

Surface Chemistry of Biological Systems

ADVANCES IN EXPERIMENTAL MEDICINE AND BIOLOGY

Editorial Board:

Nathan Back *Chairman, Department of Biochemical Pharmacology, School of Pharmacy,
State University of New York, Buffalo, New York*

N. R. Di Luzio *Chairman, Department of Physiology,
Tulane University School of Medicine, New Orleans, Louisiana*

Alfred Gellhorn *University of Pennsylvania Medical School, Philadelphia, Pennsylvania*

Bernard Halpern *Director of the Institute of Immuno-Biology, Paris, France*

Ephraim Katchalski *Department of Biophysics, The Weizmann Institute of Science, Rehovoth, Israel*

David Kritchevsky *Wistar Institute, Philadelphia, Pennsylvania*

Abel Lajtha *New York State Research Institute for Neurochemistry and Drug Addiction,
Ward's Island, New York*

Rodolfo Paoletti *Institute of Pharmacology, University of Milan, Milan, Italy, and
Institute of Pharmacology, University of Cagliari, Cagliari, Italy*

Volume 1

THE RETICULOENDOTHELIAL SYSTEM AND ATHEROSCLEROSIS

Edited by N. R. Di Luzio and R. Paoletti • 1967

Volume 2

PHARMACOLOGY OF HORMONAL POLYPEPTIDES AND PROTEINS

Edited by N. Back, L. Martini, and R. Paoletti • 1968

Volume 3

GERM-FREE BIOLOGY – EXPERIMENTAL AND CLINICAL ASPECTS

Edited by E. A. Mirand and N. Back • 1969

Volume 4

DRUGS AFFECTING LIPID METABOLISM

Edited by W. L. Holmes, L. A. Carlson, and R. Paoletti • 1969

Volume 5

LYMPHATIC TISSUE AND GERMINAL CENTERS IN IMMUNE RESPONSE

Edited by L. Fiore-Donati and M. G. Hanna, Jr. • 1969

Volume 6

RED CELL METABOLISM AND FUNCTION

Edited by George J. Brewer • 1970

Volume 7

SURFACE CHEMISTRY OF BIOLOGICAL SYSTEMS

Edited by Martin Blank • 1970

Surface Chemistry of Biological Systems

Proceedings of the American Chemical Society Symposium on
Surface Chemistry of Biological Systems held in New York
City September 11-12, 1969

Edited by
Martin Blank

*Department of Physiology
College of Physicians and Surgeons
Columbia University, New York*



PLENUM PRESS • NEW YORK-LONDON • 1970

Library of Congress Catalog Card Number 70-110799

© 1970 Plenum Press, New York

Softcover reprint of the hardcover 1st edition 1970

A Division of Plenum Publishing Corporation
227 West 17th Street, New York, N.Y. 10011

United Kingdom edition published by Plenum Press, London

A Division of Plenum Publishing Corporation, Ltd.
Donington House, 30 Norfolk Street, London W.C.2, England

All rights reserved

*No part of this publication may be reproduced in any form
without written permission from the publisher*

ISBN-13: 978-1-4615-9007-1 e-ISBN-13: 978-1-4615-9005-1
DOI: 10.1007/978-1-4615-9005-1

PREFACE

This volume of Advances in Experimental Medicine and Biology is based on an American Chemical Society Symposium entitled: "Surface Chemistry of Biological Systems", which took place in New York on September 11-12, 1969. Thanks to the special photo offset process used by the publishers, the papers are appearing very soon after their presentation, and at a lower cost than usual. These advantages are appreciated by the scientific community.

As the title of the volume indicates we have attempted to bring the scientific approach and techniques of surface chemistry to the complex problems of biological systems. Two previous symposia in this field have been published, one in the Journal of Colloid and Interface Science (24:1-127, 1967) and the other in the Journal of General Physiology (52:187S-252S, 1968). The previous publication outlets, a chemical and a biological journal, help to emphasize the interdisciplinary nature of the material and also the appropriateness of the choice of Advances in Experimental Medicine and Biology for the current symposium.

Surface chemistry continues to be useful and productive in the direct study of biological systems, and also indirectly as a context for the consideration of biological problems. There has been considerable progress in the last few years, and this volume is composed of research contributions by leading workers on a variety of problems in this general area. Along with the recent results of research on specific problems, each paper includes an up-to-date survey of the general field highlighting those areas in which there has been considerable activity in the last few years, and also indicating some of the directions in which future research will continue.

The papers can be grouped into three categories:

- 1- The first group deals with model systems, such as monolayers bilayers and dispersions, where the emphasis is on interactions between the substances themselves and also between the substances and other materials in bulk phases. These papers are directed primarily at the problems of membrane stability, and in particular the role of lipids.

- 2- The second group deals with the composition of the surfaces of natural systems and the various interactions that can result between the surfaces. These papers consider such problems as the chemical composition of a simple membrane, the substances present at the outer surfaces of various cells, the lung surfactant system, etc.
- 3- The third group deals with various aspects of transport across surfaces and the factors that influence transport. These papers emphasize the specialized mechanisms that are characteristic of transport across natural membranes, e.g. gastric secretion, pinocytosis in ameba, sugar transport in red blood cells. In the case of sugar transport it is of some interest to note that some components of the red cell which are believed to be "carriers" of sugars in membranes can be shown to act as carriers in a simple interfacial system.

There is some overlap between the groups, which is to be expected in an active field, but the groupings help one to see the trends in the general areas. For example, work is continuing on the composition and surface structure of membranes and there is a growing interest in the study of interactions in and between surfaces. There is also renewed awareness of the changes that occur in natural surfaces with time and as a result of the processes under study. This latter factor is particularly important in the study of transport processes where one must now begin to consider that membranes may change (in degree of hydration, charge, etc.) during a process and that average properties, e.g. permeability constants, may prove to be inadequate. Finally, one must note the advances that are being made in the study of medical problems, such as the characterization and the mechanism of deposition of lipids in atheromatous plaques, the development of compatible materials for intravascular prostheses, the characterization of the lung surfactant system, etc.

Although this is a rather small collection of papers, I think the reader will find that they cover a wide variety of topics and that they serve to crystallize the many recent advances in this active field of research.

Martin Blank
Department of Physiology
Columbia University
College of Physicians and Surgeons

October 1969

LIST OF PARTICIPANTS

Morris B. Abramson
The Saul R. Korey Department of Neurology
Albert Einstein College of Medicine
Bronx, New York

R. E. Baier
Applied Physics Department
Cornell Aeronautical Laboratory
Cornell University
Buffalo, New York

Jesse M. Berkowitz
Division of Gastroenterology
Department of Medicine
Meadowbrook Hospital
East Meadow, New York

Joel L. Bert
Department of Mechanical Engineering
University of California
Berkeley, California

Michael Borowitz
Cardiovascular Research Institute and
Department of Medicine
University of California Medical Center
San Francisco, California

Philip W. Brandt
Columbia University
New York, New York

Giuseppe Colacicco
York College
City University of New York
Flushing, New York

R. C. Dutton
Laboratory of Technical Development
National Heart Institute
Bethesda, Maryland

M. T. A. Evans
Unilever Research Laboratory
Colworth/Welwyn
The Frythe, Welwyn
Herts, England

Irving Fatt
Department of Mechanical Engineering
University of California
Berkeley, California

M. A. Frommer
Polymer Department
Weizmann Institute of Science
Rehovoth, Israel

Morton Galdston
Associate Professor of Medicine
New York University School of Medicine
New York, New York

Jon Goerke
Cardiovascular Research Institute and
Department of Medicine
University of California Medical Center
San Francisco, California

V. L. Gott
Department of Surgery
Johns Hopkins Hospital
Baltimore, Maryland

Helen H. Harper
Cardiovascular Research Institute and
Department of Medicine
University of California Medical Center
San Francisco, California

Klaus B. Hendil
Carlsberg Laboratory
Carlsbergvej, Valby, Denmark

L. Irons
Unilever Research Laboratory
Colworth/Welwyn
The Frythe
Welwyn, Herts, England

Robert Katzman
The Saul R. Korey Department of Neurology
Albert Einstein College of Medicine
Bronx, New York

A. Khaiat
Polymer Department
Weizmann Institute of Science
Rehovoth, Israel

Christian Mathot
Rockefeller University
New York, New York

E. Mayhew
Department of Experimental Pathology
Roswell Park Memorial Institute
Buffalo, New York

I. R. Miller
Polymer Department
Weizmann Institute of Science
Rehovoth, Israel

J. Mitchell
Unilever Research Laboratory
Colworth/Welwyn
The Frythe
Welwyn, Herts, England

Thomas Jenner Moore
St. Luke's Hospital Center and
College of Physicians and Surgeons
New York, New York

P. R. Mussellwhite
Unilever Research Laboratory
Colworth/Welwyn
The Frythe
Welwyn, Herts, England

P. A. Myers
New England Institute for Medical Research
Ridgefield, Connecticut

Martin S. Nachbar
Department of Medicine
New York University School of Medicine
New York, New York

Shinpei Ohki
Department of Biophysical Sciences
State University of New York at Buffalo
Buffalo, New York

Demetrios Papahadjopoulos
Department of Experimental Pathology
Roswell Park Memorial Institute
Buffalo, New York

Melvin Praissman
The Department of Physiology
Mount Sinai School of Medicine
New York, New York

Alexandre Rothen
Rockefeller University
New York, New York

Milton R. J. Salton
Department of Microbiology
New York University School of Medicine
New York, New York

Emile M. Scarpelli
Department of Pediatrics
Albert Einstein College of Medicine
New York, New York

Dinesh O. Shah
Surface Chemistry Laboratory
Marine Biology Division
Lamont-Doherty Geological Observatory
Columbia University
Palisades, New York

Donald M. Small
Biophysics Unit
Department of Medicine
Boston University School of Medicine
Boston, Massachusetts

H. Ti Tien
Department of Biophysics
Michigan State University
East Lansing, Michigan

D. J. Wilkins
New England Institute for Medical Research
Ridgefield, Connecticut

L. Weiss
Department of Experimental Pathology
Roswell Park Memorial Institute
Buffalo, New York

CONTENTS

The Effect of the Modification of Protein Structure on the Properties of Proteins Spread and Adsorbed at the Air-Water Interface	1
M. T. A. Evans, J. Mitchell, P. R. Mussellwhite, and L. Irons	
The Interaction of Calcium with Monolayers of Stearic and Oleic Acid	23
J. Goerke, H. H. Harper, and M. Borowitz	
Studies of Thermal Transitions of Phospholipids in Water: Effect of Chain Length and Polar Groups of Single Lipids and Mixtures	37
M. B. Abramson	
The Physical State of Lipids of Biological Importance: Cholesteryl Esters, Cholesterol, Triglyceride .	55
D. M. Small	
The Effect of Hydrocarbon Configuration and Cholesterol on Interactions of Choline Phospholipids with Sulfatide	85
M. B. Abramson and R. Katzman	
Lipid-Polymer Interaction in Monolayers: Effect of Conformation of Poly-L-Lysine on Stearic Acid Monolayers	101
D. O. Shah	
Interactions of DNA with Positively Charged Monolayers . . .	119
M. A. Frommer, I. R. Miller, and A. Khaiat	

The Effect of Modifiers on the Intrinsic Properties of Bilayer Lipid Membranes (BLM)	135
H. Ti Tien	
Asymmetric Phospholipid Membranes: Effect of pH and Ca^{2+}	155
S. Ohki and D. Papahadjopoulos	
Dissociation of Functional Markers in Bacterial Membranes	175
M. S. Nachbar and M. R. J. Salton	
RNA in the Cell Periphery	191
E. Mayhew and L. Weiss	
Immunological Reactions Carried Out at a Liquid-Solid Interface with the Help of a Weak Electric Current	209
A. Rothen and C. Mathot	
Electrophoresis and Adsorption Studies of Proteins and Their Derivatives on Colloids and Cells	217
D. J. Wilkins and P. A. Myers	
Surface Chemical Features of the Blood Vessel Walls and of Synthetic Materials Exhibiting Thromboresistance	235
R. E. Baier, R. C. Dutton, and V. L. Gott	
Lipid-Protein Association in Lung Surfactant	261
M. Galdston and D. O. Shah	
Absence of Lipoprotein in Pulmonary Surfactants	275
E. M. Scarpelli and G. Colacicco	
Relation of Water Transport to Water Content in Swelling Biological Membranes	287
J. L. Bert and I. Fatt	
Kinetic and Equilibrium Behavior of Simple Sugars in a Water-Butanol-Lipid System	295
T. J. Moore	
Use of Synthetic Membrane Models in the Study of Gastric Secretory Processes	309
J. M. Berkowitz and M. Praissman	
Properties of the Plasma Membrane of Amoeba	323
P. W. Brandt and K. B. Hendil	
Index	337

THE EFFECT OF THE MODIFICATION OF PROTEIN STRUCTURE ON THE PROPERTIES
OF PROTEINS SPREAD AND ADSORBED AT THE AIR-WATER INTERFACE

M.T.A. Evans, J. Mitchell, P.R. Mussellwhite, L. Irons

Unilever Research Laboratory Colworth/Welwyn, The Frythe
Welwyn, Herts, England

INTRODUCTION

The results of experimental biology clearly show that living systems contain complex organisations of membranes, organelles, solid-gel, solid-liquid and liquid-gel interfaces. Here proteins play key roles, the complete understanding of which requires a knowledge of their structures and interactions with surrounding substances, and a determination of how these factors govern functional relationships. With problems of this difficulty, it is usual to isolate individual components and try to understand their behaviour in simple, model systems. A classic example of this sort of approach is to be found in the study of the surface chemistry of proteins, where a vast amount of work has been concerned with the behaviour of one protein at an interface. We will examine some of the important conclusions of such work here, and in particular, we propose to analyse the relationship between the native structure of a protein and its interfacial configuration and properties.

The tremendous advance in the understanding of protein structure in solution and the crystalline state during the last two decades unfortunately has not been paralleled by a similar increase in the knowledge of their interfacial configuration. Protein chemistry in general has benefited enormously from the development and application of powerful physical methods, while the limited number of experimental techniques which are available severely restricts the study of proteins at interfaces. Present knowledge stems mainly from the measurement of surface pressure, surface potential and the rheological properties of spread and adsorbed films at the air-water and oil-water interfaces, although some work has been carried out at solid-liquid interfaces. The

state of current research is displayed and discussed in the recent reviews of Loeb¹ and James and Augenstein². Certain generally acceptable conclusions have been drawn from this extensive work on the interfacial properties of proteins. For instance, it is thought that at the air-water interface, and probably also at the oil-water interface, a protein can form two types of film:-

- (a) A dilute film, in which all the molecules are in the same extensively unfolded state.
- (b) A concentrated film, which may contain only native and unfolded molecules, or molecules in many different degrees of unfolding².

Three main factors will dictate whether a protein forms a dilute or concentrated film at an interface. They are:-

- (i) The decrease in surface free energy which will result if the protein unfolds.
- (ii) The forces which will act to maintain the protein in its native configuration at the interface.
- (iii) The surface pressure against which the molecule has to expand in order to unfold.

General considerations such as these may now be applied to particular cases. We shall show that the characteristics of certain proteins at the air-water interface can be related to differences in their tertiary structures. To illustrate this we will refer to the surface properties of β -casein, bovine serum albumin and lysozyme.

The influence of primary and quaternary structure on surface properties was investigated by the technique of selective chemical modification. For this, some derivatives of β -casein were studied at the air-water interface. In these molecules, a controlled variation of charge and hydrophobic character enabled an estimate to be made of the effect of aggregation and electrostatic repulsion on the interfacial properties of the protein.

EXPERIMENTAL

Materials

Lysozyme (β x crystallised) was obtained from Calbiochem, Los Angeles. Crystalline bovine serum albumin was supplied by the Armour Pharmaceutical Company, Eastbourne, England. Acid casein was prepared from bulk Ayrshire milk by acidification to pH 4.6 at 25°. Crude β -casein was isolated from the acid casein by urea fractionation³, and subsequently purified by chromatography on DEAE cellulose⁴.

For this study the succinyl, acetyl, n-butyryl, n-hexanoyl and n-decanoyl derivatives of β -casein were prepared. Most of these derivatives have been described by Hoagland^{5,6}. Satisfactory

compounds were prepared by reacting β -casein with the appropriate anhydride in either phosphate buffer (2% Na_2HPO_4 , pH8.0) or dimethyl sulphoxide. Exhaustive dialysis against distilled water was necessary to remove excess reagents. The derivatives were isolated by lyophilisation.

Methods

The purity of the β -casein and its derivatives was examined by gel electrophoresis.

Polyacrylamide gel electrophoresis was performed using a 10% gel slab in Tris-EDTA borate buffer at pH8.5, 400v and 50mA.

Starch-gel electrophoresis was carried out in urea-Tris-citrate buffer pH8.6, with a 12% gel⁷.

The extent of modification of β -casein was measured by the loss of ninhydrin colour in the derivatives compared to β -casein⁸. Substitution of protein hydroxyl groups was investigated by an alkaline hydroxylamine procedure⁹.

Experimental conditions for the preparation of the β -casein derivatives were chosen so that in all cases, substitution of available amino groups was greater than 90% by the ninhydrin reaction. The amino groups involved were principally the $\epsilon\text{-NH}_2$ of the lysines and the terminal amino group of the protein.

It was found that with the method of modification described, some 15-30% of available serine, threonine and tyrosine hydroxyl groups were also substituted.

Protein concentrations were measured by a semimicro Kjeldhal method.

Spreading Experiments at the Air-Water Interface

The relationship between surface concentration (c) and surface pressure (π) was determined in two ways.

(1) A pressure-area ($\pi\text{-A}$) isotherm was obtained by reducing the surface area occupied by a fixed mass of protein.

(2) The pressure-concentration ($\pi\text{-C}$) isotherm was found by spreading an increasing amount of protein onto a fixed surface area.

A Langmuir-Adam surface balance with a fused silica trough and teflon barriers was used for these measurements. The spreading area was 331 cm^2 . The force on the mica float was measured with a torsion wire system which enabled the surface pressure to be determined to an accuracy of ± 0.1 dyne cm^{-1} . The protein was spread on phosphate or glycine buffer substrates, which were maintained at $25^\circ \pm 0.5^\circ$. The buffers were as follows:-

1. 5.65mM Na_2HPO_4 , 3.05mM NaH_2PO_4 , 0.08M NaCl, pH7.0, I = 0.1.
2. 0.115M glycine in 0.1M sodium hydroxide, pH10.0, I = 0.1.
3. 0.76mM glycine in 12.4mM sodium hydroxide, 0.088M sodium chloride, pH11.7, I = 0.1.

The buffers were made up from spectroscopic grade sodium chloride and analytical grade salts. Water for surface work was double distilled, deionised and redistilled from alkaline permanganate

For the π -A isotherms, approximately 1.5×10^{-2} mg of protein was spread from a 0.03% solution in the substrate buffer onto an area of 331 cm^2 . The spreading method was similar to that of Trurnit¹⁰. A clean glass rod was wetted for 15 mm along its length by gently dipping it into the subphase. It was then clamped with 5mm of its length dipping below the interface. Protein solution from an Agla glass micrometer syringe was run onto the glass rod 10mm above the surface. The rod was then removed from the surface and the film allowed to stand for 15 minutes. For lysozyme, a period of 3 hours was allowed for equilibration. After this the film was compressed and the corresponding area measured. Measurements were made continuously up to a pressure of 1 dyne cm^{-1} . At higher pressures, 10-20 minute intervals were allowed between readings, so that the film could equilibrate.

π -C Isotherms were obtained by spreading successive aliquots of from $0.5-2.0 \times 10^{-2}$ mg of protein onto a constant area of 331cm^2 . After the addition of each aliquot, the film was allowed to equilibrate as before, then the surface pressure was measured. The spreading solution and technique were as previously described.

Compressibility data were obtained from the pressure-area isotherms by plotting $-1/A \frac{dA}{d\pi}$ against A .

Adsorption Experiments at the Air-Water Interface

The (π -t) isotherm, i.e. the change of surface tension with time as protein adsorbed to an initially clean surface was measured using a Wilhelmy plate suspended from a du Nuøy torsion head. The volume of buffer solution in a circular trough of surface area 4.7cm^2 was reduced to 100 ml by suction at the surface. 10ml of subphase were removed and 10 ml of protein solution (0.01%) injected slowly under the surface, so that the two solutions gently mixed. Measurements of surface pressure were then made over a period of 2-3 hours.

I. THE RELATIONSHIP BETWEEN NATIVE PROTEIN STRUCTURE AND INTERFACIAL CONFIGURATION

The wide variety of surface behaviour exhibited by proteins at the air-water interface is well illustrated by the properties of lysozyme, bovine serum albumin and β -casein. The π -A and π -C isotherms of the three proteins are displayed in Figure 1.

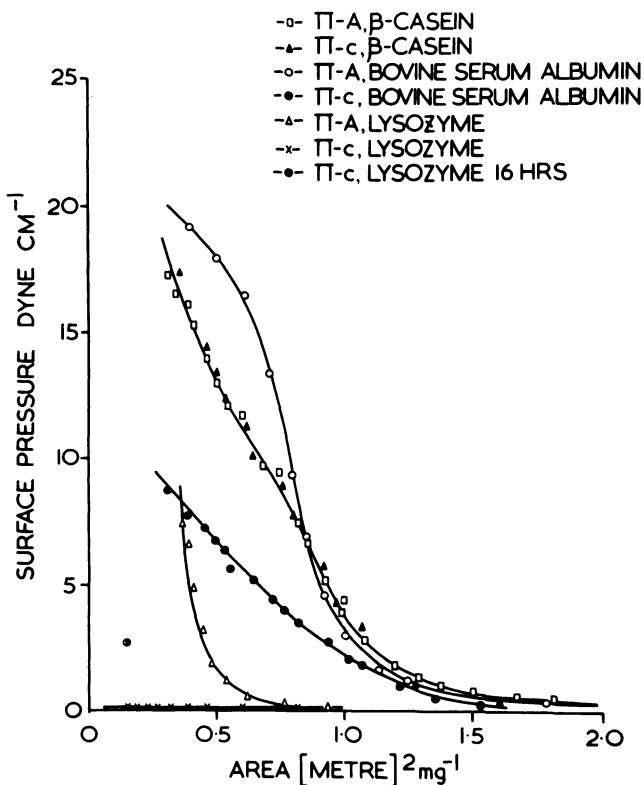


FIGURE 1: π -A and π -C isotherms of β -casein, bovine serum albumin and lysozyme on phosphate buffer (pH7) subphase at 25° .

At minimum compressibility, the π -A isotherms of bovine serum albumin and β -casein have areas of 0.85 and $0.90\text{m}^2 \text{mg}^{-1}$ respectively. Such areas are regarded as being characteristic of dilute films¹¹. Furthermore, the limiting area of the π -A isotherm for bovine serum albumin differs very little from those obtained when the protein is spread on concentrated salt solutions, or when spreading solvents are used^{12,13}. Both of these methods favour the formation of dilute films. It is, therefore, reasonable to suppose that the π -A films of β -casein and bovine serum albumin are dilute films containing only unfolded molecules.

On the other hand, even when a film of lysozyme was left for two hours to equilibrate before compression, the subsequent π -A

isotherm only gave an area at minimum compressibility of approximately $0.35\text{m}^2\text{mg}^{-1}$. This is consistent with previous work on lysozyme¹⁴, where it was found that the protein could not be spread completely on substrates of low salt concentration. The small limiting area found for lysozyme probably reflects the presence of a concentrated rather than a dilute film at the air-water interface¹⁵, together with an appreciable loss of protein to the subphase¹⁴.

Considerable differences are evident in the π -C isotherms of these proteins (Figure 1). The π -C isotherm of β -casein is in agreement with its π -A isotherm, which strongly suggests that the π -C isotherm of β -casein is also formed by a dilute film¹⁶.

Negligible surface pressures were recorded when the standard equilibration conditions were used for a π -C isotherm of lysozyme. However, after sixteen hours at a nominal surface area of $0.14\text{m}^2\text{mg}^{-1}$, a pressure of 2.7 dyne cm^{-1} was attained. Bovine serum albumin showed an intermediate behaviour. The π -A and π -C isotherms agreed up to a surface pressure of about 2 dyne cm^{-1} , but above this there was a marked divergence¹⁷. Films of pepsin¹⁸ and trypsin¹⁹ exhibit π -A and π -C isotherms with similar properties, although these were not formed under the same spreading conditions as the protein films we describe. Enzyme activity can be recovered from the π -C films of pepsin and trypsin, and this is regarded as evidence for the presence of native or incompletely unfolded molecules². By analogy, it is therefore probable that bovine serum albumin also forms a concentrated π -C film.

For lysozyme however, the π -C film generates so little surface pressure that both the surface concentration and hence the condition of the molecules at the interface are uncertain. However, other facts we will present make it reasonable to assume that lysozyme may also form concentrated films at the air-water interface.

The π -t isotherms of bovine serum albumin, lysozyme and β -casein are shown in Figure 2. These approximately reflected the maximum pressures attained in the π -C films. This was to be expected, since the adsorption of an increasing amount of protein to a constant surface area closely resembles the method of formation of a π -C film. At this concentration, β -casein lowers the surface tension more than bovine serum albumin, while lysozyme has little effect. Yamashita and Bull²⁰ have recently shown that adsorbed films of lysozyme contain native or near native molecules. The long term ageing effects shown by the gradual change in surface pressure in adsorbed films of lysozyme and bovine serum albumin (Figure 2) may then be attributed to the slow unfolding and re-orientation of native molecules in the adsorbed surface film. This is a consequence of the non-equilibrium nature of concentrated films, for since a protein can give both a dilute and a concentrated

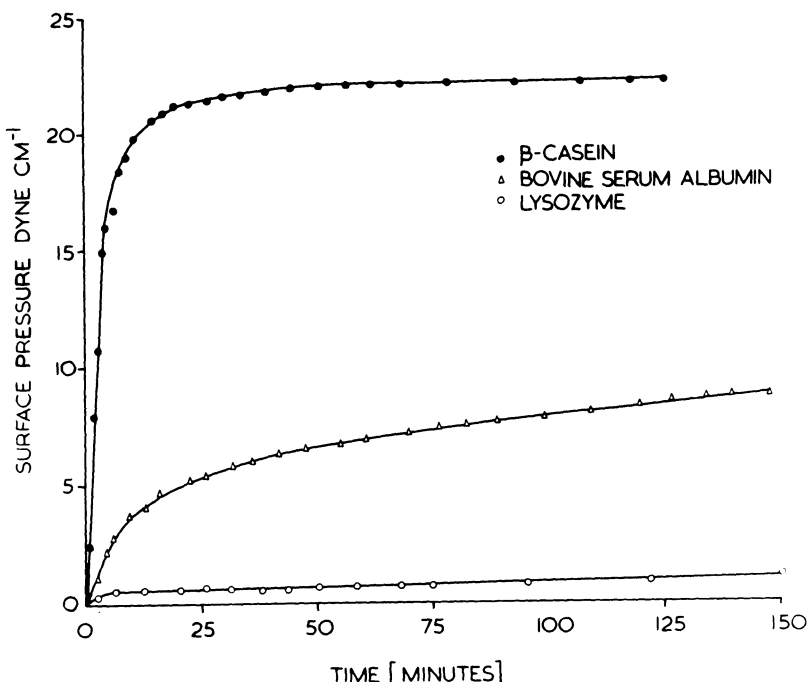


FIGURE 2: π -t Isotherms of β -casein, bovine serum albumin and lysozyme at the air/phosphate buffer (pH7) interface at 25° 0.001% protein concentration in bulk phase. After 6 hours a surface pressure of 3.3 dyne cm^{-1} was obtained for lysozyme.

film at the same concentration and on the same subphase, it follows that one type of film is metastable. As it is possible to convert a concentrated film to a dilute film by expansion, but impossible to perform the reverse process, then the dilute film is stable. In this context it is noteworthy that β -casein π -t films show no appreciable ageing effects.

Our conclusions concerning the types of films formed by these proteins are summarised in Table I, together with some structural parameters of the molecules.

We have already outlined the criteria which govern whether a molecule will readily unfold at an interface. One of these was the

TABLE I

	β -Casein	Bovine serum albumin	Lysozyme
π -A film	Dilute	Dilute	Concentrated
π -t or π -C film	Dilute	Concentrated	Concentrated
Molecular weight %age α -helix	25,000 ²¹ 10^{23}	65,000 ²² 47^{24}	14,300 ²² 23^{24}
S-S bond content per molecule	0 ²⁵	17 ²²	4 ²²
Hydrophobicity	1320 ²⁶	1120 ²⁷	970 ²⁷

surface pressure against which the protein has to spread. A consideration of this factor reveals that unfolding will be favoured in a spread π -A film as opposed to a spread π -C film, since in the former all molecules will enter a surface which is at low or zero surface pressure. In the latter, successive aliquots of protein are required to spread against the increasing surface pressure of molecules already present. Therefore, for many globular proteins of which bovine serum albumin is a typical example, adsorbed films will be of a concentrated form, and will bear little relationship to the dilute π -A spread film except at very low surface pressures.

The lack of structural barriers to unfolding of the molecule was suggested as an explanation for the pronounced surface activity of high density apolipoprotein²⁸. The differing surface activity of β -casein, bovine serum albumin and lysozyme can also be attributed to a variation in this factor. An understanding of this necessitates a brief consideration of the structure of these proteins. β -Casein is now thought to be a predominantly random coil molecule with no disulphide bonds, while both lysozyme and bovine serum albumin are globular proteins containing secondary structures, their polypeptide chains being crosslinked by disulphide bonds (Table I).

It is not obvious from Table I why bovine serum albumin should be less resistant to surface denaturation than lysozyme, since it contains about the same number of disulphide bonds per residue as lysozyme, and a greater helical content. However, studies on the denaturation of these proteins in bulk solution suggest that the barriers to unfolding in lysozyme are greater than in bovine serum albumin. For example, lysozyme at neutral pH is very stable to heat²⁹, while bovine serum albumin is not³⁰. Bovine serum albumin is denatured more readily by moderate concentrations of guanidine hydrochloride than lysozyme³¹ and unfolds at a pH slightly below its isoelectric point³⁰. Thus one of the main factors determining the

surface behaviour of these two proteins appears to be the strength of the forces maintaining tertiary structure. If these forces are weak, then the probability of unfolding is high. β -Casein, which has little tertiary structure, consequently has high surface activity. When tertiary structural content is low or absent, then secondary structure and intramolecular cohesion should become important. In this respect, the work of Malcolm³² and Loeb and Baier³³ suggests that even in dilute films proteins and polypeptides may maintain their secondary structure.

If helical regions are not disrupted at the surface, the activation energy for unfolding will not be related to secondary structure. Proteins usually contain less secondary structure than synthetic polypeptides, this structure being distributed in discontinuous segments throughout the polypeptide chain. It is therefore quite feasible for major reorientations of protein polypeptide chains to occur at the surface without disrupting the helical portions.

Solubility may be critical in determining the surface isotherm behaviour, though not necessarily the type of film that is formed. If a molecule does not unfold readily when subjected to surface forces, it will not stay long at the interface and will tend to dissolve back into the subphase. With low solubility, this tendency will be reduced, so that the molecules remain longer at the interface. The probability of unfolding then becomes greater, as desorption is less likely. Solubility considerations will, therefore, affect the time a molecule remains in the interface, but not the probability per unit time of its unfolding there. This is a property of the molecule itself.

In Table I we have included the hydrophobicity parameter derived by Bigelow²⁷. This has been calculated for many proteins on the basis of their defined apolar amino acid content. It might appear from the table that proteins with a high content of apolar amino acids are more efficient at lowering the surface tension than hydrophilic proteins, provided that tertiary structural constraints are low. This has been suggested as an additional reason for the marked surface activity of high density apolipoprotein²⁸. To examine this sort of effect we have systematically altered the hydrophobicity and charge of β -casein by selective chemical modification.

II. THE PROPERTIES OF SOME DERIVATIVES OF β -CASEIN AT THE AIR-WATER INTERFACE

The π -A isotherms of β -casein and its acyl derivatives are shown in Figure 3. An interesting feature of these isotherms is the expansion apparent at moderate and high surface pressures as the length of the n-alkyl side chain on the modifying group increases. Plots of compressibility against area for acetyl, n-butyryl and native β -casein (Figure 4) gave bimodal patterns rather than the

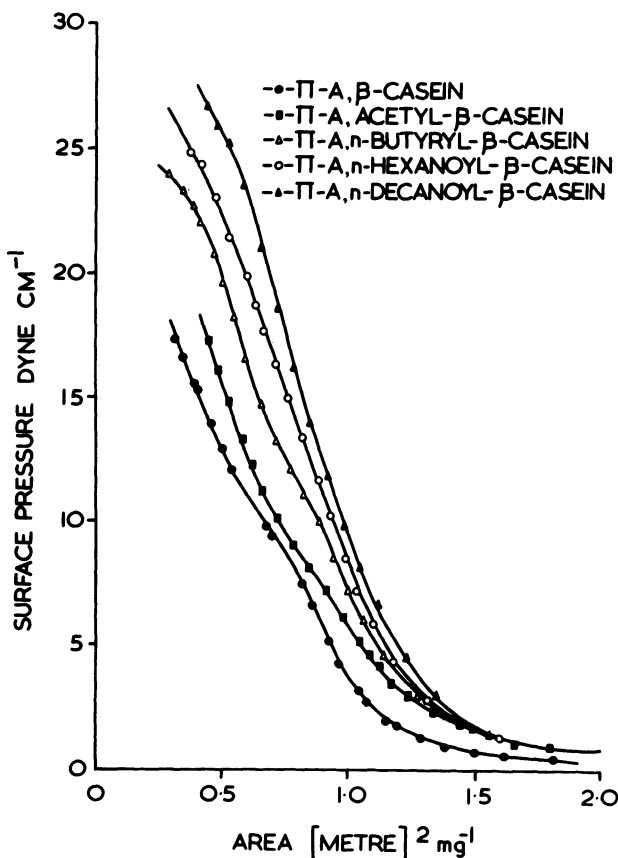


FIGURE 3: π -A isotherms of β -casein and its acyl derivatives on phosphate buffer (pH7) subphase at 25° .

single minimum normally obtained from a protein. This was caused by an irregularity in the π -A isotherms between $0.5-1.0 \text{ m}^2 \text{ mg}^{-1}$. These effects were reproducible and appeared to be unique to β -casein and its short chain acyl derivatives. Such behaviour has not been observed in other proteins studied under comparable compression conditions. However, n-hexanoyl and n-decanoyl β -caseins did not show this effect.

In Figure 5, the π -A isotherm of succinyl β -casein at pH7.0 is compared with those of β -casein at pH 10.0 and pH 11.7. Assuming a high degree of substitution of the available lysine amino groups, the charge on the succinyl derivative will be approximately three times that of β -casein, which at pH7.0 possesses a net negative

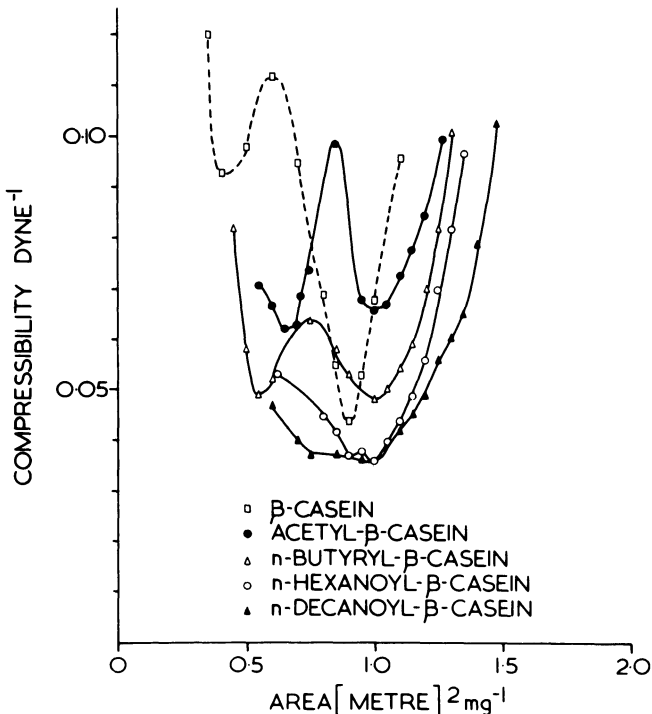


FIGURE 4: Compressibilities of β -casein and its acyl derivatives on phosphate buffer (pH7) subphase at 25°.

charge of eleven units³⁴⁺. Similarly the negative charge on the acyl derivatives will be about twice that of β -casein at pH7.0. This is because in the first case the lysine will bear a negative instead of a positive charge, while in the second the positive charge is neutralised by the modification.

Although the collapse pressures shown by the π -A isotherms of the acyl derivatives increase considerably with the chain length of the modifying group (Figure 3), the π -t isotherms do not show correspondingly large differences. It is noteworthy however, that the slow long-term changes in surface tension evident in the π -t films of n-butyryl, n-hexanoyl and n-decanoyl β -caseins are larger than those shown by native β -casein and the other derivatives.

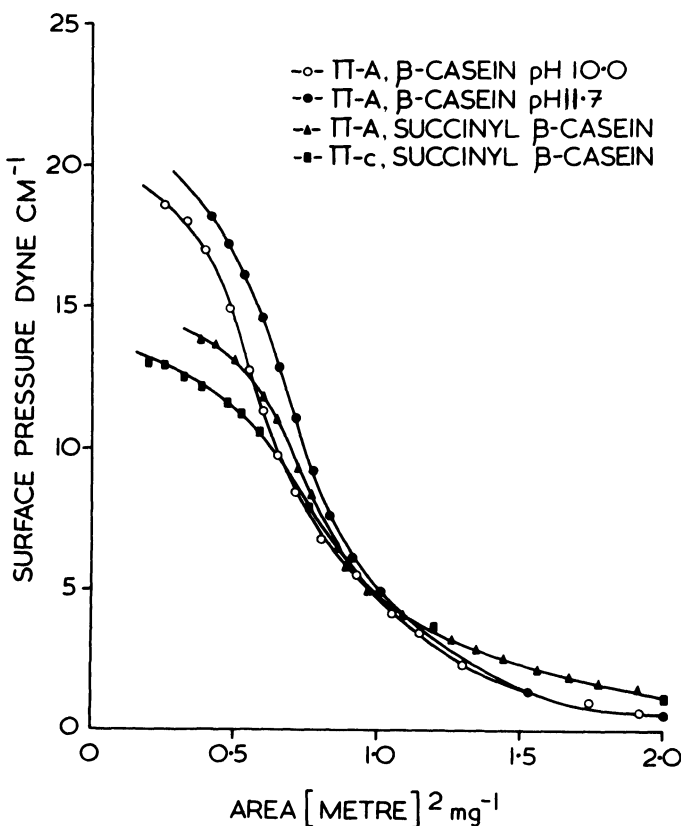


FIGURE 5: π -A isotherms of β -casein on glycine buffer (pH 10.0 and 11.7) subphases at 25°. π -A and π -C isotherms of succinyl- β -casein on phosphate buffer (pH 7) subphase at 25°.

In Figure 6 the π -C and π -A isotherms of β -casein and its acyl derivatives are compared. The π -C isotherm of succinyl β -casein is included, with its π -A isotherm in Figure 5. The π -A and π -C isotherms of β -casein and its acetyl derivative were nearly coincident over the whole pressure range measured, while at low or moderate pressures the same was true for the other acylated derivatives. For these however, divergence occurred at high pressure.

There are two possible explanations for the incremental shift of the acyl π -A isotherms with the chain length of the modifying group. Either the extra hydrophobic character imparted by the hydrocarbon side chains acts to stabilise segments of the polypeptide

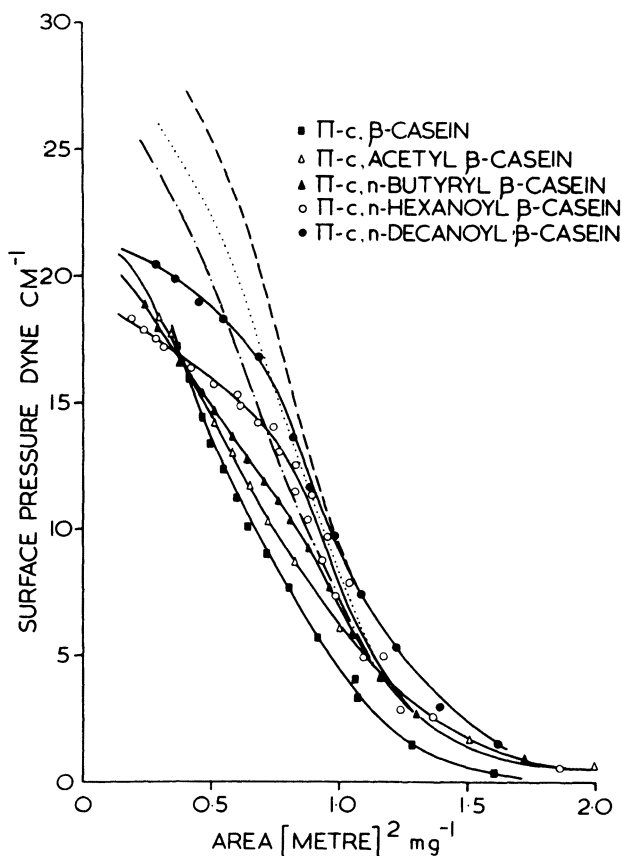


FIGURE 6: π -C Isotherms of β -casein and its acyl derivatives on phosphate buffer (pH7) subphase at 25° . The π -A isotherms of n-butyryl, n-hexanoyl and n-decanoyl β -caseins are shown as dotted lines.

chain against collapse, or the area occupied by the modified lysine residues at the interface is related to the side chain length. The first alternative seems to fit the data satisfactorily, since the expansion of the π -A isotherms of the acyl derivatives is accompanied by a decrease in compressibility, which may be associated with an increase in resistance to collapse (Figure 4). The π -A isotherm of β -casein is more compressible than that of a typical globular protein such as bovine serum albumin (Figure 1). This is because of the low degree of interaction between the amino acid residues in the film, and is in accord with the properties of a molecular structure seen as a randomly coiled thread with no covalent and little noncovalent intrachain constraint.

Modification might be expected to reduce the degree of collapse by making the energy of desorption of individual lysine residues larger and by increasing the extent of both inter and intramolecular non-polar interactions. In support of this, Hoagland⁶ has found that there is an increase in aggregate size in the bulk phase as the chain length of the modifying group in the acyl derivatives increases. High resolution n.m.r. studies also show evidence of line broadening in the n-butyryl, n-hexanoyl and n-decanoyl derivatives consistent with the presence of strong hydrophobic interactions^{7,8}.

It is difficult to determine whether the expansion of the π -A isotherms of the acyl derivatives is in any way due to a change in the area occupied by the various modified lysine residues at the interface. The basic problem is the definition of the area of close packing of a very compressible protein film, and the accurate measurement of its change. If this were feasible, it would be a simple matter to calculate the extra contribution of area per residue supplied by modified lysine groups whose side chains were oriented horizontally in the interface, and compare this with the observed alteration in area of close packing. If, however, collapse is entirely the determining factor in the differences between the π -A isotherms, then this must begin at areas greater than the first minimum in the compressibility curve ($\sim 1.0 \text{ m}^2 \text{ mg}^{-1}$).

Chemical modifications of this nature carried out on globular proteins exhibiting well defined limiting areas may well provide more accurate information as to the orientations of the modified lysines and hence to the secondary structure present in the film. We are currently investigating this possibility.

²⁷ Bigelow³⁶ has extended the work of Tanford and produced a quantitative basis for assessing the hydrophobicity of amino acids and their side chains. In this respect β -casein has an unusual distribution of amino acid content, possessing 99 residues of high hydrophobicity, between 1.5 and 3.0 k. cal/residue on Bigelow's scale, only 35 residues of moderate hydrophobicity (between 0 and 1.5 k cal/residue) and 75 polar amino acids with hydrophobicity defined as zero. Langmuir and Waugh⁷ have suggested that when protein films were compressed, polar amino acids collapsed out at low surface pressure and apolar residues at high pressure. Thus when a β -casein film is compressed, it follows that there could be a range of pressures corresponding to the region of collapse of the residues of moderate hydrophobicity; since these are few there will be a considerable change in surface pressure over a small area in the isotherm. This could be the reason for the irregularities in the π -A isotherms of β -casein and its short chain acyl derivatives. In the n-hexanoyl and n-decanoyl β -casein isotherms, where these irregularities are not observed, the degree of interaction between residues is much larger so that the idea of considering collapse in

terms of hydrophobicities of individual amino acids may not be valid. The order of amino acids in the sequence is an additional factor to be considered.

The influence of charge on the π -A isotherm is most marked at high areas. In this region the isotherms of the acyl derivatives coincide, and resemble that of β -casein at high pH (Figures 3,5). Films of both the succinyl and acyl derivatives exert a higher pressure at high areas than does the native protein.

Payens³⁸ has derived an equation for the electrostatic contribution to the film pressure of a monolayer of charge density σ esu cm⁻² on a substrate of equivalent electrolyte concentration C (equation 1).

$$(1) \quad \pi_{el} = 6.1 C^{\frac{1}{2}} \left[\cosh \left\{ \text{arc sinh } 28.10^{-6} \sigma C^{-\frac{1}{2}} \right\} - 1 \right]$$

Figure 7 shows the experimental and calculated portions of the π -A isotherms of β -casein and its derivatives at high areas. The assumption is made that the difference between the β -casein isotherm and the others is solely due to charge effects. The charge on β -casein at pH 7.0 was taken as 11 negative units, and those on the acyl and succinyl derivatives as 19 and 27 negative units respectively. These latter figures allow for slightly less than 100% substitution, as well as incomplete ionisation at pH 7.0. Agreement between the calculated and experimental isotherms was fairly satisfactory, so that it is probable that the increase in pressure exhibited by the modified caseins at high area can be ascribed entirely to electrostatic effects. From Figure 6 it also seems that the charge on β -casein at high pH closely resembles that on the acyl derivatives.

Although at areas lower than about $1.3 \text{ m}^2 \text{ mg}^{-1}$, effects other than electrostatic forces become important in determining the π -A isotherm, the lower collapse pressures of the β -casein films at high pH may also be related to the higher charge preventing cohesive interactions between the amino acid residues. The low collapse pressure of the succinyl β -casein film (Figure 6) may also be attributed to this, since the negative charge here is also greatly increased. In addition, the modified lysines are given increased polar character by the substituent carboxyl group.

Since there is a clear analogy between the method of formation of adsorbed and π -C spread films, we have made a quantitative comparison between adsorption pressures in π -t isotherms and the pressures obtained from π -C isotherms. This can be done for the β -casein derivatives by assuming that the rate of arrival of molecules at an interface in an adsorption experiment is given by an irreversible diffusion equation (equation 2)³⁹.

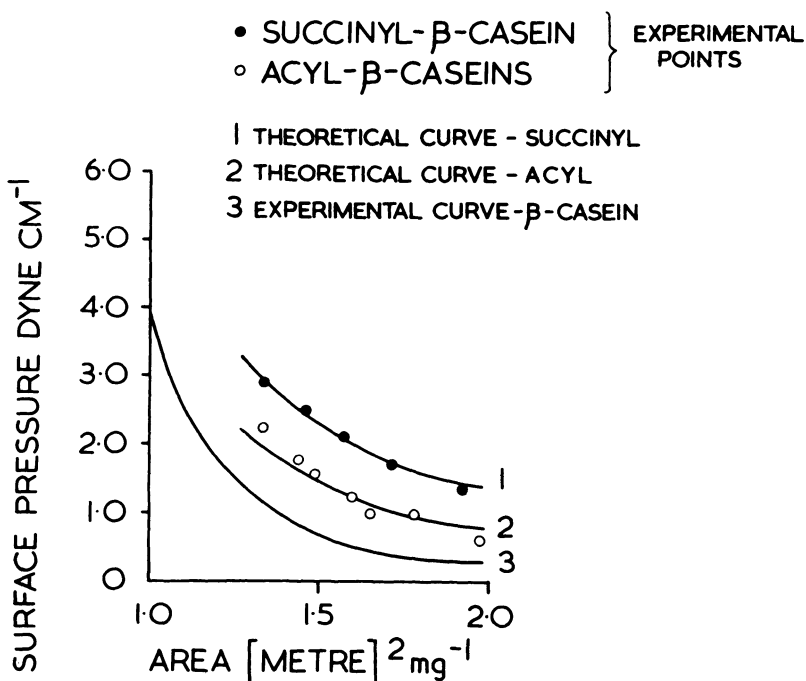


FIGURE 7: Experimental and calculated portions of the π -A isotherms of β -casein, succinyl β -casein and acyl β -caseins on phosphate buffer (pH7) subphase at 25° .

$$(2) n = 2n_0 \sqrt{\frac{Dt}{\pi_c}}$$

(n is the surface concentration of the material after time t , D is the diffusion coefficient, n_0 the bulk concentration of the protein and $\pi_c = 3.142.$)

The relationship between the surface pressure and surface concentration in the calculated π -t isotherms is derived from the π -C data. In Figures 8 and 9 the experimental isotherms are compared with the curves calculated on this basis. It can be seen that agreement between calculation and experiment is fairly good for most of the modified proteins. This would lend some support to the idea that there is a similarity between π -C and π -t films. From the work of MacRitchie and Alexander⁴⁰ it might be considered dubious to assume that the rate of adsorption was determined only by diffusion. However, these workers were concerned with globular proteins, while β -casein is disordered. It has been shown recently⁴¹ that the rate

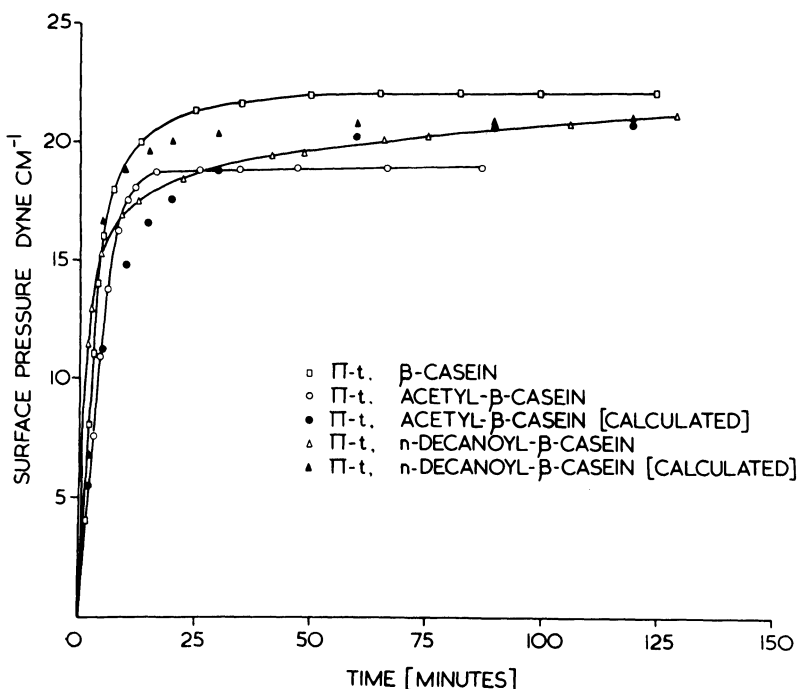


FIGURE 8: π -t Isotherms of β -casein, acetyl β -casein and n-decanoyl β -casein at the air/phosphate buffer (pH7) interface at 25° 0.001% protein concentration in bulk phase. Calculated and experimental points are shown.

of adsorption of disordered proteins to an interface more nearly corresponds to that predicted for an irreversible diffusion process.

The difference between the π -A and π -C isotherms of n-butyryl, n-hexanoyl and n-decanoyl β -caseins at high surface pressures may be due to the highly aggregated nature of these proteins. Previous work¹⁶ has shown that the divergence between the π -A and π -C isotherms of K-casein at high pressures was due to the presence of disulphide bonds which help to maintain the highly aggregated nature of this protein. In ultracentrifuge studies we have demonstrated that n-butyryl, n-hexanoyl and n-decanoyl β -caseins form stable polydisperse aggregates which do not dissociate on dilution²⁵, while β -casein, though forming a strongly aggregating system, dissociates into monomers at low temperatures and on dilution²¹. However, aggregation cannot be the reason for the divergence of the π -A and π -C isotherms of succinyl- β -casein at high pressures since this is a monomeric species at 25°⁵. Here there is possibly some loss to the subphase from the π -C film by collapse due to its enhanced polar character.

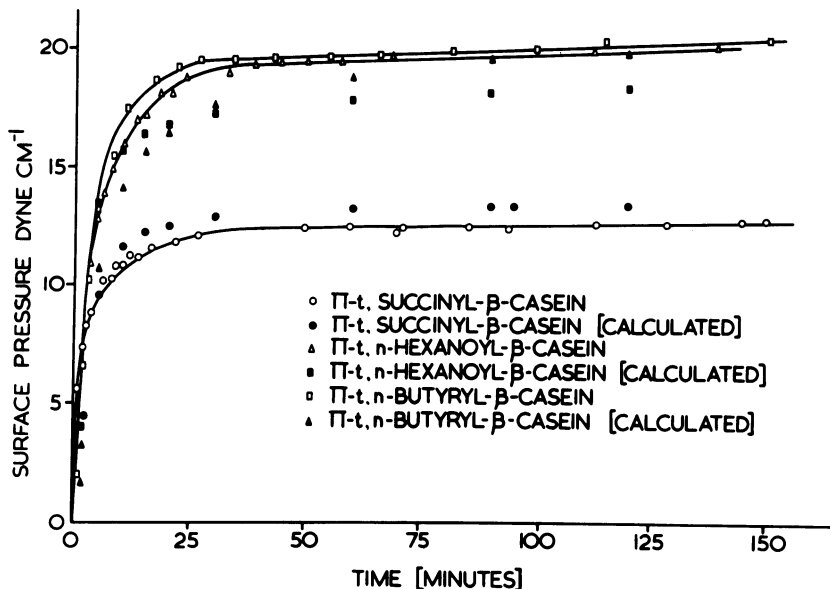


FIGURE 9: π -t Isotherms of succinyl n-butyryl and n-hexanoyl β -caseins at the air/phosphate buffer (pH7) interface at 25 °C. 0.001% protein concentration in bulk phase. Calculated and experimental points are shown.

In the π -A film, it appears that the aggregates in the acyl derivatives will unfold at the surface, since if this were not so the π -A isotherms of these proteins would be less expanded than that of β -casein. This situation does in fact occur between monomer and aggregated γ -globulin⁴².

However, when n-butyryl, n-hexanoyl and n-decanoil β -caseins are spread against high surface pressures, the aggregates appear to resist unfolding, so that the π -C and adsorbed films are of the concentrated rather than the dilute type. The greater, though gradual changes in the surface tension of adsorbed π -t films of n-butyryl, n-hexanoyl and n-decanoil β -caseins when compared with acetyl, succinyl and native β -casein tend to confirm this.

It will be useful at this point to recapitulate some of the main conclusions about the relationship between surface properties and protein structure.

- (a) A disordered protein is more surface active than a globular protein, and will be more likely to form a dilute film. It will adsorb faster to an interface, unfold more easily, and cause a larger change in interfacial tension. Disorder in this context implies a lack of intrachain restraints, not necessarily an absence of secondary structure.
- (b) We have demonstrated the influence of primary and quaternary structure on the surface properties of β -casein, by changing the chemical composition and aggregation behaviour of the protein. Caseins modified with long chain acyl groups exhibited expanded π -A isotherms, characterised by high collapse pressures. Strong apolar interactions probably occur in these films. In contrast, the π -A isotherm of succinyl β -casein shows no expansion and a low collapse pressure. Proteins which are strongly aggregated will be more likely to form concentrated films than will monomeric species.

It has been suggested that proteins present at biological interfaces possess unique surface properties²⁸. These might possibly be similar to β -casein in that they would have few tertiary structural restraints rather than a globular conformation. Such proteins, because of their high surface activity, would be the most likely to be found at, and remain at an interface. The higher collapse pressures found for the π -A isotherms of β -caseins modified with long chain acyl groups is reminiscent of the increase in pressure above the collapse pressure of the individual components, found when lipids^{38,43} or detergents⁴⁴ interact with proteins at the air-water interface. It has been proposed that the properties of these complexes are due to the intimate association of lipids and proteins in surface aggregates or mosaics. Such micellar protein aggregates may also occur in the n-hexanoyl and n-decanoyl films at high pressures in the air-water interface. We consider that certain chemically modified proteins at interfaces may display properties closely analogous to those of lipid-protein complexes, so that a study of these single protein models could perhaps clarify the understanding of more involved systems, where such structures and interactions are now thought to be present⁴⁵.

ACKNOWLEDGMENTS

The authors thank Mr. Donald Adams and Mr. Peter Miller for expert technical assistance at all stages of this work. Thanks are also due to Miss J. Greatorex for preparation of the manuscript.

REFERENCES

1. G.I. Loeb, Surface Chemistry of Proteins and Polypeptides, U.S. Naval Research Laboratory, Report 6381 (1965).
2. L.K. James and L.G. Augenstein, Advan. Enzymol., 28 (1966) 1.
3. R. Aschaffenberg, J. Dairy Res., 30 (1963) 259.
4. M.P. Thompson, J. Dairy Sci., 49 (1966) 792.
5. P.D. Hoagland, J. Dairy Sci., 49 (1966) 783.
6. P.D. Hoagland, Biochemistry, 7 (1968) 2542.
7. R.G. Wake and R.L. Baldwin, Biochim. Biophys. Acta, 47 (1961) 225.
8. E.W. Yemm and E.C. Cocking, Analyst, 80 (1955) 209.
9. A. Gounaris and G.E. Perlmann, J. Biol. Chem., 242 (1967) 2739.
10. H.J. Trurnit, J. Colloid Sci., 15 (1960) 1.
11. H.B. Bull, Adv. Protein Chem., 3 (1947) 110.
12. P. Joos, Mededel Koninkl Vlaam. Acad. Welenschap Belg., 30 (1968) 3.
13. J.T. Pearson and A.E. Alexander, J. Colloid Interface Sci., 27 (1968) 53.
14. T. Yamashita and H.B. Bull., J. Colloid and Interface Sci., 24 (1967) 310.
15. K. Hamaguchi, Bull. Chem. Soc. Japan., 31 (1958) 123.
16. J. Mitchell, L. Irons and G.J. Palmer, Proc. 5th Intern. Congr. Surface Activity, Barcelona, 1968, in press.
17. P.R. Mussellwhite and G.J. Palmer, J. Colloid Interface Sci., 28 (1968) 168.
18. L.G. Augenstein and B.R. Ray, J. Phys. Chem., 61, (1957) 1385.
19. D.F. Cheeseman and H. Schuller, J. Colloid Sci., 9, (1954) 113.
20. T. Yamashita and H.B. Bull, J. Colloid Interface Sci., 27 (1968) 19.
21. T.A.J. Payens and B.W. van Markwijk, Biochim. Biophys. Acta, 71 (1963) 517.

22. B.E. Davidson and F.J.R. Hird, Biochem. J., 104 (1967) 473.
23. T.T. Herskovits, Biochemistry, 5 (1966) 1018.
24. J.A. Gordon, J. Biol. Chem., 243 (1968) 4615.
25. R. Pion, J. Garnier, B. Dumas, P.J. de Koning and P.J. van Rooyen, Biochem. Biophys. Res. Commun., 20 (1965) 246.
26. R.J. Hill and R.G. Wake, Nature, 221 (1969) 635.
27. C.C. Bigelow, J. Theoret. Biol., 16 (1967) 187.
28. G. Camejo, G. Colacicco and M. Rapport, J. Lipid Res. 9, (1968) 562).
29. S. Beychok and R.C. Warner, J. Am. Chem. Soc., 81 (1959) 1892.
30. J.F. Foster, in F.W. Putnam, The Plasma Proteins, Vol. 1., Academic Press, New York, 1960, p.179.
31. B. Jirgensons, Arch. Biochem. Biophys., 39 (1952) 261.
32. B.R. Malcolm, Surface Activity and the Microbial Cell, Society of Chemical Industry, London, 1965, p.102.
33. G.I. Loeb and R.E. Baier, J. Colloid Interface Sci., 27 (1968) 38.
34. T.L. McMeekin, The Proteins, 2 (1954) 389.
35. M.T.A. Evans, and L. Irons, to be published.
36. C. Tanford, J. Am. Chem. Soc., 84 (1962) 4240.
37. I. Langmuir and D.F. Waugh, J. Am. Chem. Soc., 62 (1940) 2771.
38. T.A.J. Payens, Biochim. Biophys. Acta, 38 (1960) 539.
39. H.J. Trurnit, Arch. Biochem. Biophys., 51 (1954) 176.
40. F. MacRitchie and A.E. Alexander, J. Colloid Sci., 18 (1963) 453
41. J. Mitchell, L. Irons and G.J. Palmer, Biochim. Biophys. Acta., submitted for publication.
42. M. Demeny, S. Kochwa and H. Sobotka, J. Colloid Interface Sci., 22 (1966) 144.

43. G. Colaccico, J. Colloid Interface Sci. 29 (1969) 346.
44. I. Blei, Molecular Association in Biological and Related Systems, Advances in Chemistry series 84 (1968) 149.
45. J.M. Stein, Molecular Association in Biological and Related Systems, Advances in Chemistry series 84, (1968) 259.

THE INTERACTION OF CALCIUM WITH MONOLAYERS OF STEARIC AND OLEIC
ACID¹

Jon Goerke², Helen H. Harper, and Michael Borowitz

Cardiovascular Research Institute and Department of Medicine, University of California Medical Center, San Francisco, California 94122

ABSTRACT

The interaction of monolayers of stearate and oleate with Ca^{++} and H^+ have been studied in a Tris-buffered system where trans-surface potential (ΔV) and surface accumulation of Ca^{45} per mole lipid (θ) have been studied. ΔV -area data suggest that the orientation of the carbonyl dipole is the same for both lipids when the monolayers are close-packed. θ is higher for stearate than for oleate at bulk calcium concentrations in the range 10^{-7} to 10^{-4} M, but for both lipids it is far greater than would be expected from a simple mass-law relationship using the bulk affinity constant. Both the titration curves and the Ca^{45} accumulation data can be fitted reasonably well by a Donnan model which takes monolayer charge into account.

INTRODUCTION

The surface chemical properties of fatty acid monolayers have been the subject of many studies, largely because these compounds can be obtained in reasonably pure form and are among

1. Supported in part by USPHS grants HE-06285, HE-5251 and FR-00122
2. American Heart Association Established Investigator 1967-1972

the simplest agents known to lower air/water surface tension. This simplicity, while somewhat deceiving, has often been exploited so as to verify a new equation of state for the surface. Another group of studies, this among them, seeks to use such monomolecular arrays of charges as models of cell membranes, in the hope that ionic behavior near these structures will approximate that near the cell. The analysis that follows draws heavily on Danielli (1,2,3) but could as easily have followed the Stern treatment (4).

METHODS

Air/water surface tension, surface area, trans-surface electrical potential (ΔV) and surface beta-radioactivity were monitored in a Langmuir-Wilhelmy surface balance at $24.5 \pm 1^\circ\text{C}$ with Ca^{45} in the subphase and either stearic or oleic acid monolayers on the surface (fig. 1).

Stearic acid, obtained from Applied Science, had a melting point of $70.0 - 70.1^\circ\text{C}$ and showed only trace impurities on gas-

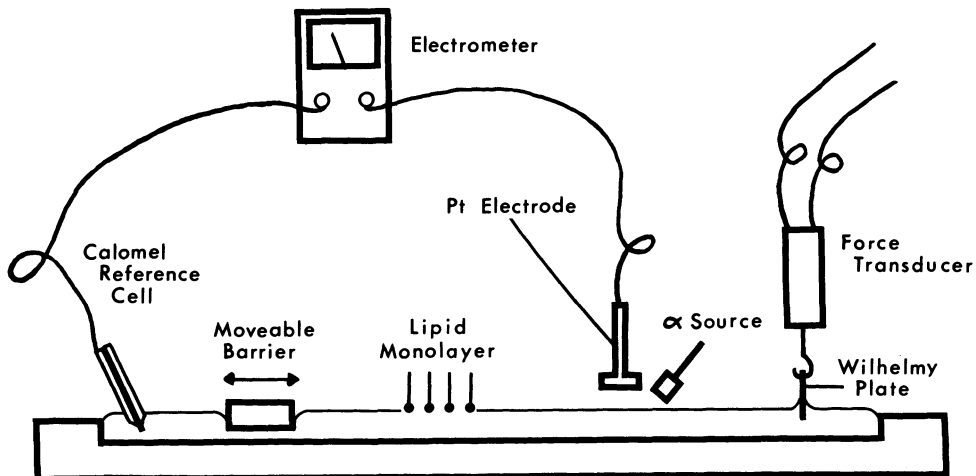


Figure 1. Langmuir-Wilhelmy surface balance.
The Geiger tube for Ca^{45} measurement is not shown, nor is the clean surface "island" for γ_0 measurement.

liquid chromatography (GLC). Oleic acid, melting point 16.4°C, was obtained from Applied Science and had less than 1% impurities by GLC. These lipids were delivered to the air-water surface in 20 to 30 µg amounts from redistilled Hexane solution using calibrated 30 to 50 µl pipettes. pH was set to 6.80 ± .02 or as otherwise indicated using 2 mM Tris buffer (International Chemical and Nuclear Company) titrated with HCl or KOH. Water for solutions was doubly or triply distilled after passage thru a mixed ion-exchange resin.

Ca^{45} , obtained as the chloride from New England Nuclear Corporation at specific activities varying from 11 to 25 c·g⁻¹, was reputedly 99% pure. Cold $\text{CaCl}_2 \cdot 2\text{H}_2\text{O}$ (Baker Analyzed Reagent) was used to vary the subphase Ca concentration. Chemical calcium from both sources was checked by flame photometry and the specific activity of the Ca^{45} was reassayed by the method of Goldstein (5).

The trough for the Langmuir-Wilhelmy surface balance was milled from white virgin teflon securely mounted on 0.5 inch stainless steel leaving inner dimensions of 40 × 10.1 × 0.5 cm. A tightly fitting teflon barrier was motor driven at linear rates of 0.1 cm·sec⁻¹ between measurements for the radioactivity series, and at rates of 0.05 cm·sec⁻¹ (stearate) and 0.1 cm·sec⁻¹ (oleate) for the pH potential-area isotherms. The entire trough and measurement assembly was contained within an electrically shielded enclosure. Barrier position was monitored with a potentiometer linked to the barrier mechanism.

Surface tension was measured by the Wilhelmy method using a roughened platinum plate 4 × 0.5 × 0.015 cm flamed just before use. Force on the plate was determined by a force transducer (Statham model G10B) with amplifier (Sanborn model 311A).

A Radium²²⁶ ionizing electrode (5 µC, U.S. Radium Corp.) was used solely as a removeable alpha-radiation source to ionize the air gap between the surface and a well aged platinum electrode connected to an electrometer amplifier (Keithley model 603). A calomel cell at the other end of the trough acted as the reference electrode. Source and electrode were incorporated in a teflon carriage which could be positioned via a teflon slide either over the experimental solution surface or over an area of the surface isolated by a teflon ring. This latter area could easily be cleaned by aspiration, and surface potential measurements taken over it were used as reference potentials, V_o . The trans-surface potential difference (ΔV) due to the monolayer was then determined by subtracting this clean surface reading from that obtained over the monolayer. V_o was found to vary by as much as 10 mV during a day for aged platinum electrodes and far more for newly made ones.

Prior to each experiment the solution surface was cleaned by aspiration until ΔV was less than 5 mV. The potential titration curves (fig. 3) represent single experiments at each pH.

A Geiger tube (Amperex #18536) and ratemeter (Tracerlab model SC-34) were used to monitor surface beta-radioactivity due to Ca⁴⁵ for 20 minute periods at different values of surface tension. The tube was calibrated for Ca⁴⁵ by summing the readings taken from the surface of a 10 x 10 cm lucite plate which had been sprayed with a Ca⁴⁵ solution and allowed to dry. The plate surface Ca⁴⁵ was subsequently eluted and counted in a liquid scintillation counter to assay the amount of isotope involved. Because of its density, lucite was assumed to give a back-scattering effect close to that of water. It was found that the readings were substantially independent of distance from 0.3 to 0.7 cm over the planar source although tube-to-surface distance was kept constant in all experiments. Surface accumulation of Ca was determined from the difference in counts between the clean solution surface and the monolayer covered surface.

Replicate 50 μ l samples of the mixed subphase were counted in a beta-scintillation counter (Packard model 3003) and used with bare surface radiation counts to determine Geiger tube efficiency for each experiment. Counting vials contained PPO and POPOP in 10 ml toluene, 5 ml absolute ethanol, and 50 μ l IN HCl.

Two separate Ca⁴⁵ experiments were performed at each pCa and the results averaged except for those stearate experiments (fig. 4) employing a concentration range of 4 to 8 Gibbs (4 to 8 x 10⁻¹⁰ Moles.cm⁻²) where single experiments were done. In these last experiments, Ca⁴⁵ uptake was measured at 4 to 6 positions over the lipid covered surface and the average of these readings was used in the calculations.

The four electrical outputs developed as above were appropriately scaled with voltage dividers and led into four channels of a 10 inch multi-point chart recorder (Leeds and Northrup Speedomax W) with sampling time of one second per point. Thus each channel was sampled once every four seconds.

Surface pressure (π) (dyne.cm⁻¹) for any given monolayer was taken to be the difference between the surface tension of the clean air-water interface (γ_0) and the tension of the interface with a monolayer present (γ_m):

$$\pi = \gamma_0 - \gamma_m$$

When an attempt was made to hold monolayers for 20 minutes at pressures exceeding 5 dyne.cm⁻¹ for oleate and 20 dyne.cm⁻¹ for stearate it was found necessary to decrease the trough area

periodically. This was interpreted as a movement of lipid out of the film either into solution, onto the teflon walls and barrier or into a folded configuration. In order to compensate for this phenomenon separate π -A isotherms were obtained at successively faster barrier speeds, starting with $0.025 \text{ cm} \cdot \text{sec}^{-1}$. Several isotherms at the slowest speed giving constant patterns were then averaged to produce reference stearate and oleate isotherms for the full range of calcium concentrations employed. The values of π chosen for obtaining experimental data (1, 2, 5, 10, 20 and 30 dyne \cdot cm $^{-1}$) were then referred to these isotherms to obtain the surface area per molecule of the lipid species. Oleate molecular areas determined in the above manner were used to calculate the upper of the lower pair of curves in figure 5. The lowest oleate curve was calculated using the measured area and weight of lipid applied.

RESULTS

Representative surface tension-area data (fig. 2) has been plotted as π versus molecular cross-sectional area. The smallest area obtainable for oleate just prior to film collapse is seen to exceed that for stearate, presumably reflecting both the inclination of the oleate hydrocarbon chain enforced by its 9-cis double bond and the tendency of such a rotating structure to sweep out larger areas. While there were minor changes in oleate isotherms with increasing bulk calcium (C_{ab}), there was a rather marked condensation of stearate isotherms in the 1-20 dyne \cdot cm $^{-1}$ region as has been reported by other authors (6). Figure 2 shows two typical isotherms obtained at pC_{ab} of 7 and 3.

Trans-surface potential (ΔV) measurements have been expressed in terms of the effective surface dipole moment. ΔV is commonly thought to be the sum of a number of components (3), the most important of which are due to the average electrostatic potential (Ψ_o) and the average vertical component of the permanent molecular dipole (μ)

$$\Delta V = \Psi_o + \frac{12\pi\mu}{A} \quad (1)$$

In equation 1 mixed units have been used for convenience: ΔV and Ψ_o will be in millivolts if μ is expressed in milliDebyes and A in A^2 . After multiplying both sides by $A/12\pi$ we equate the left hand side with μ' .

$$\mu' = \frac{\Delta V A}{12\pi} = \frac{\Psi_o A}{12\pi} + \mu \quad (2)$$

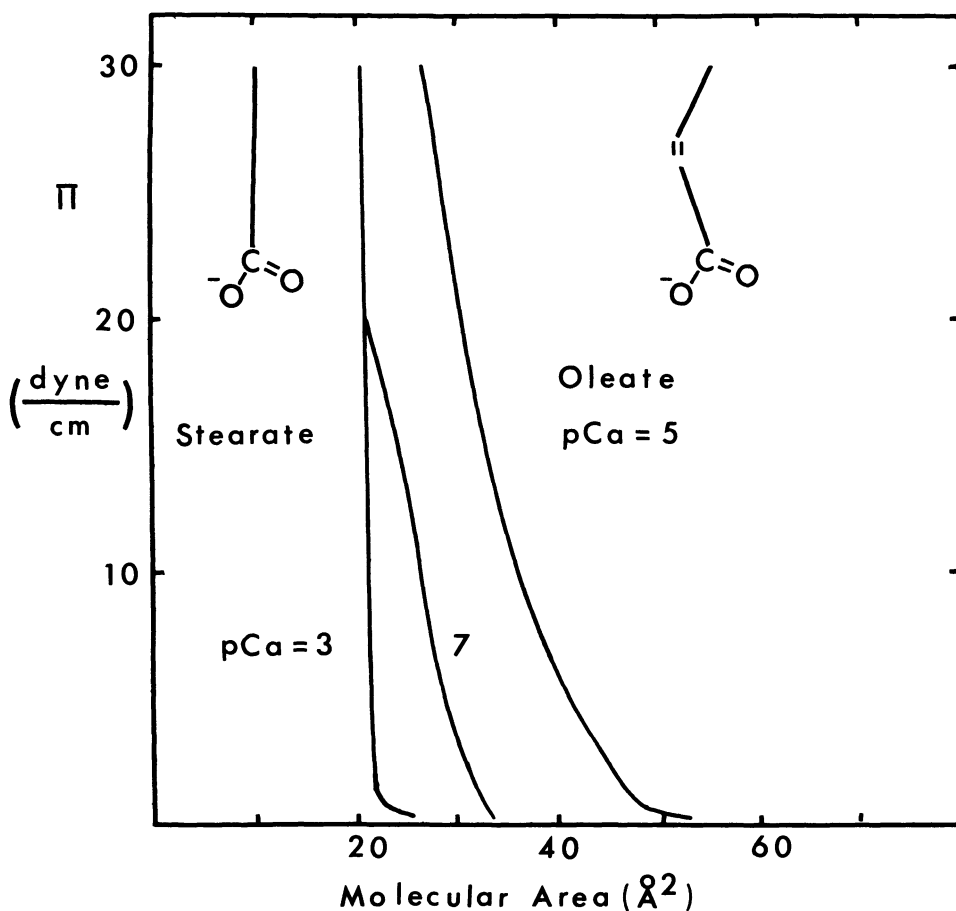


Figure 2. Pressure-Area isotherms.

The larger molecular area of oleate is evident as is the lowering of π in stearate monolayers by the addition of Ca.

μ ought to be nearly identical for both lipids, hence at low pH where ionization is suppressed, stearate and oleate values for μ' should be identical if polar group orientation is the same. Figure 3 shows titration data for the range pH 2-11 at high surface pressures where the molecular orientations would be best defined. At the acid end of both data sets μ' approaches +200 mD which agrees well with the figure of 210 mD given by Goddard and Ackilli (6) for stearate.

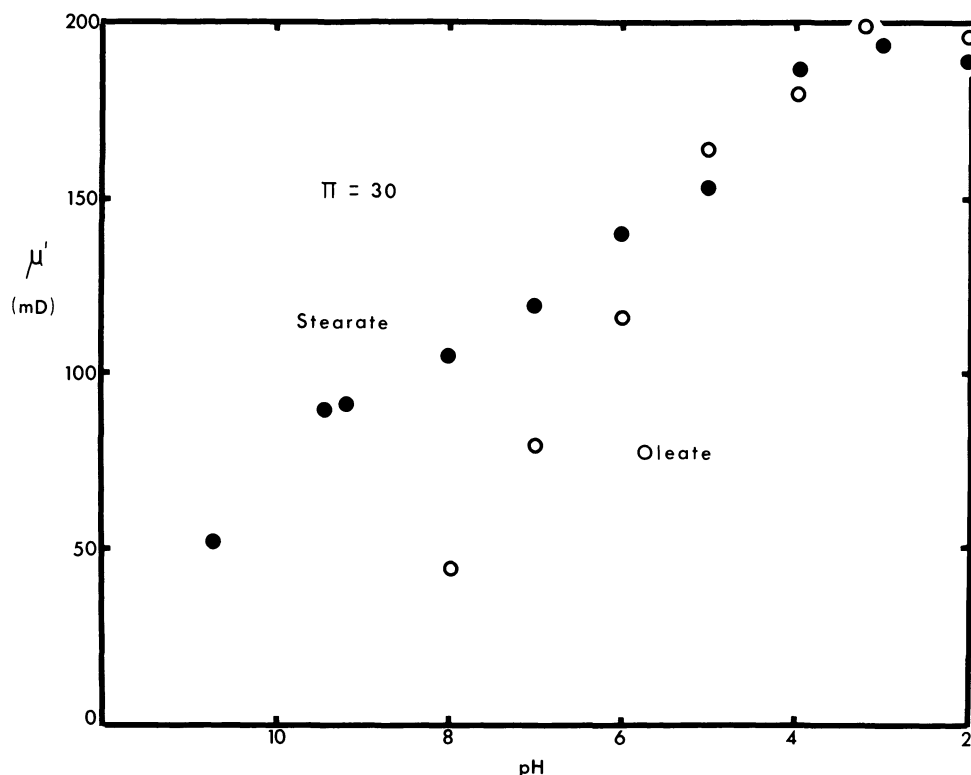


Figure 3. Potential curves.

$\mu' \equiv \frac{\Delta V}{12\pi} A$. 2 mM Tris buffer was titrated with KOH or HCl.

Equal values at pH 2 presumably reflect the vertical component of permanent dipole terms.

At higher pH with increased ionization μ' decreases and for oleate seems to become negative in this system. If the value of 200 mD at pH 2 were due solely to the rather strong carbonyl dipole (2300 mD), then its oxygen would appear to be inclined downwards approximately 5° from the horizontal. The rapid decline of stearate ΔV at pH somewhat greater than 9 was also observed by Goddard and Ackillii and by Spink (7).

Data from Ca^{45} uptake measurements has been expressed using the ratio (θ) of excess surface Ca per unit area to the total applied lipid per surface area. The effect of merely increasing surface lipid concentration is thereby normalized out. Figure 4 is a plot of θ versus lipid concentration (L_s) in Gibbs lipid, and

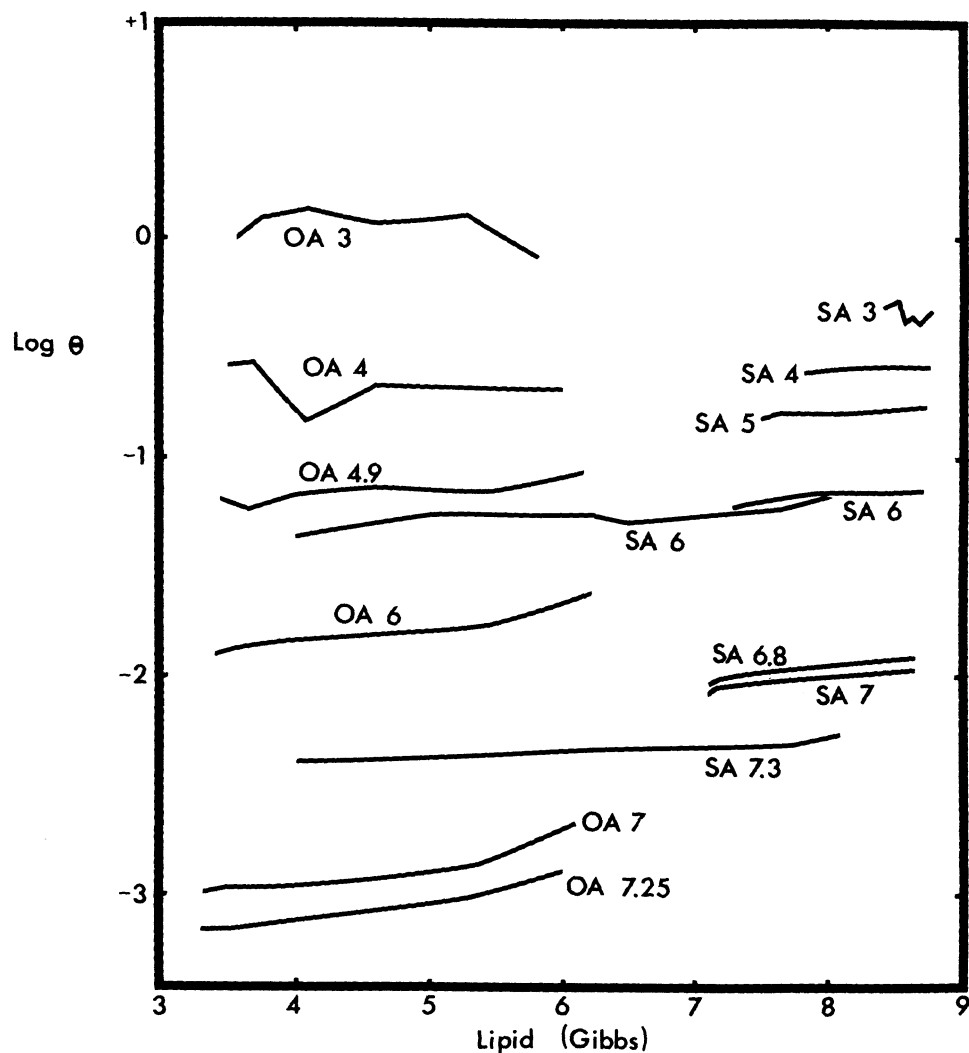


Figure 4. Log (calcium/lipid surface ratio) versus surface lipid concentration. OA = oleic acid, SA = stearic acid, numerical values adjacent to curves are bulk pCa. $\theta = 0.5$ seems to be the limiting value for stearate.

shows the strong dependence of θ on pCa for both stearate and oleate. In the range of L_s studied there was a tendency for θ to increase as the monolayers became more concentrated. At comparable values of L_s and for the lower range of calcium concentrations, θ was appreciably higher for stearate than for oleate. At higher calcium concentrations however, the reverse appeared to be true, although the dispersion of oleate data at the low specific activities used in these runs renders this finding less significant.

In those stearate experiments where Ca^{45} uptake was measured at low L_s there was a considerable variation of counting rates: at 4 Gibbs the area most remote from the spreading region had no increase in activity whatsoever whereas another area had 5 times the clean solution count. Since the physical diameter of the Geiger window was 2 cm and the pattern was stable for over an hour, this was taken as evidence of the presence of large "islands" of stearate in the surface. The effect was still present but markedly diminished at $\pi = 5 \text{ dyne} \cdot \text{cm}^{-1}$.

Figure 5 is a graph of $\log(\theta/(1-\theta))$ versus $p\text{Ca}_b$ for stearate and oleate near the lower limits of their cross-sectional areas. Curves at other surface pressures were similarly shaped.

DISCUSSION

These experiments illustrate the markedly increased affinity of fatty acids for calcium and hydrogen ions when these lipids are arrayed in monolayers. Figure 6 reproduces the stearate potential data with superimposed theoretical curves. The steeper right-hand curve, reminiscent of bulk titration curves, is an attempt to predict μ' from the bulk dissociation constant for long chain fatty acids, ignoring any effect the monolayer field might have on counter-ion distribution. Using a K_a of 1.1×10^{-5} (8) to determine surface charge density σ in $\text{esu} \cdot \text{cm}^{-2}$ one can calculate

Ψ_o in statvolts from

$$\Psi_o = \frac{2 kT}{Ze} \sinh^{-1} \left(\frac{\sigma}{c_i T/2} \left(\frac{500 \pi}{DRT} \right)^{1/2} \right) \quad (3)$$

which is the potential in the plane of monolayer head groups relative to the bulk phase as developed by Gouy (9) and Chapman (10). c_i is the ionic strength in $\text{moles} \cdot \text{l}^{-1}$, e is the electronic charge and the other terms have their usual meanings. μ' was calculated from equation 2 using $\mu = 194 \text{ mD}$, the maximum value obtained with this data set. It should be noted that the Gouy-Chapman relation has been used solely to relate surface charge to potential and that the usual Boltzmann counter-ion double layer distribution has been specifically omitted. This simple approach to the problem indicates that either our value K_a is a gross overestimate or our analysis has excluded an important force peculiar to the arrangement

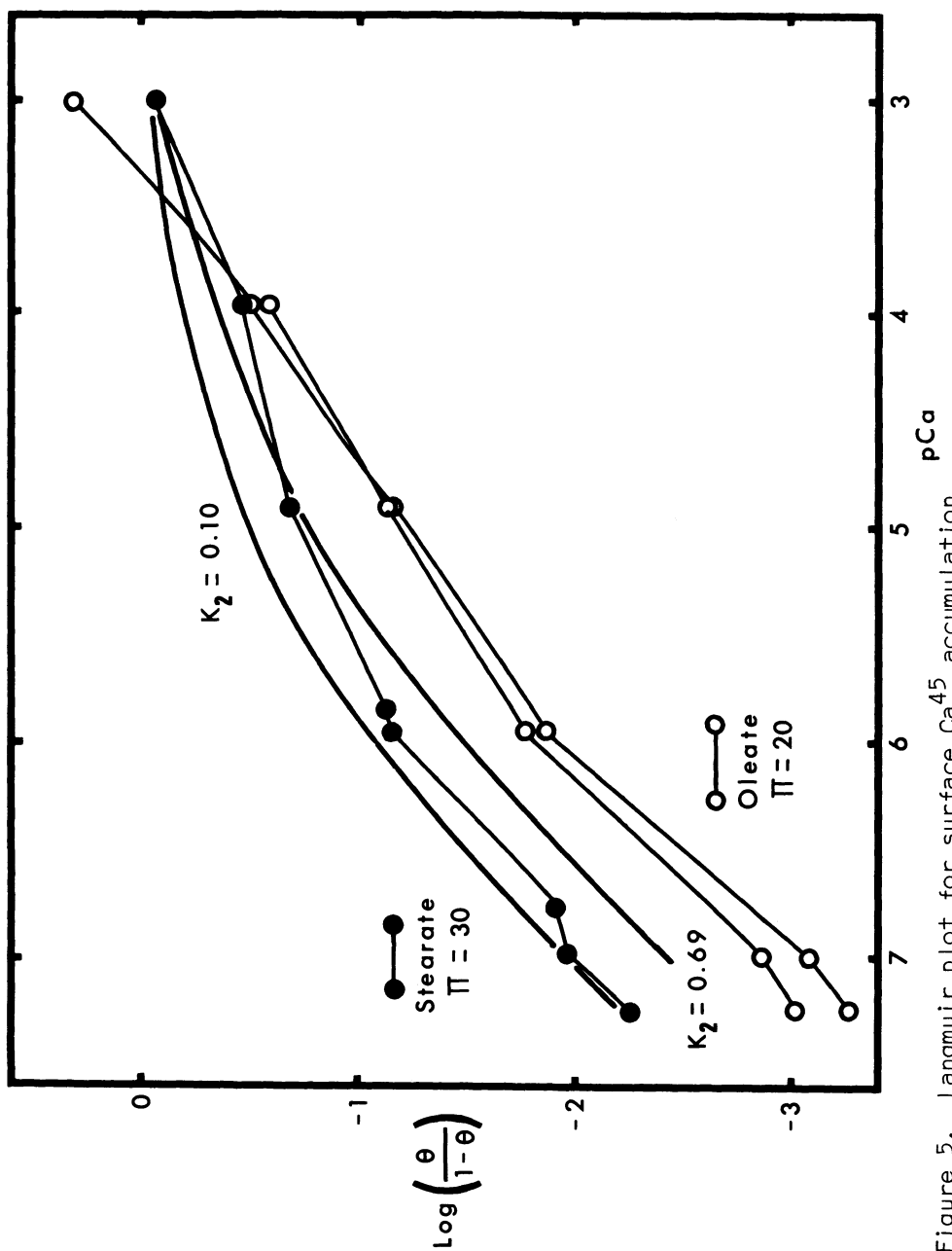


Figure 5. Langmuir plot for surface Ca^{45} accumulation.

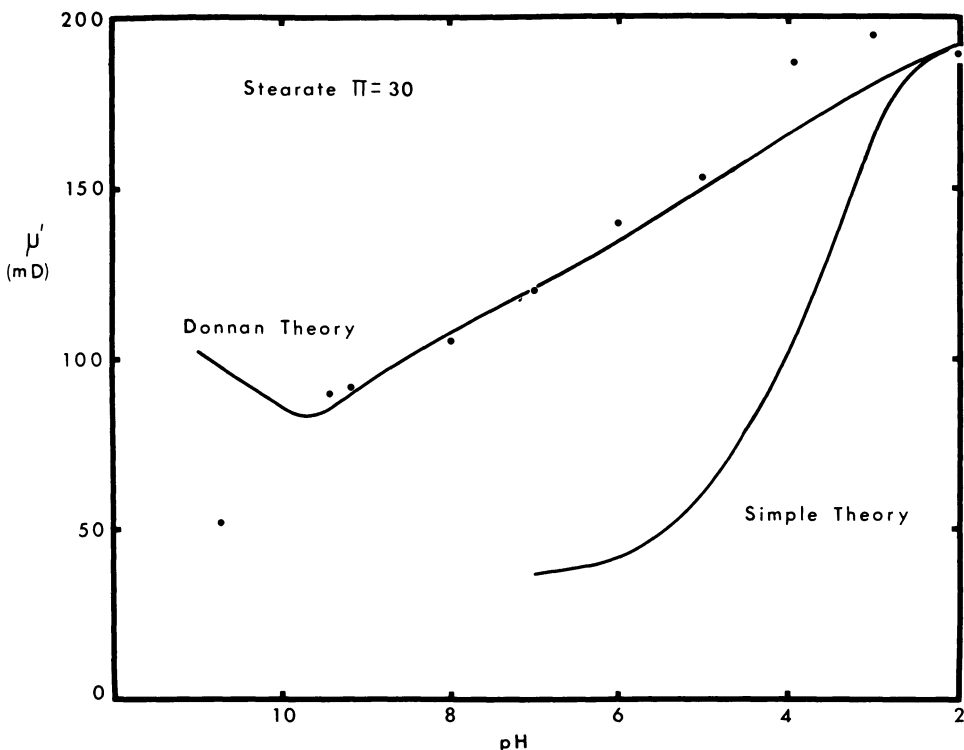


Figure 6. Stearate potential titration.

Curve at right uses Gouy potential Ψ_0 , ignoring Boltzmann distribution of counter-ions. Curve at left uses Donnan potential and counter-ion distribution.

of carboxyl groups in a monolayer. The importance of such a monolayer array of charge can be shown by including it in a model to predict surface potential or μ' . In the subsequent Donnan analysis the solution is considered to have two phases, bulk and surface, with the lipid head groups restricted to the surface phase. The thickness of this latter phase is taken arbitrarily as the Debye-Hückel distance $1/\kappa$ with

$$\kappa^2 = \frac{4\pi e^2}{kT} c_i$$

where c_i is the bulk ionic strength. In the pH range of these experiments $1/\kappa$ varied from 28 to 438 Å. Using the usual Donnan relations as in equation 4, surface phase electroneutrality and the K_a given above for lipid and surface phase hydrogen ions

$$\frac{\text{Tris}_s^+}{\text{Tris}_b^+} = \frac{\text{OH}_b^-}{\text{OH}_s^-} = \left(\frac{\text{Ca}_s^{++}}{\text{Ca}_b^{++}} \right)^{1/2} \quad \text{etc. (4)}$$

(H_s^+) , one obtains a third degree equation in H_s^+ which can be solved numerically using different values of bulk hydrogen (H_b^+) and L_s . L_s was set equal to 5.3 Gibbs for a representative close-packed oleate curve and to 8.3 Gibbs for stearate. With an assumed maximum of $\mu' = 194$ mD the smooth curve at the left of figure 6 is a good representation of the data, particularly in the midrange. The same simple and Donnan analyses for oleate are shown in figure 7. The fit is less good here, perhaps due to the instability of oleate monolayers at alkaline pH or more probably to the change of μ with film expansion.

The Donnan treatment can also be applied to the interaction of Ca with lipid monolayers. Considering first a simpler analysis which ignores surface electrostatic forces, one can calculate an apparent affinity constant K for Ca and lipid from:



Using $\theta = \text{CaL}/L_T$ (where CaL is the total excess of calcium per unit area in the surface as measured, say, by the Geiger tube, and L_T is the total lipid per unit area) one can easily show that

$$\log \left(\frac{\theta}{1-\theta} \right) = \log K - p\text{Ca}$$

By fitting the data of figure 5 from pCa 7 to 6 to this relation one obtains for oleate $K_{OA} = 1 \times 10^4$, and for stearate $K_{SA} = 8 \times 10^4$. From other considerations Danielli (2) gives the comparable bulk lipid-calcium affinity constant as 1.45. Again, this disparity can be largely explained by considering the "surface" calcium in a Donnan model to be composed of an ionized surface phase component (Ca_s^{++}) and a lipid-bound component (CaL^+) having an affinity constant $K = 1.45$ in equilibrium with Ca_s^{++} . With the same considerations as above for the hydrogen binding case including the same value of K_a one can obtain a fourth degree equation in Ca_s^{++} . Solving this numerically yields the lower smooth curve in figure 5 where $\text{Ca}_s^{++} + \text{CaL}^+$ has been used to calculate the surface excess of Ca and hence θ . K_2 values given in figure 5 represent dissociation of CaL^+ and are the reciprocals of the above affinity constants. By arbitrarily increasing K to 10, one obtains the upper smooth curve which fits the extremes of the stearate data better.

Nowhere in the foregoing analysis has there been a suggestion as to why stearate can attract more Ca to the surface than can oleate. The data at hand do not allow strict determination of

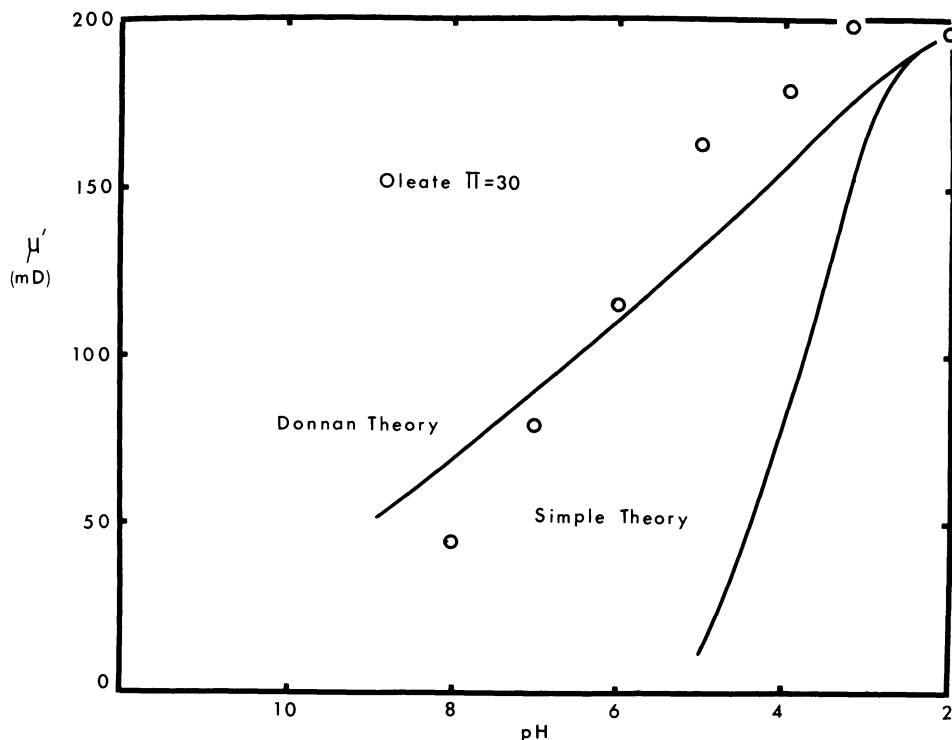


Figure 7. Oleate potential titration.
Curves calculated as for Figure 6.

μ at pH 6.8 for either acid, and hence a difference in Ψ_0 cannot be invoked as the cause. The presence of islands would be expected to enhance surface accumulation, but of course only at low L_s . At pCa 6 for example, one can predict only a 30% enhancement of θ in a Donnan calculation. Perhaps there is a real increase in binding through coordination as suggested by Deamer and Cornwell (11).

These demonstrations of the power of negative surfaces are quite relevant to biology, where for instance cell membranes and intracellular membranes composed of charged phospholipids, fatty acids and proteins abut the aqueous environment. Any consideration of the interaction of charged species in the aqueous phase with a membrane containing charged groups must therefore consider the effect of charge array in addition to the usual group affinity constants.

We wish to express our thanks to Professor John A. Clements for his interest and advice, and to Miss Sarah Jones and Mrs. Lynne Kalnasy for technical assistance.

BIBLIOGRAPHY

1. Danielli, J.F., Proc. Roy. Soc. Lond., Ser. B, 1937, 122, 155.
2. Danielli, J.F., J. Exptl. Biol., 1944, 20, 167.
3. Danielli, J.F. and J.T. Davies, Adv. in Enzymology, 1951, 11, 35.
4. Stern, O., Z. Elektrochem., 1924, 30, 508.
5. Goldstein, G., Nucleonics, 1965, 23, 67.
6. Goddard, E.D., and J.A. Ackillli, J. Coll. Sci., 1963, 18, 585.
7. Spink, J.A., J. Coll. Sci., 1963, 18, 512.
8. Garvin, J.E., and M.L. Karnovsky, J. Biol. Chem., 1956, 221, 211.
9. Gouy, M., J. de Phys., Ser. 4, 1910, 9, 457.
10. Chapman, D.L., Phil. Mag., 1913, 25, 475.
11. Deamer, D.W., and D.G. Cornwell, Biophys. Acta, 1966, 116, 555.

STUDIES OF THERMAL TRANSITIONS OF PHOSPHOLIPIDS IN WATER: EFFECT
OF CHAIN LENGTH AND POLAR GROUPS OF SINGLE LIPIDS AND MIXTURES*

Morris B. Abramson

The Saul R. Korey Department of Neurology, Albert
Einstein College of Medicine, Bronx, New York

ABSTRACT

Several phospholipids and mixtures of phospholipids in water-rich systems were studied by differential thermal analysis and polarized light microscopy. Sharp transition temperatures were observed for all lipids which were single molecular types. This transition is associated with the melting of the hydrocarbon chains and formation of the liquid crystalline form. For mixtures of lecithin of different hydrocarbon chain lengths, the transition temperature range was broadened and increased with the concentration of the long chain component. The transition temperatures of a series of lipids, which had the same hydrocarbon chains but different polar groups, phosphatidyl ethanolamine, N,N-dimethyl phosphatidyl ethanolamine, and lecithin, were lowered as the methylation of the amine increased. Mixtures of lecithin and phosphatidyl ethanolamine with the same hydrocarbon chains showed that the transition temperature of the phosphatidyl ethanolamine is lowered by the presence of lecithin and in some compositions two transition temperatures were observed. The mixing of an acidic lipid, dicetyl phosphoric acid, with lecithin showed that small concentrations of the acid lower the transition temperature of lecithin. At concentrations of the acid above 21 mole percent, the transition temperature of dicetyl phosphoric acid is observed.

*This work was supported by Multiple Sclerosis Grant 503A and U.S. Department of the Interior, Office of Saline Water Grant 14-01-0001-1277.

INTRODUCTION

Several recent investigations have indicated the value of thermal studies as another method for obtaining knowledge of the ultrastructure of biologic systems. Interesting investigations of the membranes of Mycoplasma laidlawii were made by Steim and co-workers (1969) who used differential scanning calorimetry to show the effect of fatty acid content on the thermal transitions of these biomembranes. Other thermal studies gave information on the organization of lipids in ox brain myelin and of the lipids of human erythrocyte ghosts (Ladbrooke et al., 1968a,b).

The success of these studies rests in good measure on the establishment of sufficient information concerning the thermal properties of relatively simple systems containing compounds important in biologic structures. Some of these properties for phospholipids are described in other publications (Chapman et al., 1966, 1967; Ladbrooke et al., 1968c). Since knowledge of the properties of phospholipids in water-rich systems is of major significance toward the understanding of biomembranes, the present paper describes some of the thermal transitions of lipid-water systems as observed by differential thermal analysis (d.t.a.) and microscopic studies. Synthetic lipids are used in which the hydrocarbon chain structures as well as the polar groups are of one type. These well-defined compounds have characteristic and sharp transition temperatures which may be used as indicators to gain an insight into the inter-relationships of lipids in mixed systems.

EXPERIMENTAL

Materials

The lipids used in this study came from the following sources: L-2,3-dipalmitoyl lecithin, L-2,3-dipalmitoyl phosphatidyl ethanolamine, L-2,3-dipalmitoyl-glycerine-1-phosphoryl N,N-dimethyl ethanolamine, L-2,3-dihexadecyl-glycerine-1-phosphoryl choline, L-2,3-dihexadecyl-glycerine-1-phosphoryl ethanolamine, and lysolecithin from Mann Research Laboratories, New York. Dicetyl phosphoric acid was from K and K Laboratories, Plainview, New York. L-2,3 dimyristoyl lecithin was a gift from Professor Eric Baer. Egg lecithin obtained from Sylvana Company, Milburn, New Jersey was purified by silicic acid chromatography. All lipids used gave single bands on thin layer chromatograms.

Mixed lipid systems were prepared by weighing the solids into a small test tube so that 7-10 mg total solid was present. This was dissolved in 1 ml chloroform-methanol (2:1 by volume) and mixed thoroughly. The solvent was evaporated in a stream of nitrogen and the tube was then kept in vacuum overnight. Removal of all solvents was checked by reweighing the tube and its contents. Single lipid systems were prepared from 7-8 mg weighed into a small test tube. Dispersions were prepared by adding 0.1 ml redistilled water and crushing the solid particles in water with a small spatula. After standing for 2 hours, the solid was crushed again and the suspension mixed vigorously in a cyclo-mixer. This was repeated after a second 2 hour period. After standing overnight at 4° the systems were mixed again and forced repeatedly through a narrow-tipped pipette until no large aggregates were visible.

Thermal Analysis

Differential thermal analyses were performed using the DuPont 900 Thermal Analyzer. Samples of 25 μ l of the mixed suspension containing 7-10% lipid were transferred by pipette to the 4 mm diameter sample tube. Most of the determinations were at a heating rate of 10°/min and a sensitivity of 0.1°/inch. Powdered silica was used as reference solid. At the completion of the thermal analysis, the system and the heating block were cooled by careful application of dry ice and the heating cycle was repeated to determine reversibility of the changes. In most instances second aliquots of the lipid system were taken and the thermal diagram was repeated. All determinations of single lipid systems were repeated with second preparations of the aqueous dispersion.

Polarized Light Microscopy

Small aliquots of all systems used for d.t.a. studies were viewed in a polarizing light microscope equipped with a Kofler heating stage. The sample on a glass slide was heated from room temperature to 70°C and changes in structure of the lipid aggregates were observed.

RESULTS

In order to interpret the thermal diagrams shown below, several points can be reviewed. An endothermic transition is indicated by a peak in a downward direction. The onset of this transition occurs at the temperature at which the curve shows a

downward departure from the baseline. The transition is complete when the peak is at its lowest point and absorption of heat by the change is complete. Baselines which are not horizontal are common for solids dispersed in liquids. These may result from shifting of the particles with respect to the thermocouple position, change in packing of the solid or other mechanical change.

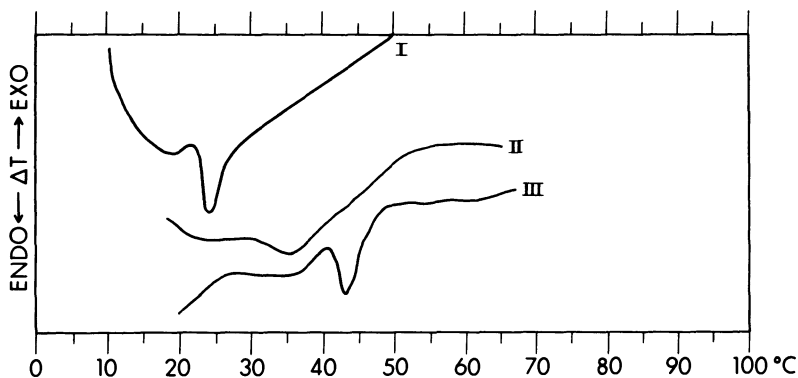


Fig. 1 - D.T.A. diagrams for synthetic lecithins of different hydrocarbon chain lengths and a mixture of two forms of lecithin. Systems contained 7-10% lecithin in water. The peak indicates the transition from the gel to the lamellar liquid-crystalline form.

I L-2,3 dimyristoyl lecithin

II L-2,3 dimyristoyl lecithin 40 mole %
L-2,3 dipalmitoyl lecithin 60 mole %

III L-2,3 dipalmitoyl lecithin

Mixed Hydrocarbon Structures

Thermal diagrams of dimyristoyl lecithin and dipalmitoyl lecithin both show sharp transitions, the former at 23° - 24° , the latter at 41° - 43° . These values are in agreement with the findings of Chapman et al. (1967) who used somewhat more concentrated aqueous mixtures. These changes are attributed to the transition from a gel structure to the lamellar or smectic liquid crystal form. Mixtures of these two forms of lecithin showed transitions over a temperature range varying roughly from 20° to 39° . In Figure 1 the d.t.a. diagrams are shown for aqueous systems of dimyristoyl lecithin, dipalmitoyl lecithin and a mixture of 40 mole percent dimyristoyl and 60 mole percent dipalmitoyl lecithins. In the latter (Curve II), a broad transition range is observed

from 31-38°. This transition at a temperature closer to that of dipalmitoyl lecithin is consistent with the larger percentage of this component in the mixture. Inspection of this system by polarized light microscopy showed the typical spherical structures observed for lecithin systems. These were highly bi-refrinent and did not show any inhomogeneities. The two forms of lecithin appeared to be completely intermixed in these systems and exhibited transition temperatures intermediate between those of the single lipids.

Since egg lecithin is a mixture of compounds that differ in the length and degree of unsaturation of their hydrocarbon chains, it is anticipated that its thermal transitions would take place over a broad temperature range. In Figure 2, Curve I, the d.t.a.

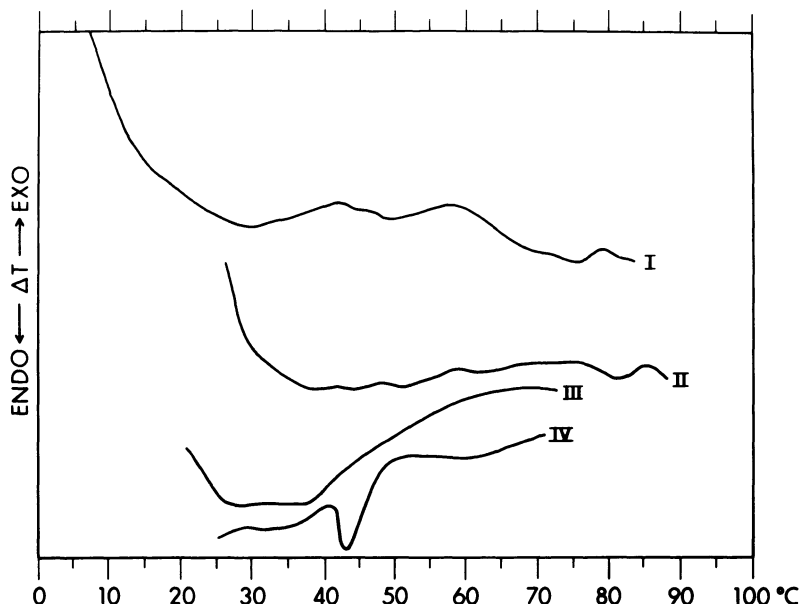


Fig. 2 - D.T.A. diagrams for egg lecithin, dipalmitoyl lecithin and mixtures of these forms of lecithin. Systems contained 7-10% lecithin in water.

I egg lecithin

II egg lecithin 63 mole %
L-2,3 dipalmitoyl lecithin 37 mole %

III egg lecithin 23 mole %
L-2,3 dipalmitoyl lecithin 77 mole %

IV L-2,3 dipalmitoyl lecithin

diagram for egg lecithin in water shows an endothermic change from 10-40° with smaller changes at approximately 50° and 75°. A mixture of 37 mole percent dipalmitoyl lecithin with egg lecithin showed the initial transition beginning at about 22° with a smaller transition at 80°, Curve II. A mixture containing 77 mole percent dipalmitoyl lecithin showed a much reduced transition range from roughly 20-40°. The diagrams for egg lecithin alone and those of egg lecithin with dipalmitoyl lecithin in which the added dipalmitoyl component increased the percent of saturated acyl chains indicate that the different molecular forms of lecithin are intermixed. When the mixture contains a wide range of hydrocarbon chain lengths and degrees of unsaturation the transition is over a broad temperature range. Increasing the presence of one molecular form then brings the transition temperature closer to that of the predominant species.

Mixed Lipid Types

In another series of experiments, mixtures were prepared of dipalmitoyl lecithin and dipalmitoyl phosphatidyl ethanolamine. These compounds are alike in the length and saturation of the hydrocarbon chains. They differ only in the nature of the terminal amino group of the polar moiety of the molecule. The lecithin contains the tri-methyl amine while diacyl phosphatidyl ethanolamine contains the primary amine. The thermal diagrams for three mixtures of these phospholipids are shown in Figure 3, Curves II, III, IV. These diagrams can be compared with the ones for the single compounds, dipalmitoyl lecithin, Curve I and dipalmitoyl phosphatidyl ethanolamine Curve V. In Curve II the peak associated with the transition of dipalmitoyl lecithin (the major component in the mixture) at 40° is present and another smaller and broader peak at 54-56° appears. A mixture of almost equi-molar amounts of the two compounds (Curve III) shows no evidence of the peak at 40° but the peak at the higher temperature is more pronounced and appears at a slightly higher temperature (52-59°) than in Curve II. With a further increase of the phosphatidyl ethanolamine component to 72 mole percent (Curve IV), the peak at the higher temperature is sharply defined, ranging from 53-60.5°. Dipalmitoyl phosphatidyl ethanolamine alone shows a transition from 62-65°.

Polarized light microscopy of these systems showed two types of structures. Lecithin alone gave spherical particles with heavy walls which were highly bi-refringent. Phosphatidyl ethanolamine consisted of amorphous masses, also bi-refringent. At the transition temperature these formed myelin figures in a strikingly sharp transformation. These figures were structures with parallel walls extruded from the amorphous mass. In some

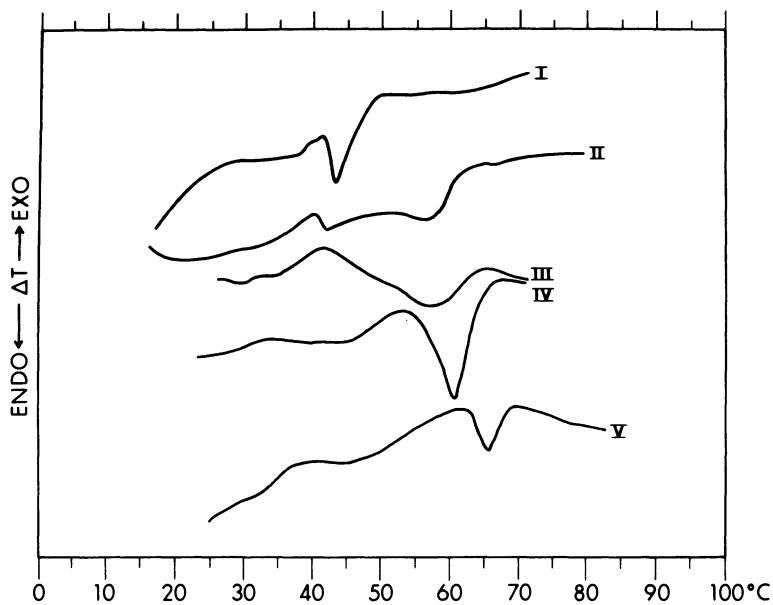


Fig. 3 - D.T.A. diagrams for dipalmitoyl lecithin, dipalmitoyl phosphatidyl ethanolamine and mixtures of these two lipids showing the effect of different polar groups. Systems contained 7-10% lipids in water.

I	L-2,3 dipalmitoyl lecithin	
II	L-2,3 dipalmitoyl lecithin	66 mole %
	L-2,3 dipalmitoyl phosphatidyl ethanolamine	34 mole %
III	L-2,3 dipalmitoyl lecithin	49 mole %
	L-2,3 dipalmitoyl phosphatidyl ethanolamine	51 mole %
IV	L-2,3 dipalmitoyl lecithin	28 mole %
	L-2,3 dipalmitoyl phosphatidyl ethanolamine	72 mole %
V	L-2,3 dipalmitoyl lecithin	- - - -

instances stacked arrays of these structures formed. Mixtures of the two lipids contained both types of aggregates. The temperatures at which they underwent a change differed in the mixed

systems from that observed for the single lipids. At the lower transition temperature the spherical bodies became deformed in shape when in contact with other particles and the walls became thinner.

Addition of Acidic Lipid

The effects of the addition of negatively charged groups of an acidic component were studied in another series of mixtures. In these, dicetyl phosphoric acid was mixed with dipalmitoyl lecithin. Figure 4 shows the thermal diagrams of the single compounds, dipalmitoyl lecithin and dicetyl phosphoric acid, in Curves I and VII respectively. In Curves II, III, and IV in which the mole percent of dicetyl phosphoric acid is 5, 10, and 18%, the transition characteristic of dipalmitoyl lecithin is present but at a slightly lower temperature beginning at 39°. In Curve IV this transition is broadened and extends beyond 50°. A mixture containing 21 mole percent of the acidic component (Curve V) does not show the transition for lecithin but a broad peak beginning at 58° appears. A mixture of 39 mole percent dicetyl phosphoric acid shows a sharp peak at 69° beginning at 65° as in Curve VI. This does not differ greatly from dicetyl phosphoric acid alone with a transition beginning at 67° and exhibiting a peak at 71°.

Figure 5 shows thermal diagrams for related compounds which have specific chemical differences. Curves I, II, and III permit a comparison of L-2,3-dipalmitoyl lecithin, L-2,3-dipalmitoyl-glycerine-1-phosphoryl N,N-dimethyl ethanolamine and L-2,3-dipalmitoyl phosphatidyl ethanolamine in Curves I, II, and III respectively. Each of these compounds shows a single sharp transition temperature. The transition in Curve II beginning at 48° and reaching a peak at 50° is somewhat closer to the related lecithin than to the phosphatidyl ethanolamine. Thermal diagrams were also obtained for L-2,3-dihexadecyl-glycerine-1-phosphoryl choline and L-2,3-dihexadecyl-glycerine-1-phosphoryl ethanolamine. The former shows a sharp peak at 46° beginning at 43° (Curve IV), the latter has a major peak at 69° beginning at 68° (Curve V). A smaller thermal transition occurs from 52-56°. In both these compounds the transition to the liquid crystalline form occurs at a temperature about 3-4 degrees above that for the related diglyceride compound.

The thermal diagrams of another series of mixtures are shown in Figure 6. These mixtures are similar to the ones in Figure 3. They contained dipalmitoyl lecithin mixed with L-2,3-dihexadecyl-glycerine-1-phosphoryl ethanolamine in place of the L-2,3-dipalmitoyl phosphatidyl ethanolamine in the mixtures shown in

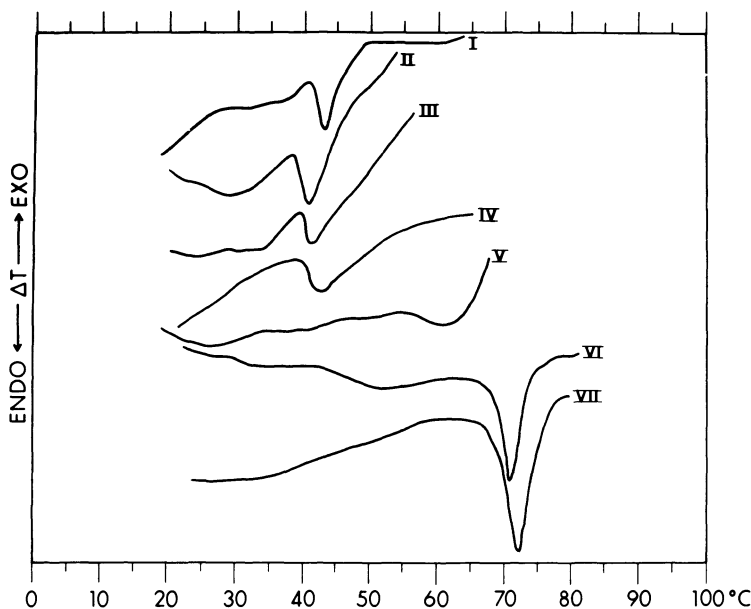


Fig. 4 - D.T.A. diagrams for dipalmitoyl lecithin, dicetyl phosphoric acid and mixtures of these compounds showing the effect of an acidic component. Systems contained 7-10% lipids in water.

- I L-2,3 dipalmitoyl lecithin
- II L-2,3 dipalmitoyl lecithin 95 mole %
dicetyl phosphoric acid 5 mole %
- III L-2,3 dipalmitoyl lecithin 90 mole %
dicetyl phosphoric acid 10 mole %
- IV L-2,3 dipalmitoyl lecithin 82 mole %
dicetyl phosphoric acid 18 mole %
- V L-2,3 dipalmitoyl lecithin 79 mole %
dicetyl phosphoric acid 21 mole %
- VI L-2,3 dipalmitoyl lecithin 61 mole %
dicetyl phosphoric acid 39 mole %
- VII dicetyl phosphoric acid

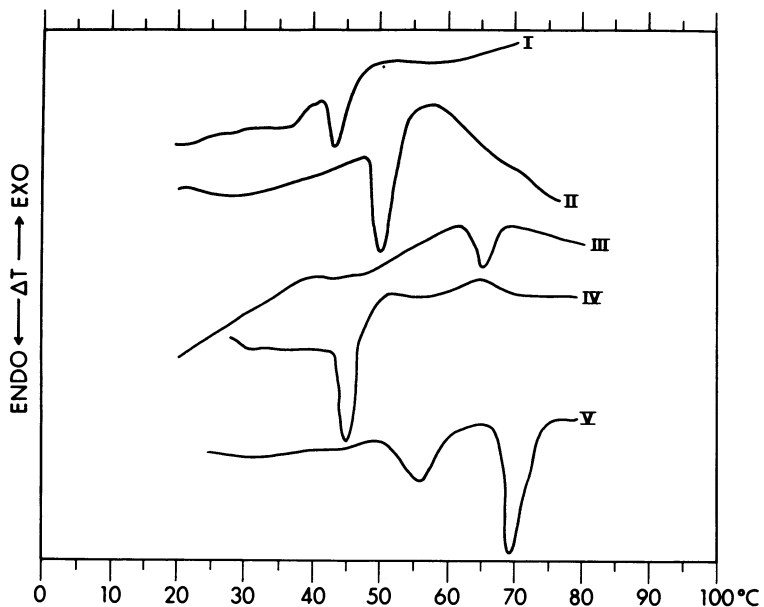


Fig. 5 - D.T.A. diagrams for different phospholipids showing in I, II and III the effect of methylation of the amine and IV, V diether analogues of I and III. Systems contained 7-10% lipids in water.

- I L-2,3 dipalmitoyl lecithin
- II L-2,3 dipalmitoyl-glycerine-1-phosphoryl N,N-dimethyl ethanolamine
- III L-2,3 dipalmitoyl phosphatidyl ethanolamine
- IV L-2,3-dihexadecyl-glycerine-1-phosphoryl choline
- V L-2,3-dihexadecyl-glycerine-1-phosphoryl ethanolamine

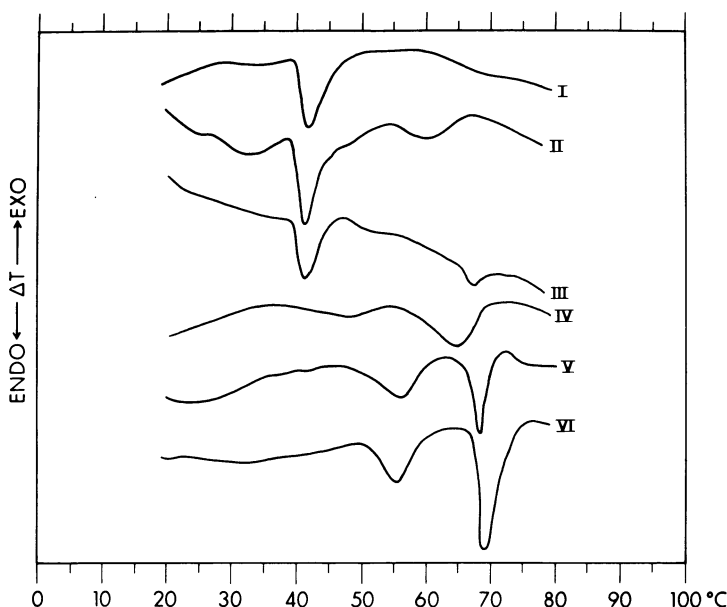


Fig. 6 - D.T.A. diagrams of mixtures of A. L-2,3 dipalmitoyl lecithin and B. L-2,3 dihexadecyl-glycerine-1-phosphoryl ethanolamine showing the effect of mixtures of two different polar groups and diether and diester linkage to glycerine. Systems contained 7-10% lipids in water.

I A - 83 mole %
 B - 17 mole %

IV A - 31 mole %
 B - 69 mole %

II A - 80 mole %
 B - 20 mole %

V A - 16 mole %
 B - 84 mole %

III A - 49 mole %
 B - 51 mole %

VI B - 100 mole %

- - - -

Figure 3. The peak associated with the transition of dipalmitoyl lecithin is evident in Curves I, II and III and in which its concentration decreases from 83 to 49 mole percent. It is not detected in Curve IV where its concentration is 31%. The transition for L-2,3-dihexadecyl-glycerine-1-phosphoryl ethanolamine may be seen in all curves except I. In Curve II this is a broad peak beginning at 56°. In Curve III for the roughly equi-molar mixture the peak is less broad and begins at 65°. Curves IV and V show two peaks which approach the two transitions for the single compound L-2,3-dihexadecyl-glycerine-1-phosphoryl ethanolamine in

sharpness and in temperature. This series compares well with the series shown in Figure 3 in which L-2,3 dipalmitoyl phosphatidyl ethanolamine was present. One difference that may be noted is that the peak for lecithin in the equi-molar mixture is quite definitely present in Figure 6 but not in Figure 3.

Several experiments were performed with mixtures of dipalmitoyl lecithin and lysolecithin which contained 70% C₁₆ chains and 30% C₁₈ chains. Lysolecithin in water showed no sharp thermal transition from 15-80°C. A mixture containing 9.5 mole percent lysolecithin lowered the transition temperature of dipalmitoyl lecithin 2-3 degrees. A mixture containing 26% lysolecithin did not give the same diagram when reheated. Another mixture containing 34% lysolecithin gave a sharp peak at 50° but this was not repeated on the second heating of the sample. Apparently the changes produced by lysolecithin are more complex than those observed in other mixtures of lipids. These will require further investigation.

TABLE I

Major Transition Temperatures	°C
Single Lipids in Water	
L-2,3-dimyristoyl lecithin	23-24
L-2,3-dipalmitoyl lecithin	41-43
L-2,3-dipalmitoyl-glycerine-1-phosphoryl-N,N-dimethyl ethanolamine	48-50
L-2,3-dipalmitoyl phosphatidyl ethanolamine	62-65
dicetyl phosphoric acid	67-71
L-2,3-dihexadecyl-glycerine-1-phosphoryl choline	43-46
L-2,3-dihexadecyl-glycerine-1-phosphoryl ethanolamine	68-69

DISCUSSION

Chapman and his coworkers have shown (Chapman et al., 1967) that synthetic forms of lecithin mixed with 30% or more by weight of water, underwent a mesomorphic transition at temperatures much below the transition temperatures for the anhydrous or the mono-hydrate forms of that lecithin. For aqueous systems of

dimyristoyl lecithin this transition was observed at 23° and for dipalmitoyl lecithin at 41°. At this transition the lecithin changes from a gel structure to the smectic liquid crystalline form. The structural changes involved are the melting of the hydrocarbon chains and penetration of water between the layers of polar head groups of the molecules. In the smectic state the hydrocarbon groups are in a fluid condition with freedom of movement within the bimolecular layers of the liquid crystal. Movement of the molecules within the plane is conceivable, but movement between planes is not possible because the polar groups are bound to water at the interface and quite possibly by intermolecular bonds established between the polar moieties of neighboring molecules. In this form the phospholipids exist in structures resembling biomembranes. The difference in the sharp transition temperatures encountered with myristoyl lecithin as compared with dipalmitoyl lecithin results from the lower temperature required to disrupt the Van der Waals forces between hydrocarbon chains which decreases with the smaller number of CH₂ groups in dimyristoyl lecithin. Mixtures of dimyristoyl and dipalmitoyl lecithin show a transition that takes place over a broader temperature range intermediate between the transition temperatures of the two single lipids. It, therefore, appears that the two forms of lecithin become intermixed with the resulting hydrocarbon layer composed of a mixture of chains melting at temperatures determined by the mole percent of the components. The polar regions immersed in the aqueous layers are the same for the single forms of lecithin and the mixtures. The thermal diagrams for egg lecithin in Figure 2 shows the broad range of melting of the mixture of hydrocarbon moieties present. Egg lecithin contains a high percentage of unsaturated chains which have lower melting points than the corresponding saturated chains. The transition to the smectic form begins at a low temperature. When dipalmitoyl lecithin is mixed with egg lecithin the transition range becomes narrower and approaches that of dipalmitoyl lecithin as its concentration in the mixture increases. This again points to the mixing of the chains of the different forms of lecithin with a resulting transition temperature dependent upon the composition of the hydrocarbons.

When two different lipid types are mixed, it is quite possible that more complex changes take place. In the mixing process as performed in the experiments reported here, several changes may be inferred. These may be complex and many aspects of them have not yet been fully explored. When a lipid is dissolved in chloroform-methanol or other organic solvent, the lipid is either dispersed at the molecular level or in the form of micelles. The micelles in these instances have the polar groups directed away from the solvent. A mixture of two lipids in such a solvent may contain a mixture of molecules or micelles containing a mixture of molecules

or some mixture of micelles. Furthermore, on evaporation of the solvent, differences in the solubilities of the lipids in the solvent may lead to the formation of different forms of solid deposit as the amount of solvent decreases. In the d.t.a. studies of mixed lecithins and phosphatidyl ethanolamine, the endothermic peak characteristic of dipalmitoyl lecithin is seen in Figure 3, Curve II, where it is present in a concentration of 66 mole percent but is not seen in Curve III at 49%, whereas the peak for phosphatidyl ethanolamine is seen in Curve II where its concentration is 34 mole percent and more strongly in Curve III at 51%. This may indicate that the structure established by the phosphoryl ethanolamine in water is more stable than that of phosphorylcholine. The microscopic examination of the systems used for Curves II and III showed two forms of aggregates, the bi-refringent spheres characteristic of lecithin systems and amorphous masses which were found with dipalmitoyl phosphatidyl ethanolamine below the transition temperature. On heating the mixed system the two types of particles showed changes at different temperatures. In all the curves for mixtures of the two lipids, the transition temperature for the dipalmitoyl phosphatidyl ethanolamine is lower than that shown by dipalmitoyl phosphatidyl ethanolamine alone. This presumably results from the incorporation of lecithin molecules into the particles of phosphatidyl ethanolamine which is nevertheless predominant in determining the physical characteristics of the particles when its concentration is greater than some value between the 34 mole to 51 mole percentages of Curves II and III.

Although phosphorylcholine lipids and phosphorylethanolamine lipids are both relatively abundant in biologic membranes, they are not equivalent or interchangeable, each maintaining its unique character. An interesting finding related to this is the work of Tomasz (1968) who showed that ethanolamine can be incorporated in place of choline into the structural components of the cell wall of pneumococcus with resulting changes in cell characteristics. With ethanolamine the cells remain associated after cell division and cannot be lysed as readily as cells containing choline. This difference in the amine groups is further supported by Zull and Hopfinger (1969) who calculated the potential energy fields about the nitrogen atom in choline and ethanolamine. They find that in ethanolamine a stronger potential energy field exists in the region of the nitrogen atom than in choline. This could result in a stronger interaction with anions in inter- or intra-molecular bonding. The higher temperature that is found for the transition to the liquid crystalline form for dipalmitoyl phosphatidyl ethanolamine as compared with dipalmitoyl lecithin, and the persistence of the structure characteristic of the ethanolamine phospholipid over that of the choline phospholipid as shown by the d.t.a. curves of Figure 3 are consistent with the

greater force field at the positive charged sites of the ethanolamine. In Figure 5, the Curves I, II and III show that in the dimethylethanolamine phospholipid the steric effect of the two methyl groups is not as great as the effect in choline and the forces between molecules is intermediate between that of choline and ethanolamine as shown by their transition temperatures. In a parallel sequence in the structure of the pneumococcal cell walls, incorporation of N,N-dimethylamino ethanolamine results in organisms more closely resembling the normal one containing choline than does ethanolamine incorporation (Tomasz, 1968).

The phospholipids of biomembranes are either bi-ionic as lecithin or phosphatidyl ethanolamine or anionic as the phosphoinositides, phosphatidylserine or phosphatidic acid. In recent studies of the permeabilities of model lipid systems the properties of liposomes have been explored. In these liposomes, the addition of an acidic lipid to lecithin permits the formation of lipid aggregates in which membrane-like structures entrap small volumes of aqueous solution (Bangham et al., 1965). The acidic component used is often dicetyl phosphoric acid. The thermal diagrams of Figure 4 show that small concentrations of dicetyl phosphoric acid are incorporated into the structure of dipalmitoyl lecithin and a small lowering of the transition temperature of the lecithin results. When the concentration of the acid reaches roughly 21 mole percent there is no sharp transition and the lecithin is in the liquid-crystal state at a temperature below its normal transition. These experiments do not, however, indicate whether this change results from the presence of negative phosphate groups which disrupt the network of polar groups of lecithin in the aqueous boundary layer or whether it stems from the intrusion of hydrocarbon chains which are not carboxy acid ester linked to glycerine. The appearance of a sharp peak at 65° for a mixture containing 39 mole percent dicetyl phosphoric acid shows the stronger intermolecular bonding of this acid component. Microscopy showed two forms of aggregates in these systems with a large amount of amorphous material which melted at a temperature near 70°. An interpretation of these mixed systems is that two forms of mixed aggregates arise. In one the presence of small amounts of dicetyl phosphoric acid affects the transition of dipalmitoyl lecithin so that it is in the liquid-crystal form over a wide temperature range. The other aggregate contains lecithin incorporated into the dicetyl phosphoric acid structure which has a transition temperature a few degrees lower than dicetyl phosphoric acid alone.

The diagrams shown in Curves IV and V, Figure 5 and Table I permit a comparison of closely related analogs of dipalmitoyl lecithin and dipalmitoyl phosphatidyl ethanolamine whose thermal diagrams are shown in Curves I and III. The compounds which

contain the ether linkage to glycerine in place of the ester linkage exhibit transitions that are much like those of the normal lipid type but at a small increase in temperature. This may be the result of closer packing of the hydrocarbon chains with increased Van der Waals forces in the ether bonded compounds.

In the series of mixtures of dipalmitoyl lecithin with L-2,3-dihexadecyl-glycerine-1-phosphoryl ethanolamine not only are the compounds different in their polar moieties but also in the linkage of the hydrocarbon chain to glycerine. This series of thermal diagrams (Fig. 6) resembles the ones depicted in Figure 3 with some differences. The transition for dipalmitoyl lecithin is present and sharp in the equi-molar mixture with the ether linked ethanolamine lipid but is broadened and at a lower temperature in the mixture with phosphatidyl ethanolamine. It is conceivable that the dipalmitoyl lecithin becomes intermixed with the more closely related phosphatidyl ethanolamine more readily than it does with the somewhat different ether linked ethanolamine analog. The lecithin then loses its structural characteristics and its sharp transition in the equi-molar mixture with phosphatidyl ethanolamine.

Chapman (1966) reviewed some of the biologic significance of the liquid crystalline state of membrane lipids as a result of the studies of the physical properties of lipid systems. It is interesting, although still hazardous, to draw inferences concerning the nature of biomembranes from the results described here for lipid-water systems. In the mixture of lipids found in most biomembranes, it is possible that some of the lipid types could influence the transition from the gel to lamellar form more strongly than other types. This effect would be related to the nature of the polar groups and their interactions with the polar groups of other molecules. In this connection, the mesomorphic transitions of bi-ionic lipids could be strongly influenced by the incorporation of small amounts of anionic lipid. Furthermore, the lipids in biomembranes may not be distributed uniformly through the bilayer but may exist in regions or domains with different compositions and physical characteristics. These associations of lipids would in large measure be determined by the interactions between the polar groups of like and unlike molecules with each other and with water. As seen in some of the thermal diagrams given here, these lipid associations or domains may undergo liquid crystalline transitions at different temperatures. Conceivably, changes in the environment may also influence these regions differently. It is then possible that some microscopic regions of the membrane may be in the fluid smectic state while others remain in the gel form. This could strongly affect the permeabilities of these lipid structures as shown by de Gier et al.

(1969) in studies of the effect of temperature on the permeability of liposomes.

The author is grateful to Dr. W.T. Norton for reviewing the manuscript and Mr. C. Gryte for technical assistance.

REFERENCES

- Bangham, A.D., Standish, M.M., and Watkins, J.C. (1965). J. Mol. Biol., 13:238.
- Chapman, D., (1966). Ann. N.Y. Acad. Sciences, 137:745.
- Chapman, D., Byrne, P., and Shipley, G.G., (1966). Proc. Roy. Soc. London A 290:115.
- Chapman, D., Williams, R.M., and Ladbrooke, B.D., (1967). Chem. Phys. Lipids, 1:445.
- de Gier, J., Mandersloot, J.G., and Van Deenen, L.L.M., (1969). Bioch. Biophys. Acta, 173:143.
- Ladbrooke, B.D., Jenkinson, T.J., Kamat, V.B., and Chapman, D., (1968A). Bioch. Biophys. Acta, 164:101.
- Ladbrooke, B.D., Williams, R.M., and Chapman, D., (1968B). Bioch. Biophys. Acta, 150:333.
- Ladbrooke, B.D., Williams, R.M., and Chapman, D., (1968C). Bioch. Biophys. Acta, 150:333.
- Steim, J.M., Tourtellotte, M.E., Reinert, S.C., McElhaney, R.N., and Rader, R.L., (1969). Proc. Nat. Acad. Sci. U.S., 63:104.
- Tomasz, A., (1968). Proc. Nat. Acad. Sci. U.S., 59:86.
- Zull, J.E., and Hopfinger, A.J., (1969). Science, 165:512.

THE PHYSICAL STATE OF LIPIDS OF BIOLOGICAL IMPORTANCE:

CHOLESTERYL ESTERS, CHOLESTEROL, TRIGLYCERIDE

Donald M. Small⁺

Biophysics Unit, Dept. of Medicine, Boston University

School of Medicine, Boston, Massachusetts

Introduction

Alpha and beta serum lipoproteins and the lipids of the lesions of atherosclerosis contain a large fraction of cholesterol esters. Further, the lipid droplets of the fatty streak of the atherosclerotic lesions are probably nearly pure cholestryl ester. Although there is a vast literature concerning the metabolism (1,2) and transport of cholesterol and its esters, very little is known of the physical state of the biologically important cholestryl esters and even less about the physical state of these esters in mixtures of other naturally occurring lipids. Even more important, the state of these compounds in vivo has not even been studied. While it is true that pure cholestryl esters of saturated fatty acids have been carefully examined (3-7), there has been no report of the state of monounsaturated and polyunsaturated cholestryl esters as a function of temperature. Yet, it is these most important but neglected unsaturated and polyunsaturated esters which make up the bulk of cholestryl esters of biologic or pathologic origin. The purpose of this report is to discuss briefly the physical state of cholestryl esters of saturated, cis monounsaturated and cis polyunsaturated long chain fatty acids. Next, since about 70-80% of the cholestryl esters in α and β lipoprotein (8) and atheromatous lesions (9-12) are cholestryl oleate and cholestryl linoleate a condensed binary phase diagram will be presented to show the physical state of all mixtures of these two esters over a temperature range (0°C to 90°C) encompassing most temperatures encountered by living organisms. Finally, because free cholesterol and triglycerides are also present in very high

+ Markle Scholar in Academic Medicine

concentration in certain lipoprotein fractions (2,8) and possibly in atheromatous plaques (9-12), the interactions of these substances with each other and with cholesteryl esters will be discussed. The specific interrelations will be illustrated using the binary phase diagrams, cholesterol-cholesteryl oleate, cholesterol-triolein and triolein-cholesteryl oleate and the ternary system (3 components) cholesteryl oleate-cholesterol-triolein.

While cholesterol and triglycerides melt from a crystalline form directly to an isotropic liquid, cholesteryl esters behave differently. They form thermotropic liquid crystals (13,14) or mesophases (4). It is well known that many organic substances do not melt simply from a crystalline solid to an isotropic liquid, but melt through a series of mesomorphic phases before finally melting to an isotropic liquid (4,13,14). These mesomorphic phases have been called "liquid crystalline" phases since they have characteristics of both liquids and crystals. The long chained fatty acid esters of cholesterol characteristically show two mesophases, a cholesteric liquid crystalline phase and a smectic liquid crystalline phase. The cholesteric liquid crystal phase forms from an isotropic melt. It has a conic focal texture with a negative sign of birefringence and often exhibits a wide range of reflected colors. The smectic liquid crystalline phase forms from the cholesteric phase. It is more grossly opaque, colorless, and transmits polarized light more intensely than the cholesteric mesophase. The smectic mesophase has a very obvious conic focal texture but the sign of birefringence is positive.

Certain esters (e.g. cholesteryl myristate) have inantiatropic phase transformations (5,6,15), that is, the transitions are reversible and occur either on heating or cooling. However, many of the liquid crystalline phases of other cholesteryl esters are monotropic with respect to a crystalline phase, that is, they have a lower transition temperature than the melting point of the crystal and do not appear when the crystal is melted. They only appear when the melt is cooled below the melting point of the crystal. These monotropic mesophases may be more or less stable. Nearly all of the liquid crystal transitions (Isotropic melt \leftrightarrow cholesteric mesophase; cholesteric mesophase \leftrightarrow smectic mesophase) are perfectly reversible, if they can be supercooled and reheated before crystallization of a true crystal occurs. If however, crystallization occurs to a crystal of higher melting point, no liquid crystalline transformation will form on reheating; the crystal will simply melt to an isotropic liquid. Some of the monotropic mesophases are very stable and remain unchanged for several days or even weeks and months, whereas others are highly unstable and true crystals grow from the liquid crystals within seconds after the phase appears. Although in some cases the monotropic liquid crystals seem to be stable, it would be expected that, with proper nucleating agents and temperature or with long periods of time,

crystals would finally grow from these phases since the crystalline phases with melting points higher than the cholesteric to isotropic transitions are, from the thermodynamic point of view, the most stable state.

Materials and Methods

Materials

Cholesteryl esters of saturated fatty acids of the purest grade were obtained from Eastman Kodak and from Hormel Institute, Austin, Minn. Esters of unsaturated fatty acids were obtained from the Hormel Institute and were judged to be 99% pure with less than 5% trans double bonds. The esters were stored at -4°C in small vials under nitrogen.

Methods

All pure compounds or mixtures of pure compounds were observed grossly, by polarizing microscope, and by differential scanning calorimetry (DSC).

Preparation or Mixtures

Mixtures were prepared by two techniques. 1) Solutions of pure components were made in appropriate organic solvents mixed to give a desired weight proportion and the solvent evaporated under N₂. 2) Pure compounds were weighed directly onto the microscopic slide, melted and mixed by stirring with a small platinum wire. For some of the gross studies compounds were weighed into thick-walled glass tubes melted under a stream of N₂ and sealed. For DSC runs compounds were weighed directly into the DSC pan. A melting curve was obtained and the mixture was allowed to remain well above the melting point for 1 hour to assure mixing. A cooling curve was then obtained. The rest of the DSC procedure is as outlined below.

Microscopic and gross examination of sample. The sample was placed on a clean glass slide and a coverslip was placed over the sample so that one edge of the coverslip came in contact with the slide and the other with a thin (0.16 mm) piece of glass. This arrangement produces a wedge-shaped sample varying in thickness from 0 to 0.16 mm. The temperature of the sample was then raised on the stage of a polarizing microscope fitted with a special heating chamber described previously (16) at about 1-2°/min until the sample melted to the isotropic state. The sample was then cooled at about 1-2°/min and both the gross and microscopic changes were observed. After each phase change the temperature was reversed at a rate of 1°/min to verify the reversibility of the phase change. When all liquid crystalline phase transformations were observed, the sample was allowed to cool slowly to 20°C until crystallization occurred. The sample was then reheated slowly to note the transition temperature of the crystalline phase. Rapid quenching of the sample from the isotropic melt was then performed by placing the sample on an

aluminum block at -20°C or on a piece of dry ice. The sample was reheated and the phase changes noted. Finally, the sample was melted to an isotropic liquid and the entire procedure repeated. Each sample was studied in duplicate.

The changes in gross appearance of the sample were followed by observing the wedge of sample against a black background on a heated stage under a bright light over a wide range of angles of the incident beam. The first evidence of phase change noted in going from isotropic liquid to the cholesteric liquid crystalline phase was often a sudden appearance of a purple or blue color in the thicker part of the sample. Under crossed nicols this phase appeared to be isotropic unless the sample was perturbed by pressing on or moving the coverslip. When perturbed the sample became birefringent. In some cases there appeared to be a change from this apparent isotropic condition (homeotropic) to a fine conic focal texture with an obvious negative sign of birefringence somewhat below the original change from colorless to purple. Grossly a slight turbidity is noted coincident with this change. Gray (5) has previously described these changes for some saturated cholesteryl esters. As the sample is cooled and the cholesteric phase transforms to the smectic phase, an obvious turbidity occurs in the gross specimen and all color is lost. A marked sudden increase in the birefringence occurs to a conic focal texture with an obvious positive birefringence. The accuracy of determining transition temperatures by the gross microscopic methods is limited to $\pm 0.2^\circ\text{C}$.

Differential Scanning Calorimetry. (see Fig. 1) Two to four mg of sample were weighed into an aluminum sample pan on a Kahn Microbalance. This sample was sealed and placed in a differential scanning calorimeter fitted to a DuPont 900 Differential Thermal Analyzer. An empty sealed aluminum sample pan served as the reference standard. A heating curve was obtained at 2.5, 5 or 10°/min until the sample was entirely melted. The sample was then cooled at the same rate until the liquid crystalline phase transformations were observed. The sample was then reheated at the same rate to observe the reversibility of the phase transformations. The sample was then cooled to -50°C and allowed to remain at that temperature for 30 min. A new heating curve was then obtained at 2.5, 5 or 10°C/min until the sample melted. The entire procedure was then repeated. The transition temperature was taken from the intersection of the flat part of the curve with line drawn through the steepest part of the melting curve. Repeated studies on the same sample and different sized samples of the same material showed that the transition temperature of pure materials were accurate to $\pm 0.5^\circ\text{C}$. The transition temperatures in the liquid crystalline state always varied by less than a degree for both heating and cooling, showing the almost perfect reversibility of the liquid-cholesteric and cholesteric-smectic transitions. These temperatures agreed ($\pm 0.5^\circ\text{C}$) with the transitions observed grossly or by microscope.

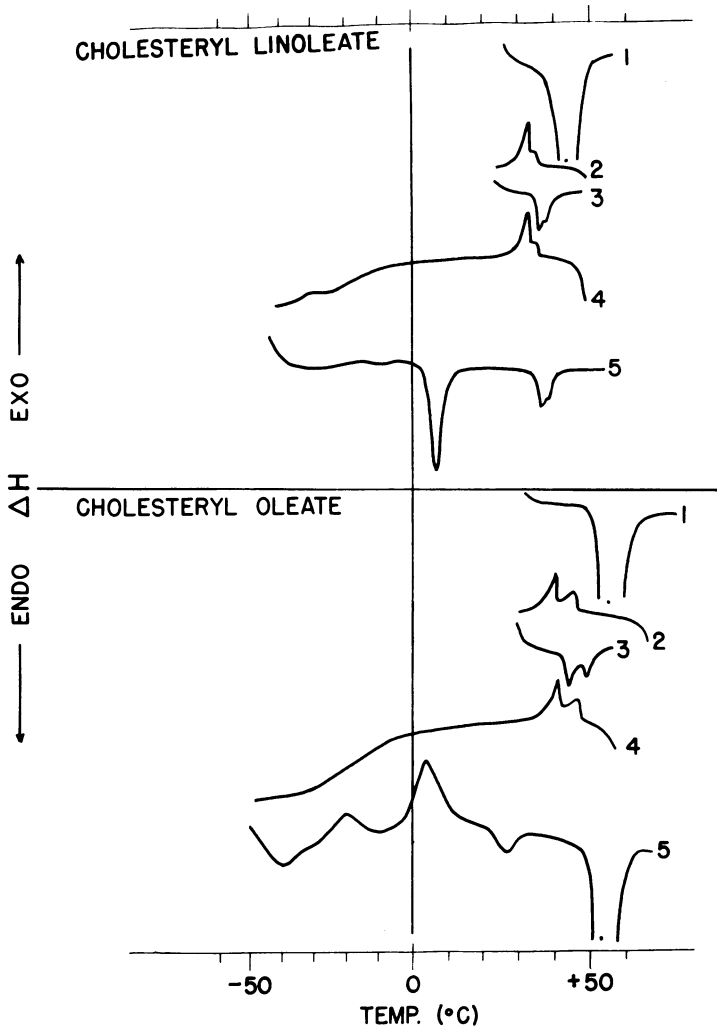


Figure 1. Differential scanning calorimetry curves of cholesteryl linoleate and cholesteryl oleate. Above-cholesteryl linoleate.

1) First heating curve from room temperature; C_1 melts at 42°C.
 2) First cooling curve from melt. Exothermic liquid crystalline transformations at 36.5 and 34°C are present. 3) Reheating from a liquid crystalline state. The liquid crystalline transformations are reversible. 4) Recooling to -50°C. 5) Reheating after 30 min at -50°C. The endothermic peak at 3°C represents the melting of crystalline phase C_2 to the smectic liquid crystalline phase.
 Below-cholesteryl oleate. The numbers 1-5 refer to heating and cooling curves as stated above. Note that C_1 melts at 51°C in both 1 and 5. The liquid crystalline transitions are at 47.5 and 42°C.

The heat of transitions can be calculated from triangulation or planography of the areas under the curves. These heats of transition have previously been reported by Barrall, Porter and Johnson (17) for the liquid crystalline transitions of some cholesteryl esters of saturated fatty acids. Both isotropic to cholesteric and cholesteric to smectic transitions are small, being of the order of 0.5 Cal/gm. These changes are illustrated in Fig. 1. The heats of these two transitions for the unsaturated cholesteryl esters are likewise small, being of the same order as those reported for saturated esters. The cholesteric to isotropic heat of transition is about half that of the smectic to cholesteric.

Results

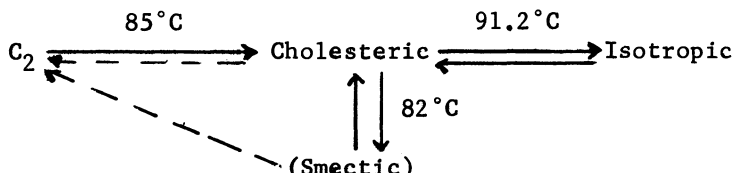
The results will be presented in diagrammatic fashion utilized for instance by Gray (10). The symbols used are the following:

- C_1 = crystal having a melting point higher than the highest liquid crystal transition
- C_2 = crystals having melting point lower than the highest liquid crystal transition
- Cholesteric = cholesteric mesophase
- Smectic = smectic mesophase
- Isotropic = isotropic liquid melt
- () refer to monotropic phases

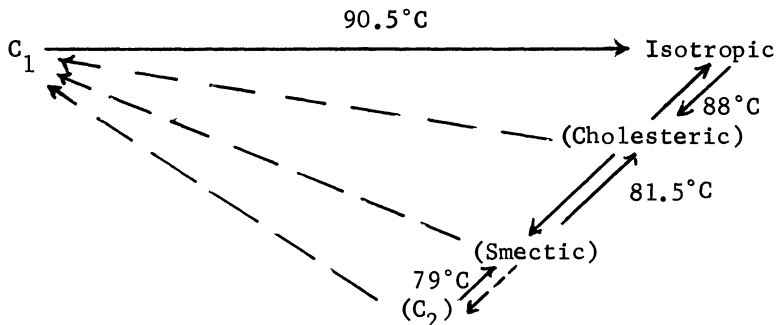
The temperature above or beside the arrow indicates the temperature transition from one state to another. A dotted arrow indicates a transition occurring with supercooling.

Saturated Fatty Acid Esters of Cholesterol

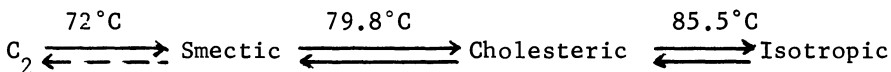
Cholesteryl decanoate



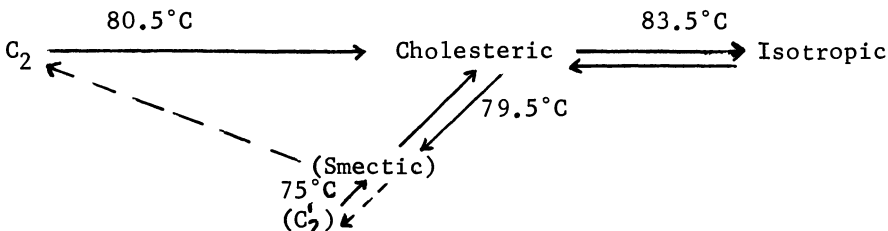
The crystalline form of cholesteryl decanoate (C_2) melts sharply to the cholesteric mesophases at 85°C. The cholesteric mesophase is enantiotropic and melts quite sharply to an isotropic liquid at 91.2°C. On cooling the liquid to cholesteric phase is reversible. Cooling further there is a cholesteric to smectic transformation at 82°C which is also reversible. This monotropic smectic mesophase is quite stable and only after several hours at lower temperatures does C_2 grow from the smectic mesophase.

Cholesteryl laurate (cholesteryl dodecanate)

C₁ melts at 90.5° to an isotropic liquid. On cooling there are transformations to the cholesteric phase at 88° and to a smectic phase at 81.5°. If the sample is allowed to cool quickly a second crystalline form C₂ forms from the smectic mesophase. This crystalline form melts to the smectic mesophase at 79°C. The two monotropic mesophases formed in this system are very unstable and within minutes crystals of C₁ will grow from both the cholesteric and the smectic mesophase. The crystals thus formed (C₁) melt at 90.5°C.

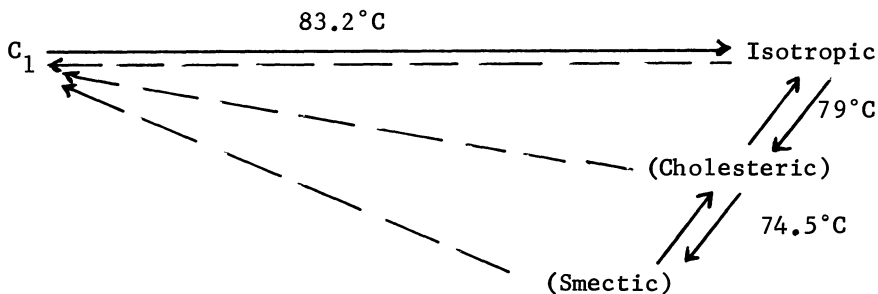
Cholesteryl myristate (cholesteryl tetradecanoate)

Cholesteryl myristate shows two enantiotropic mesomorphic phase transformations. C₂ melts to the smectic phase at 72°C and the smectic phase melts to the cholesteric phase at 79.8°C. The cholesteric phase melts to an isotropic liquid at 85.5°C. The liquid-cholesteric transformation and the cholesteric-smectic transformation show no supercooling effects. However, the smectic phase may be cooled well below 72° before recrystallization of C₂ occurs. Thus the transitions of cholesteryl myristate are similar to those of cholesteryl laurate except no C₁ crystal form is found in cholesteryl myristate.

Cholesteryl palmitate (cholesteryl hexadecanoate)

Cholesteryl palmitate (CP) shows 1 enantiotropic mesophase transition ($\text{CH} \longleftrightarrow \text{I}$). The behavior of CP is similar to that of cholesteryl dodecanoate, although the phase transformations are lower. A second unstable monotropic crystalline phase (C_2) forms when the smectic phase is supercooled rapidly. C_2 melts to SM at 75°C.

Cholesteryl stearate (cholesteryl octadecanoate)

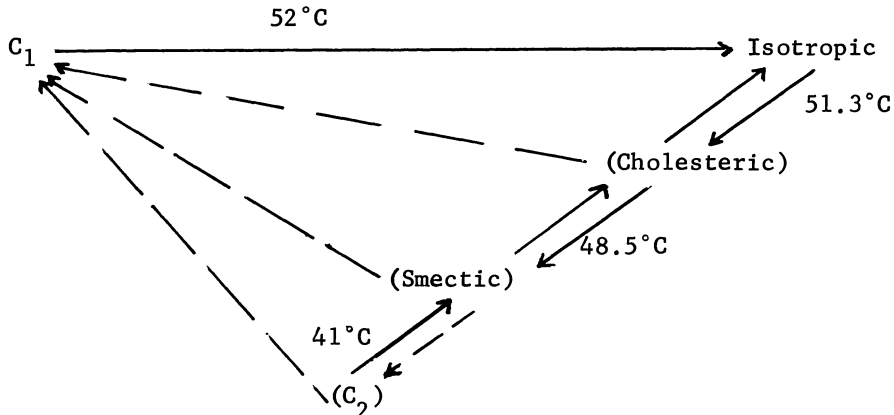


Cholesteryl stearate shows two monotropic mesophase transformations at 79 and 74.5°C. These phases are highly unstable and crystals of C_1 grow from both liquid crystalline phases very quickly after their formation. Further, the liquid phase cooled slightly below 83.2° will grow crystals of C_1 .

These phase transformations are very similar to those described by Gray (5) and by Barrall, Porter and Johnson (6). There are slight differences in the transition temperatures of some of the esters which may reflect purity or variations in technique.

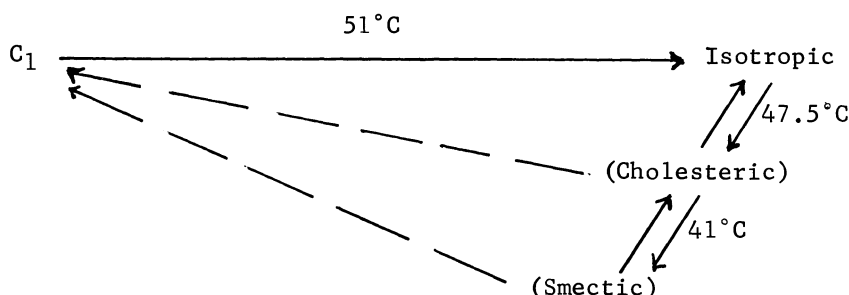
Esters of Monounsaturated and Polyunsaturated Fatty Acids

Cholesteryl palmitoleate (cholesteryl cis 7-8 hexadecenoate)



Crystals of cholesteryl palmitoleate (C_1) melt to an isotropic liquid at 52°C. On cooling, the isotropic liquid forms a cholesteric phase at 51.3° and the smectic mesophase at 48.5°C. These phases are reversible without supercooling effects. When the smectic mesophase is cooled to room temperature a second crystalline phase (C_2) forms. These crystals melt to the smectic mesophase at 41°C. Samples left at room temperature for several days undergo a polymorphic crystal transformation from C_2 to C_1 . The monotropic cholesteric and smectic mesophases of this cholesterol ester are fairly stable.

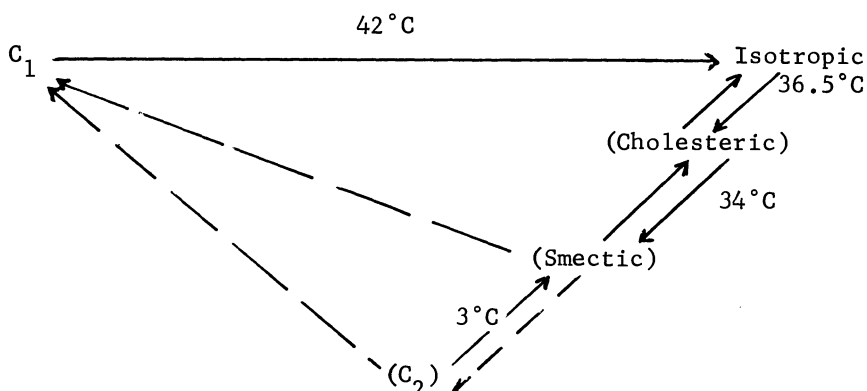
Cholesteryl oleate (cholesteryl cis 9-10 octadecenoate)



Crystals of cholesteryl oleate (C_1) melt sharply to an isotropic melt at 51°C. Monotropic cholesteric and smectic phases are formed at 47.5°C and 42°C, respectively. The monotropic cholesteric mesophase is fairly stable, but C_1 crystals will grow from the smectic mesophase cooled to room temperature after several minutes.

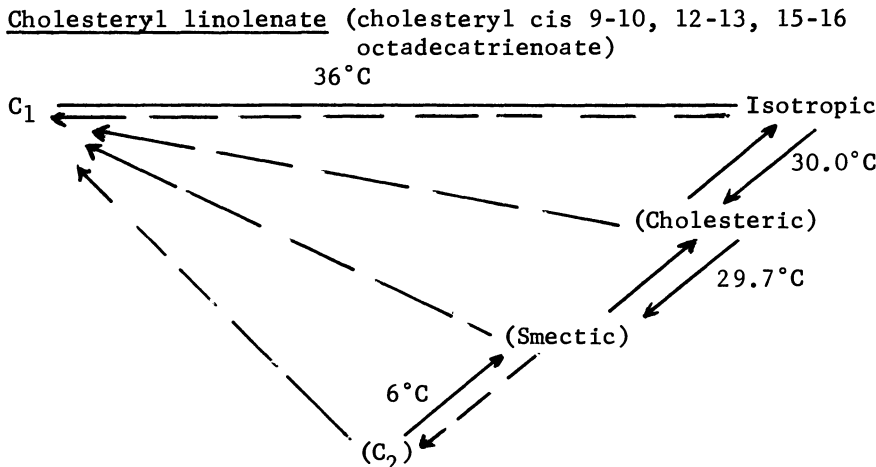
Polyunsaturated Fatty Acid Esters of Cholesterol

Cholesteryl linoleate (cholesteryl cis 9-10,12-13 octadeca-dienoate)



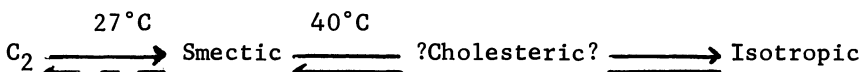
Crystalline cholesteryl linoleate (C_1) melts to the isotropic

liquid at 42°C. Two reversible monotropic phase transformations to the cholesteric phase and smectic phase occur at 36.5°C and at 34 °C. On cooling to room temperature, recrystallization from the smectic phase to C₁ will occur very slowly (only after days). If the sample is cooled rapidly to -40°, a second crystalline form, C₂, will be formed which melts at 3°C to the smectic mesophase.



On the initial heating, crystals of cholesteryl linoleate melt to an isotropic liquid at 36°C. On cooling two monotropic mesophases are formed. The cholesteric phase forms abruptly at 30.0°C and at 29.7° the cholesteric phase transforms to the smectic phase. Note that there is only 0.3° between the phase transformations. This was difficult to detect on the DSC curve as the cholesteric-liquid endotherm appeared as a shoulder on the smectic-cholesteric endotherm. However, these transformations were quite evident from gross and microscopic examination of the sample. The mesophases of cholesteryl linoleate are unstable and C₁ grows from a supercooled isotropic phase, the cholesteric phase and the smectic mesophase. If the sample is cooled rapidly to -40°C the smectic phase transforms to a second crystalline phase (C₂) which melts to the smectic phase at 6°C.

Cholesteryl cis 11-12, 14-15, 17-18 eicoso trienoate



This ester of the trienoic C₂₀ fatty acid belongs to the linolenic fatty acid series (that is, the first double bond counting from the end methyl group of the fatty acid occurs at the 3 position). Acids of the linoleic series and the oleic series have their first double bond placed at the 6 and 9 positions respectively. The crystals of this cholesteryl ester melt at 27° to the smectic

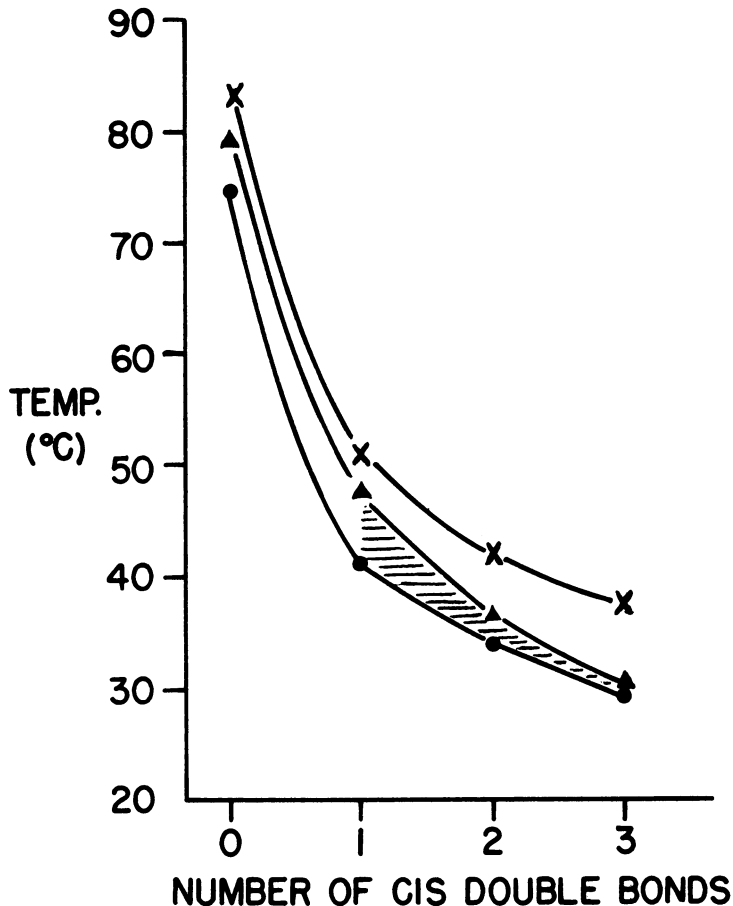
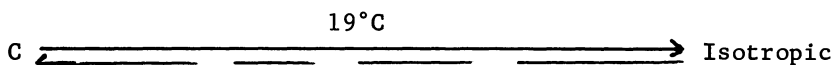


Figure 2. Transition temperature vs the number of cis double bonds in C-18 fatty acids esterified with cholesterol. X, the crystal ($C_1 \rightarrow$) isotropic transition; \blacktriangle , the cholesteric \leftrightarrow isotropic transition; \bullet , the smectic \leftrightarrow cholesteric transition. Shaded area refers to the temperature domain of the cholesteric mesophase. For further explanation see text.

mesophase. No cholesteric mesophase was observed. However, when the smectic mesophase melts to the isotropic phase a slight flash of color seems to occur coincident with the transition which suggests that there may be a cholesteric phase which exists over such a small temperature range that it is undetected by microscope or DSC.

Cholesteryl arachidonate (cholesteryl cis 5-6,8-9,11-12,14-15 eisoco-tetraenoate)



Cholesteryl arachidonate shows no mesophases. Crystals (C) of this ester melt sharply at 19.0° to the isotropic liquid. On cooling recrystallization to this crystalline phase occurs. In some slightly less pure samples a second polymorphic form was present at lower temperatures and on heating melted at 15° and immediately recrystallized to C which melted again at 19°C.

Cholesteryl cis 4-5,7-8,10-11,13-14,16-17,19-20 docoso hexenoate

This C22 hexenoic acid ester of the linolenate series was a liquid at 0°C. It did solidify at -72°, but no liquid crystalline phases were noted on melting.

Results show that both the melting points of the crystalline material and the liquid crystalline transitions of the unsaturated and polyunsaturated cholesteryl esters are considerably lower than those of their saturated homologues. To illustrate this graphically the crystalline to isotropic transitions ($\text{C}_1 \longrightarrow \text{isotropic}$), the isotropic to cholesteric transitions and cholesteric to smectic transitions are plotted as a function of the number of cis double bonds in C18 fatty acids in Figure 2. There is a fall in all 3 transition temperatures as the number of double bonds increases. Further, considering only the unsaturated cholesteryl esters the temperature domain of the cholesteric mesophase (shaded area in Fig. 2) decreases sharply with the number of double bonds. Thus, for cholesterol oleate the cholesteric phase extends from 42 to 47.5° or covers a domain of 5.5°. The dieonic ester, cholesteryl linoleate, has a domain of 2.5°C, but cholesteryl linolenate has a domain of only 0.3°C. In the C20 homologue of cholesteryl linolenate no cholesteric phase could be clearly detected. Further, in those polyunsaturated cholesteryl esters having 4-6 cis double bonds, the melting points of the crystals were considerably lower and no mesophases were observed.

While the specific position of the cis double bonds is undoubtedly important in determining the phases present and the transition temperatures of the phase it can be generally stated

that the more double bonds the lower the transition temperatures. Cholesteryl esters having four or more cis double bonds do not form mesophases.

Two Component Systems

Cholesteryl oleate-cholesteryl linoleate condensed binary phase diagram. Because the 2 most abundant esters of cholesterol in biological systems are cholesteryl oleate and cholesteryl linoleate I have studied the binary mixtures of these 2 cholesterol esters to determine the physical state of mixtures of these compounds as a function of temperature. In Fig. 3 an attempt has been made to construct the condensed binary phase diagram of cholesteryl oleate and cholesteryl linoleate. The temperature is plotted on the vertical axis the percent cholesteryl linoleate or cholesteryl oleate on the horizontal axis. This diagram has been constructed from the DSC heating curves and from gross and microscopic examination. At the lower temperatures it appears that the cholesteryl oleate and cholesteryl linoleate from a compound (X) which contains about 70% cholesteryl oleate and 30% cholesteryl linoleate. Below 3°C in concentrations of cholesteryl linoleate greater than about 65% a crystalline solid solution (SS) of the 2 esters is present (lower right side of Fig. 3). The crystalline form of SS is probably identical to the C₂ form of cholesteryl linoleate which melts to the smectic phase at 3°C (point D). Mixtures containing a high proportion of cholesteryl linoleate form a smectic liquid crystalline phase (SM) at temperatures above 3°C. Depending on the temperature this phase (SM) can contain up to about 50% cholesteryl oleate (point E). The compound X of cholesteryl oleate and cholesteryl linoleate has a melting point about 30°C and melts to form a smectic mesophase and crystals of cholesteryl oleate. Mixtures containing less than 30% cholesteryl oleate form a cholesteric mesophase (CH) before melting to an isotropic solution (I).

For the sake of explanation let us examine several mixtures of different composition of see what happens as the temperature is raised. For example, observe a mixture containing 20% cholesteryl linoleate and 80% cholesteryl oleate as the temperature is increased along line abcdef. Between 0°C and 27°C (point a) this mixture is made of two phases, a polymorphic crystalline type CR' of cholesteryl oleate and crystals of the compound. As the temperature is raised CR' undergoes a polymorphic change to CR at about 27°C. CR is identical to the stable crystalline form (C₁) of cholesteryl oleate. At 30°C (point b) the behavior is similar to a peritectic system and theoretically 3 phases can coexist, CR, X and SM. However, as X melts it forms more CR and a second phase SM such that at a temperature just above 30°C only CR and SM are present (point c). On further heating SM transforms to the cholesteric mesophase (CH) at point d. In the process more CR is

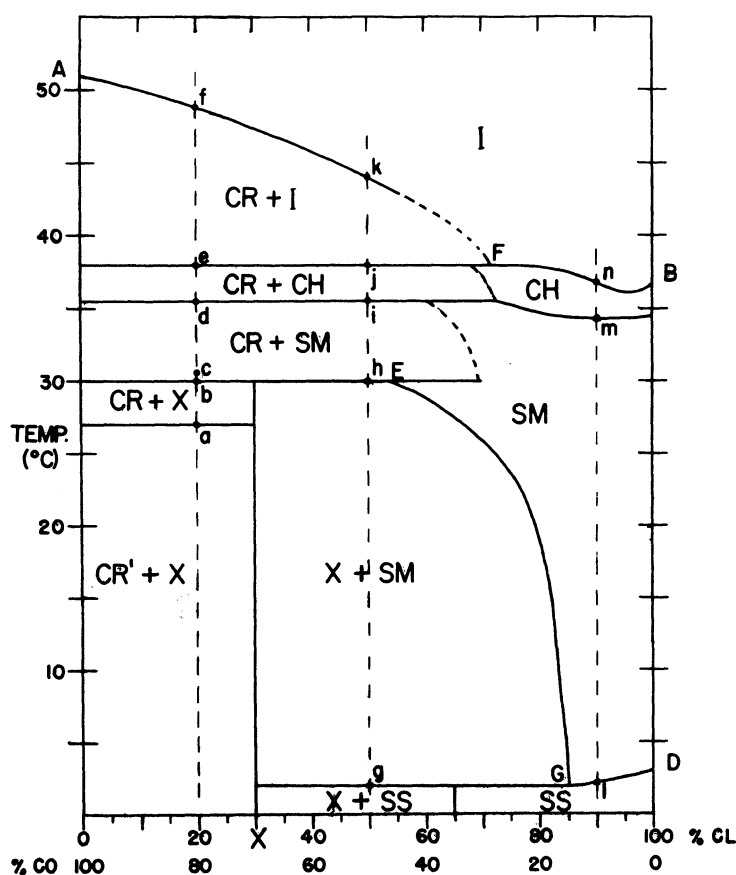


Figure 3. The cholesteryl oleate-cholesteryl linoleate condensed phase diagram. Vertical axis, temperature °C; horizontal axis weight % cholesteryl linoleate (CL) or cholesteryl oleate (CO). CR, crystals of cholesteryl oleate (C_1). CR' polymorphic form of cholesteryl oleate; X, the crystalline compound of cholesteryl oleate and cholesteryl linoleate; SS, solid solution of cholesteryl linoleate containing limited quantities of cholesteryl oleate; SM, smectic liquid crystalline phase; CH, cholesteric liquid crystalline phase; I, isotropic liquid phase. Points A, B, D, E, F, G are points explained in the text. Lines abcdef, ghijk and lmn are explained in the text. Phase boundaries represented by broken lines are only approximate.

formed. Between d and c gradual melting of CR occurs and the composition of the melt (I) becomes richer in cholesteryl oleate (following line fF). At point f the last of CR melts producing an isotropic solution (I) of composition identical to the original mixture.

Now consider the behavior of a mixture having a composition of 50% of each component as it is heated along line ghijk. At 0°C this mixture is made up of two solids, compound X and the solid solution (SS) containing about 35% cholesterol oleate. At about 2°C (point g) the solid solution melts to form a mixture of X and smectic liquid crystalline phase (SM) having a composition of about 85% cholesteryl linoleate (point g). As the temperature is increased along gh more X melts to SM having a composition given by GE. At h theoretically 3 phases can be present (as with point b, see above), CR, X and SM. At this temperature the reaction $X \rightarrow CR + SM$ occurs and at a slightly higher temperature only CR and SM remain. Points i, j and k are analogous to points d, e and f respectively. The behavior of this mixture is similar to the previous mixture (80 cholesteryl oleate/ 20 cholesteryl linoleate) above 30°C, except that the final melting point of CR (point k) is somewhat lower because the mixture contains more cholesteryl linoleate.

Finally consider a mixture containing 90 cholesteryl linoleate, 10 cholesteryl oleate as it is melted along lmn. At 0°C this mixture is a single phase of crystalline solid solution (SS). At 3° (point l) SS melts directly into another single phase SM. At 34.5°C (point m) there is a phase change to a second liquid crystalline phase, the cholesteric phase (CH). At 37°C (point n) CH melts to an isotropic liquid.

One important point should be made about this phase diagram. As was pointed out in the earlier section on pure cholesteryl esters, both the mesophases of cholesteryl oleate and cholesteryl linoleate are monotropic with respect to crystallizing phase C₁. However, the mesophases of the oleate ester are unstable and cholesteryl oleate crystals (C₁) can be readily made to form from the mesophases by cooling or by being allowed to stay at room temperature for several hours. However, the mesophases of cholesteryl linoleate are quite stable under certain conditions. The specific conditions under which this diagram was produced involve the cooling of the mixture from isotropic melt to -50°C at a rate of 5°/min. The mixture is then allowed to stand for 30 min at -50°C and then reheated at a rate of 5°/min. While crystallization of C₁ invariably takes place (labelled CR on fig 3) in mixtures having 30% or more cholesteryl oleate no recrystallization of C₁ takes place with less cholesteryl oleate. AF is the final melting of the oleate crystals while FB is the melting of the cholesteric

phase. Further, if each mixture is allowed to cool slowly to 25°C and is then left for 48-72 hrs those mixtures containing less than 30% cholestryl oleate remained in the smectic mesophase (SM) at 25°C. On heating, these mixtures form the cholesteric phase (CH) at 34.5 to 35.5°C and melt to an isotropic solution along FB. Many of the mixtures were stable for 6 months. Nevertheless, since SM and CH are probably monotropic phases one would expect that under the appropriate conditions of time, nucleation and temperature a more stable crystalline form (C₁) would be present. Thus, the true phase (equilibrium) diagram would contain no monotropic phases and line FB would be replaced with a line representing the melting of C₁. It is possible that a eutectic exists between the stable crystalline form (C₁) of cholestryl oleate and cholestryl linoleate. Whether this possible eutectic would have a lower melting point than the mesophases at that composition has not yet been determined. If the eutectic melting point was lower then a stable mesophase would be present at the eutectic composition. Experiments are now in progress to resolve this problem. Nevertheless, from a biologic point of view it seems likely that the phase diagram presented, although probably not truly representing equilibrium conditions, has importance because of the great stability of the smectic and cholesteric mesophases containing large amounts of cholesterol linoleate.

Cholestryl oleate-cholesterol condensed binary phase diagram. The condensed phase diagram of cholesterol and its ester of oleic acid is presented in Fig. 4. The melting point of crystals of cholesterol is depressed continuously along line AC by increasing amounts of cholesterol oleate. The melting point of cholesterol oleate is also depressed by small quantities of cholesterol along line BC. Point C represents a eutectic composition of 95% cholestryl oleate, 5% cholesterol (8.4 mole% cholesterol). This composition melts quite sharply at 46°C to an isotropic fluid. To illustrate the phase diagram, let us observe a mixture containing 96% cholesterol oleate - 4% cholesterol. At 25°C crystals having a spherolyte configuration are present. At 46°C, melting is not complete until the temperature is raised to 47.5°C. Now, examine a mixture containing 92% cholestryl oleate and 8% cholesterol. Again, one recognizes at 25°C a spherolyte type of configuration of the crystals (Fig. 5a). These crystals melt between 45.5 and 46°C. However, there remains a radial network of thin crystals of cholesterol which now form a ghost-like outline of the spherolyte (Fig 5b). These crystals gradually melt as the temperature is raised, melting completely only at 65°C to an isotropic liquid. The condensed phase diagram may be divided into the following regions. Below line DCE-pure cholesterol crystals and crystals of cholesterol oleate exist. There is a eutectic composition at point C which has the lowest melting point (46°C). Above ACB a single isotropic melt is present. In the region ADC crystals of

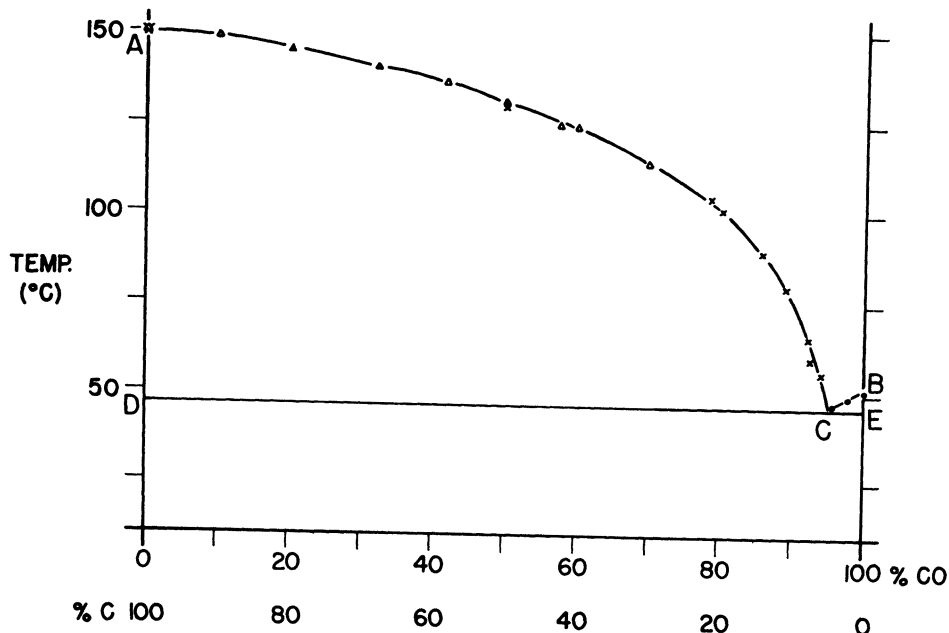


Figure 4. Cholesterol-cholesteryl oleate condensed binary phase diagram. Vertical axis, temperature (°C); horizontal axis weight % cholesteryl oleate (CO) or cholesterol (C). The triangles represent peak of melting curve of cholesterol by DSC, X the final microscopic melting point of crystals of cholesterol in each mixture and the solid circles the final melting points of cholesteryl oleate. Point A is the melting point of pure cholesterol, Point B the melting point of the crystalline (C_1) form of cholesteryl oleate and point C the melting point of the eutectic composition.

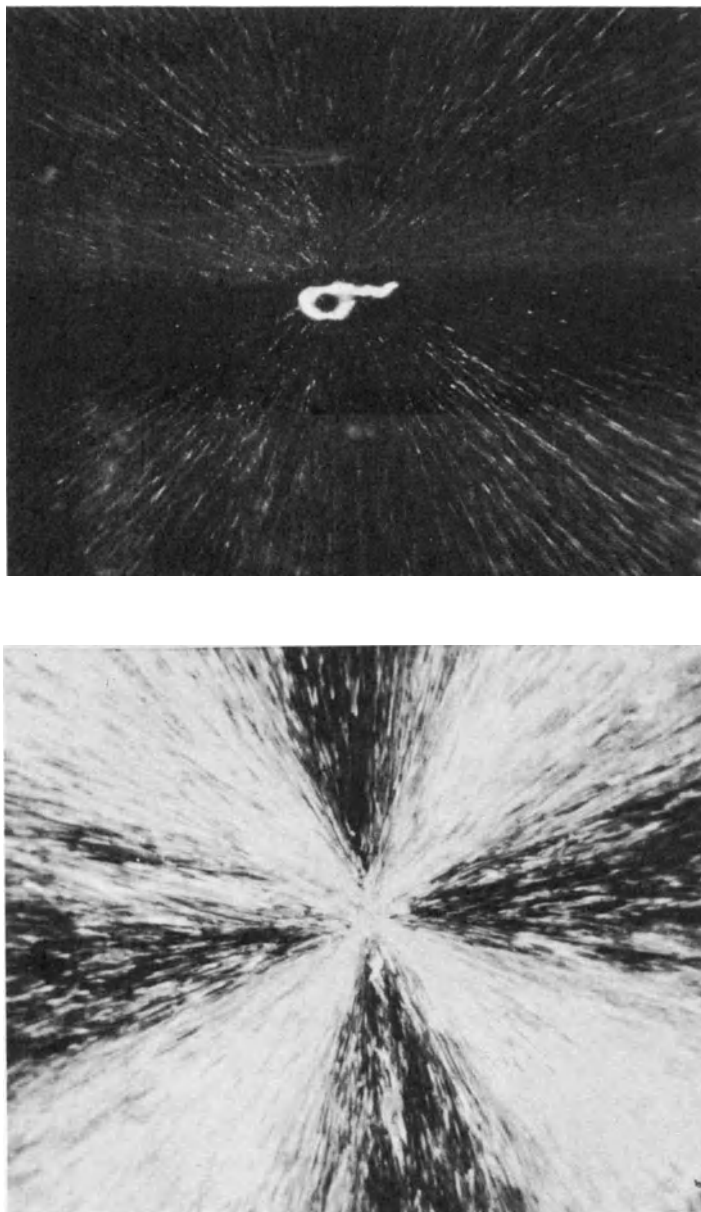


Figure 5. Mixture containing 92% cholestearyl oleate-8% cholesterol. Crossed nicols, 50X. Left, mixture at 35°C showing a sphereolitic crystalline configuration, consisting primarily of crystalline (C_1) cholestearyl oleate. Right, same mixture at 56°C after the eutectic composition had melted. Only a fine network of cholesterol crystals remain. Bright spot in center is dust particle, which served as a nidus for crystallization. For further explanation see text.

cholesterol are in equilibrium with a liquid having a composition lying along AC. In the area marked BEC crystals of cholesteryl oleate are in equilibrium with a liquid lying along line BC. It should be noted that those mixtures containing a high proportion of cholesteryl oleate (greater than 80%) can be supercooled readily to produce liquid crystalline transformations similar to those formed with cholesteryl oleate alone. However, since these transformations are monotropic and rather unstable, they will not be discussed further.

Cholesteryl oleate-triolein condensed binary phase diagram. The binary phase diagram formed by the mixture of triolein and cholesteryl oleate is given in Fig. 6. The melting point of the crystalline form (C_1) of cholesteryl oleate is depressed by increasing concentrations of triolein. There appears to be a eutectic at about 4% cholesteryl oleate--96% triolein, although the melting point of the eutectic mixture was only half a degree lower than that of pure triolein. On heating a mixture containing 50% triolein and 50% cholesteryl oleate from 0°C, one notes that the eutectic mixture (nearly pure triolein) melts at about 4°C. Cholesteryl oleate crystals remain and gradually melt until only an isotropic solution is present (46.5°C). Mixtures containing less than 5% cholesteryl oleate could not be nucleated or made to grow cholesteryl oleate crystals. The phase diagram is thus composed of the following regions. Above line ACB a single isotropic liquid phase is present. Below DCE crystals of triolein and of cholesteryl oleate are present. In the very small zone labeled ADC, there is a mixture of pure triolein and crystals of cholesteryl oleate which melt along line AC. In zone BCE crystals of cholesteryl oleate are present which melt along line CB.

The cholesterol-triolein condensed phase diagram. In Fig. 7 the phase diagram of cholesterol-triolein system is presented. Triolein, like cholesteryl oleate (Fig. 4), also depresses the melting point of cholesterol. The line AC, in fact, gives the solubility of cholesterol in triolein as a function of temperature. The shape of AC suggests that a eutectic is present at C but this could not be demonstrated clearly by microscope or DSC curves. Partington (18) produced similar diagrams for long chain fatty acids and concluded, as must also be concluded from this diagram, that no compounds are formed between either long chain fatty acids or triolein and cholesterol.

Three Component Systems (Ternary systems)

Cholesterol-cholesteryl oleate-triolein. In order to get an idea of the interrelations of these three lipids as a function of temperature, a large series of mixtures of the three lipids were made up in thick-walled glass tubes and the mixtures sealed under

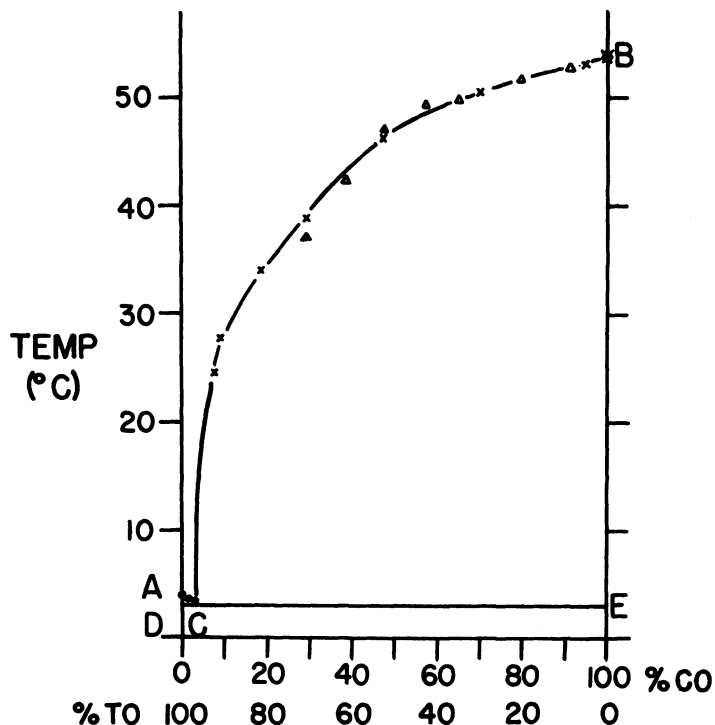


Figure 6. Triolein-cholesteryl oleate condensed binary phase diagram. Vertical axis, temperature, horizontal axis percent cholesteryl oleate (CO) or triolein (TO). Triangles represent the peak of the cholesteryl oleate melting DSC curve, X the final melting point of cholesteryl oleate in the mixture and the solid circles represent the final melting point of triolein. Point A represents the melting point of pure triolein, B the melting point of crystals (C_1) of pure cholesteryl oleate and C the melting point of the eutectic composition.

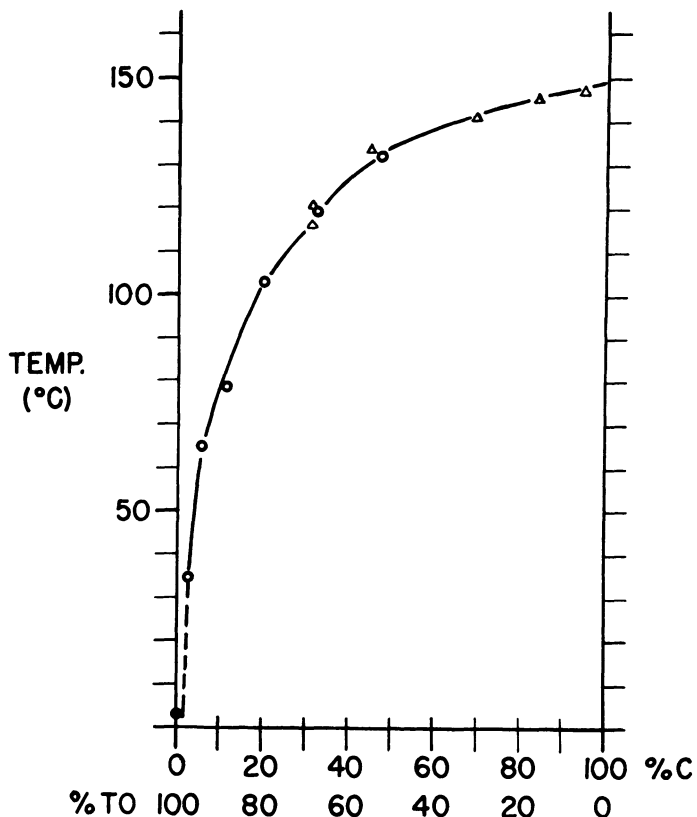


Figure 7. Triolein-cholesterol condensed binary phase diagram. Vertical axis, temperature °C, horizontal axis percent triolein (TO) or cholesterol (C). Triangles represent peak of the DSC melting curve of cholesterol, open circles represent the final melting point of cholesterol crystals in triolein and the solid circle represents the melting point of pure triolein. Although a eutectic may be present at about 1% cholesterol it could not be clearly defined.

nitrogen. Each mixture contained approximately 1 gram. The mixtures were then heated until all solids had melted, shaken and were then cooled to 0°C. After one week the temperature of the mixtures was raised at approximately 5° levels and allowed to stay at each temperature level for a period of 7-14 days. The mixtures were agitated intermittently and observed for the amount of solid present. When equilibrium was reached (no further decrease in the amount of solid present) the temperature was raised to the next level. When the mixture was completely melted the temperature was noted. The phase diagram given in Figure 8 shows only the composition range of the mixtures which were completely liquid at the temperature of the experiment.

At 25°C only mixtures very close to 100% triolein are liquid. This could have been predicted from the binary phase diagrams cholesterol-triolein and cholesteryl oleate-triolein. As the temperature is increased, the cholesteryl oleate melts into the triolein but only a small amount of cholesterol is melted so that at 38° the zone of one liquid phase has increased appreciably only in relation to cholesteryl oleate. At 52°C cholesteryl oleate and triolein are mutually soluble in all proportions. A total of about 12% cholesterol can be dissolved in a mixture fairly high in cholesteryl oleate. As the temperature is increased the amount of cholesterol that can be dissolved in mixtures of cholesteryl oleate and triolein gradually increases. Of course, at 150° the entire system is one single oily phase.

Discussion

Generally speaking, from a biologic point of view, lipids may be lumped into two large classes. The first class are those lipids which are involved in the structure of plasma membranes, the membranes of cellular organelles and the circulating lipoproteins. The second class are those lipids which are primarily stored to be either used later as sources of energy or as building blocks for structural lipids. The former group includes primarily the complex lipids such as phospholipids, glycolipids and sulfolipids, which for the most part are insoluble, but swell in water to form lyotropic crystals (16,19,20). Many individual species and mixtures of these lipids are capable of forming an endless series of bimolecular leaflets (the lamellar liquid crystalline phase) which bears analogy to the plasma and organelle membranes found within the cell. Cholesterol, while not capable of swelling alone in water, is often found in association with plasma membranes and indeed has been shown to interdigitate between lecithin molecules in the bilayers of the lecithin liquid crystalline lattice (21,22, 23) and the lipids of the erythrocyte membrane (24). Thus, while pure cholesterol has a melting point greatly above normal body temperature, it can be solubilized within a lamellar liquid crystalline lattice in ratios up to 1 molecule of cholesterol

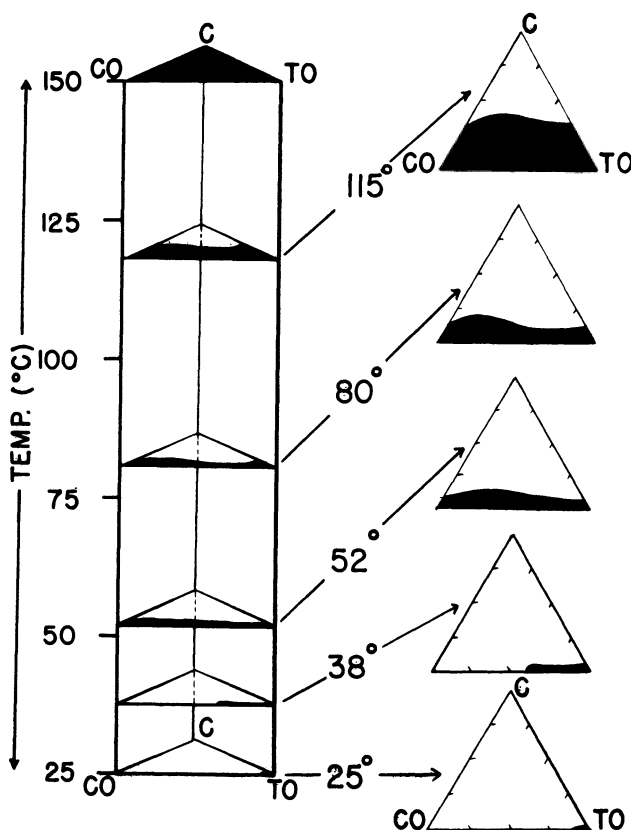


Figure 8. The cholesteryl oleate-cholesterol-triolein ternary phase diagrams as a function of temperature. On the left the ternary phase diagram is expressed as a regular prism with each edge representing one of the three components. Representative ternary (3 component) systems at specific temperatures are shown on the right. CO, cholesteryl oleate; C, cholesterol; TO, triolein. The darkened area of the triangle represents those compositions forming one single isotropic liquid. The rest of the phase diagram is made up of mixtures of two or three phases. As the temperature is increased the domain of compositions which are in the completely melted state increases. For further explanation see text.

to 1 molecule of phospholipid (21 22 23). The storage lipids, for the most part, are less polar lipids and while some, such as triglycerides, fatty acids and free cholesterol are capable of spreading at an oil-water interface (19), others such as the long chain fatty acid esters of cholesterol are almost completely nonpolar and will not spread. The major storage lipids include triglyceride, cholesteryl esters of long chain fatty acids and to some extent free cholesterol and fatty acids. Because living organisms require mobility, it would seem important that the storage lipids be maintained in a liquid state. It is hard to imagine how storage lipids in a crystalline state could readily diffuse to be metabolized by enzymes or even to be mobilized for transport. Thus, I have begun a series of studies designed to define the physical state of a number of chemical classes of those lipids which can be roughly defined as storage lipids. Biologically, these lipids are found in adipose tissue, liver, adrenal glands, the gonads and circulating lipoproteins in small drops which, on superficial examination, appear to be composed of a single liquid (oil) phase. In this preliminary paper the physical state of cholesteryl esters, free cholesterol and triglyceride alone and in mixtures is reported. These studies give a general idea of the physical state of individual components and solubility relationships of mixtures of these lipids as a function of temperature.

The present studies show that the individual cholesteryl esters of biological origin show a marked variability in their transition temperatures. The esters of saturated long chain fatty acids have melting points some 40° above body temperature. This makes them unsuitable to function as storage lipids, at least in the pure state, since they would be solid and quite insoluble. On the other hand, the esters of the unsaturated fatty acids have transition temperatures and melting points fairly close to body temperature. It would, however, appear that the monounsaturated esters, cholesteryl oleate and cholesteryl palmitoleate, have transition temperatures far enough above body temperature and unstable enough monotropic liquid crystalline phases that they would probably also be unsuitable as a storage lipid in pure states. On the other hand, cholesteryl linoleate, which has 2 cis double bonds, could exist, at least in part, in a liquid crystalline state at body temperature, and therefore might be considered suitable as a storage lipid. The binary system cholesteryl oleate and cholesteryl linoleate show that there are a range of compositions high in cholesteryl linoleate which form very stable liquid crystalline phases in the temperature range present in warm-blooded animals. While the liquid crystalline phase consists of molecules in a partly organized state which gives the mesomorphic phases a viscosity considerably higher than that of the liquid phase (13,14), these states are rather fluid and therefore may represent a suitable structure for storage lipid. However, because of the viscosity and the partial orientation of the molecules within these phases, it is

a non-liquid state. There are, obviously, other cholesteryl esters present in both beta lipoproteins and in the cholesteryl ester fraction isolated from lipids of the plaque. These include small amounts of saturated esters (mainly cholesteryl palmitate) and some polyunsaturated fatty acid esters. It would be premature to try to predict the physical state of the lipids in the plaque without 1) examining the effect of the other esters on the physical state of the total mixture and 2) without further careful study of both the chemical composition of the lipid and the distribution of lipid within the plaque. However, droplets of lipid present a single phase and the composition of that phase in the long run must be determined by the physical characteristics of the molecules within the phase.

In the past it has been shown that large amounts of cholesterol can be solubilized in phospholipid bilayers (21,22,23). What about the solubility of cholesterol in the major storage lipids, such as triglycerides and cholesterol ester? The present work clearly shows that the solubility of free cholesterol in either cholesteryl oleate (Fig. 4) or triolein (Fig. 7) is very small at body temperature. Further, the three component system shows that cholesterol is only sparingly soluble in mixtures of cholesteryl oleate and triolein and only when temperatures well above body temperatures are large amounts of cholesterol solubilized. Reports on the amount of free cholesterol in atherosclerotic plaques vary. Luddy et al (12) and Dayton et al (11) found quite large amounts of free cholesterol in plaques taken from autopsy specimens. However, these high values could be due to postmortem hydrolysis of cholesterol ester. Smith et al (9,10) find somewhat less free cholesterol. Theoretically the free cholesterol could partition between an oil phase which consists primarily of cholesteryl ester and into the phospholipid bilayers of cell membranes and organelles associated with the plaque. It is also possible that cholesterol is solubilized by other substances (protein, nucleotides, glycoproteins, etc.), but this has not yet been shown to be quantitatively important. Is the total amount of cholesterol present greater than the total solubilizing capacity of these two systems? This cannot be answered at the present time, but it might appear that in the plaques containing a high amount of "amorphous material" (9,10) that there is an excess of free cholesterol beyond that which can be solubilized readily by 1) an oil phase containing small amounts of glyceride and large amounts of cholesteryl ester and 2) the phospholipids present in that plaque. If this is the case, one might expect to find crystals of true cholesterol occurring in these lesions.

Triglycerides are storage lipids found in adipose tissue, liver and lipoproteins of low density. In higher animals dietary fat is hydrolyzed in the intestinal lumen, absorbed and then resynthesized to triglyceride in the intestinal mucosal cell. It is

quite possible that the process of transport out of the phase either of molecules in their intact chemical state or through biochemical reactions such as hydrolysis might proceed at a much slower rate and thus allow the accumulation of lipid in this state. In the atherosclerotic plaque, it has been shown that a large proportion of the lipid is cholesterol ester (9-12). Although no vigorous studies on the physical state of the lipids in the atherosclerotic plaque have been carried out to date, Stewart (25) has shown that some substance (presumably lipid) present in both betalipoprotein and in atherosclerotic plaques was anisotropic and had a negative sign of birefringence. Unfortunately, the substance observed was not analyzed and careful temperature studies were not carried out. He, nevertheless, suggested that perhaps the lipids in arterial walls and perhaps in beta lipoprotein could be in the liquid crystalline state. Considering the sign of birefringence, the liquid crystalline state would have to be the cholesteric liquid crystalline phase. Since about 60-80% of cholesteryl esters of the beta lipoproteins (2,8) and of the cholesteryl esters found in atherosclerotic lesions (9-12) are cholesteryl oleate and cholesteryl linoleate, the condensed phase diagram of these systems may be important. Again, the condensed phase diagram shows that at body temperature mixtures of cholesteryl oleate and cholesteryl linoleate in which there is less than about 30% cholesteryl oleate present are in a fairly stable cholesteric liquid crystalline phase. Thus, it is possible that the anisotropic lipid droplet which Stewart observed with negative birefringence represented the cholesteric liquid crystalline phase. If that were the case, one would predict that these droplets would be made up of almost pure cholesterol esters with very little triolein or free cholesterol dissolved in them. We have, in fact, recently found that isolated lipid droplets of the fatty streaks of human atherosclerotic plaques are nearly pure cholesteryl ester and are present in a liquid crystalline phase which has a transition point from cholesteric to isotropic (varying on the source of the lipid) from 37° to 42°. Smith et al (9,10) have recently described histologically two types of oil droplets occurring in the atherosclerotic plaque, the first type, perifibrinous lipid, is extracellular and has a cholesteryl oleate to cholesteryl linoleate ratio very similar to beta lipoprotein in that it is relatively high in cholesteryl linoleate. On the other hand, the second type designated, intracellular fat droplets, have a different distribution of fatty acids in their cholesteryl esters, being very high in cholesteryl oleate. Although no attempt was made to examine the physical state of these deposits in the natural state, one might predict that if these droplets are in the liquid state that they would be unstable and that precipitation of cholesteryl oleate could readily occur within these drops. Once the excess cholesteryl oleate was precipitated, it would not be normally removed and could act as a nidus for accumulation of further esters. It could well be that a portion of the cholesteryl oleate in the plaque is in

released into the lymph in large dietary (exogenous) chylomicrons. These particles are transported in the plasma to the liver and other parts of the body by the systemic circulation. Smaller endogenous chylomicrons are probably synthesized primarily in the liver and released into the circulation. While these particles have been called lipoproteins they are really small emulsion droplets to which a very small amount of protein is attached. The oil phase is largely triglyceride and the emulsifiers are primarily phospholipids, free cholesterol and perhaps to some minor degree fatty acid and protein. The composition of the oil phase of exogenous chylomicrons like that of adipose tissue is analogous to the oil phase shown in Fig. 8 for the cholesteryl oleate-cholesterol-triolein diagram at 25°C (i.e. very little cholesteryl ester or free cholesterol is present in the oil phase). The monolayer of emulsifier at the surface of the oil droplet has a composition which obeys the cholesterol-lecithin-water phase diagrams (21,22, 23) in that less than one cholesterol molecule per phospholipid molecule is present in this layer (26).

This discussion has been largely speculative in nature principally for two reasons: 1) data concerning the composition and physical state of specific lipid phases occurring naturally or pathologically is not readily available and 2) the application of the data obtained in the present studies is limited because the number and types of lipid species studied has been limited. Nevertheless, the broad outline of the interrelations between cholesterol, its esters and triglycerides described here may be applicable to the interrelations of these lipids in biological systems and in pathological states. Only time and more data will tell.

Acknowledgements

The author wishes to thank Mr. John Steiner for excellent technical assistance and Mrs. C. Castles for secretarial help.

Supported by NIH Public Health Research Grant AM 11453.

REFERENCES

1. Bloch, K. Science, 150:3692, 19, 1965.
2. Frederickson, D.S., R.I. Levy and R.S. Lees. New Eng. J. Med. 276:1, 34; 276:3, 148; 276:4, 215 and 276:5, 273, 1967.

3. Jaeger, Rec. Trav. chim. 25:334, 1906.
4. Friedel, G. Ann. Physique, 17:273, 1922.
5. Gray, G.W. J. Chem. Soc. pt. 3, 3733, 1956.
6. Barrall, E.M., II., R.S. Porter and J.F. Johnson. J. Physical Chem. 70:385, 1966.
7. Chistyakov, I.G. Soviet Physics - Crystall. 8:1, 57, 1963.
8. Freeman, N.K., F.T. Lindgren and A.V. Nichols. Progress in Chem. of Fats and other Lipids. 6:215, 1963.
9. Smith, E.B., P.H. Evans and M.D. Downham. J. Atheroscler. Res. 7:171, 1967.
10. Smith, E.B., R.S. Slater and P.K. Chu. J. Atheroscler. Res. 8:399, 1968.
11. Dayton, S., S. Hashimoto and M.L. Pearce. Circulation, 32: 911, 1965.
12. Luddy, F.E., R.A. Barford and R.W. Riemenschneider. J. Biol. Chem. 232:843, 1958.
13. Brown, G.H. and W.G. Shaw. Chemical Rev. 56:6, 1049, 1957.
14. Gray, G.W. Molecular Structure and the Properties of Liquid Crystals. Academic Press Inc., New York, N.Y., 1962, p. 114.
15. Barrall, E.M., R.S. Porter and J.F. Johnson. Mol. Crystals, 3:103, 1967.
16. Small, D. M. J. Lipid Res., 8:551, 1967.
17. Barrall, E.M., II, R.S. Porter and J.F. Johnson. J. Physiol. Chem. 71:1224, 1967.
18. Partington, J.R. J. Chem. Soc. 99:313, 1911.
19. Small, D.M. J. Am. Oil Chem. Soc. 45:108, 1968.
20. Dervichian, D.G. in Progress in Biophysics and Molecular Biology, 14, 263. (Butler, J. and H. Huxley, Eds. Academic Press, New York, 1964).

21. Small, D.M., M. Bourges and D.G. Dervichian. *Nature*, 211: 816, 1966.
22. Small, D.M. and M. Bourges. *Mol. Crystals*, 1:541, 1966.
23. Bourges, M., D.M. Small and D.G. Dervichian. *Biochim. et Biophys. Acta* 137:157, 1967.
24. Rand, R.P. and V. Luzzati. *Biophys. J.* 8:1, 125, 1968.
25. Stewart, G.T. in *Ordered Fluids and Liquid Crystals. Adv. in Chem. Series* 63, p. 141, 1967.
26. Zilversmit, D.B. *J. Lipid Res.* 9:180, 1968.

THE EFFECT OF HYDROCARBON CONFIGURATION AND CHOLESTEROL ON
INTERACTIONS OF CHOLINE PHOSPHOLIPIDS WITH SULFATIDE*

Morris B. Abramson and Robert Katzman

The Saul R. Korey Department of Neurology, Albert
Einstein College of Medicine, Bronx, New York

ABSTRACT

Mixtures of sphingomyelin and sulfatide or lecithin and sulfatide showed a titration capacity in the acid range that was greater than that of any of these lipids titrated alone. This is explained as the results of the ionic interaction of the sulfate and quaternary amine of neighboring molecules thus making the phosphate of the choline lipid available for titration.

This effect was greatest for sulfatide with sphingomyelin or with dipalmitoyl lecithin and decreased with egg lecithin and soybean lecithin. This order follows the increase in molecular cross-sectional area of the choline lipid and the increased separation of the charged groups of the mixed lipids. Incorporation of the neutral lipid, cerebroside, into sphingomyelin-sulfatide had little effect. Cholesterol, however, decreased the interaction of sulfatide with sphingomyelin or lecithin. This probably resulted from the separation of the charged lipids by the molecules of cholesterol. These data point to an intermolecular ionic linkage of choline lipids with anionic compounds in lipid membrane systems. The absence of any effect of cholesterol on the titration of choline lipids alone supports the view that lecithin and sphingomyelin without acidic components exist as dipolar ions with intramolecular bonding.

*This work was supported by Multiple Sclerosis Grant 503A, U.S. Department of the Interior, Office of Saline Water Grant 14-01-0001-1277, and U.S. Public Health Service Grants NB 03356 and NB 01450.

The addition of salts to systems of sphingomyelin-sulfatide or lecithin-sulfatide at pH 4.0 gave a cation-proton exchange with $K^+ = Na^+ > choline^+$.

Sodium dodecyl sulfate mixed with sphingomyelin or lecithin gave reactions similar to but less than those of sulfatide with these lipids.

Titrations were also performed on mixed dispersions of dipalmitoyl lecithin and sodium dicetyl phosphate. These systems showed that all the phosphate groups of the latter were available for titration and lends weight to the assumptions made in the interpretations of the systems containing sulfatide.

Despite the widespread occurrence and involvement of the choline phospholipids, lecithin and sphingomyelin, in biologic membranes (O'Brien, 1967), our knowledge of the molecular structures of these compounds in membrane systems and their interaction with other lipid components is fragmentary. In a report from this laboratory (Abramson and Katzman, 1968), we described the change of the dipolar structure of sphingomyelin or lecithin systems upon the addition of sulfatide. In these mixed lipid aggregates, the interaction between the fully ionized acid groups of sulfatide with the positive region of the choline of a neighboring lipid molecule leads to the freeing of the phosphate of that molecule. The change of the phosphate group is easily recognized by the difference in the titration characteristics of the single lipids and the mixed lipids between pH 3.5 and 10.

In this paper we describe further studies of the ionic interactions of choline lipids. The effects of different hydrocarbon structures and the inclusion of cholesterol on the interaction with sulfatide is given.

EXPERIMENTAL

Materials

Sphingomyelin obtained from freshly slaughtered beef brain was purified by the method described earlier (Abramson, et al., 1965). Sulfatide, also from beef brain, was extracted and converted to the sodium salts as in earlier work (Abramson, et al., 1967). Egg lecithin (Sylvana) was purified by silicic acid chromatography. The L- α -dipalmitoyl lecithin was from Mann Research Laboratories, New York. The cerebrosides were a gift from Dr. W.T. Norton. Cholesterol was obtained from Eastman Kodak. Sodium dodecyl sulfate and dicetyl phosphoric acid were

obtained from K and K Laboratories, Plainview, New York. The former was recrystallized 3 times. Dicetyl phosphoric acid was converted to the sodium salt by dissolving in chloroform-methanol (2:1, v/v) and partitioning with 0.1M NaCl maintained at pH 8.5. The sodium salt was separated and repartitioned. All lipids used gave single bands on thin-layer chromatograms performed as described below.

Dispersed Systems

Lipid systems were prepared in a 20 ml glass tube. Egg lecithin which was stored at -10° in solution in chloroform-methanol (2:1, v/v) was deposited in a weighed tube by vacuum evaporation of the solvent. The other lipids used were in solid form and were weighed into the glass tube. For single and mixed lipids, the weighed solids were first dissolved in chloroform-methanol (2:1, v/v). To dissolve the sodium sulfatide required gentle warming. On evaporation of the solvent by nitrogen and then in vacuum, a deposit of lipids was formed on the bottom of the tube. After adding 5 ml water, the system cooled in an ice-water bath, was dispersed by a 1 minute exposure of ultrasonic radiation using an MSE ultrasonic generator. All systems containing anionic lipids dispersed readily and showed low turbidity with no tendency to settle. Addition of cholesterol produced more turbid systems. Representative systems produced this way were studied by polarized light and electron microscopy. They showed structures similar to those reported by Bangham, et al., 1965.

Titrations

Titrations were performed at $24 \pm 1^\circ C$ in the 20 ml tube covered by a plastic cap. A stirrer, combined glass and reference electrode, 0.1 ml microburet (Manostat), and a tube supplying CO_2 -free moist nitrogen, fit tightly into the plastic cover. Additions of 1 to 3 μl of standard 0.100 N NaOH or HCl were made by means of the microburet, and the system after mixing was stirred at a very slow constant rate for 10 to 30 minutes until a stable pH value was measured on a pH meter (Corning Model 12). Most titrations were performed with duplicate samples. Blank titrations were made under identical conditions except for the absence of lipids in the system. By subtracting the blank from the titration curve, a corrected curve was obtained.

Thin-layer Chromatography

To assess the extent of degradation of the compounds during the course of the experiments, 0.1 ml samples were taken before and after the titration. In some instances, additional samples were taken at selected points during the titration. These samples were dried by a stream of nitrogen and dissolved in chloroform-methanol (2:1, v/v). Thin-layer chromatograms were obtained in silica gel G (Merck). Small quantities of the original lipids were run on each chromatogram as standards. Chromatograms were developed with chloroform-methanol-water-ammonia (29%) (70:30:4:1, by volume). They were stained with iodine vapor and charred with sulfuric acid. Sphingomyelin, sulfatide and dipalmitoyl lecithin showed very slight or no degradation products. Egg lecithin underwent a small amount (<5%) of degradation after titration in the basic range. Soybean lecithin, however, degraded to a much greater degree.

RESULTS

Effect of Area of Choline Molecule

Titrations were carried out on aqueous systems of sodium sulfatide, sphingomyelin, and three forms of lecithin. Comparable systems were prepared using sodium sulfatide mixed with sphingomyelin or lecithin. The titrations of these mixed systems under similar conditions showed an increased acid capacity in the pH range studied compared with the titration of sodium sulfatide alone or of any choline lipid alone. For these mixed systems, we then envisage analogous reactions between the anionic sulfate with the positive nitrogen of the choline moiety (Fig. 1). In comparing the extent of interaction of the 2 lipids, we measured the number of μ mole H^+ bound per μ mole of 1:1 lipid complex between pH 7 and 3.5. Titrations to lower pH levels were avoided because of flocculation and the greater possibility of degradation of the lipids. Since the titration curve is nearly vertical at pH 7 (Fig. 2), measurements can be made from this point.

Quantitative differences are shown by the different choline compounds (Table 1). Whereas the system of either sphingomyelin or dipalmitoyl lecithin with sulfatide showed extremely large acid capacity, reacting with 0.42 - 0.44 μ mole of H^+/μ mole complex between pH 7.0 and 3.5, the other two systems with egg or soybean lecithin and sulfatide showed much smaller effects.

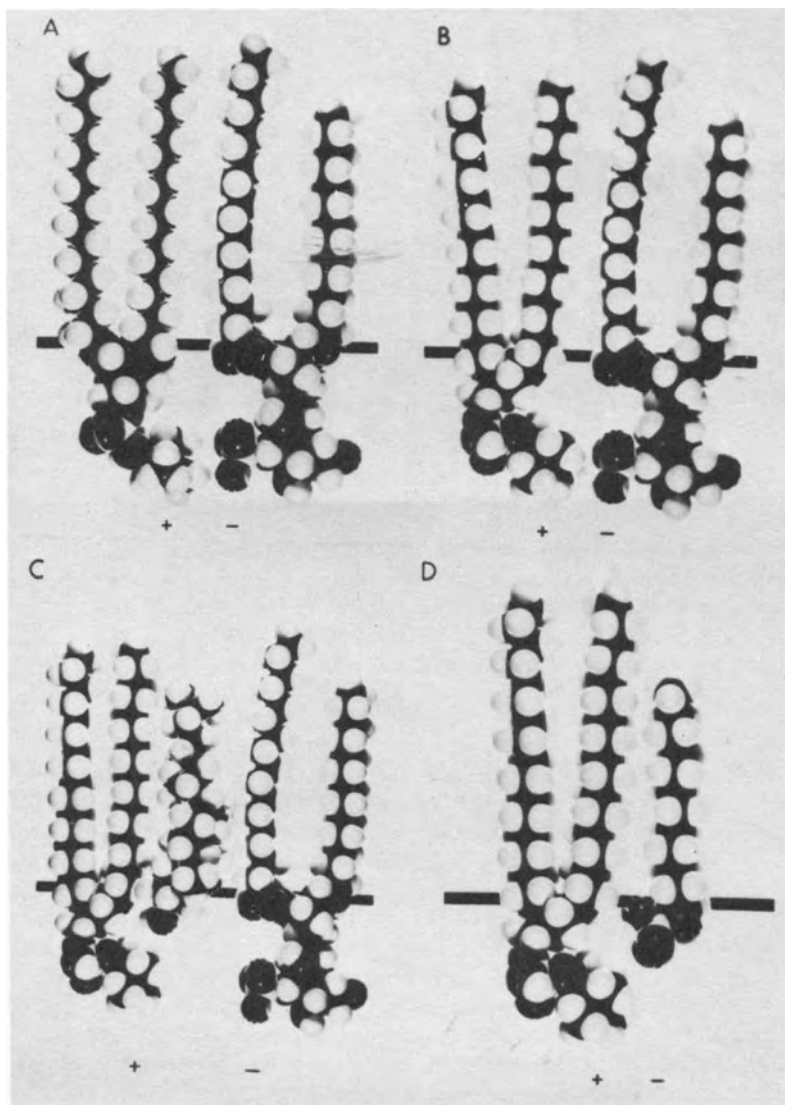


Fig. 1. Corey-Pauling Models of interacting lipid molecules. The continuous aqueous phase is below the horizontal line. The $-N(CH_3)_3^+$ of sphingomyelin or lecithin and $-SO_3^-$ groups of sulfatide are indicated by their charges. The metallic cations are not shown.

- A. sphingomyelin - sulfatide
- B. dipalmitoyl lecithin-sulfatide
- C. dipalmitoyl lecithin-cholesterol-sulfatide
- D. dipalmitoyl lecithin-dodecyl sulfate

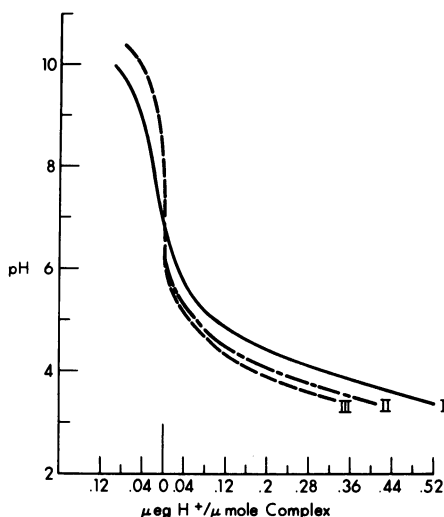


Fig. 2. Titrations of mixed sulfatide-sphingomyelin systems (1:1 molar ratio) performed at 24° in 5 ml using 0.100 N HCl or NaOH. Each curve was corrected by subtracting a blank.

- I 7.9 μ mole sulfatide-sphingomyelin complex in H₂O.
- II 7.7 μ mole sulfatide-sphingomyelin complex in 0.01 M NaCl.
- III 7.5 μ mole sulfatide-sphingomyelin complex in 0.05 M NaCl.

Analogous experiments were carried out with mixtures of dipalmitoyl lecithin and the sodium salt of dicetyl phosphoric acid. These experiments served two purposes: first to demonstrate the degree of dispersion of lecithin systems and the availability of all the ionic groups for interactions; secondly to determine whether the measure of the equivalents of H⁺ that react with these mixtures between two set pH levels gives a relative measure of the equivalents of the ionized component in the lipid systems. We prepared systems containing 9-11 μ mole dipalmitoyl lecithin with increasing amounts of sodium dicetyl phosphate. All of these dispersed easily with small amounts of ultrasonic energy and had low turbidities. The action of the anionic phosphate was similar to that of sulfatide in increasing the dispersibility of lecithin.

Typical titration curves of such mixed systems in water or 0.06M NaCl are shown in Fig. 3. Identifiable equivalence points in salt-free systems were seen at pH 4.25 and 9.3. In this range, the contribution of the dipalmitoyl lecithin to the titration is small. In Fig. 4 is shown the reasonably good agreement of the μ equivalents H⁺ that react in this range with the μ moles sodium dicetyl phosphate present in the systems. This gives support to the view that the anionic component is completely codispersed with

TABLE I: Effect of Dimensions of Choline Lipid on its Interaction with Sodium Sulfatide. Titrations were performed at 24°.

The acid capacity of the mixed lipid systems can be compared with the single lipids given below.

Systems (1:1 molar ratio)	Monolayer		Radius (A) ^o Choline Lipida
	Acid Capacity (μmole H ⁺ /μmole complex)	pH 7.0-4.0	
	pH 7.0-3.5		
Sphingomyelin-sulfatide	0.30	0.44	3.7
Dipalmitoyl lecithin-sulfatide	0.29	0.42	3.7
Egg lecithin-sulfatide	0.19	0.30	4.3
Soybean lecithin-sulfatide	0.10	0.21	4.5
<u>Single Lipids</u>		(μeq H ⁺ /μmole lipid)	
Sphingomyelin	0.083	0.14	
Egg lecithin	0.044	0.058	
Dipalmitoyl lecithin	0.078	0.12	
Sodium sulfatide	0.085	0.16	
Phosphatidylinositol	0.28	0.37 ^b	

a The radius was calculated from the monolayer molecular area at moderate surface pressure (20 dyne/cm), from data of Shah and Schulman (1967 a,b,c).

b Abramson, et al., (1968)

the lecithin and that all the ionic groups are exposed to the aqueous medium. To carry further the parallel between these systems and those with lecithin and sulfatide, we assume that the former could not be titrated below some arbitrarily set pH level such as pH 6. A linear relation is seen in Fig. 4 for the μequivalents H⁺ that react from the equivalence points of pH 9.3 to this cut-off point of pH 6. In this way these μequivalents of H⁺ can give a measure of the relative amounts of anionic compound present in the mixture.

Effect of Cholesterol or Cerebroside on the Ionic Interaction of Lipids

We titrated 1:1 mixtures of sulfatide with choline lipid admixed with varying amounts of cholesterol. The presence of cholesterol in all instances decreased the interaction of the other two lipids (Table 2). The presence of 0.5 μmole cholesterol per μmole complex reduced the acid capacity of sphingomyelin-

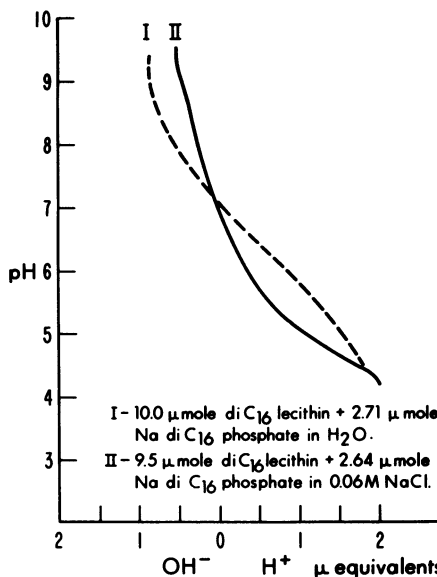


Fig. 3. Titrations of dipalmitoyl lecithin codispersed with sodium salt of dicetyl phosphoric acid at $T = 24^{\circ}$. The minor contribution of the lecithin was subtracted. All systems were brought to pH 10 with NaOH and then titrated with HCl.

- I 10.0 μ mole dipalmitoyl lecithin + 2.7 μ mole Na dicetyl phosphate in H₂O.
- II 9.5 μ mole dipalmitoyl lecithin + 2.6 μ mole Na dicetyl phosphate in 0.06M NaCl.

sulfatide systems to that found for the egg lecithin-sulfatide system alone. Furthermore, a 1 μ mole mixture of cholesterol with 1 μ mole sphingomyelin-sulfatide complex had an acid capacity comparable with that of egg lecithin-sulfatide containing a 0.5 mole ratio of cholesterol. In systems with dipalmitoyl lecithin replacing sphingomyelin and also mixed with sulfatide and cholesterol, the effect of the cholesterol was essentially the same as with the sphingomyelin systems.

Since myelin contains a relatively large percentage of cerebrosides (kerasin and phrenosin) which are structurally related to both sphingomyelin and sulfatide, it was desirable to study the effect of the uncharged cerebrosides on the other two. Sphingomyelin admixed with phrenosin or phrenosin and keratin showed minor differences in titration behavior compared with sphingomyelin alone. This was also true for sulfatide with phrenosin. Systems of sphingomyelin and sulfatide complex

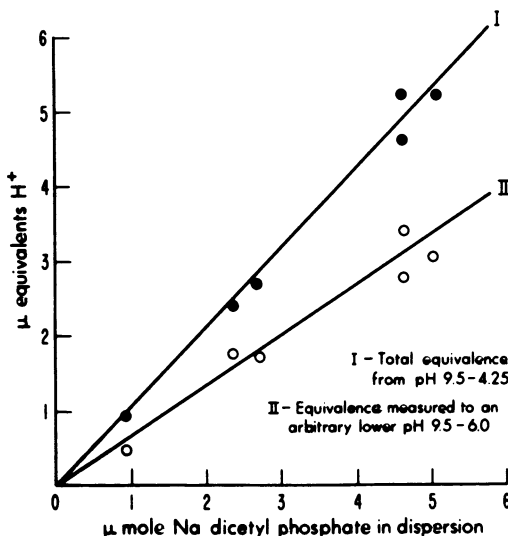


Fig. 4. Relation between the μ mole of Na dicetyl phosphate (co-dispersed with 0.5 - 11.0 μ mole dipalmitoyl lecithin) and the μ equivalents of H^+ reacted in titrations in aqueous systems. This relation shows the complete dispersion of the lipids with availability of the acid groups for reactions.

- I Total number of μ equivalents H^+ that react between equivalence points indicated by the titration curves (pH 9.3 - 4.25)
- II Number of μ equivalents H^+ that react from the equivalence point at pH 9.3 to an arbitrary lower value at pH 6.0.

containing phrenosin showed almost the same titration capacity as observed in the absence of phrenosin (Table 2).

Reactions with Sodium Dodecyl Sulfate

The question arises whether an ionic interaction takes place between a choline lipid and an insoluble long-chain anion with a structure simpler than that of sulfatide. To study such an interaction, sodium dodecyl sulfate was dissolved in chloroform-methanol with choline lipids, and the dried solid was dispersed in water as in the previous experiments. The titration characteristics of these systems are given in Table 3.

An interaction between the long-chain alkyl sulfate with the choline is evident from the titration data. The acid capacity of the phosphate, however, is somewhat less than in the comparable system containing sulfatide. Other similarities, however, do persist; the effect with egg lecithin is less than with sphingo-

TABLE II: Effect of Neutral Lipids on Titration Characteristics of Ionic Lipids in Aqueous Systems at 24°.

Choline Lipid (A)	Molar Ratios			Acid Capacity	
	Acidic Lipid (B)	Neutral Lipid		pH 7.0-3.5 (μmole H ⁺ /μmole Lipid (A))	
Sph*	1.0	-	Chol	2.3	0.091
Egg PC	1.0	-	Chol	1.2	0.063
(μmole H ⁺ /μmole A-B complex 1:1)					
Sph	1.0	Sulf	1.0	-	0.44
Sph	1.0	Sulf	1.0	Chol	0.5
Sph	1.0	Sulf	1.0	Chol	1.0
Dipalm PC	1.0	Sulf	1.0	-	0.42
Dipalm PC	1.0	Sulf	1.0	Chol	0.5
Dipalm PC	1.0	Sulf	1.0	Chol	1.0
Egg PC	1.0	Sulf	1.0	-	0.30
Egg PC	1.0	Sulf	1.0	Chol	0.5
Sph	1.0	Sulf	1.0	Phren	1.0
Sph	1.0	Sulf	1.0	Phren	2.2
Sph	1.0	Sulf	0.5	Phren	2.2
Dipalm - dipalmitoyl Chol - cholesterol Phren - phrenosin					
*Sph - sphingomyelin					
PC - lecithin					
Sulf - sulfatide					

myelin, and the inclusion of cholesterol reduces the effect.

Cation-Proton Exchange

When solutions of calcium chloride or alkali metal chloride were added to aqueous systems of the single lipid, sulfatide, lecithin or sphingomyelin, very small and non-reproducible changes in pH resulted. When a mixed system of sulfatide and sphingomyelin or sulfatide and egg lecithin was brought to pH 4.00 by the addition of hydrochloric acid, and solutions of these chloride salts, also brought to pH 4.00, were added, a sharp drop in pH resulted. A definite relationship was found for the H⁺ ion released and the type and concentration of cation added to the system. To study this relationship the experimental procedure

TABLE III: Titration Characteristics of Aqueous Dispersions of Systems Containing Sodium Dodecyl Sulfate (NaDS) at 24°.

		Acid Capacity μmole H ⁺ /μmole pH 7.0-3.5
NaDS	Molar Ratio	μmole H ⁺ /μmole Complex
Sphingomyelin+NaDS	1:1	0.29
Egg Lecithin+NaDS	1:1	0.18
Sphingomyelin+NaDS	1:1 Cholesterol 0.5	0.16
Egg Lecithin+NaDS	1:1 Cholesterol 1.0	0.065

followed was the addition of a small amount of a concentrated solution of the salt, the system was then permitted to come to a stable pH. The volume of standard NaOH required to return the system to pH 4.00 gave a measure of the cation-proton interaction. With increasing concentrations of salt the release of protons diminished so that little further change resulted at concentrations greater than 0.05 M univalent cation or 1 mM CaCl₂ (Fig. 5). For a 1:1 sphingomyelin-sulfatide system at pH 4.00 and 24°, the effects of KCl and NaCl were roughly alike. At a concentration of 0.05 M salt, 0.24 - 0.26 μmole H⁺ was exchanged per μmole of complex, with a small further increase at 0.100 M salt. Calcium chloride solutions produced an equal effect at a concentration of 1 mM. Solutions of choline chloride produced a somewhat smaller effect, exchanging 0.10 μmole H⁺/μmole complex at a concentration of 0.05 M choline. A noteworthy observation is that the total effect of the calcium ion was not greater than that of the alkali metals, as it is in other acidic lipid systems (phosphatidic acid or phosphatidylinositol). This may be the result of the reduced ability of the bivalent cation to bridge two negative charge sites in the mixed lipid systems studied here.

In mixed systems consisting of egg lecithin and sulfatide at pH 4.0 and 24°, the exchange of cations for H⁺ was less than in comparable sphingomyelin-sulfatide systems. At 0.05 M NaCl or KCl, 0.09 μmole of H⁺ per μmole complex was exchanged. In these systems, the effectiveness of choline was the same as NaCl or KCl.

The interaction of cations with sphingomyelin-sulfatide systems is also shown by their titrations in 0.01 and 0.05 M salt as compared with salt free systems (Fig. 2). Here again, a greater effect of NaCl or KCl as compared with choline chloride was shown.

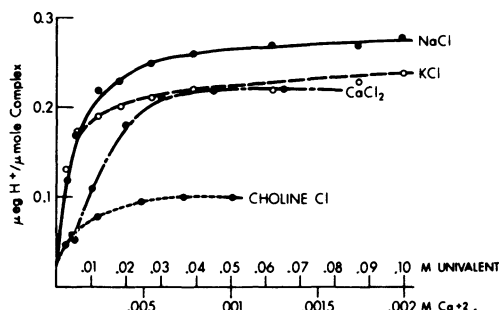


Fig. 5. Cation-proton exchange with mixed sulfatide-sphingomyelin systems (1:1 molar ratio) maintained at pH 4.0 and 24°. Each system contained 7.5 to 7.8 μ moles of 1:1 complex in 5 ml. After each addition of concentrated salt solution at pH 4.0 the μ eq of NaOH required to maintain constant pH gave a measure of the μ eq H⁺ exchanged.

DISCUSSION

In explaining the differences in the extent of the interaction of sulfatide with the four choline lipids studied, we compare the hydrocarbon chains in these compounds. Unlike dipalmitoyl lecithin in which the acyl chains are fully saturated, egg lecithin contains approximately 50% unsaturated fatty acids, while in soybean lecithin 75% of the hydrocarbon chains are unsaturated with many polyunsaturations (Shah and Schulman, 1967a). Sphingomyelin contains a small percent of unsaturated chains. It has been shown (Shah and Schulman, 1967b; Demel et al., 1967) that the area of choline lipids as measured by monolayer experiments increased with the unsaturation of the hydrocarbon chain. Assuming that the lipid aggregates we studied are at moderate and roughly equal surface pressures, then using the radius calculated from the molecular area at 20 dyne/cm (Shah and Schulman, 1967a, b,c), the distance between a negative charge site on the sulfatide molecule and the positive nitrogen of the neighboring choline lipid would probably increase as the area of the fatty acid chains increase. If such factors as polarization and dielectric constants are presumed to be unchanged, the extent of the ionic interaction of the two lipids would decrease with the square of the charge separation. Although the actual distance between charges cannot be given precisely, the increased dimensions of the choline lipid give some indication of the increasing separation as the lipid becomes more unsaturated. The resulting decrease in acid capacity in Table I may be compared with the changes in radius of the choline lipid.

When cholesterol, sulfatide, and choline lipid are dissolved in warm chloroform-methanol (2:1, v/v) and stirred, the 3 components become intermixed, and on evaporation of the solvent, the solid residue is this mixture of lipids. We assume that when this solid is dispersed in an aqueous medium, each particle contains a mixture of the lipids. The decreased interaction between sulfatide and the choline lipids (Table 2) can be interpreted as the result of the interpenetration of the cholesterol between the other lipid molecules.

It is interesting to relate these changes in the titration characteristics of mixed lipid systems containing cholesterol with some of the data available from studies of mixed monolayers. Shah and Schulman (1967b) find that lecithin-cholesterol monolayers in the absence of Ca^{+2} ions remain in the liquid state except at high surface pressures. If this condition persists with the additional presence of sulfatide, the mobility of the molecules in the lamellar aggregates should permit the arrangement leading to minimum free energy. Since the ionic interaction between the sulfatide and choline lipid is reduced by increasing the concentration of cholesterol in the lipid systems, this leads us to the view that the coulombic forces are not able to "squeeze out" the cholesterol molecules. This may be either the result of ion-dipole interaction between cholesterol and the choline lipid or due to the geometric structures of these molecules which permit a favorable packing arrangement. From Table 3, we can see that cholesterol produces a similar decrease in the interaction between sodium dodecyl sulfate and choline lipids such as occurs with sulfatide and choline lipids. If we assume an association of cholesterol with the choline lipid persisting in the presence of a third component (sulfatide), we may then use data obtained from mixed monolayers for the average molecular areas in lecithin-cholesterol systems (Table 4). A 1:1 molar mixture of dipalmitoyl lecithin-cholesterol monolayer at 20 dyne/cm surface pressure has an area of 80 \AA^2 for the two molecules, whereas a 1:0.5 mixture of these lipids has an average molecular area of 45 \AA^2 , giving an apparent area of 68 \AA^2 for the lecithin-cholesterol association. At an equal surface pressure, a mixed egg lecithin monolayer in 1:0.5 mole ratio with cholesterol has an area of 84 \AA^2 for the mixture and for egg lecithin alone, a molecular area of 71 \AA^2 . The reasonable agreement between the changes in the combined molecular area for the lecithin cholesterol association and the decreased interaction between sulfatide and lecithin adds weight to a relatively simple explanation based upon the combined area of the cholesterol with the choline lipid as the predominant factor in determining the extent of interaction with the sulfatide in these mixtures. This is further supported by the almost identical results obtained with sphingomyelin and dipalmitoyl lecithin which, despite their different nonpolar structures, are alike in molecular area and in their phosphoryl choline portions.

TABLE IV: Relation Between I. Molecular Area of Lecithin-Cholesterol Association and II. Acid Capacity of 1:1 Complex of Lecithin-Sulfatide with Added Cholesterol

Molar ratio	Average Molecular area ^a Å ²	I Combined molecular area lecithin-cholesterol association Å ²	II Acid Capacity 1:1 lecithin-sulfatide complex pH 7 - 3.5 μmole H ⁺ /μmole complex
Dipalmitoyl lecithin-cholesterol 1:0.5	45	68	0.31
Dipalmitoyl lecithin-cholesterol 1:1	40	80	0.23
Egg lecithin	71	-	0.30
Egg lecithin-cholesterol 1:0.5	56	84	0.24
Soybean lecithin	78	-	0.21

^aAdapted from monolayer measurements Shah and Schulman (1967 b).

As shown by Table 2, the addition of phrenosin to the sphingomyelin-sulfatide complex does not have the same effect as cholesterol. From the structural similarity of phrenosin and the other two lipids as well as their occurrence together in biologic systems, it would appear that the cerebroside (phrenosin) enters the lipid lamellar structure with its molecules parallel to the other sphingolipids, the polar galactose moiety of the cerebroside extending into the aqueous medium. However, the positions taken by the cerebroside molecules are between the units of bimolecular complexes and not between the molecules of the complex, as though the cerebroside is unable to break the ionic bond. In this way, the ionic characteristics of the complex remain unchanged.

To explain the smaller effect produced by sodium dodecyl sulfate than by sulfatide in the reaction with the choline lipids, the structural features of these two sulfates are compared. In sodium dodecyl sulfate the negative charge site is not far removed from the hydrocarbon chain. At the lipid-aqueous interface, the anionic site is close to the phase boundary. Sulfatide is

somewhat more hydrophilic due to the galactose present so that the sulfate will be further below the interface than in the case of the alkyl sulfate. As seen in Fig. 1, Corey-Pauling models of the choline lipids and sulfatide show the choline-positive and sulfatide-negative groups on a plane parallel to the lipid-water interface, but this arrangement is not seen when sulfatide is replaced by an alkyl sulfate.

It is well-established that the acid and base groups of choline lipids are not available for titration (except at very low and very high pH levels) and are presumably bound in some manner. This may be an intermolecular salt linkage between the quaternary amine of one molecule and the phosphate of another as suggested by Pethica (1965). Alternatively, it may involve an intramolecular bond between the ionic groups, or as suggested by Sundaralingam (1968) a bond between the nitrogen and the phosphate-ester oxygen. Intermolecular ion binding between choline lipid molecules could add to membrane cohesion. Our titrations of sphingomyelin-cholesterol reveal no increase in titrability of the acid group as compared with sphingomyelin alone. Similar results were found with egg lecithin-cholesterol systems. This may be evidence of the absence of intermolecular ion bonds between lecithin or sphingomyelin molecules. However, in the presence of an amphipathic anion (sulfatide or dodecyl sulfate), an intermolecular ionic linkage is established.

The release of H^+ ions that takes place on adding salt solutions to our choline lipid-sulfatide systems can be interpreted along either of two alternative paths: I: The effect may be the result of a change in the phosphate that was made available by the interaction of the sulfatide with the choline lipid. This reaction may resemble the changes that take place when cations are added to incompletely ionized phosphatidic acid or phosphatidylinositol (Abramson et al., 1968). Another possible explanation that would be unique for the inter-lipid ionic bond is: II: The increased ion concentrations in the system may lead to a rupture of the bond between the sulfate and the positive site of the choline molecule. This then permits the phosphate to re-establish its normal intra-molecular phosphoryl-choline bonding. Since the phosphate has been shown to be ionic in lecithin and sphingomyelin (Abramson et al., 1965), the change from an incompletely ionized to a fully ionized phosphate leads to a release of protons. If the latter mechanism is the actual one, it signifies the breaking of an ionic intermolecular linkage between lipids, with attending structural changes, produced by cations in solution. Earlier studies of cation-proton exchange with phosphatidylinositol systems in water at pH 3.5 showed that on bringing the system to 0.05 M Na^+ or K^+ , roughly 0.16 μ mole H^+/μ mole lipid was exchanged, whereas titrations showed the maximum protons available as determined by the fraction

of unionized phosphatidylinositol at pH 3.5 is 0.30. In the system of sphingomyelin-sulfatide, at pH 4.0 the H⁺ ions available for exchange are 0.30 μmole/μmole complex, while the exchange with alkali metal ions is 0.24 - 0.26 μmole/μmole complex. A much greater proportionate change takes place than with phosphatidyl-inositol. This may be an indication that the two reactions are not alike, and that the H⁺ ion release detected in our mixed lipid systems results from the rupture of the intermolecular bond as described in mechanism II.

In a theoretical treatment of lecithin in water systems, Parsegian considers the positive choline regions of the lecithin as constituting a diffuse layer of counterions bordering the surface of lipid molecules given negative charges by the ionic phosphate (Parsegian, 1967). The positive charges are free to diffuse within a distance of 5Å from the surface at the ends of the flexible -CH₂-CH₂- linkage. In our studies of mixed lipids we can visualize the positive choline as shifting its position from a counterion for phosphate to the sulfate. The limitation of the 5Å length of the CH₂ linkage then explains the decreased effect when the intermolecular distances increase with increased unsaturation of the lecithin molecule.

REFERENCES

- Abramson, M.B., and Katzman, R. (1968), Science, 161, 576.
Abramson, M.B., Colacicco, G., Curci, R., and Rapport, M.M. (1968), Biochemistry, 7, 1692.
Abramson, M.B., Katzman, R., Curci, R., and Wilson, C.E. (1967), Biochemistry, 6, 295.
Abramson, M.B., Norton, W.T., and Katzman, R. (1965), J. Biol. Chem., 240, 2389.
Bangham, A.D., Standish, M.M. and Watkins, J.C. (1965), J. Mol. Biol., 13, 238.
O'Brien, J.S. (1967), J. Theoret. Biol., 15, 307.
Parsegian, V.A. (1967), Science, 156, 939.
Pethica; B.A. (1965) In Surface Activity and the Microbiol Cell, Soc. Chem. Ind. (London) 19, p. 85.
Shah, D.O., and Schulman, J.H. (1967a), J. Colloid Interface Sci., 25, 107.
Shah, D.O., and Schulman, J.H. (1967b), Jour. Lipid Res., 8, 215.
Shah, D.O. and Schulman, J.H. (1967c), Biochim. Biophys. Acta, 135, 184.
Sundaralingam, M. (1968), Nature, 217, 35.

LIPID-POLYMER INTERACTION IN MONOLAYERS: EFFECT OF
CONFORMATION OF POLY-L-LYSINE ON STEARIC ACID MONOLAYERS

Dinesh O. Shah

Surface Chemistry Laboratory, Marine Biology Division
Lamont-Doherty Geological Observatory of Columbia
University, Palisades, New York

ABSTRACT

Surface pressures and surface potentials of stearic acid monolayers were measured at various pH values in the presence and absence of poly-L-lysine in the subsolution. The presence of poly-L-lysine strikingly influences the state of stearic acid monolayers. Surface potential measurements indicated that the maximum interaction between poly-L-lysine and stearic acid monolayers occurred between pH 10 and 11. Poly-L-lysine solutions exhibited surface activity in the same pH range. Air bubbles covered with poly-L-lysine films showed maximum stability at pH 11. These results indicate that in the pH range 10-11, where coil-to-helix transition occurs in solution, poly-L-lysine has partial or complete helical conformation which causes the slowest rate of drainage of water in bubble lamellae, and which also exhibits surface activity and hence, increases the interaction of poly-L-lysine with stearic acid monolayers. The implications of these findings for lipid-protein associations in biomembranes are discussed.

INTRODUCTION

Lipid-protein interactions are of great interest to understand the structure and function of biological membranes. Various approaches have been taken to elucidate the interaction of lipids and proteins in biological membranes. In recent years, nuclear magnetic resonance and electron spin resonance spectroscopy have been used profitably to investigate these interactions (1-4). Phospholipid bilayers and monolayers have served as useful models for these studies (5-6). The monolayer

*Lamont-Doherty Geological Observatory Contribution No. 1404.

approach has been found very useful to understand molecular mechanisms presumably occurring at the cell surface (7-10).

Earlier studies on lipid-protein interaction in monolayers were reported by Schulman and his co-workers (11-12) who investigated the interaction of albumin, globulin and haemoglobin with cholesterol, cephalin, cardiolipin, alkyl sulfate and alkyl trimethylammonium monolayers. Eley and Hedge (13,14) studied protein-protein and protein-lipid interactions in fibrinogen, thrombin, albumin, lecithin and cephalin monolayers. The interaction of synthetic dihydroceramide lactoside monolayers with globulin, albumin, and ribonuclease was investigated by Colacicco, Rapport and Shapiro (15). These workers (16) have also shown from their studies on the interaction of apoprotein with various lipid monolayers, that the unusual surface activity of apoprotein may be intimately related to the mechanism of formation of the lipo-protein. Recently, Arnold and Pak (17) have investigated protein-protein interaction in monolayers.

To investigate the interaction of water with films, Trapeznikov (18) and Garrett (19) have studied the stability of bubbles covered with a monolayer of surface-active materials. In general, the stability of such bubbles is related to the rate of drainage of water in the bubble lamellae. The interaction of polar groups with water (i.e. hydration of polar groups) impedes the drainage of water in the lamellae, and, hence, increases the time required to reach a critical thickness where bubble lamellae break. Therefore, more strongly hydrated molecules increase the bubble stability. This method was used in the present study to investigate the hydration of stearic acid and poly-L-lysine films.

It has been recognized that both ionic and hydrophobic interactions play a role in the lipid-protein association. A simple model system of stearic acid and poly-L-lysine was selected to investigate various aspects of the ionic interaction in the present studies, since the ionic properties of stearic acid monolayers (20,23) and of poly-L-lysine solutions (24) have been established. The objective of the present studies was to investigate how the ionization of carboxyl groups in the monolayer and the conformation of poly-L-lysine in the subsolution influence interactions at the interface.

EXPERIMENTAL

Materials: Poly-L-lysine hydrochloride (molecular weight 100,000 - 200,000) was bought from Mann Research Laboratories Inc. (New York, N.Y. 10006). Highly purified (>99%) stearic acid was purchased from Applied Science Laboratories, Inc. (State College, Pa., 16801). Inorganic chemicals of reagent grade and distilled-deionized water were used in all experiments.

For pH close to 2, the solutions of 0.05 M HCl were used; for pH 3 to 6, 0.05 M buffer solutions of citric acid-sodium citrate were used; for pH 7 to 9, 0.05 M buffer solutions of tris-HCl were used; for pH 10 to 11, 0.05 M buffer solutions of glycine-NaOH were used; for pH 12 to 13, 0.05 M and 0.1 M solutions of NaOH were used. The buffer solutions were prepared according to Biochemists' handbook (25). A stock solution of 5 mg poly-L-lysine per ml of distilled water was prepared. 2.4 ml (containing 12 mg of poly-L-lysine) of this solution was added to 100 ml of the subsolution for surface measurements. The stearic acid was dissolved in chloroform-methanol-hexane (1:1:3 v/v/v) in a concentration of about 0.8 mg/ml.

Methods: The surface pressure was measured by a modified Wilhelmy plate method, and the surface potential by a radioactive electrode, as described previously (26). The state of the monolayers was determined qualitatively by the talc method (27). The monolayers of stearic acid were spread on buffered subsolutions in the presence and absence of poly-L-lysine (12 mg/100 ml subsolution).

Bubble stability: The survival time (i.e., the time interval between the formation and collapse) of bubbles was measured with a stopwatch after producing a small air bubble by a dropper (tip diameter 1 mm) under monolayers and subsolutions in the following manner. When a monolayer was compressed to its limiting area ($\approx 20 \text{ } \mu\text{m}^2/\text{molecule}$), a bubble was produced on each side of the compression glass barrier. For subsolutions containing poly-L-lysine, the monolayer side of the compression barrier showed surface properties of stearic acid + poly-L-lysine, whereas the other side of the barrier showed those of adsorbed film of poly-L-lysine alone. At least ten measurements were made for bubble stability. It should be pointed out that since the collapse of a bubble produces considerable structural reorganization and rearrangement of molecules in the monolayer, a second bubble should not be produced in the same region of the monolayer. Therefore, all ten bubbles were produced in different parts of the monolayer and their average survival time was calculated.

The surface tension of buffered solutions of poly-L-lysine was measured with a Roller-Smith surface tensiometer. The surface pressure (π) of poly-L-lysine solutions is defined as $\pi = \sigma_0 - \sigma_p$, where σ_0 is the interfacial tension without poly-L-lysine and σ_p is that with poly-L-lysine in the subsolution; hence, π represents the lowering of the surface tension of buffer solutions by the presence of poly-L-lysine.

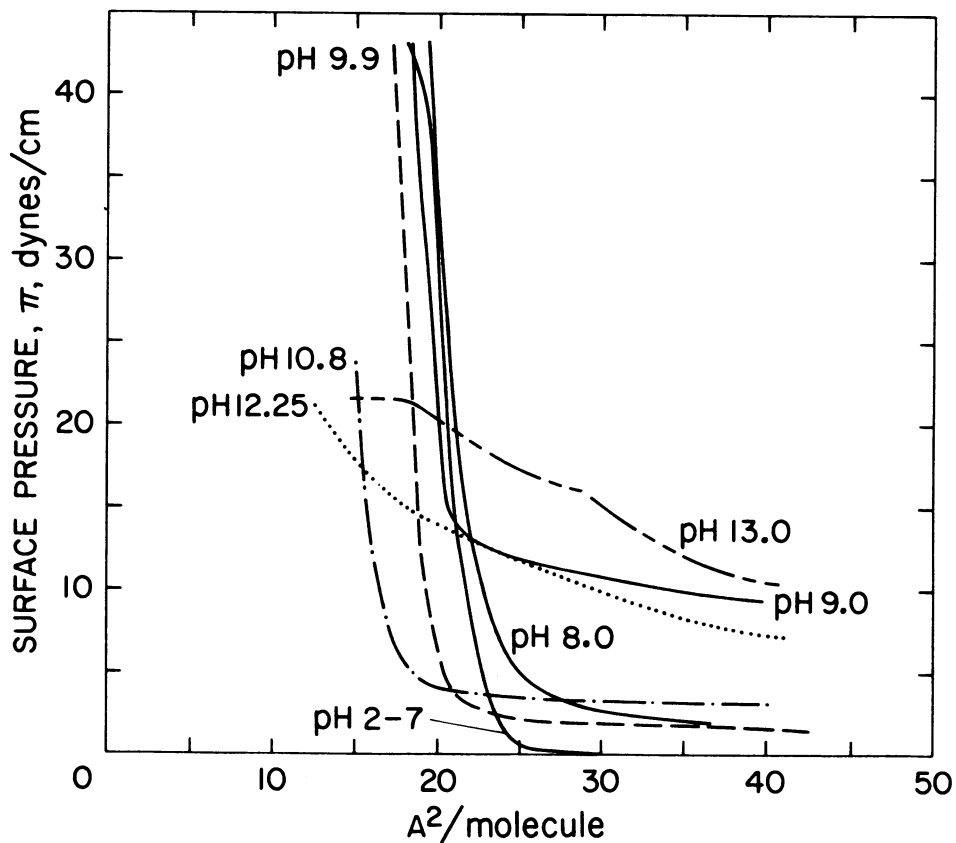


Fig. 1. Surface pressure-area curves of stearic acid monolayers on buffered subsolutions at various pH values at 22°C.

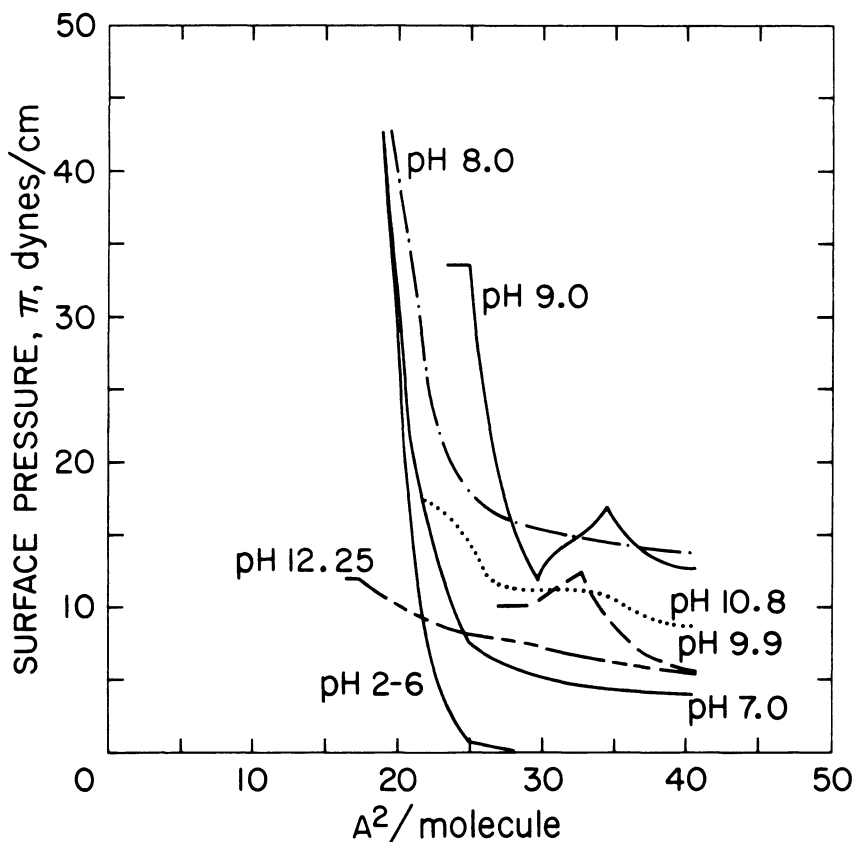


Fig. 2. Surface pressure-area curves of stearic acid monolayers on buffered subsolutions containing 0.02 mg/ml of poly-L-lysine at various pH values at 22°C.

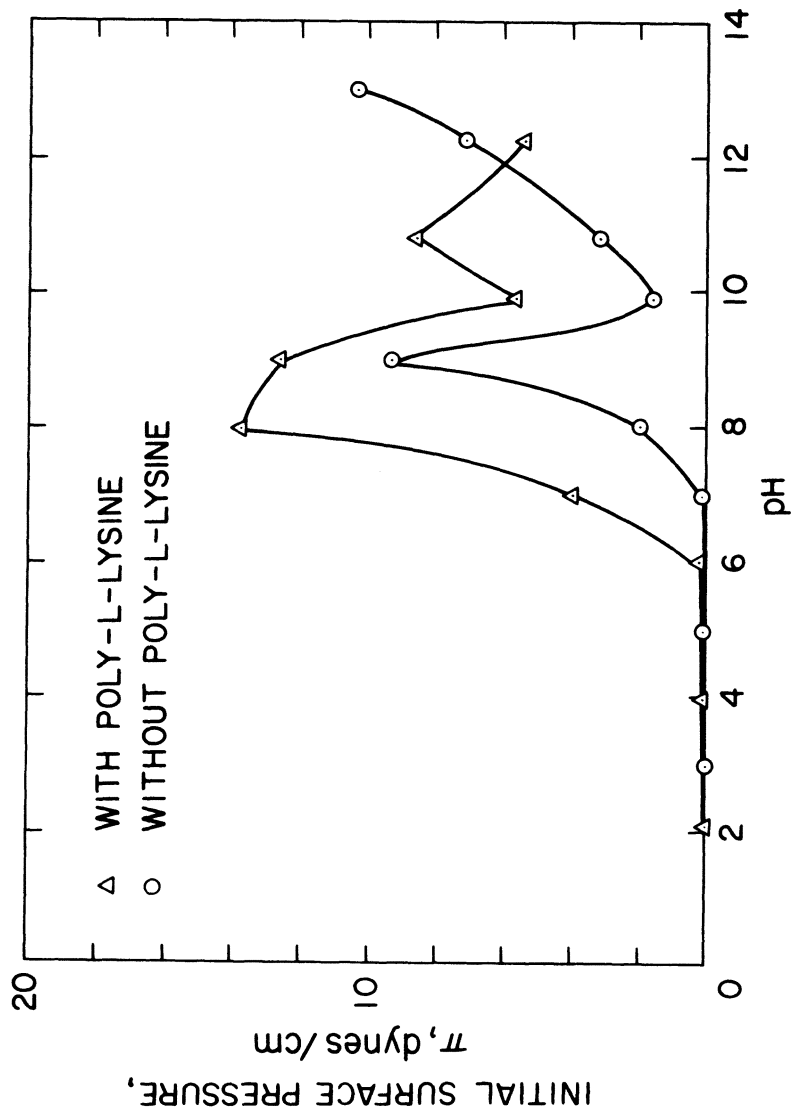


Fig. 3. Initial surface pressure values of stearic acid monolayers on buffered sub-solutions in the absence (○) and presence (△) of poly-L-lysine (0.12 mg/ml) at various pH values at 22°C.

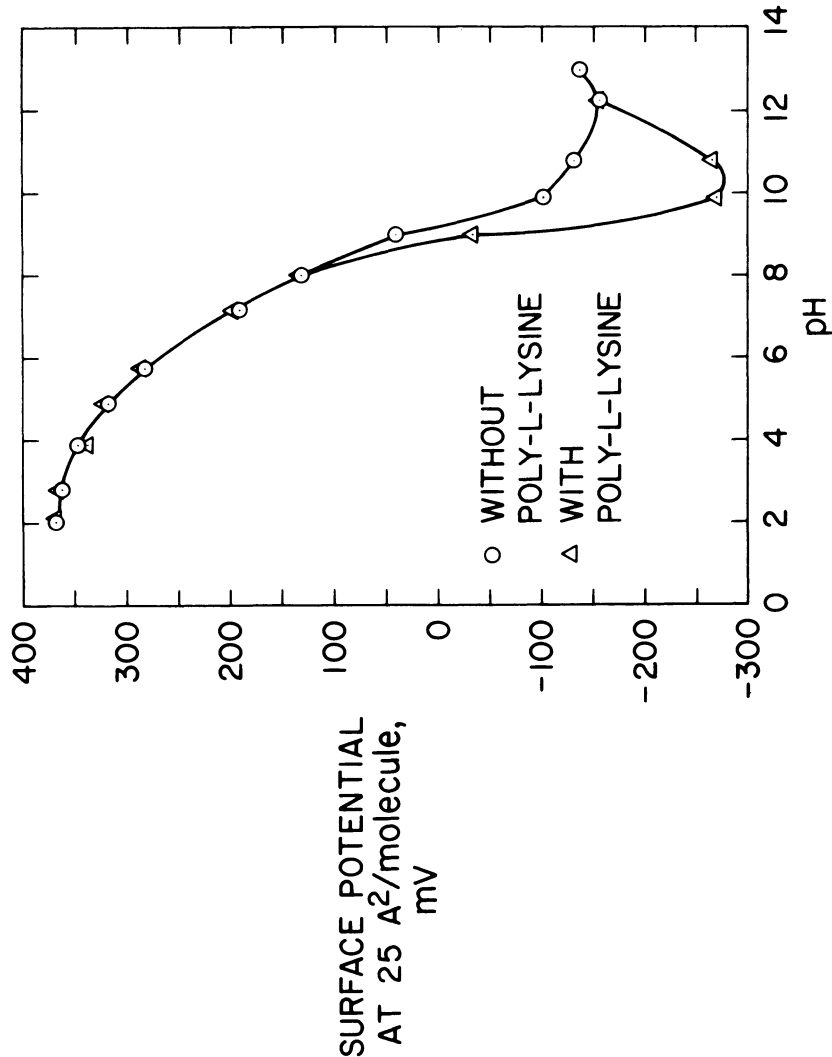


Fig. 4. Surface potentials of stearic acid monolayers at $25 \text{ A}^2/\text{molecule}$ molecule on buffered subsolutions in the absence (○) and presence (△) of poly-L-lysine (0.12 mg/ml) at various pH values at 22°C .

RESULTS

Figures 1 and 2 show surface pressure-area curves of stearic acid monolayers in the absence and presence of poly-L-lysine in subsolutions of different pH values. It has been shown (28) that the plateau region in the surface pressure-area curves of stearic acid at large area per molecule is directly related to repulsion in the monolayers because of ionization of carboxyl groups. Figure 3 shows the surface pressure values where the plateau region begins for different pH values. In general, the presence of poly-L-lysine increases these initial surface pressure values and shifts the curve to the left (or acid side).

Figure 4 shows the surface potentials of stearic acid monolayers at $25 \text{ \AA}^2/\text{molecule}$ in the presence and absence of poly-L-lysine at various pH values. It is evident that the interaction of poly-L-lysine with stearic acid monolayers lowers the surface potential and that the maximum interaction occurs in the pH range 10 to 11.

Table I summarizes the state of stearic acid monolayers near the collapse pressure in the presence and absence of poly-L-lysine in the subsolution at various pH values. It shows that the interaction between stearic acid monolayers and poly-L-lysine in the pH range 9 to 11 solidifies the monolayers.

The upper part of figure 5 shows the data of Applequist and Doty (24) on poly-L-lysine solutions. The lower part of figure 5 shows our data on the bubble stability of stearic acid monolayers in the presence of poly-L-lysine in the subsolution. The bubble stability for stearic acid monolayers alone, which is not shown in figure 5, did not exceed 10-15 seconds over the whole pH range. The surface activity (or surface pressure) of poly-L-lysine solutions and bubble stability at various pH values are also shown in figure 5. It is evident from figure 5 that at pH 11, the conformation of poly-L-lysine molecules, which is nearly helical and surface-active, affords maximum stability to bubble lamellae.

DISCUSSION

Figure 1 shows that for pH values from 2 to 9, the limiting area of stearic acid is approximately the same ($\approx 20 \text{ \AA}^2/\text{molecule}$), implying that the monolayers are insoluble in this pH range. At pH 9.9 and 10.8, the limiting areas are respectively 16 and $18 \text{ \AA}^2/\text{molecule}$, which may be due to slight solubility of ionized stearic acid molecules in the subsolution, or to rearrangement of molecules in the monolayers. The initial surface pressure values

TABLE I

pH	Subsolution	Subsolutions without Poly-L-lysine		The state of monolayers	The state of monolayers
		The state of monolayers	Subsolutions with Poly-L-lysine		
2.0	HCl solution	liquid		liquid	liquid
2.8	citric acid-sodium citrate buffer	liquid		liquid	liquid
3.9	citric acid-sodium citrate buffer	liquid		liquid	liquid
4.9	citric acid-sodium citrate buffer	liquid		liquid	liquid
5.75	citric acid-sodium citrate buffer	liquid		liquid	liquid
7.15	tris - HCl			solid	solid
8.0	tris - HCl			solid	solid
9.0	tris - HCl		gel (+)*	solid	solid
9.9	glycine-NaOH buffer		gel (+)	solid	solid
10.8	glycine-NaOH buffer		gel (++)	solid	solid
12.25	NaOH solution	gel (+++)	gel	gel	gel

*The number of + signs indicates qualitatively the increasing surface viscosity of the monolayers.

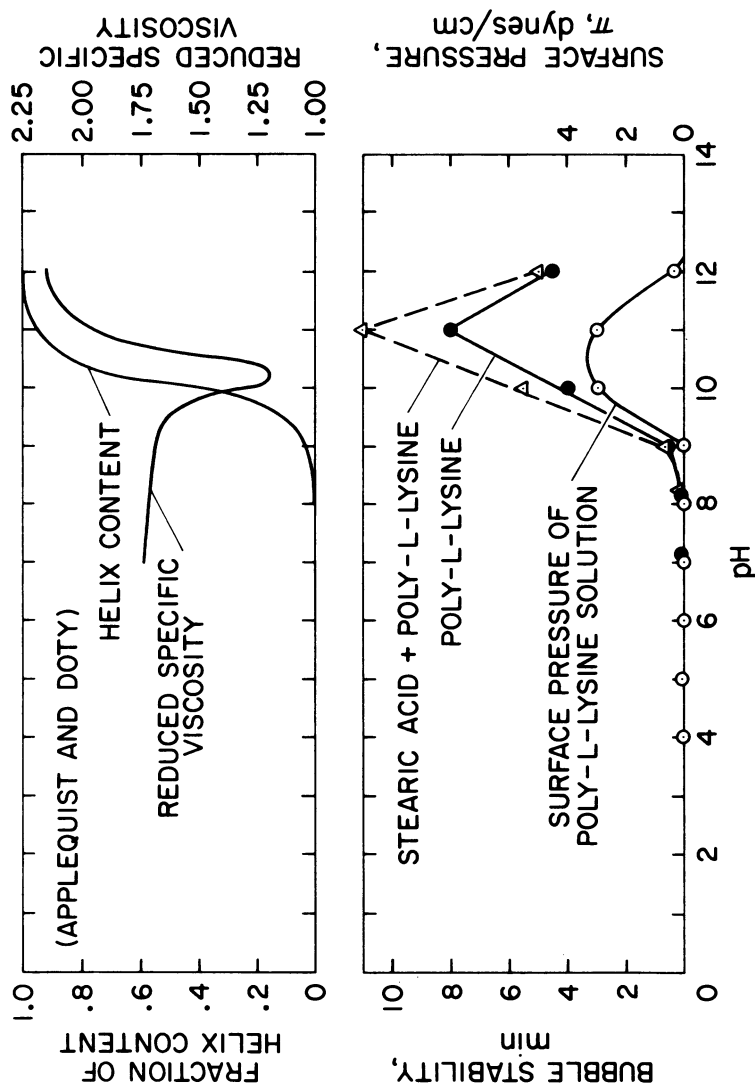


Fig. 5. Data of Applequist and Doty on helix content and reduced specific viscosity of poly-L-lysine solutions (upper part) surface pressure (or surface activity), and bubble stability of poly-L-lysine solutions (lower part). The bubble stability of stearic acid monolayers in the presence of poly-L-lysine is shown by a broken line, whereas that of stearic acid alone was 10–15 seconds in the whole pH range.

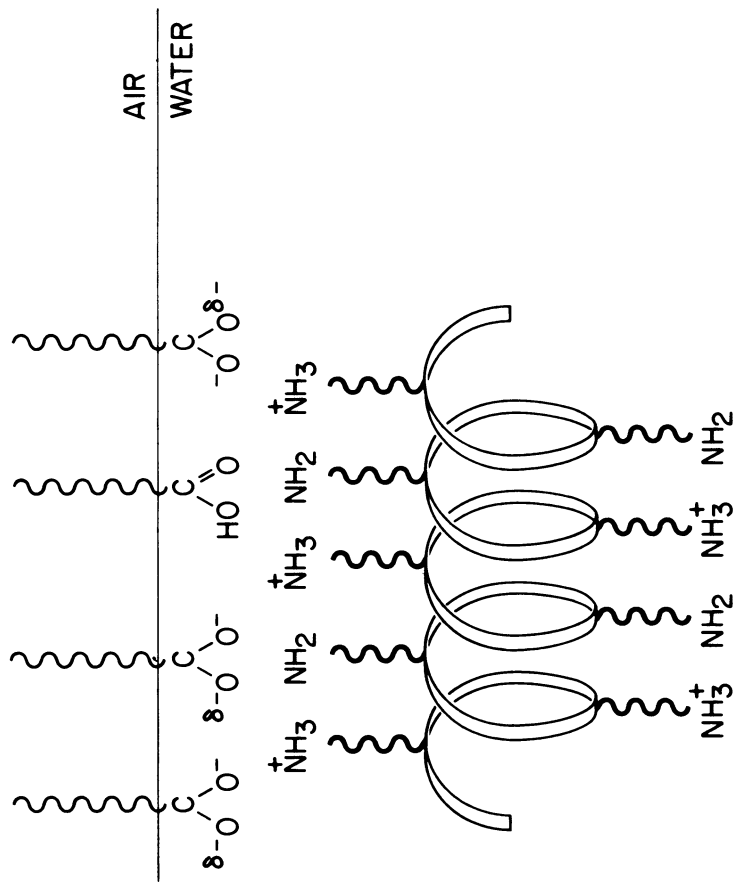


Fig. 6. Schematic representation of interaction between stearic acid and poly-L-lysine in monolayers at pH 11. δ^- represents a partial ionic charge on oxygen atoms.

of the plateau region indicate the extent of ionic repulsion in monolayers (fig. 1). As shown in figure 2, the presence of poly-L-lysine strikingly alters the surface pressure-area curves of stearic acid monolayers above, but not below pH 6, indicating that poly-L-lysine does not interact with stearic acid monolayers in the pH range 2 to 6.

It is interesting to compare the effect of cations such as calcium with poly-L-lysine on stearic acid monolayers. It has been shown (29-31) that the binding of calcium ions to stearic acid monolayers begins to occur at about pH 5; this causes condensation of the monolayers. In contrast, the interaction between poly-L-lysine and stearic acid expands the monolayers presumably due to penetration of side chains of poly-L-lysine in the monolayers. The kinks in the surface pressure area curves at pH 9.0 and 9.9 at about $35 \text{ A}^2/\text{molecule}$ indicate the areas at which presumably some of the penetrated side chains of poly-L-lysine are squeezed out of the monolayers (fig. 2).

Figure 3 shows the initial surface pressure values of the plateau region in the presence and absence of poly-L-lysine in subsolutions. Stearic acid monolayers without poly-L-lysine show a maximum at pH 9, whereas, the maximum occurs at pH 8.0 in the presence of poly-L-lysine in the subsolution.

It has been shown (28, 32) that at pH 9, where 50% of the molecules are ionized (i.e., $\text{pK} = 9$), there is maximum separation between the molecules in stearic acid monolayers. It is clear that in the presence of poly-L-lysine in subsolutions, the maximum separation occurs at pH 8.0, which suggests that the pK value has shifted by one pH unit. A similar decrease in the pK of oleic acid by the presence of calcium ions was reported by Benzonana and Desnuelle (33). A second maximum observed at pH 11 may be due to the penetration of poly-L-lysine into the monolayers. In general, the initial surface pressure values above pH 6 are higher in the presence of poly-L-lysine in the subsolution than in the absence of it. This can be explained as follows: because of coulombic attraction the cationic side chains of poly-L-lysine may penetrate the negatively charged stearic acid monolayers. This will increase the surface concentration of molecules and, hence, the surface pressure in monolayers.

Figure 4 shows the surface potentials of stearic acid monolayers in the presence and absence of poly-L-lysine in subsolutions. It shows that the maximum interaction occurs in the pH range 10-11 where the surface potential decreases by about 175-185 mv. It is interesting to note that the presence of calcium ions in the subsolution also decreases the surface potential of stearic acid monolayers by about 200 mv (31). Hence, the

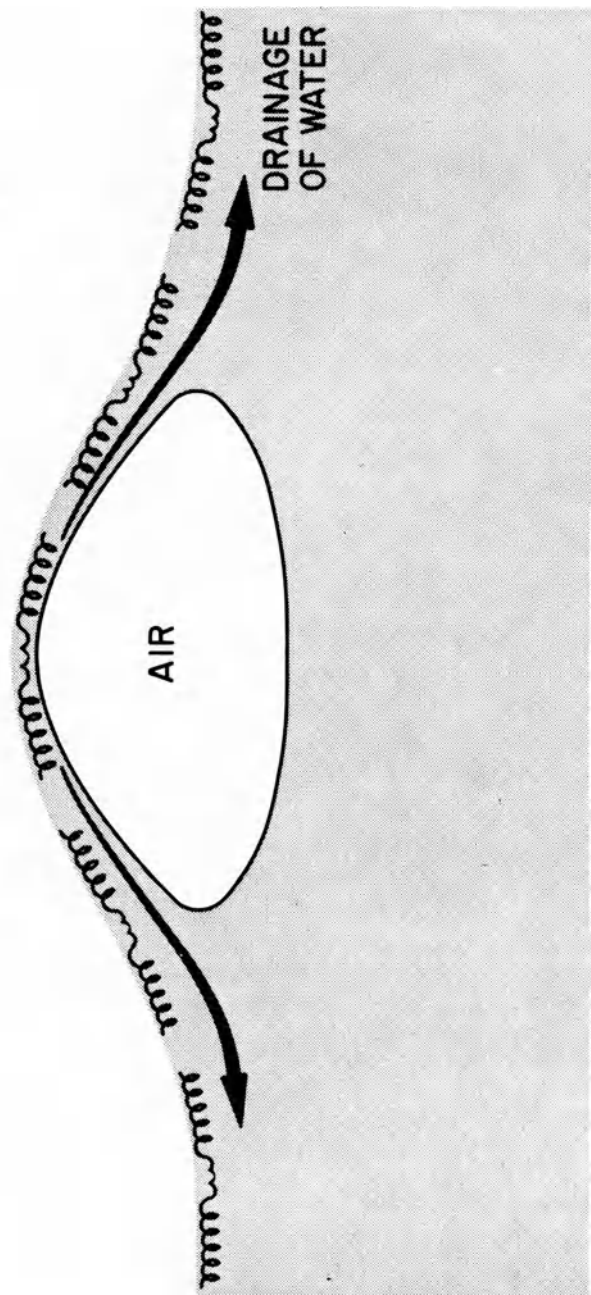


Fig. 7. Schematic representation of the mechanism governing the stability of an air bubble covered with a film. A faster rate of drainage of water in the lamellae decreases the bubble stability.

mechanism of action of poly-L-lysine on stearic acid monolayers is presumably the same as that of calcium ions. In contrast, the interaction of calcium ions with lecithin, sphingomyelin, cardiolipin and dicetyl phosphate monolayers increases the surface potentials (26, 34, 35).

Applequist and Doty (24), using birefringence, viscosity, sedimentation and optical rotatory dispersion measurements, have shown that random coil-to-helix transition in poly-L-lysine solutions occurs in the pH range 10 to 11. The dissociation of NH_3^+ groups also takes place in this pH range. Figure 6 schematically shows the interaction of poly-L-lysine with stearic acid monolayers at pH 11 where poly-L-lysine molecules have nearly helical conformation.

Figure 5 shows that poly-L-lysine solutions exhibit surface activity (or surface pressure) in the pH 10 to 11. Although the surface pressure of poly-L-lysine is very low (3 dynes/cm), it strikingly influences the bubble stability. Below pH 9, the bubble stability of poly-L-lysine solution is about 10 seconds, whereas at pH 11, its bubble stability is 8 minutes.

The bubble stability of stearic acid monolayers in the absence of poly-L-lysine is about 10-15 seconds over the whole pH range, whereas that of stearic acid in the presence of poly-L-lysine is about 11 minutes at pH 11. It is evident that this enhancement of bubble stability is due to the presence of poly-L-lysine since it also shows maximum bubble stability (8 mins.) without stearic acid monolayers. The upper part of figure 5 shows that at pH 11, poly-L-lysine has almost helical conformation in solution.

Figure 7 schematically shows the mechanism of bubble stability in the presence of a film. If the rate of drainage is rapid, the bubble has a shorter survival time. If the molecules in the film impede the drainage of water due to film-water interaction, the stability of the bubble increases. The data presented in this paper suggest that helical conformation of poly-L-lysine decreases the rate of drainage of water in the bubble lamellae and, hence, increases the bubble stability. The interaction between stearic acid and poly-L-lysine causes further increase in the bubble stability.

The question may be raised whether poly-L-lysine molecules at pH 11 retain their helical conformation at the interface or not. In this author's opinion, the helical conformation is preserved at the interface. If poly-L-lysine molecules are denatured at the interface, one would not observe the striking properties in the pH range 10 to 11. Moreover, using deuterium exchange, infra-red spectroscopy and electron diffraction methods

to study skimmed monolayers, Malcolm (36, 37) has shown that helical conformation of poly-peptides is retained in the monolayer at the air-water interface.

It is difficult to extrapolate the results of monolayer studies to interactions in biological membranes. However, the correlation of these studies with those of others on biological membranes should be mentioned. It has been established by various workers with different techniques that membrane proteins have partially helical conformation (38-40). From the results reported in this paper it appears that partially helical conformation of proteins in biological membranes may cause maximal interaction with water (i.e., maximum hydration) and enhance the interaction with lipids presumably because of the surface activity of the proteins in such conformation.

In summary, the results presented in this paper indicate that the lipid-polymer interaction in monolayers is strikingly influenced by the conformation of the polymer. Extensive studies on the interaction between various lipids and poly-peptides in monolayers are in progress in this author's laboratory.

ACKNOWLEDGEMENTS

The author wishes to express his sincere gratitude to the National Research Council for providing an NRC-NASA Resident Research Associateship, and to Dr. L.P. Zill and Dr. M.R. Heinrich of Ames Research Center, and Dr. O.A. Roels of Lamont-Doherty Geological Observatory, for providing helpful suggestions and encouragement at various stages of this work. Part of this work was supported by Sea Grant GH-16, and was completed at the Lamont-Doherty Geological Observatory of Columbia University. Special thanks are also extended to Mr. E.J. Murphy (Senior Research Scientist) for help in the preparation and to Dr. O.A. Roels for critical review of this manuscript.

REFERENCES

1. D. Chapman, V.B. Kamat, J. De Gier, and S.A. Penkett, J. Mol. Biol., 31 (1968) 101.
2. D. Chapman, V.B. Kamat, J. De Gier, and S.A. Penkett, Nature 213 (1967) 74.
3. M.D. Barratt, D.K. Green, and D. Chapman, Biochim. Biophys. Acta, 152 (1968) 20.
4. J.M. Stein, O.J. Edner and F.G. Bargoot, Science, 162 (1968) 909.

5. T. Hanai, D.A. Haydon and J. Taylor, J. Theoret. Biol., 9 (1965) 422.
6. L.M. Tsofina, E.A. Liberman, and A.V. Babakov, Nature, 212 (1966) 681.
7. D.O. Shah and J.H. Schulman, J. Colloid Interface Sci. 25 (1967) 107.
8. D.O. Shah and J.H. Schulman, Advances Chem. Ser., 84 (1968) 189.
9. A.D. Bangham, B.A. Pethica and G.V.F. Seaman, Biochem. J. 69 (1958) 12.
10. B.A. Pethica and J.H. Schulman, Biochem. J., 53 (1953) 177.
11. P. Doty and J.H. Schulman, Faraday Soc. Disc., London 6 (1949) 27.
12. R. Matalon and J.H. Schulman, Faraday Soc. Disc., 6 (1949) 27.
13. D.D. Eley and D.G. Hedge, Proc. Roy. Soc., Ser. B, 145 (1956) 554.
14. D.D. Eley and D.G. Hedge, J. Colloid Sci., 11 (1956) 445.
15. G. Colacicco, M.M. Rapport, and D. Shapiro, J. Colloid Sci., 25 (1967) 5.
16. G. Camejo, G. Colacicco, and M.M. Rapport, J. Lipid Res., 9 (1968) 562.
17. J.D. Arnold and C.Y. Pak, J. Am. Oil Chemists' Soc., 45 (1968) 1.
18. A.A. Trapeznikov, Acta Physicochemica (U.S.S.R.), 13, (1940) 265.
19. W.D. Garrett, Deep-Sea Res., 14 (1967) 661.
20. D.O. Shah, J. Colloid Interface Sci., in press
21. J. Bagg, M.D. Haber and H.P. Gregor, J. Colloid Interface Sci., 22 (1966) 138.
22. A.P. Christodoulou and H.L. Rosano, Advances Chem. Series, 84 (1968) 210.
23. E.D. Goddard and J.A. Ackilli, J. Colloid Sci., 18 (1963) 585.
24. J. Applequist and P. Doty, In Polyamino Acids, Polypeptides, and Proteins, Ed. M.A. Stahmann. The University of Wisconsin Press, Madison, (1962) 161.
25. C. Long, ed. "Biochemists' Handbook", Van Nostrand, Princeton (1961) p. 30.
26. D.O. Shah and J.H. Schulman, J. Lipid Res. 6 (1965) 341.
27. D.O. Shah and J.H. Schulman, Lipids, 2 (1967) 1.
28. D.O. Shah, J. Colloid Interface Sci., in press, (1969).
29. J. Bagg, M.B. Abramson, M. Fichman, M.D. Haber and H.P. Gregor, J. Am. Chem. Soc., 86 (1964) 2759.
30. D.W. Deamer, D.W. Meek and D.G. Cornwell, J. Lipid Res., 8 (1967) 255.
31. J.V. Sanders and J. A. Spink, Nature, 175 (1955) 644.
32. J. Bagg, M.D. Haber, and H.P. Gregor, J. Colloid Interface Sci., 22 (1966) 138.

33. G. Benzonana and P. Desnuelle, Biochim. Biophys. Acta, 164 (1968) 47.
34. D.O. Shah and J.H. Schulman, J. Lipid Res., 8 (1967) 227.
35. D.O. Shah and J.H. Schulman, Biochim. Biophys. Acta, 135 (1967) 184.
36. B.R. Malcolm, Proc. Roy. Soc. (London) Ser A. 305 (1968) 363.
37. B.R. Malcolm, Nature, 219 (1968) 929.
38. J.M. Steim, Advan. Chem. Ser., 84 (1968) 259.
39. J. Lenard and S.J. Singer, Proc. Natl. Acad. Sci., 56 (1966) 1828.
40. D.W. Urry, M. Mednieks, and E. Bejnarowicz, Proc. Natl. Acad. Sci., 57 (1967) 1043.

INTERACTION OF DNA WITH POSITIVELY CHARGED MONOLAYERS

M. A. Frommer*, I.R. Miller and A. Khaïat

Polymer Department, Weizmann Institute of Science
Rehovoth, Israel

ABSTRACT

Surface pressures and potentials of monolayer complexes between DNA and cetyltrimethylammonium or positively charged poly-peptides (copolymers of L-lysine and L-phenylalanine) were measured. The areas per molecule of the different components in the surface were determined by direct measurement of their surface concentrations, using tritium labelled substances.

It was found that the surface pressures of the condensed monolayers were only slightly affected by the presence of the DNA in the surface. The effect of the DNA is more pronounced on the surface potential and on the surface pressure of the expanded monolayers. The effect of DNA on these properties is analogous to that of high salt concentrations.

A model for the structure of the DNA containing surface complex is proposed.

INTRODUCTION

The surface properties of DNA adsorbed at the air-water (1,2) mercury-water (3,4) and solid-water (5,6) interfaces have been studied quite extensively. However, due to the high solubility of DNA there is no information about its properties when

*Present address: Hydronautics Israel Ltd., Kiryat Weizmann,
Rehovoth, Israel

spread as a monolayer at the A/W interface. The claimed stability of monolayers of the pure sodium salt of DNA on 2 N NaCl substrate reported by James and Mazia 15 years ago (7) was found to be incorrect. This is presumably due to high protein content in the DNA used by these authors. It was shown by Kleinschmidt and co-workers (8) and by Cheesman (9) that binding DNA to proteins stabilizes it at the A/W interface. Stable monolayers of DNA can also be obtained by substituting some of its counter-ions with surface active ions. In this article we shall describe observations on the properties of long chain quarternary ammonium salts of DNA as well as on the interaction of DNA with monolayers of a basic polypeptide.

EXPERIMENTAL:

Materials

Calf thymus DNA was purchased from Worthington Corp. Its tritiation by the Wilzbach method is described in our previous publication (2).

Cetyltrimethyl ammonium bromide (CTABr) was a gift from "Fluka AG". Elementary analysis of this product yields practically the theoretical formula C₁₉H₄₂NBr. To prepare tritiated CTA hexadecylamine (a Fluka AG product) was allowed to react for 24 h. at room temperature with an equivalent amount of tritiated methyl iodide (obtained from the Radiochemical Center, Amersham, England) in nitromethane over sodium bicarbonate powder. A large excess of methyl iodide was then added and the reaction was permitted to continue at 60°C for two days. The solution concentration was determined on the basis of nitrogen content.

Solutions of long chain quarternary ammonium salts of DNA were prepared by mixing solutions of 0.5-0.7 mg/cc of DNA in 1:1x10⁻³ N NaCl: isopropyl alcohol, and 0.6-0.8 mg/cc of cetyltrimethylammonium bromide in the same mixed solvent (12,13). The concentrations of the DNA were determined by optical density measurements of the aqueous solution prior to addition of isopropyl alcohol. In the case of CTABr solution, its concentration was calculated from the dry weight of the long chain salt.

Copolymers of L-lysine hydrobromide and L-phenylalanine were supplied by "Yeda" Research and Development Co., Rehovoth, Israel. Their exact composition as well as their concentration in the spreading solutions were determined by amino acid analyzer manufactured by Beckman-Spinco. All other salts and liquids were commercial products of highest purity grade and in many cases were further purified by distillation (i-PrOH) crystallization (MgCl₂) or

TABLE I

Influence of: a) amount of CTA-DNA spread, b) long chain salt content in the spreading solution and c) salt concentration in the substrate on: 1) the ratio of the measured DNA surface concentration to that expected from the amount spread, and on 2) the surface concentration of the DNA

NaCl concentration in the substrate	0.001 N		0.01 N		0.1 N		1 N	
	Volume of CTA-DNA solutions spread in ml/cm ²	2x10 ⁻⁴	2x10 ⁻³	2x10 ⁻⁴	2x10 ⁻³	2x10 ⁻⁴	2x10 ⁻³	2x10 ⁻⁴
CTA Mole DNA Nucleotides	Conc. of DNA in spread soln. ratio mg/ml	ratio mg/m ²						
0.69	0.9	0.41	0.8	3.7	0.9	0.41	0.5	2.3
0.87	1.0	0.57	0.8	4.6	1.0	0.57	0.5	2.8
0.93	0.8	0.49	0.6	3.6	0.9	0.55	0.3	1.8
0.85	0.8	0.61	0.5	3.8	1.0	0.77	0.4	3.1
0.45	1.15	0.5	0.46	0.3	2.7	0.7	0.64	0.3
0.22	1.38	0.5	0.46	0.3	2.7	0.7	0.64	0.3
0.09	1.57	0.3	0.31	0.1	1.0	0.5	0.52	0.2
0.04	1.77	0.2	0.23	0.08	0.94	0.4	0.47	0.1
						0.1	1.2	
						0.5	0.59	
						0.5	0.59	
						0.3	3.5	
						0.3	3.1	
						0.3	0.6	
						0.3	0.62	
						0.3	0.4	
						0.3	0.47	
						0.3	3.5	

heating to high temperatures (NaCl).

Techniques

Measurements of surface concentration, surface pressure, and surface potential were performed as described in previous communications (10,11). Monolayers of 1.15:1 L-lysine:L-phenyl alanine were spread from a 1 mg per cc solution of 1:2 dichloroacetic acid: chloroform. Spreading was performed by the Trurnit method (18) on a glass rod sticking out above the liquid surface.

RESULTS

Surface Concentrations of Monolayers of Cetyltrimethylammonium Salts of DNA (CTA-DNA)

The surface concentrations of the components of spread monolayers of CTA/DNA were determined by utilizing tritiated DNA or tritiated CTA and measuring the surface radioactivity. It was found that if the CTA content in the CTA/DNA complex was above 0.1 mole CTA per mole nucleotides, and the area per CTA ion was higher than about 90 Å², the spread CTA remained quantitatively in the surface. Table 1 summarizes the influences of: a) the amount of CTA/DNA spread, b) the long chain salt content in the spreading solution, and c) salt concentration in the substrate, on the ratio of the measured surface concentration of H³-DNA to that expected from the amount spread. It is obvious from the results of Table 1 that increasing the volume spread, from 0.001 ml to 0.01 ml, causes dissolution of the H³-DNA from monolayer, and the ratio of the measured surface concentration to the "theoretical" one decreases. However, when the salt concentration in the substrate is low and the CTA content high enough, practically all the DNA remains at the interface. This is in full agreement with the reported non-solubility of long chain quaternary ammonium salts of DNA (12,13).

Considering now the changes in the stability of the monolayer with the salt concentration, one finds two contradictory influences. When the CTA to DNA ratio is high, an increase in the salt concentration of the substrate causes increased solubility of the DNA from the interfacial film. On the other hand, when the CTA content in the monolayer is low, increasing NaCl concentration enhances the persistence of the DNA in the monolayer. In intermediate compositions when about half of the counter-ions of the DNA are sodium ions, maximal DNA retention in the monolayer is found in medium salt concentrations. These observations demonstrate that increasing salt concentration causes, on the one hand, an increased exchange of the

long chain counter-ions with sodium ions, and thus to an increased dissolution of the DNA from the monolayer, and on the other hand, to an enhanced adsorption of the DNA at the air-water interface. When the CTA content is high, the influence of the exchange reaction predominates and increasing salt concentration enhances desorption of DNA, while, in sodium rich monolayers, the result is the contrary. The highest surface concentration obtained was about 4.6 mg per m², corresponding to 12 Å² per nucleotide. This area of 12 Å² per nucleotide is significantly smaller than the value of 35 Å² per nucleotide reported for native DNA adsorbed at the mercury-water interface (3,4) and it seems therefore that the excess of the insoluble CTA-DNA complex remains in the surface forming a thick interfacial film.

Surface Pressure and Potential of CTA-DNA Monolayers

It is obvious from Table 1 that monolayers of CTA-DNA remain quantitatively on the surface of a low salt concentration substrate, provided the CTA to DNA ratio is higher than about 0.5 mole CTA per nucleotide. It was possible therefore to measure the dependence of the surface pressure (π) and surface potential (ΔV) on the area occupied by such monolayers. The experimental results are presented in Figures 1 and 2.

Figure 1 describes the π -A curves of monolayers of cetyltrimethylammonium chloride (CTACl) on 1 N NaCl solution and of CTA-DNA salts of varying CTA content on 10⁻³ N NaCl solutions. It is obvious that the surface pressure of all CTA/DNA salts at high surface areas is very small, and is even smaller than that of CTACl occupying the same area on 1 N NaCl. Moreover, Figure 1 also demonstrates the unexpected observation that the "limiting area" occupied by a CTA residue is almost unaffected by its being bound to DNA and is similar to that of CTACl on high salt concentration substrate. The slight shift to higher "limiting area" for CTA to DNA ratio of 0.64 and 0.75 mole per equivalent can account for steric effects exerted by the DNA in the sublayer on the CTA monolayer. It seems that the maximal areas per CTA at CTA/DNA ratios around 0.7 is related to the difficulty of binding CTA ions anchored at the interface to the negative groups on the DNA double helix which point toward the solution. It is thus assumed that about one third of the charges on the DNA in the surface area is inaccessible to the CTA ions. Figure 3 describes a possible surface configuration conforming with these steric requirements. The area occupied by a CTA residue when the CTA to DNA ratio is about 0.7 is approximately 110 Å². It is obvious from Fig.3 that when increasing the CTA:DNA ratio above 0.7, the area per CTA ion decreases since the additional CTACl molecules may arrange themselves between two CTA/DNA molecules. Eventually the average area per CTA, at CTA/DNA ratios the DNA becomes too soluble to penetrate the CTA monolayer, and it tends to

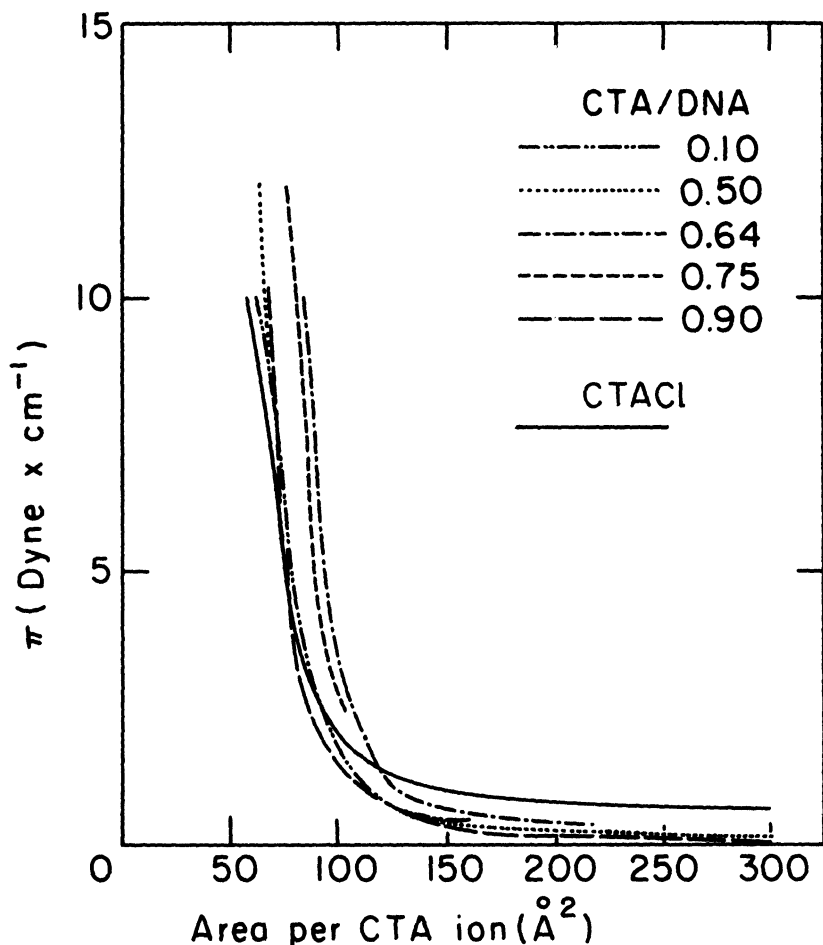


Fig. 1. The dependence of surface pressure- π on the area-(A) occupied by a monolayer of CTACl on 1 N NaCl substrate (full curve), and by monolayers of CTA/DNA of varying CTA content on 10^{-3} N NaCl substrate. The composition of the CTA/DNA monolayers are expressed in unit of moles CTA per nucleotide residue.

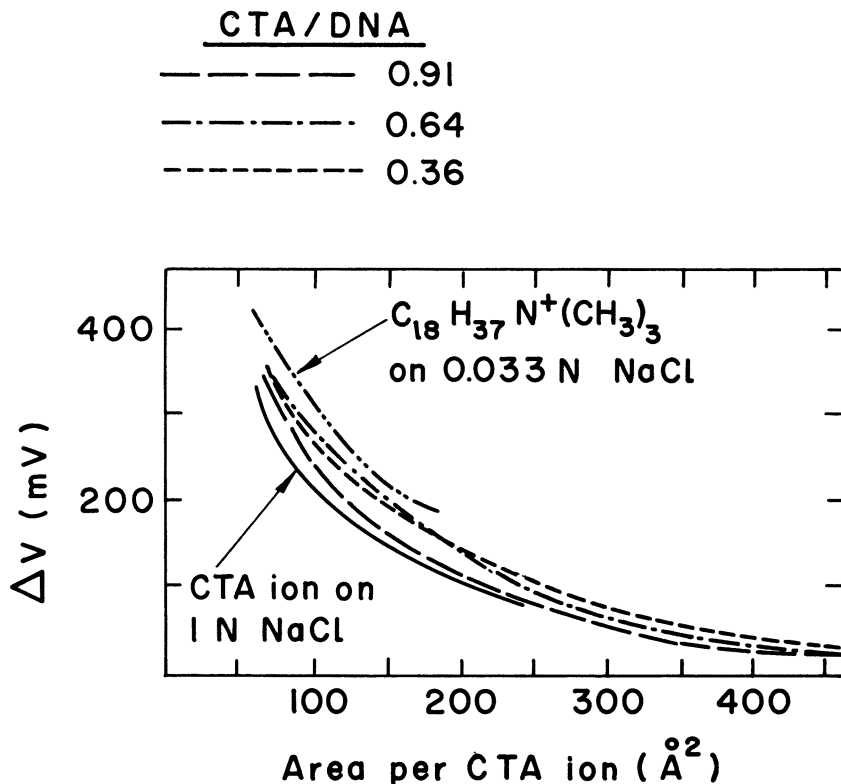


Fig. 2. The dependence of surface potential- ΔV , on the area-(A) occupied by monolayer of CTACl on NaCl substrate, by monolayer of $\text{C}_{18}\text{H}_{37}\text{N}^+(\text{CH}_2)_3\text{Cl}^-$ on 0.033 N NaCl substrate, and by monolayers of CTA/DNA of varying CTA content on 10⁻³ N NaCl substrate. The compositions of the CTA/DNA monolayers are expressed in units of moles CTA per nucleotide residue. The data on the behaviour of the $\text{C}_{18}\text{H}_{37}\text{N}^+(\text{CH}_3)_3\text{Cl}^-$ monolayer is reproduced from Davies' measurements (14).

form a sublayer without any effect on the area per CTA.

The assumption inherent in this model, that the DNA retains its native structure, is based on the weak interaction forces evident from the small effect on the surface tension. Moreover, it will be shown in the discussion of the surface potential data, that the distorting vector of these forces is probably very small and the interacting monolayer charges can conform with the DNA structure. Supporting evidence for this assumption is the native structure of the NaDNA regenerated from the CTA/DNA precipitate (15). The presence of the DNA at the interface (proved by our surface concentration measurements presented above) can easily be confirmed by its influence on the shape of the π -A isotherms. As shown in Figure 4, the "character" of π -A curves of CTAC1 changes gradually from an "expanded" isotherm at low salt concentrations to a condensed one at high salt concentrations. The CTA/DNA monolayers which were spread on a 10^{-3} N NaCl substrate are of a "condensed" type, with a low surface pressure at high areas.

The surface potential-area (ΔV -A) curves of CTAC1 on 1 N NaCl solution of $C_{18}H_{37}N(CH_3)_3Cl^-$ on 0.033 N NaCl substrate, and of CTA/DNA salts of varying CTA content, on 10^{-3} N NaCl substrate are presented in Figure 2. We see again that the surface potential properties of the CTA/DNA monolayers are determined quite exclusively by the long chain hydrophobic counter-ion. Again, the practical identity of the ΔV -A curves of CTAC1 on 1 N NaCl solution and the various CTA/DNA monolayers on 10^{-3} N NaCl cannot be explained by dissolution of the DNA. As shown by Davies (14) a tenfold increase in the salt concentration of the substrate causes a decrease of 55 mV in the ΔV in the ΔV -A curves of monolayers of $C_{18}H_{37}N^+(CH_3)_3$. In Figure 2 Davies's results dealing with $C_{18}H_{37}N^+(CH_3)_3$ monolayers on 0.033 N NaCl concentration are compared with our results and indicate that the DNA attached to the CTA monolayer acts as if it would contribute a local ionic strength of ≈ 1 . This is much larger than our experimental error of ± 15 mV. The small shift to higher ΔV values in the CTA/DNA monolayers cannot be interpreted more quantitatively due to lack of knowledge on the contribution to the surface potentials of the small fraction of DNA anchored at the interface, and the non-avoidable configurational changes in the long chain salt.

Monolayers of Lysine-Phenylalanine Copolymers and Their Interaction With DNA

Figure 5 describes the dependence of π -A curves of monolayers of copolymers of L-lysine:L-phenylalanine on the composition of the substrate. Let us consider first the influence of the salt concentration and of the composition of the copolymer on the π -A relation.

The limiting area occupied by a lysine residue increases considerably with increasing phenylalanine content in the copolymer. This is expected of course, since the hydrophobic phenylalanine groups are those which anchor the polymeric molecule at the interface. Consequently increasing phenylalanine content in the copolymer by a factor of about ten should cause an increase in the limiting area per lysine residue by a similar factor and this is indeed the case. However, whereas the π -A relation of the 1:9.6 L-lysine:L-phenylalanine copolymer is independent of salt concentration in the range 5×10^{-3} M to 1 M [Na⁺] (and is practically independent of pH), the surface pressure-area relation of 1.15:1 L-lysine:L-phenylalanine copolyptide depends considerably on the ionic strength. The limiting area per amino acid residue of the 1:9.6 copolymer is 21.5 \AA^2 , practically independent of salt concentration and pH. The limiting area per amino acid residue of the 1.15:1 copolyptide is however about 9 \AA^2 on 10^{-3} N NaCl substrate, and increases to 17 \AA^2 on 0.1 - 1 N NaCl solution. Limiting areas of 15-17 \AA^2 per amino acid residue are typical of many proteins and polypeptides at the air-water interface (19,20,22) and are usually attributed to the β -keratin conformation. The increased limiting area of the 1:9.6 copolymer is typical of phenylalanine polypeptides (21).

The extraordinarily low limiting area of 1.15:1 L-lysine:L-phenylalanine on 10^{-3} N NaCl solution seems to result from a partial dissolution of the lysine residues in the substrate. Indeed it is well known (22,23) that polylysine monolayers can only be spread on very concentrated salt solutions. The penetration of the lysine groups into the surface at high ionic strength is therefore confirmed by our measurements. We do not believe that the abnormal low limiting area of 9 \AA^2 per amino acid residue might be due to helical conformation, since such conformation of charged polypeptide is expected to be more stable on a high, rather than on a low, ionic strength substrate.

In a preliminary qualitative study of the adsorption of DNA onto a monolayer of copolyptide of 1:1 L-lysine: L-phenylalanine, reported in part in our previous communication (11), it was found a) that DNA adsorbs from a low salt concentration substrate [e.g. 0.004 M (NH₄)₂SO₄] onto such monolayers at a rate corresponding approximately to a diffusion controlled mechanism, b) that the amount of DNA adsorbed on a fairly compressed copolyptide monolayers is smaller than that expected from a stoichiometric ratio between the free amino groups and the phosphate anions. Thus, when the area occupied by an amino acid residue was 19.5 \AA^2 only 0.65 nucleotides were adsorbed per each lysine residue at the interface. The amount adsorbed was decreased to 0.4 nucleotides per lysine residue when the monolayer was further compressed and the area available per amino acid residue was only 10 \AA^2 . Since in the bulk phase the interaction between polylysine and DNA was found to be a stoichiometric one (15,16) it seems that steric hindrance at the interface is responsibl

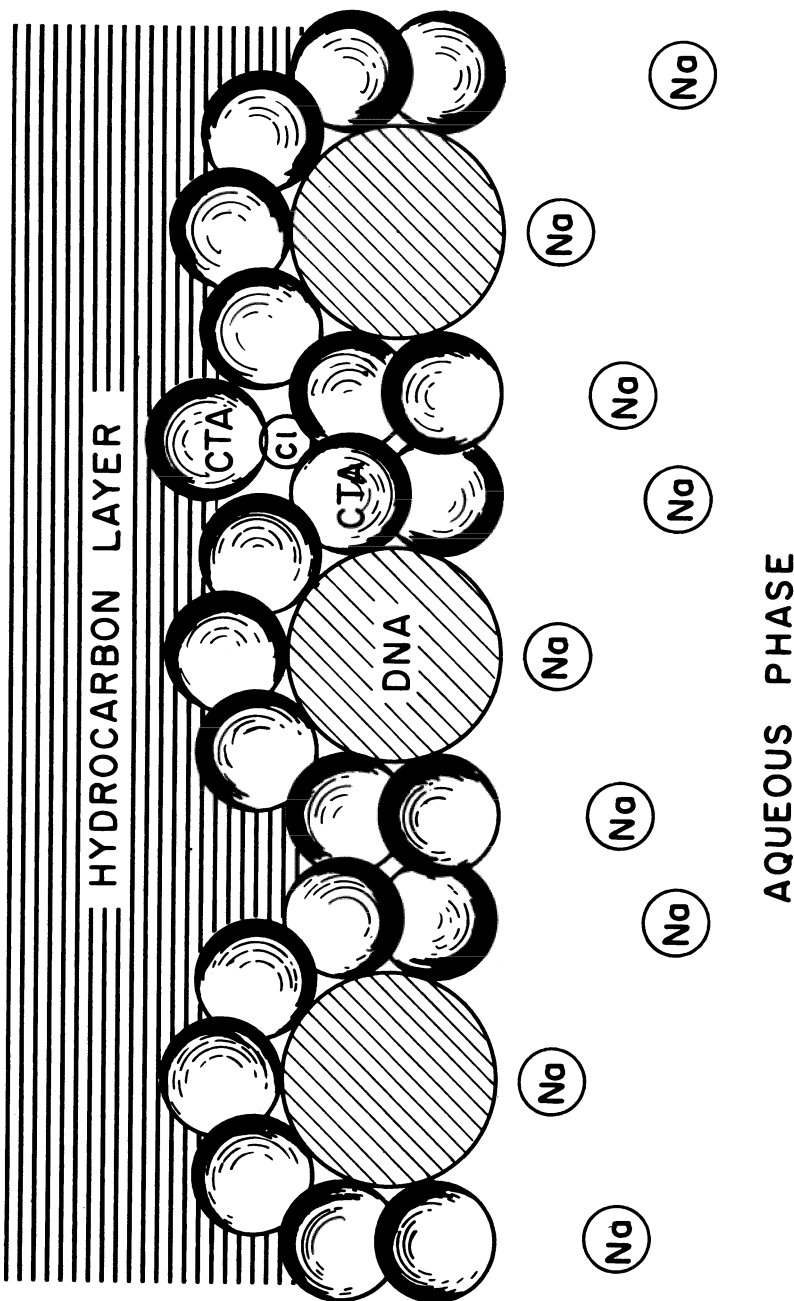


Fig. 3. Schematic representation of the arrangement of CTA ions around the DNA bihelix at the air-water interface.

for the non-stoichiometric ratio. This restriction indicates that the interacting DNA tends to preserve its stiff double helical structure. It might be recalled that in the adsorption of polyacids on positively charged mercury it was found that only a small fraction of the polyelectrolyte is anchored at the interface (17) and neutralized by surface charges. In the present case it is also possible that not all the adsorbed DNA charges are neutralized by the charges of the polypeptide monolayers, even though the interaction between the polymeric charges in the surface may be facilitated by protrusion of the positively charged lysine residues into the sublayer.

The influence of substrate DNA on the surface pressure of a monolayer of 1.15:1 L-lysine:L-phenylalanine is shown also in Figure 5. As in the case of monolayers of CTA/DNA, the interaction of the DNA with the basic polypeptide changes the shape of its π -A curve from that typical to a "gaseous" monolayer to that characteristic of condensed ones. However, the interaction between the DNA and the monolayer does not cause an increase in the limiting area.

DISCUSSION

The most striking phenomenon displayed either by monolayers of CTA/DNA or by monolayers of basic polypeptides containing DNA is the fact that despite its unquestionable existence at the interface (proved by radioactive and surface pressure and potential measurements) DNA penetrates the compressed positively charged monolayer only weakly, and has little effect on the limiting areas. This resembles the "surface potential and tension paradox" described in a previous communication on "the adsorption of DNA at the air-water interface" (1). Adsorption of DNA at the A/W interface is not followed by any detectable changes in surface tension or potential. It was shown that this can happen only when a very small fraction of the adsorbed molecule is anchored at the surface, or when the adsorption forces are too weak to cause an appreciable reorientation of the residues near the surface. Similarly, it seems that when the DNA is held at the surface by interaction with hydrophobic counter-ions, only a small fraction of the molecule is really anchored at the air boundary, and the electrostatic binding takes place in the monolayer.

What is the conformation of the DNA at the interface? To know this we have to determine the exact composition of the DNA at the surface. Let us consider the implications of a 1:1 interaction of DNA with CTA. If as in the bulk phase all sodium ions of the DNA are substituted by CTA ions to yield pure CTA/DNA (12), then if the DNA retains its double helical conformation it must affect the structure of the long chain salt at the surface. This is because the

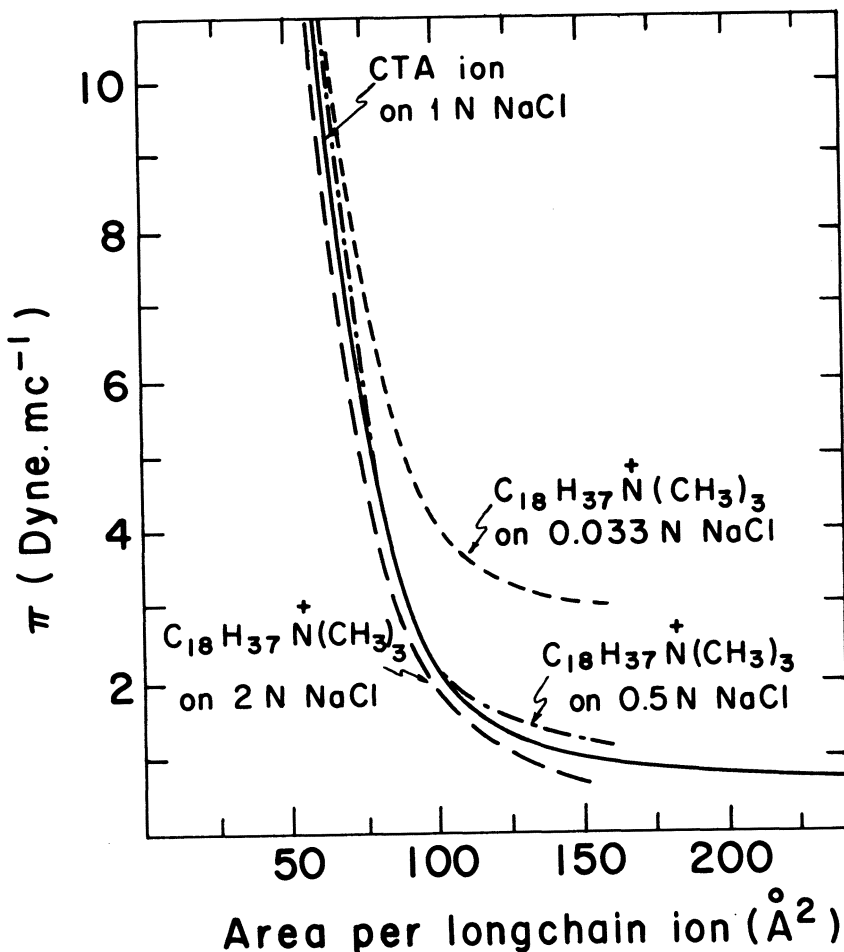


Fig. 4. The dependence of surface pressure π on the area-(A) occupied by a monolayer of CTACl on 1 N NaCl substrate, and by monolayers of $\text{C}_{18}\text{H}_{37}\text{N}^+(\text{CH}_3)_3\text{Cl}^-$ on 2 N, 0.5 N, and 0.033 N NaCl substrate. The data on the behaviour of the $\text{C}_{18}\text{H}_{37}\text{N}^+(\text{CH}_3)_3\text{Cl}^-$ monolayer is reproduced from Davies' measurements (14).

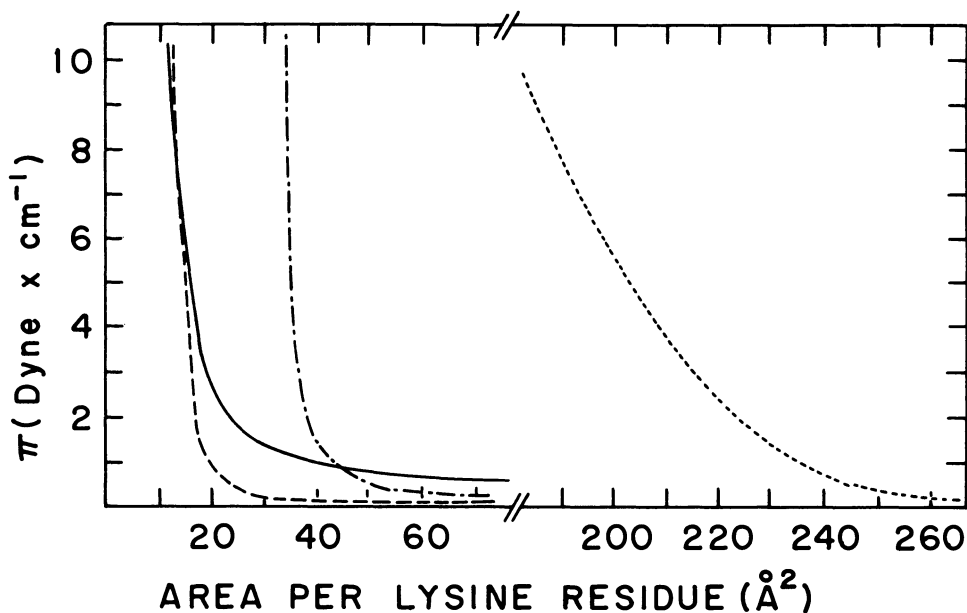


Fig. 5. The dependence of surface pressure- π on the area-(A), occupied by monolayers of copolymers of L-lysine, L-phenylalanine on various substrate,

- 1.15:1 lys:φ-al on 10^{-3} N NaCl
- - - - 1.15:5 lys:φ-al on 10^{-3} N NaCl containing 0.0016%–0.0032% DNA
- 1.15:1 lys:φ-al on 0.1–1 N NaCl
- - - - - 1:9.6 lys:φ-al on Na_2HPO_4 – KH_2PO_4 buffer yielding neutral pH.

double helix is a rigid structure having a surface charge density of 35 \AA^2 per negative charge. The limiting area of CTACl is however about 90 \AA^2 per positively charged ion. If, as assumed, the DNA is fully neutralized by CTA ions, they must penetrate into the solutions to various depths around the rigid DNA cylinder so that each of its negative charges is neutralized. Since the surface potential of the CTA/DNA monolayer is similar to that of CTACl on a high salt concentration substrate, the orientation of the dipoles and the packing of the long chain salt ions cannot be altered by this arrangement. Interaction of CTA without dipole orientation can be visualized only with those charges on the rigid DNA rod which do not point towards the solution, as shown in Figure 3. In this arrangement there is no rigid binding, and the CTA dipoles can "slide" around the cylindrical structure without change in orientation. It is very likely that the structure of charged monolayers, where the ionic components penetrate into the solution to various depths, is not unique for the case of polymeric "counter-ions", but may be a general feature of charged monolayers.

The lack of stoichiometry in the interaction of DNA with a polylysine monolayer, as well as steric effects in the CTA/DNA monolayers, hint very strongly that the DNA attached to the surface retains its double helical structure. This rigid structure eliminates the possibility of complete neutralization of the monolayer by the interacting DNA.

ACKNOWLEDGMENTS

The authors acknowledge the help of Mr. Mei-Marom who performed part of the surface pressure measurements of copolypeptides.

This work was sponsored by the National Institute of Health under research grant No. GM-08-519 and under research agreement No. 615134.

This paper is abstracted from the Ph.D. thesis submitted by M.A. Frommer to the Feinberg Graduate School of the Weizmann Institute of Science.

REFERENCES

1. Frommer, M.A. and Miller, I.R., J. Phys. Chem., 72, 2862 (1968).
2. Frommer, M.A. and Miller, I.R., Biopolymers, 6, 1461 (1968).
3. Miller, I.F., J. Mol. Biol., 3, 229 (1961).
4. Miller, I.R., J. Mol. Biol., 3, 357 (1961).

5. Winsten, W.A., *Biopolymers*, 2, 337 (1964).
6. Miller, I.R., *Biochim. et Biophys. Acta.*, 103, 219 (1965).
7. James, I.W. and Mazia, D., *Biochim. et Biophys. Acta.*, 10, 367 (1953).
8. Kleinschmidt, A., Rutter, H., Hellmann, W., Zahn, R.R., Doctor, A., Zimmermann, E., Rubner, H. and Al-Ajwady, A.M., *Z. Naturforschg.*, 146, 770 (1959).
9. Cheesman, D.F., *Biochim. et Biophys. Acta.*, 11, 439 (1953).
10. Frommer, M.A. and Miller, I.R., *Rev.Sci.Instr.*, 36, 707 (1965).
11. Frommer, M.A. and Miller, I.R., *J. Colloid and Interface Sci.*, 21, 245 (1966).
12. Aubel-Sadron, G., Beck, G., and Ebel, J.P., *Biochim. Biophys. Acta.*, 53, 11 (1961).
13. Ebel, J.P., Aubel-Sadron, G., Weil, J.H., Beck, G., and Hirth, L., *Biochim. Biophys. Acta.*, 108, 30 (1965).
14. Davies, J.T., *Proc. Roy. Soc.*, A 208, 224 (1951).
15. Zubay, G. and Wilkins, M.H.F., and Blout, E.R., *J. Mol. Biol.*, 4, 69 (1962).
16. Bonner, J. and Ts'o, P.O.P. (editors), "The Nucleohistones", Holden-Day Inc., San Francisco, (1964).
17. Miller, I.R. and Katchalsky, A., "Proc. 4th Intern. Cong. Surface Activity", J.Th.G. Overbeek Ed., Vol. 2, p.275, Gordon and Breach Sci. Pub., New York (1967).
18. Trurnit, H.J., *J. Colloid Sci.*, 15, 1 (1960).
19. Cumper, C.W.N. and Alexander, A.E., *Trans. Farad.Soc.*, 46, 235 (1950).
20. Isemura, T. and Yamashita, T., *Bull. Chem.Soc. Japan*, 32, 1 (1959); 35, 929 (1962).
21. Mishuck, E. and Eirich, F.R., *J. Poly.Sci.*, 16, 397 (1955).
22. Davies, J.T., *Biochem. J.*, 56, 509 (1954).
23. Davies, J.T., *Trans. Farad. Soc.*, 49, 949 (1953).

THE EFFECT OF MODIFIERS ON THE INTRINSIC PROPERTIES OF BILAYER
LIPID MEMBRANES (BLM)

H. Ti Tien

Department of Biophysics, Michigan State University
East Lansing, Michigan

INTRODUCTION

Black lipid membranes (BLM), as model systems for studies of biological membrane function, offer an opportunity for carrying out measurements which may pertain to cellular mechanisms of many important biological activities. For example, the mechanisms of nerve excitation, of water permeation, of active transport, and of energy transduction are just a few of the problems being actively investigated with the use of BLM. A number of comprehensive reviews covering the earlier studies on BLM have been published recently (1-4).

Although biological membranes are known to be complex and highly variable both in structure and function, it seems probable that there is a common construct basic to all of them (5). The strongest experimental evidence in support of such a supposition is provided by the electron microscopy of cellular membranes and organelles, which has led to the "unit membrane" hypothesis (6). Under the electron microscope, all the natural membranes thus far examined are in the order of 100 Å in thickness and are generally interpreted to be as consisting of a lipid bilayer of the Gorter-Grendel type with adsorbed protein or nonlipid layers (7,8). The structure of BLM is frequently depicted to be similar to that of a Gorter-Grendel bimolecular lipid leaflet at a water-oil-water biface (9). This paper will attempt to present a unifying view that modified BLM are useful experimental models for at least five basic types of biological membranes. These types are the plasma membrane of erythrocyte, the nerve membrane of axon, the cristae membrane of mitochondrion, the thylakoid membrane of chloroplast, and the rod outer segment sac membrane of retina. Schematic and

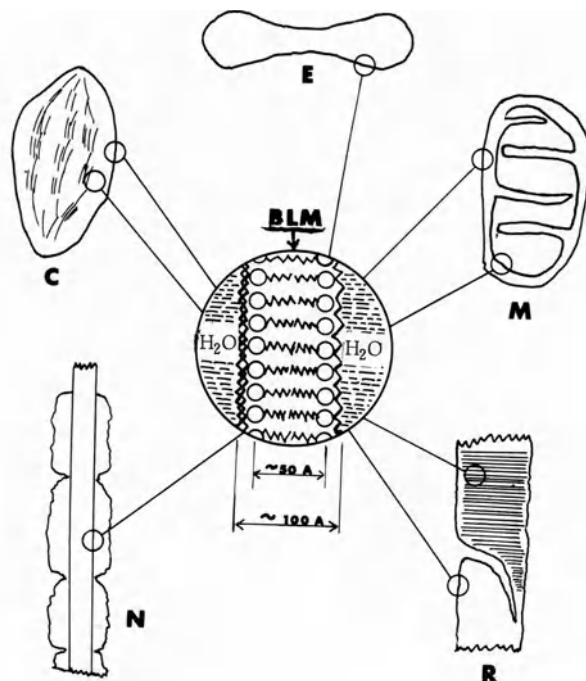


Figure 1. Schematic illustration of the five basic types of biological membranes as they are generally visualized under the electron microscope and their molecular interpretation according to the bimolecular leaflet model (BLM). E erythrocyte (plasma membrane). C chloroplast (thylakoid membrane). M mitochondrion (cristae membrane). N nerve axon (myelin). R rod outer segment membrane.

highly idealized pictures illustrating these basic units of life processes are shown in Fig. 1. In describing these model systems, the effects of modifiers on the intrinsic properties of unmodified BLM will be stressed.

BLM VS. ULTRATHIN LAYER OF LIQUID HYDROCARBON

The intrinsic properties of an unmodified BLM generated from either phospholipids or oxidized cholesterol in an alkane solvent are strikingly similar to those expected of a thin layer of liquid hydrocarbon of equivalent thickness. A comparison of the properties of the unmodified BLM with the extrapolated properties of a 100 Å layer of liquid hydrocarbon is summarized in Table 1. It is evident from the data given that an unmodified BLM appears to be a

Table 1. COMPARISON OF PROPERTIES OF UNMODIFIED BLM AND A LAYER OF LIQUID HYDROCARBON OF EQUIVALENT THICKNESS

<u>PROPERTY</u>	<u>UNMODIFIED BLM (EXPERIMENTAL)</u>	<u>LIQUID HYDROCARBON (EXTRAPOLATED)</u>
Thickness (Angstroms)	40-130	100
Resistance ($\Omega\text{-cm}^2$)	$10^7\text{-}10^9$	10^8
Capacitance ($\mu\text{F}\text{-cm}^{-2}$)	0.3-1.3	1.0
Breakdown Voltage (V/cm)	$10^5\text{-}10^6$	10^6
Dielectric Constant	2-5	2-5
Refractive Index	1.4-1.6	1.4-1.6
Water Permeability (μ/sec)	8-24	35
Interfacial Tension (dynes/cm)	0.2-6	50
Potential Difference per 10 fold Concentration of KC1 (mV)	0	0
Electrical Excitability	None	None
Photoelectric Effects	None	None

poor model for the biological membrane. For instance, it is well known that biological membranes are ion-selective. In the case of nerve membrane, electrical "excitability" is one of the most unique features.

In an attempt to modify the intrinsic properties of the BLM, literally several hundreds of compounds were evaluated in the beginning (10). Among these the following groups of materials have been tried: common proteins, enzymes, surfactants, fermentation products, vitamins, tissue extracts (eg. retina), and a variety of organic and inorganic compounds. This broad and preliminary testing of materials has led to the discovery of a modifier of uncertain composition (still not known to date) termed "excitability inducing material" (or EIM) which not only dramatically reduced the BLM resistance but induced electrical "excitability" as well (10,11). Beginning with EIM, a number of modifying agents (or modifiers) has been discovered which, when present in the BLM, impart new properties that are of biological interest. Since a detailed review of these BLM modifiers will be given elsewhere (12), only a general classification is given in Table 2. The present paper will be concerned with the effects of modifiers on four different BLM systems, which have been studied recently in this laboratory.

Table 2. CLASSIFICATION OF BLM MODIFIERS

<u>CATEGORIES</u>	<u>EXAMPLE</u>
A. Those Altering the Basic Electrical Properties	EIM ^a , KI
B. Those Conferring Ion Specificity	Valinomycin, I ₂
C. Those Inducing Electrical Excitability	EIM ^a , Alamethicin(13)
D. Those Changing the Mechanical Properties	HDTAB ^b , Various Proteins
E. Those Generating Photoelectric Effects	Chlorophylls, Retinenes, Phthalocyanines, Various Organic Dyes, Inorganic Ions

^aEIM - Excitability Inducing Material (10)^bHDTAB - Hexadecyltrimethylammonium BromideTable 3. COMPOSITION OF BLM-FORMING SOLUTIONS

MAJOR LIPID COMPONENT OR SOURCE	MODEL FOR	REFERENCE
A. Brain lipids	Plasma membrane	(10)
Phospholipid and Cholesterol	" "	(14)
Erythrocyte extract	" "	(15)
E. Coli extract	" "	This work ^a
B. Brain lipids	Nerve membrane	(10)
Oxidized Cholesterol + DAP ^b	" "	(16)
C. Phospholipid + Cholesterol	Mitochondrial membrane	(17)
DAP ^b + Oxidized Cholesterol	" "	(16)
D. Chlorophylls + Phospholipid	Thylakoid membrane	(18)
Chloroplast extract	" "	(18)
E. Carotenoid pigments & Phospholipid + oxidized Cholesterol	Visual receptor membrane	(19)

^aDetails given in this paper^bDAP - Dodecyl acid phosphite (16)

In Table 3 the major component or source of lipids which has been used for the generating of BLM as models for various biological membranes is given. Further details concerning these BLM-forming solutions may be found in the published literature.

E. COLI BLM (Reconstituted Plasma Membrane)

Unlike most mammalian cells, E. Coli contain little lecithin or cholesterol. In spite of this difference in lipid composition, E. Coli also develop a high K^+ and low Na^+ interior when the nutrient solution is low in K^+ and high in Na^+ . It was decided to study the effect of modifiers on BLM formed from E. Coli extract. The simple procedure for obtaining BLM-forming solution is shown in the flow chart (Fig. 2).

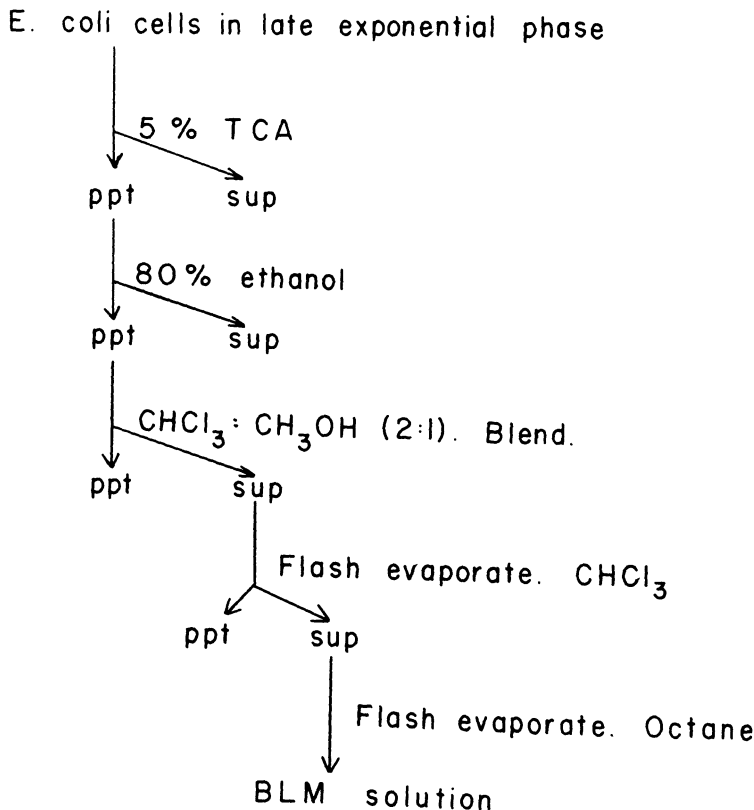


Figure 2. Procedure for preparation of E. Coli BLM-forming solution.

E. Coli, strain K-12, were grown at 37°C in DIFCO culture medium with 3g/l sucrose added. The cells were harvested in the logarithmic phase of growth and treated first with 5% cold TCA, the 80% ethanol. The treated cells were dissolved in 20 ml/gm chloroform:methanol (2:1) and the mixture was blended in a Waring blender for 5 minutes. After centrifugation the supernatant was flash evaporated and the residue was redissolved in chloroform and filtered. This supernatant was flash evaporated and the final residue was dissolved in a hydrocarbon solvent. Dodecane was used in preliminary experiments; however it was found that black membranes formed faster and more smoothly in octane, and this solvent was subsequently used in all extractions.

A description of the apparatus has previously been given in detail (20). Briefly, membranes were formed on a 1.5 mm hole in a thin teflon sleeve which separated two chambers, each filled with aqueous solution. Temperature was maintained with a constant temperature bath connected to polyethylene or glass tubing which coiled around twice through the outer chamber. By keeping the inner chamber stirred, equilibration of temperature could be achieved in a short period of time. Calomel electrodes with agar-saturated KC1 bridges were inserted in each chamber to measure electrical properties. For measurements of resistance and capacitance a small current at known potential (30-40mV) was passed across the membrane and through a standard resistor placed in series with the membrane. The potential drop across the BLM was measured with a Keithley-610 electrometer and the time course of this potential was recorded on a Bausch and Lomb VOM-5 recorder for capacitance determinations. Resistance was calculated from an application of Ohm's law and capacitance was calculated from the well-known DC discharge technique. For measurements of transmembrane potential all electronic components were switched out of the circuit except the electrometer and recorder. Lipid solution was applied to the teflon sleeve using a trimmed sable brush (10). At 37°C thinning was complete within two minutes.

The DC electrical resistance of E. Coli BLM was 10^7 - $10^8 \Omega\text{-cm}^2$. After correcting for area, usually 1 mm^2 , the corrected resistance value was 10^5 - $10^6 \Omega\text{cm}^2$. The resistance was slightly increased in more dilute salt solutions, roughly a two-fold increase for every ten-fold dilution in the range of 10^{-3} - 10^{-1}M salt solution. The change in resistance observed with changing temperature is shown in Fig. 3. From a plot of $\log R$ versus $1/T$ using the Arrhenius equation, the activation energy was calculated to be 18.6 Kcal/mole.

The capacitance of the E. Coli BLM was $.75\mu\text{F}/\text{cm}^2$ in 0.1N NaCl at 37°C. Variations in this parameter have not been studied in detail.

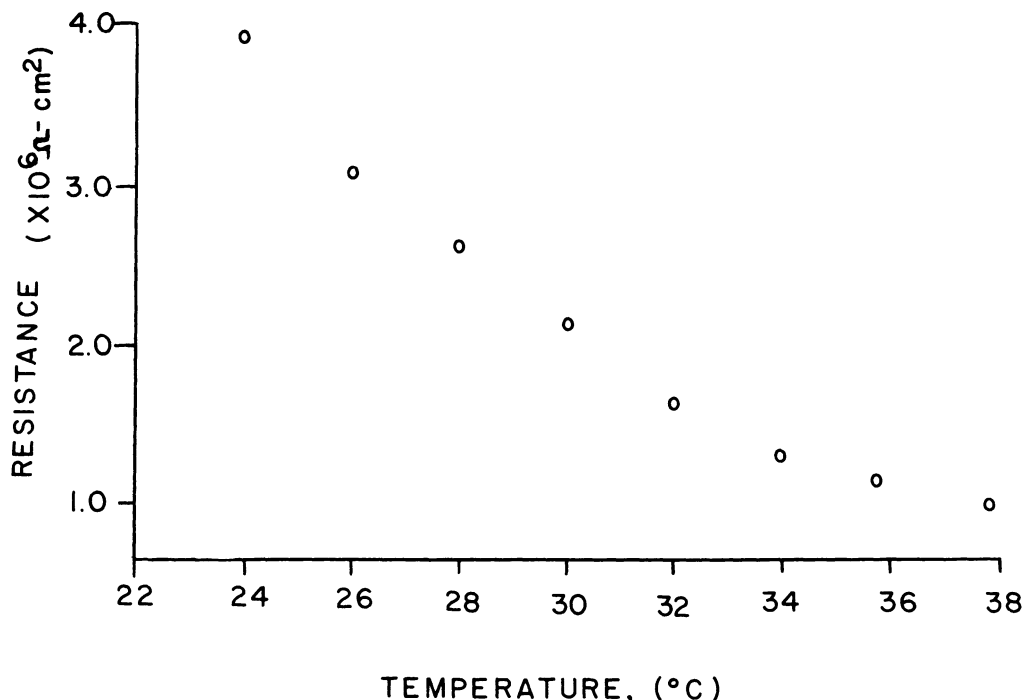


Figure 3. Temperature dependence of E. Coli BLM resistance.
Activation energy, 18.6 Kcal/mole.

The Effect of EIM

Two compounds which have a dramatic effect on most black membrane systems were tested on E. Coli BLM. Both iodine and EIM caused drops in resistance down to the level of $5 \times 10^3 \Omega\text{-cm}^2$. The effect with iodine was immediate, while the addition of EIM took 1-2 minutes to show its effect. The lowering of BLM resistance by EIM (added to one side) as a function of time is shown in Fig. 4. It is interesting to note that the membrane became asymmetric.

The Effect of Surfactants

In an effort to determine qualitatively the net charge on the BLM surfaces, various anionic and cationic surface active materials were added to one side of the membrane and the transient transmembrane potential was measured. The cationic materials tested were hexadecyltrimethylammonium bromide (HDTAB) and protamine sulfate; the anionic agents were sodium dodecyl sulfate

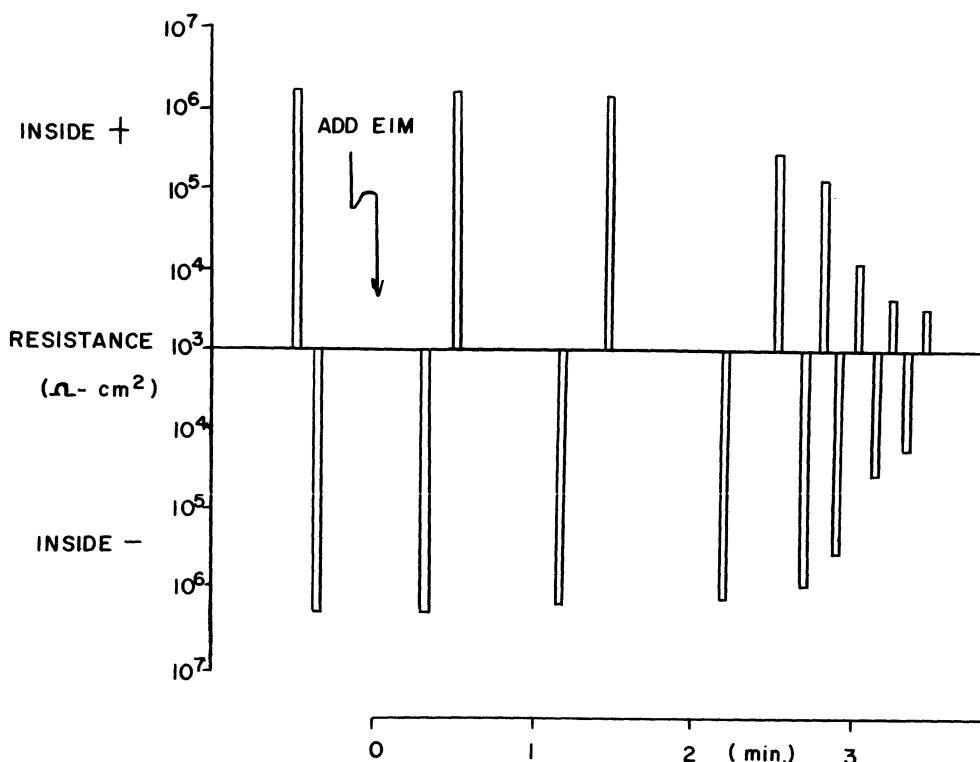


Figure 4. The effect of EIM on membrane resistance as a function of time measured with both polarities. Note the membrane resistance is asymmetrical.

and casein. Of these compounds, both of the positively charged surface active materials produced large transmembrane potentials when added to the aqueous solution on one side of the membrane.

The results of a set of experiments in which HDTAB was used is shown in Fig. 5. Addition of HDTAB to one side of the BLM produced a transmembrane potential which was positive on that side. The potential developed a few seconds after the material was added, the short delay being due to the amount of time required for the stirring motion to bring the material to the membrane interface. The potential developed across the membrane was transient and began decaying in an exponential manner after ten seconds or so. The total time course of the potential was in the range of 1-3 minutes. The transmembrane potential increased with increasing concentrations

of HDTAB until the detergent caused the membrane to rupture. Similar results were produced with protamine sulfate except that the potential developed was much smaller.

The effect of these cationic surface-active materials was much more pronounced when the salt concentration in the aqueous solution was low. The negatively charged materials had little effect, although casein was not tested at high concentrations due to its very limited solubility in neutral salt solution. It was concluded from these experiments that the net interfacial charge on the E. Coli BLM was negative.

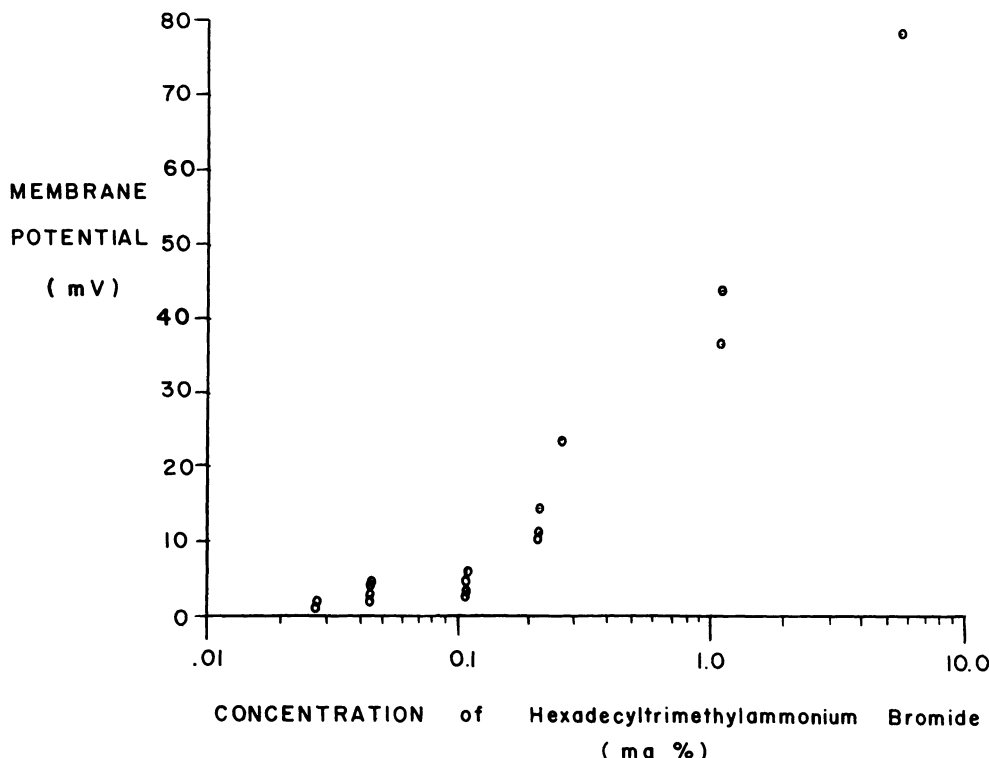


Figure 5. The effect of HDTAB on E. Coli BLM potential.

OXIDIZED CHOLESTEROL BLM

One of the difficulties in studying BLM is to find a lipid solution from which stable BLM can be formed. Oxidized cholesterol solution has been found to give very stable membranes (21), and it is by far the easiest to work with. The intrinsic electrical properties of oxidized cholesterol BLM are as follows: resistance -- $5 \times 10^9 \Omega \text{cm}^2$, capacitance-- $0.57 \mu\text{F}/\text{cm}^2$, and breakdown voltage--300 mV (16).

The effect of I_2 and KI on BLM was first observed by Lauger et al (22). They reported that the electrical resistance of lecithin BLM is lowered by 3 orders of magnitude when KI- I_2 was present in the bathing solution. Lauger et al. have also reported that a steady concentration potential of about theoretical value was observed, implying the BLM is highly specific for I^- .

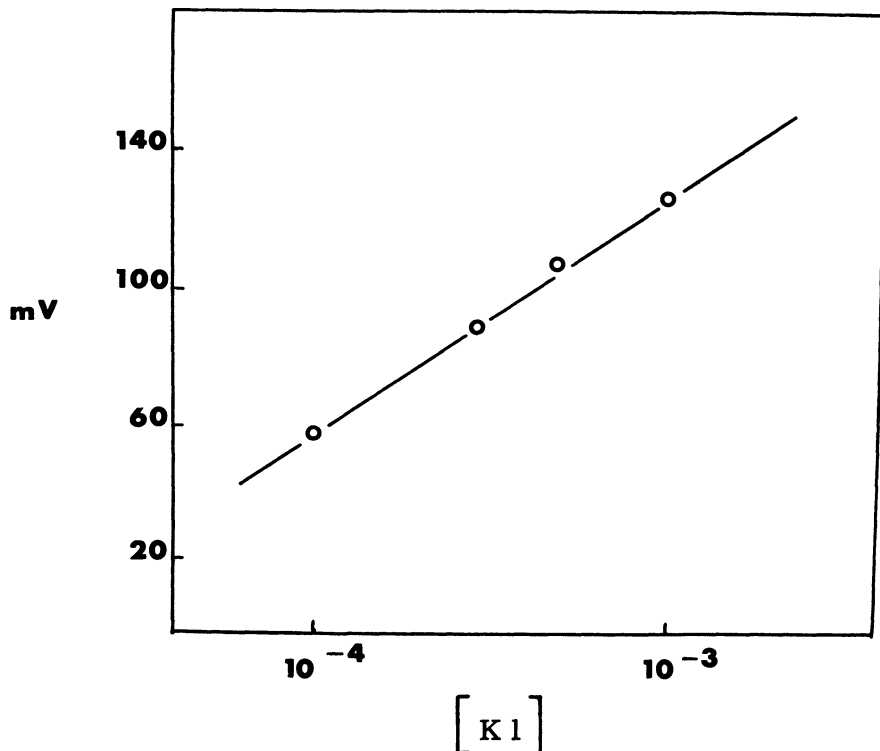


Figure 6. Typical response of an iodine-modified BLM to KI in 0.1 M KCl. The response to I^- depends only on the presence of I_2 and irrespective of BLM-forming solution.

In pursuing the effect of KI-I₂ on BLM, we have found that a BLM can be made into an iodide-specific electrode by simply incorporating a minute amount of I₂ into the lipid solution prior to BLM formation. For example, BLM formed from an oxidized cholesterol solution containing 0.2 mg of I₂ (per 5 ml) responded ideally to I⁻. A typical curve is shown in Fig. 6. The presence of other ions such as Cl⁻, SO₄²⁻ or F⁻ did not interfere with the "electrode" response to iodide ion.

In another series of experiments, we have measured the current/voltage (I/V) curves of oxidized cholesterol BLM in 0.1 M K I + 0.1 g I₂ with Na₂S₂O₃ added to one side of the BLM. The I/V curve shown in Fig. 7 has been obtained with the aid of an automatic recording polarograph (Polarecord Model E, Metrohm Ltd.). The presence of Na₂S₂O₃ on one side of the BLM generated a potential difference of about 45 mV. It is evident that the I/V curve is no

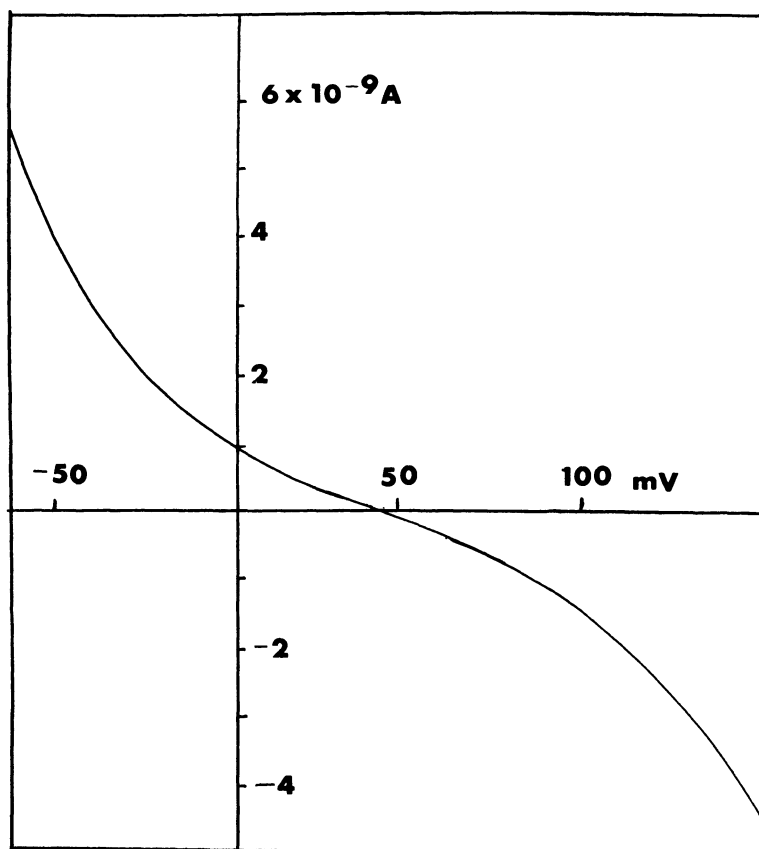


Figure 7. Current/voltage curve of an oxidized cholesterol BLM in 0.1 N K I + 4x10⁻⁴ M iodine. In addition, the inner chamber contained 5x10⁻³ M Na₂S₂O₃.

longer linear but still entirely symmetrical. Our findings on the effect of KI-I₂ on BLM are consistent with the observations reported by other workers (22,23). The presence of I₂ in the BLM facilitates the selective iodide transport, which in turn is manifest in the development of a concentration potential in accordance with the Nernst equation. A possible explanation for the non-linear portion of the I/V curve will be given later.

CHLOROPLAST BLM (CHL-BLM)

The third type of BLM which has been studied is constituted of spinach chloroplast extracts (18). The chloroplast black lipid membrane (Chl-BLM) is of special interest in that upon illumination with light, two basic photoelectric effects can be induced. The photovoltaic effect has been found to be dependent both on light intensity and wavelength. In addition, the electrical properties of Chl-BLM can be altered by a number of modifiers. The results of some recent experiments are summarized in the following paragraphs.

The Effect of Fe⁺³ and Ferredoxin

Unlike other BLM, Chl-BLM have been found highly specific to H⁺ below pH 8. For example, in the pH region 4-6, a potential difference of theoretical value has been observed (i.e., 58 mV/pH). This implies that the surface of Chl-BLM is negatively charged (presumably due to sulfolipids and phospholipids). In the dark the d.c. resistance of the membrane is ohmic when separating two identical solutions. The unmodified Chl-BLM exhibits photoconductivity. When Fe⁺³ is added to one side of the Chl-BLM, a "rectification" effect can be produced. The current/voltage curve for an asymmetrical system containing 10⁻³M Fe⁺³ on one side is shown in Fig. 8A. Similar effect can be induced when spinach ferredoxin is used in place of Fe⁺³ (see Fig. 8B).

The Effect of 2,4-dinitrophenol (DNP) and pH

The separation of charges by light in chloroplasts is believed to be among the first steps involved in the primary process of photosynthesis. Chemical compounds such as 2,4-dinitrophenol (DNP) can uncouple electron transfer from energy accumulation in the electron transport chain. The similar effect of DNP on oxidative phosphorylation in the mitochondria is well known (24). With the availability of BLM as model systems for the biological membranes (see Fig. 1), various uncouplers including DNP have been tested (16,25). In addition to DNP, we have investigated the effect of carbonylcyanide-p-trifluoromethoxy-phenolhydrazone (FCCP) on the electrical properties of Chl-BLM.

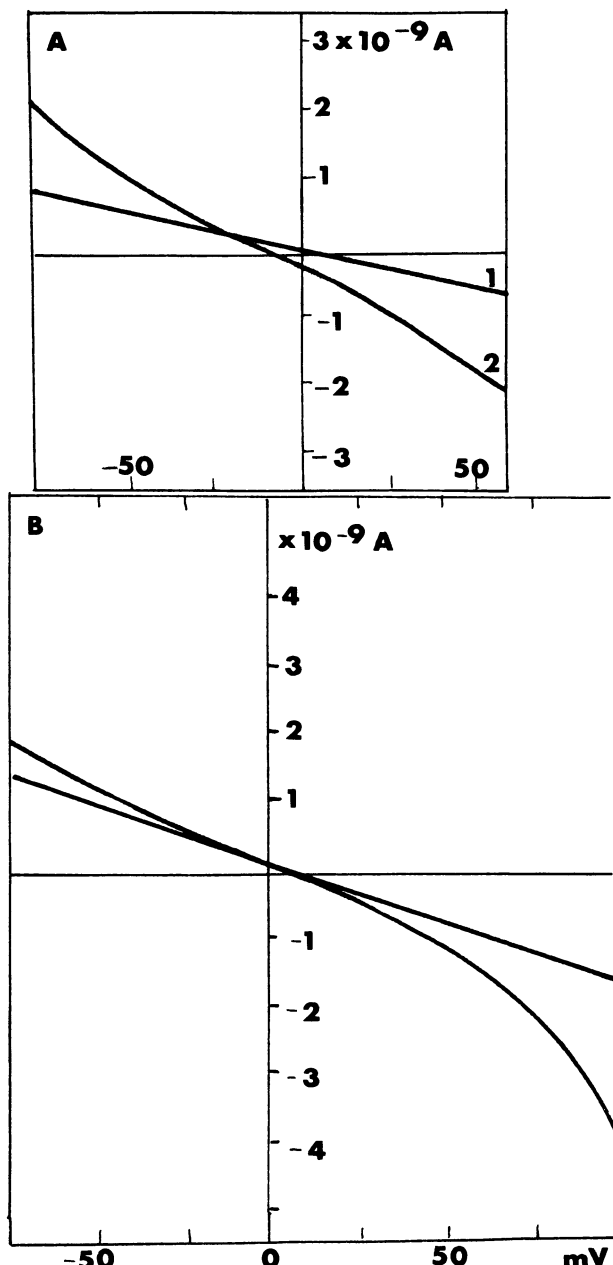


Figure 8. Current-voltage curves of chloroplast BLM in 0.1 M citrus-phosphate buffer at pH 5. A. Inner chamber containing 10^{-3} M Fe^{+3} ; curve 1 obtained in the dark, curve 2 with white light. B. Inner chamber containing 0.1 mg ferredoxin preparation; curve 1 in the dark, curve 2 with light.

In low concentrations (10^{-6} - 10^{-5} M), both DNP and FCCP dramatically lowered the Chl-BLM resistance, FCCP being twenty times more effective.

The efficiency of FCCP and DNP on Chl-BLM has been found to be pH dependent. Fig. 9A presents the results obtained with a Chl-BLM as a function of pH (0.1M citrate-phosphate buffer). It is interesting to note that in the absence of an uncoupler, the electrical resistance of Chl-BLM itself exhibits a pH-dependency (Fig. 9B).

The effect of these modifiers on non-linear I/V curves (iodine, FCCP, and DNP) may be explained in terms of ion association (26) in the lipid moiety and dissociation of the ionizable groups of the Chl-BLM. At the BLM biface (i.e., the two co-existing membrane/solution interfaces), dissociation of the ionizable groups of the lipids must be governed by the pH of the bulk solution and possibly also by the electric field. Thus, the selectivity of the BLM would be controlled by the ionizable groups at the biface whereas the specificity depends upon the solubility

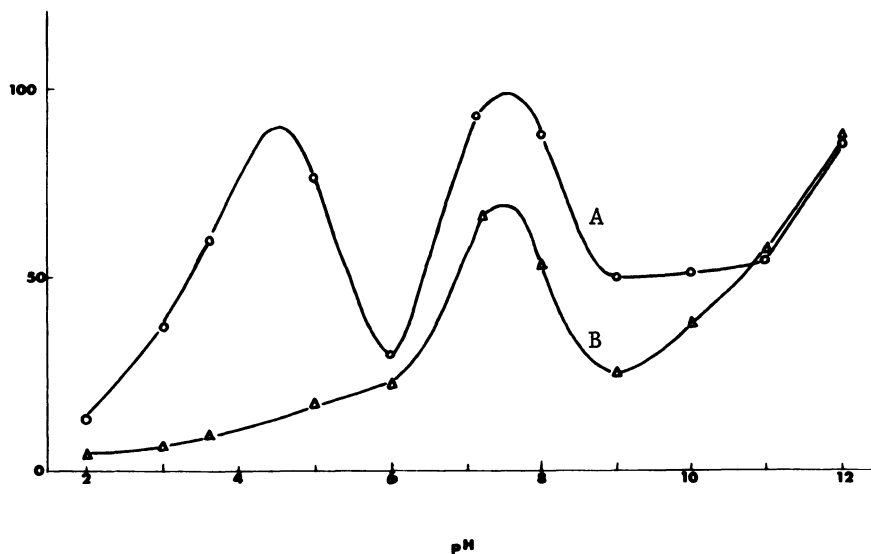


Figure 9. pH dependence of BLM current. BLM-forming solution was prepared from spinach chloroplast extract. Aqueous solution= 0.1 M citrate-phosphate buffer; Applied voltage: 60 mV. Curve A was with 2,4-dinitrophenol (DNP) as the modifier and curve B without modifier. Applied voltage = 60 mV.

of lipid-soluble complex. According to Bjerrum's theory of ion association (26), the equation governing the following reaction



is given by

$$K^{-1} = \frac{4\pi N}{1000} \left(-\frac{e^2}{DkT} \right)^3 Q(b) \quad (2)$$

where K is the dissociation constant for the reaction (1), and where N , D , R , T , and e have the usual significance. The quantity $Q(b)$ is a definite integral, which is a function of (b) defined by the following equation

$$b = \frac{e^2}{DkTa} \quad (3)$$

where "a" is the distance between the ion pair. In principle one should be able to calculate the dissociation constant of the ion pair in the hydrophobic region of the BLM ($M^-—C^+$, where M^- stands for a negatively charged modifier, and C^+ is its counter ion). The Bjerrum theory of ion association has been quantitatively confirmed for aqueous solutions and non-aqueous systems by the work of Kraus and Fuoss (27). Whether the theory can be extended to BLM systems remains to be seen. The evidence at hand suggests that, when modifiers or ionizable species are present in the BLM system, the current/voltage curves are no longer linear (Figs. 7 and 8). It seems probable that the dissociation of ion-pairs under the condition of intense field ($\sim 1-5 \times 10^5$ V/cm) may be responsible for the non-linear I/V behavior. In fact, the production of additional charge carriers as a function of the electric field (the Wien effect) has been considered recently in conjunction with nerve excitation (28). The possibility that a similar mechanism is also operative in the BLM system under the influence of modifiers and electric field seems quite likely.

The Photoelectric Spectrum of Chl-BLM

As has been mentioned above, the observation of photoelectric effects provides ample evidence that a separation of charges (electrons and holes) by light is taking place in Chl-BLM. To study further the light-induced phenomena, we have now developed a quantitative technique to obtain the spectra of the Chl-BLM (29). The method is based upon the measurement of photoresponse of the BLM as a function of wavelength. The action spectrum of a Chl-BLM together with its absorption spectrum is shown in Fig. 10. Within the experimental error of detection instruments, the two spectra are practically identical. This finding is consistent with the observation that the spectral excitation curve of most organic photoconductors (semiconductors) is generally found to be very similar to that of the absorption spectrum.

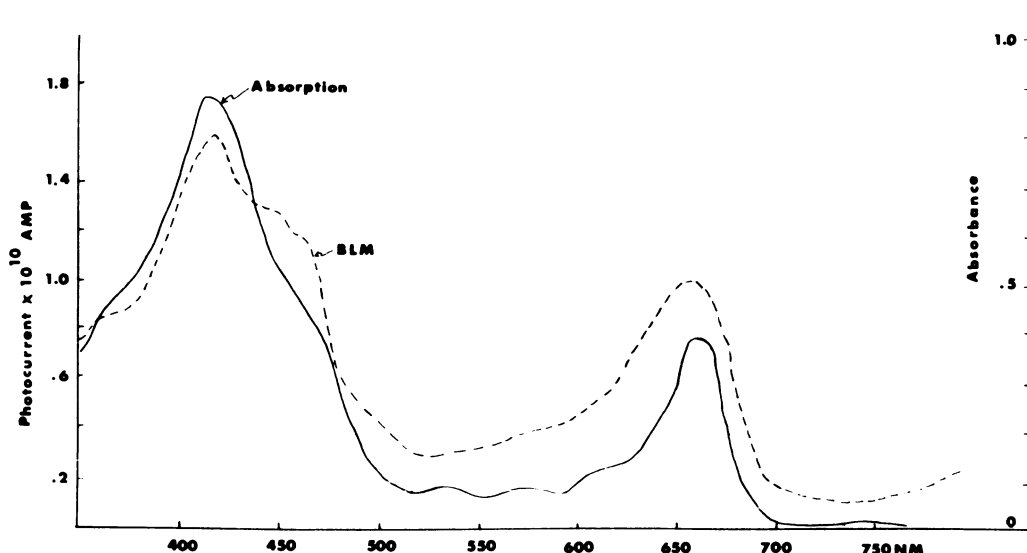


Figure 10. Absorption and photoelectric spectra of chloroplast extract (29).

CAROTENOID BLM

In the earlier studies BLM have been used as models for various types of biological membranes (Fig. 1). Attempts were made to incorporate visual pigments such as rhodopsin into the BLM but no significant results were obtained (30). More recently, β -carotene has been incorporated into a BLM system but no marked lowering of electrical resistance was observed (31). With availability of more stable BLM-forming solutions and improved experimental techniques, we have initiated a new series of experiments with the aim of constituting a different type of BLM as a model for the visual receptor membrane (19). The following paragraph summarizes our preliminary findings on black lipid membranes containing carotenoid pigments (or carotenoid BLM for short).

The experimental techniques used in the formation of the carotenoid BLM have been described previously (4). The lipid solutions used consisted of various carotenoids (*all-trans* retinal, *9-cis* retinal, *all-trans* retinol, and β -carotene), phospholipids, and oxidized cholesterol dissolved in liquid alkanes. The dark d.c. resistance of the membrane is ohmic ranging from 10^6 to $10^7 \Omega\text{-cm}^2$, which is about 2-3 orders of magnitude lower than that of carotenoid-free BLM. Upon illumination with white light (DFG tungsten lamp, Sylvania) a maximum photo-emf of about 6 mV was observed in a BLM containing a mixture of *all-trans* retinal and β -carotene. All carotenoid BLM were found to be

photoconductive. In addition, we have found that the photoresponses of these carotenoid BLM were more complex as the experimental conditions were altered. Depending upon the carotenoid pigments used and external factors (e.g. modifiers and applied voltage), the voltage/time curves can vary from a simple monophasic response to a typical biphasic wave-form not unlike those found in vertebrate retina (32). The various modes of responses which have been observed in our initial experiments are illustrated in Fig. 11.

The relevance of carotenoid BLM as an experimental model for the visual receptor membrane may be viewed from the standpoint of visual organelles (see Fig. 12). As has been revealed by the electron microscope, the outer segment membranes of rods and cones are highly organized (5). The structure of the outer segment membranes is believed to be similar to that of the unit membrane (6,34). Thus, the carotenoid BLM is one of the ideal systems with which not only initial energy transduction mechanism from photons to electrons and holes but also the triggering mechanism for ionic permeability across the membrane can be readily investigated. For example, Hagins *et al* (35) have reported that the initial membrane depolarization of the sacs of the rod outer segment is

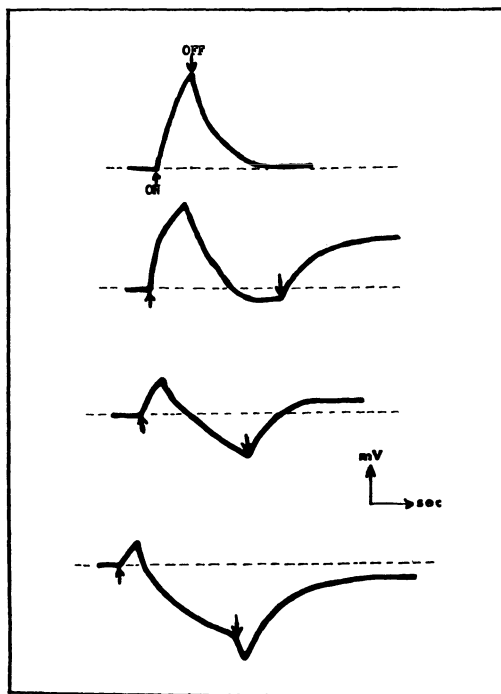


Figure 11. Modes of photoelectric response of a carotenoid BLM under different experimental conditions (19).

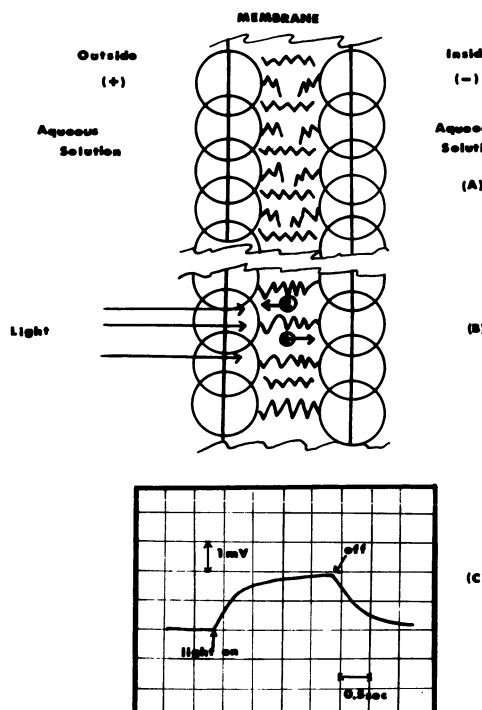


Figure 12. The effect of light on a carotenoid BLM containing β -carotene and retinal. (a) illustrating a hypothetic structure of the BLM in the dark, (B) generation of charge carriers by light, (C) an oscilloscope trace of a carotenoid BLM in response to illumination.

fairly localized while the outer plasma membrane depolarization occurs with a large latency and delocalization. We are at the present carrying out further experiments with the carotenoid BLM with the object of understanding the mechanisms of excitation and energy conversion. It is hoped that the results will be useful in analyzing the complicated electroretinogram (32,33).

SUMMARY

At the present time the molecular structure of biological membranes has not been definitely settled. Nevertheless, the general picture of membrane structure widely accepted today, is that based upon the bimolecular leaflet model. In view of this acceptance, a black or bilayer lipid membrane (BLM) upon suitable modification appears to be the closest approach to the biological membrane.

We have shown that an unmodified BLM in common salt solutions

(NaCl or KCl) exhibits characteristics expected of a liquid hydro-carbon layer of equivalent thickness. Upon the addition of modifiers, the intrinsic properties of a simple BLM can be drastically altered. The BLM modifiers can be broadly divided into 5 groups: (1) those altering the passive electrical properties, (2) those changing the mechanical properties, (3) those conferring ion selectivity, (4) those inducing excitability, and (5) those generating photoelectric effects. The results of some recent studies from this laboratory using a number of modifiers on a variety of BLM systems as models for various biological membranes have been described.

ACKNOWLEDGMENTS

The author acknowledges the invaluable collaboration of his colleagues: Drs. A. L. Diana, S. P. Verma, N. T. Van, Mr. W. A. Huemoeller and Mr. N. Kobamoto in the experimental work described in this paper. The E. Coli cells were kindly supplied to us by Professor Harold Sadoff. A sample of FCCP was provided by Dr. W. W. Prichard of E. I. duPont Co. These investigations were supported by Grant GM-14971 from National Institutes of Health.

REFERENCES

1. J. A. Castleden, *J. Pharm. Sci.*, 58, 149 (1969).
2. A. D. Bangham. *Progress in Biophysics*, 18, 29 (1968).
3. L. Rothfield and A. Finkelstein, *Ann. Rev. Biochem.*, 37, 480 (1968).
4. H. T. Tien and A. L. Diana, *Chem. Phys. Lipids*, 2, 55 (1968).
5. F. S. Sjöstrand, *Radiation Res. Suppl.*, 2, 349 (1960).
6. J. D. Robertson, *Protoplasma*, 63, 219 (1967).
7. E. Gorter and F. Grendel, *J. Exptl. Med.*, 41, 439 (1925).
8. H. Davson and J. F. Danielli, "The Permeability of Natural Membranes", Cambridge, London, (1952).
9. H. T. Tien, *J. Gen. Physiol.*, 52, 125s (1968).
10. P. Mueller, D. O. Rudin, H. T. Tien, and W. C. Wescott, in "Recent Progress in Surface Science", 1, 379 (1964).
11. P. Mueller, D. O. Rudin, H. T. Tien, and W. C. Wescott, *Nature*, 194, 979 (1962).
12. H. T. Tien, in "The Chemistry of Bio-Surfaces", M. L. Hair, ed., Marcel Dekker, Inc., New York, to be published.
13. P. Mueller and D. O. Rudin, *Nature*, 217, 713 (1968).
14. T. Hanai, D. A. Haydon, and J. Taylor, *J. Theoret. Biol.*, 9, 422 (1965).
15. R. E. Wood, R. P. Wirth, and H. E. Morgan, *Biochim. Biophys.* 163, 171 (1966).
16. H. T. Tien and A. L. Diana, *Nature*, 215, 1199 (1967).
17. Bielawski, T., E. Thompson and A. L. Lehninger, *Biochem. Biophys. Res. Commun.*, 24, 948 (1966).

18. H. T. Tien, W. A. Huemoeller, and H. P. Ting, Biochem. Biophys. Res. Commun., 33, 207 (1968).
19. H. T. Tien and N. Kobamoto, Nature, in press (1969).
20. H. T. Tien and A. L. Diana, J. Colloid Int. Sci., 24 287 (1967).
21. H. T. Tien, S. Carbone, and E. A. Dawidowicz, Nature, 212, 718 (1966).
22. P. Lauger, W. Lesslauer, E. Marti, and J. Richter, Biochim. Biophys. Acta, 135, 20 (1967).
23. A. Finkelstein and A. Cass, in "Biological Interfaces: Flows and Exchanges, Little, Brown & Co., New York, 1968. p. 145.
24. P. Mitchell, Biol. Rev., 41, 445 (1966).
25. E. A. Liberman, E. N. Mokhova, V. P. Skulachev, and V. P. Topaly, Biofizika, 13, 188 (1968).
26. N. Bjerrum, "Selected Paper", Emar Munksgaard, Copenhagen (1949). pp. 108-119.
27. R. M. Kraus and C. A. Fuoss, J. Am. Chem. Soc., 55, 1010 (1933).
28. L. Bass and W. J. Moore, Nature, 214, 393 (1967).
29. N. T. Van and H. T. Tien, Biochim. Biophys. Acta., (1969) to be published.
30. D. O. Rudin and H. T. Tien, unpublished data (1961-1962).
31. R. B. Leslie and D. Chapman, Chem. Phys. Lipids, 1, 143 (1967).
32. K. T. Brown, Vision Res., 8, 633 (1968).
33. W. L. Pak and R. A. Cone, Nature, 204, 836 (1964).
34. J. J. Wolken, J. Am. Oil Chemists' Soc., 45, 251 (1968).
35. W. A. Hagins, H. V. Zonada, and R. G. Adams, Nature, 194, 844 (1962).

ASYMMETRIC PHOSPHOLIPID MEMBRANES: EFFECT OF pH AND Ca^{2+}

Shinpei Ohki and Demetrios Papahadjopoulos

Dept. of Biophysical Sciences, State University of New York at Buffalo and Dept. of Experimental Pathology Roswell Park Memorial Institute, Buffalo, New York

SUMMARY

Phosphatidylserine membranes (either as liquid-crystalline vesicles or as bilayers) in 0.1M NaCl and neutral pH, are very impermeable to cations or anions and exhibit high electrical resistance ($5 \times 10^7 \Omega\text{cm}^2$). However, the same membranes become unstable under conditions of asymmetric distribution of Ca^{2+} or H^+ : Addition of Ca^{2+} to the aqueous salt solution only on one side of the membrane, produces a lowering of the d.c. resistance, and above a certain concentration results in breakage of the membrane. On the other hand, if Ca^{2+} is present on both sides, the membranes are stable and show very high electrical resistance ($5 \times 10^8 \Omega\text{cm}^2$) over a wide pH range. The above phenomena were not observed with membranes made of phosphatidylcholine. It is suggested that the instability of PS membranes observed in this study is due to the difference in surface energy between the two opposing sides of the bilayer. The biological implications of membrane instability following an asymmetric distribution of Ca^{2+} or H^+ is discussed.

INTRODUCTION

Phospholipid membranes have recently become the subject of intensive research as models for biological membrane function (4, 47). Since most biological membranes are complex mixtures composed predominantly of lipids and proteins, artificial membranes composed exclusively of lipids can serve only as very simplified models. However some of the properties of such artificial membranes bear striking similarity to those of the biological membranes (20, 19,

39, 6). Thus it appears that within certain limitations, artificially produced phospholipid membranes are very promising tools for studying "in isolation" certain molecular events relating to specific membrane functions.

Most of the published work on artificial phospholipid membranes has been performed either with neutral purified phospholipids or with ill-defined lipid-extracts from various natural sources (4, 47). However, it would appear that for studies relating to electrical excitation where binding of ions on fixed charges is an important factor, the phospholipids of choice would be some of the species that carry formal charges (17, 26, 31). Anionic phospholipids (PS, PA, PI, PG, diPG, triPI) are present in most membranes in widely varying proportions, although the percentage of each species within a given membrane is fairly characteristic (51, 3).

Recent work on the surface properties of anionic phospholipids indicates that they bind bivalent metals with high stability constants and even in the presence of high concentration of monovalent salts (2, 13, 26, 5). In contrast, it has been shown that unsaturated PC does not bind appreciable amounts of Ca^{2+} in the presence of 0.1M Na^+ or K^+ (15, 36, 40, 26, 11).

Studies concerned with the permeability properties of anionic (acidic) phospholipids indicate that these compounds are able to form bilayer structures with very high resistance to the diffusion of ions (17, 28, 34, 33). Membranes composed of PS either in the form of unilamellar vesicles or as planar bilayers are characterized by high electrical resistance, high capacitance and low diffusion of Na^+ , K^+ and Cl^- (34, 31, 21, 22). However, bivalent metals appear to have a pronounced effect on these permeability properties. Thus, it has been shown that Ca^{2+} increases the diffusion rate of Na^+ and K^+ out of unilamellar PS vesicles (28, 34, 33). It has also been shown that PS bilayers formed in the presence of Ca^{2+} and Na^+ are more stable and have higher electrical resistance than those formed in the presence of only NaCl (21, 22).

This intriguing dual role for Ca^{2+} in its ability to produce both an increase and a decrease in the permeability of PS membranes has recently been investigated further by the present authors (31). The data obtained indicate that the stability of a phospholipid membrane is markedly effected by the asymmetric distribution of fixed charges and counterions on the two opposing sides of a phospholipid bilayer.

The present communication is a review of recent data concerning the effect of Ca^{2+} and H^+ on the stability of PS bilayers and an account of the biological implications of such a system.

RESULTS AND DISCUSSION

Effect of pH on Conductivity of Phospholipid Membranes:

Bilayer membranes composed of PS show a very high resistance (10^7 to $10^8 \Omega\text{cm}^2$) when made in 0.1 N NaCl and slightly acidic solutions, pH 3 to 7 (Fig. 1). This range of electrical resistance values is remarkably similar to those calculated (34, 33) from data of K^+ diffusion rates through PS vesicles (2×10^{-15} equiv/cm² sec = $1 \times 10^8 \Omega\text{cm}$). The decrease in resistance with pH lower than 3.0 shown in Figure 1 could be explained by the protonation of the phosphate group which would render both phospholipids positively charged or alternatively by the permeability to protons. The decrease in resistance between pH 4 and 8 (also observed with PC bilayers (21)), is more difficult to explain in terms of ionization of specific groups on the molecules. Titrations of monomolecular films indicate no changes in surface potential

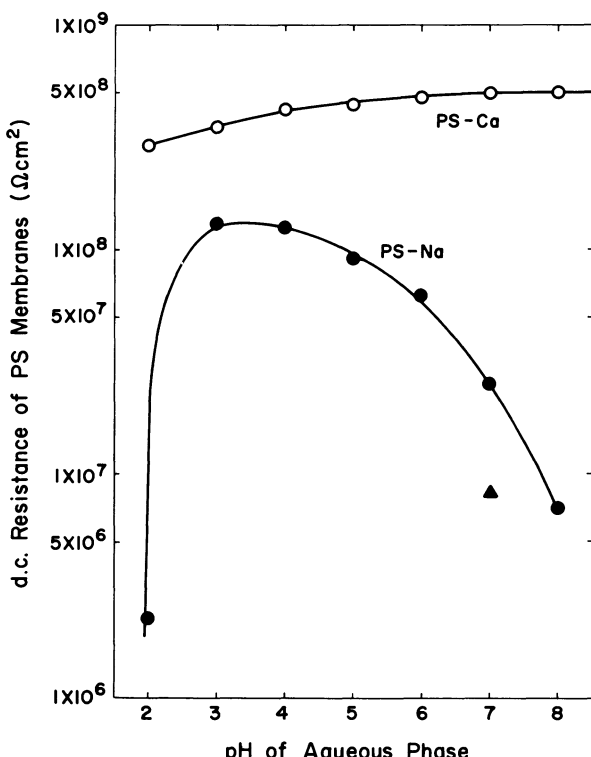


Fig. 1. Electrical resistance of PS membranes at different pH: The membranes were formed in the following solutions: in 0.1 M NaCl, ●; in 0.1 M NaCl and 1.0 mM CaCl₂, ○; point ▲ indicates the resistance of a PS membrane formed in 0.1 M NaCl, with 1.0 mM CaCl₂ added to one side of the membrane after the formation.

between pH 3 and 11 for PC, and between pH 6 and 9 for PS (26). A possible explanation could be the presence of small amounts of fatty acids which are either present from the beginning or are produced by hydrolysis during the experiment. However, changes in resistance due to ionization seem to be much more pronounced than changes in ΔV . Thus, the ionization of the amino group in PS produces a change of 40 mV in ΔV and the ionization of the secondary phosphate of PA only 25 mV (26). Thus, a small degree of ionization (1%) would not produce appreciable changes in ΔV (less than 1 mV) but it would be expected to affect the conductivity. This would explain the instability of PS membranes above pH 8 although it is still difficult to apply the same argument for PC with a quaternary ammonium group.

Figure 1 also shows the effect of small amounts of Ca (1mM) in the presence of 100 mM NaCl on the resistance of PS bilayers. In this case the resistance is very high ($4-5 \times 10^8 \Omega\text{cm}^2$) and shows no change over a wide range of pH. This result is very similar to the titration curves of PS monolayers in the presence of the same concentrations of Ca^{2+} and Na^+ (26). Low concentrations of Ca^{2+} have no effect on PC resistance, although an increase in resistance is noted with high Ca^{2+} (0.1N) at high pH (21). It should be noted here that PS bilayers in 0.1 NaCl show generally lower resistance in the presence of EDTA. Obviously small amounts of contaminant bi- and multi-valent metals stabilize the membrane and might explain the higher resistance of PS compared to PC (21, 33). Small amounts of bi- and multi-valent metals are usually present as contaminants in the monovalent salts and are also extracted along with PS from natural sources. Metal determinations performed by SPANG Micro-analytical Laboratory indicated the following: For a sample of bovine PS purchased from Applied Science Laboratories there was 204 parts per million Ca^{2+} and 4030 parts per million Mg^{2+} . For a sample of bovine brain PS prepared in our laboratory, there was 100 parts per million Ca^{2+} and 40 parts per million Mg^{2+} .

Asymmetric Distribution of Ca^{2+} :

When CaCl_2 is added on one side of a PS membrane prepared in 0.1 N NaCl (pH 7.0) the electrical resistance of the bilayer drops by a factor of more than two (Fig. 1). Above a certain concentration of Ca^{2+} the membrane becomes unstable and breaks. In a representative experiment where the resistance of PS was $6.8 \times 10^7 \Omega\text{cm}^2$ As it has been noted in the previous section, when 1 mM CaCl_2 is present on both sides, the resistance is much higher ($3 \times 10^8 \Omega\text{cm}^2$). The concentration of CaCl_2 necessary to produce breaking is highly dependent on the pH. As Figure 2 shows, while 1 mM is enough to break the membrane at pH 7.8 it takes 5 mM CaCl_2 at pH 7.0 and even higher at lower pH (curve a). These experiments were conducted in the presence of 0.1 mM EDTA in order to remove any higher valency metals either contributed as contaminants of the NaCl or extracted

with the PS fraction from natural sources. When EDTA is not included in the solution, the concentration of Ca^{2+} required for breaking are usually higher (point b in Fig. 2). The presence of Tris-Cl also has an inhibitory effect on the ability of Ca^{2+} to break the membrane. Points 1, 2, 3, 4 in figure 2 were obtained with 0.1, 1.0, 5.0 and 10 mM Tris-Cl respectively. EDTA was present in these experiments at 0.1 mM concentration which rules out contamination by bivalent metals and points to the possibility of a competitive interaction. Similar instability and breaking is observed with membranes of PS formed in 1 mM CaCl_2 solution (with 100 mM NaCl), equimolar amounts of EDTA are added on one side only. However, it should be noted here that membranes made of PC do not show any instability at all with concentrations of Ca^{2+} up to 20 mM on one side only.

The above results bear remarkable similarity to the effect of Ca^{2+} on the permeability properties of PS vesicles (28, 34). The addition of 1 to 2 mM CaCl_2 s to the outside solution of such vesicles produces complete discharge of the Na^+ and K^+ trapped inside the

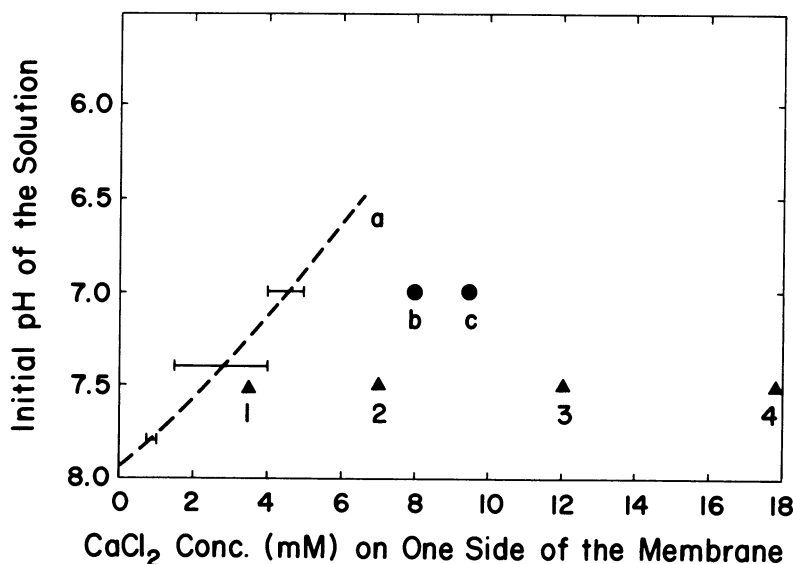
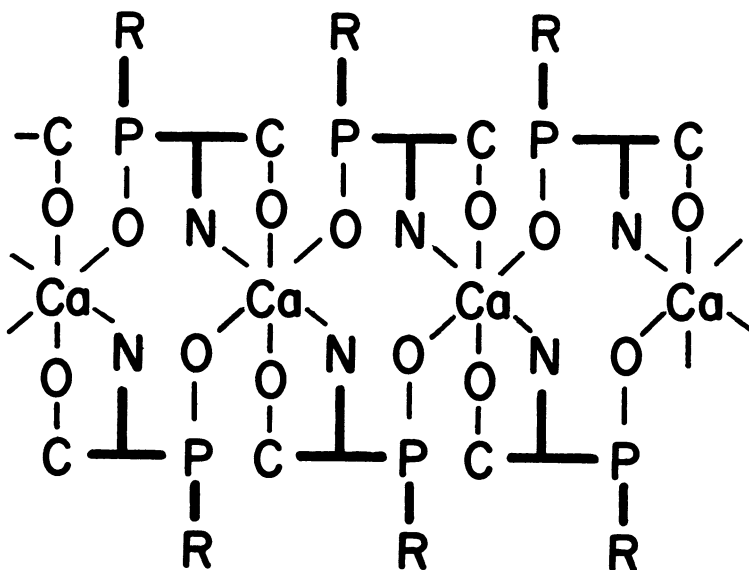


Fig. 2. Stability of PS membranes with asymmetric distribution of Ca^{2+} . Membranes were formed in 0.1 M NaCl and 0.05 mM EDTA. Curve a (----) indicates the amount of Ca^{2+} (in mM) added to one side of the membrane before breakage. Points 1, 2, 3, 4 (\blacktriangle) indicate the presence of increasing amounts of Tris-Cl (0.2, 1.0, 2.0, 10.0 mM respectively). Point b (\bullet) indicates the amount of CaCl_2 needed in the absence of EDTA (other conditions same as points of curve a). Point c (\bullet) indicates the effect of CaCl_2 on a PS-cholesterol membrane.

vesicles within minutes. Smaller amounts of Ca^{2+} produce a slow increase in K^+ or Na^+ diffusion (33). Using the same vesicles it has been shown that at a concentration of 1mM of Ca^{2+} in 145mM KCl , PS binds one equivalent of Ca^{2+} per molecule (5). Titration of PS monolayers has shown (5, 26) that the same concentration of Ca^{2+} produces a decrease in film pressure (increase in surface tension, $\Delta\overline{\text{I}} = 6$ dynes/cm) and an increase in surface potential (40mV). In spite of the binding of one equivalent of Ca^{2+} per PS molecule, microelectrophoresis of PS vesicles in the presence of 1mM CaCl_2 (and 145 NaCl) indicates that the surface is still electronegative: potential = -35 mV. This was interpreted (26) as evidence for the discharge of the amine proton during Ca^{2+} binding also shown earlier by titrimetric techniques (1). The binding of Ca^{2+} to PS (Fig. 3) is tentatively illustrated as a hexadentate complex involving four neighboring PS molecules in a linear polymeric arrangement.



PS- Ca^{2+} complex, TOP VIEW

Fig. 3. Diagrammatic representation of PS-calcium complex. In this illustration the phospholipid molecules are placed with the fatty acid chains perpendicular to the plane of the page. The letter R signifies the rest of the molecule (diglyceride) connected to the head group phosphorylserine. Each Ca^{2+} is bound to a total of six groups (two phosphates, two carboxyls and two amines) of four different molecules. The whole complex is a linear polymeric arrangement.

arrangement. Not shown in figure 3 are the other counter-ions (Na^+ or K^+ which must be present as a diffuse layer adjacent to the $\text{PS}-\text{Ca}^{2+}$ complex which is still electronegative. The instability of PS membranes following an asymmetric distribution of Ca^{2+} in respect to the two planes of the membrane was recently interpreted as the result of differences in the surface energy between these two planes (23).

Counterbalancing of Ca^{2+} with H^+

If PS membranes are formed at a certain pH and the pH of the solution facing only one side of the membrane is changed subsequently, a point of instability is reached (breaking) which is characteristic of the initial pH of the solution. Figure 4 illustrates some of the

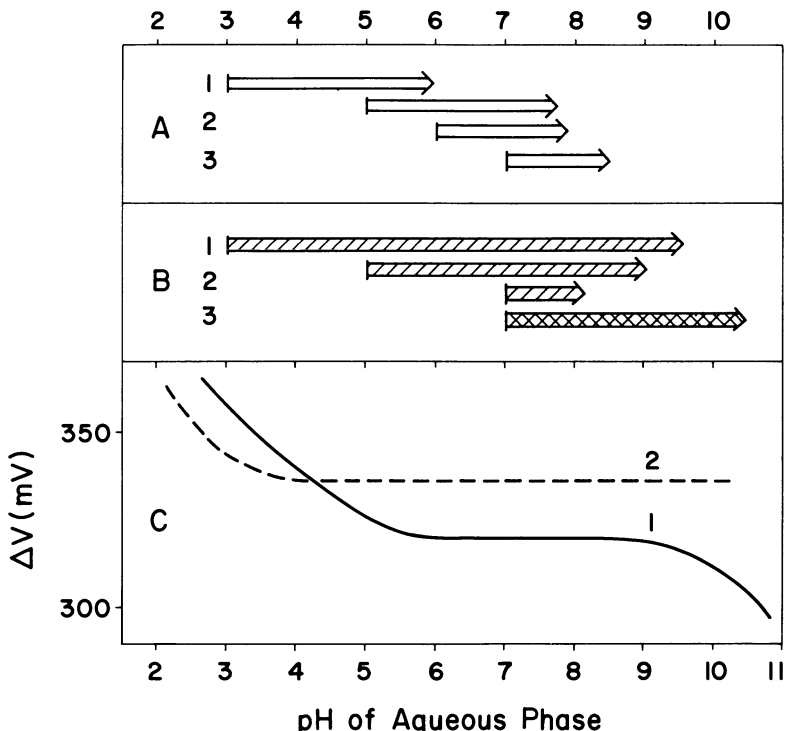


Fig. 4. Limits of stability of PS membranes under asymmetric distribution of H^+ and Ca^{2+} . Each horizontal bar represents the difference in pH between the two sides of the membrane, before the membrane breaks. The beginning of each bar is the initial pH and the end point of each bar the final pH of the solution on the outside aqueous compartment. A: experiments in 0.1 M NaCl only. B1 and B2: experiments in 0.1 M NaCl with 1 mM Ca^{2+} added to the outside before the change in pH. B3: experiments in 0.1 N NaCl and 1.0 mM CaCl_2 . C: Titration of PS monolayers. 1: in 0.1 M NaCl , 2: in 0.14 M NaCl and 1.0 mM CaCl_2 (for details see ref.).

results indicating the stability of PS membranes under asymmetric distribution of H^+ . Figure 4A represents experiments without Ca^{2+} . If a PS membrane is formed at pH 3.0, it reaches the point of instability (breaking) when the outside pH is increased to 6.0 (Fig. 4A, 1). However when the initial pH is higher (Fig. 4A, 2 and 3), the outside pH at which the membrane breaks is also higher. It is thus apparent that the stability of the membranes is defined by the difference in ionization of the three head-groups (phosphate, carboxyl and amino) between the two sides of the membrane. At pH 3.0 PS should be near the isoelectric point (Fig. 4C, curve 1) while at pH 6.0 each molecule carries one extra negative charge per molecule. This difference of one charge per molecule (zero vs. one) produces instability as shown in A1. If both sides are charged with one charge per molecule (at pH 6 or 7) the membrane is stable. However when the amine starts losing its protons above pH 6 or 7, a fraction of the extra charge per molecule is enough to produce breaking (Fig. 4A, 2 and 3).

The remarkable ability of Ca^{2+} in stabilizing asymmetric membranes is seen in Fig. 4B. Here the membranes were made at pH 3.0. Then 1 mM $CaCl_2$ was added outside only, followed by NaOH to increase the pH. At this point the PS membranes were neutral on one side (pH 3.0) and charged on the other (pH 3.0-9.5) but with Ca^{2+} binding on the charged groups. Such membranes were stable up to pH 9.5. This stability up to high pH decreases as initial pH becomes higher and H^+ do not counterbalance Ca^{2+} (Fig. 4B, 2). When Ca^{2+} is present on both sides, PS membranes formed at pH 7.0 can be titrated on one side with NaOH up to pH 10.5 (or with HCl down to pH 2.5) before they become unstable (Fig. 4B, 3). This stability over a wide pH range is also found upon titration of PS monolayers in the presence of Ca^{2+} (Fig. 4C, curve 2).

Effect of Cholesterol, Alcohols, Local Anaesthetics:

The presence of cholesterol in the membrane forming solution (1/1 W/W or 1/2 mole/mole PS/cholesterol) has generally a stabilizing effect on the membranes. It increases electrical resistance and decreases capacitance (32) of bilayer membranes. When mixed with PS in 1/1 molar proportion before the formation of sonicated vesicles, it reduces the diffusion rate to both Na^+ and Cl^- and increases the activation energy for the diffusion of these ions (32, 27). Cholesterol also has an inhibitory effect on Ca^{2+} induced permeability changes. As shown in Figure 2 (point c) it takes twice as much Ca^{2+} to break the membrane compared to the amount needed to break the membranes in the absence of cholesterol. The same effect was noticed with PS vesicles (32). This is probably due to the dilution of surface charge by the neutral molecules of cholesterol. A similar phenomenon has also been noticed with mixtures of PS and PC (33).

General and local anaesthetics have been used in conjunction with studies on the permeability of PC multilamellar vesicles. It has been reported (6) that alcohols tend to increase, while local anaesthetics tend to decrease the diffusion rate of K^+ through such model membranes. More recently, we have studied the effect of alcohols and local anaesthetics on the ability of Ca^{2+} to induce permeability changes in PS membranes. Both groups of anaesthetics seem to have a pronounced inhibitory effect on Ca^{2+} action. When PS membranes (bilayers) are made in 0.1 N NaCl solution containing 0.1 mM Butanol, addition of Ca^{2+} on one side has no effect up to 20 mM, the highest concentration studied. Presumably, this is again the effect of "dilution" of the PS molecules at the surface of the membrane by butanol molecules. Capacitance and resistance of the membrane ($C \approx 0.4 \mu F/cm^2$, $R \approx 4 \times 10^7 \text{ cm}^2$) indicate that the bilayers are still intact. The effect of nupercaine on PS vesicles is shown in Figure 5. Nupercaine alone (0.5 mM) has no effect on permeability (Fig. 5, A and B). $CaCl_2$ alone (1mM) increases the diffusion rate of

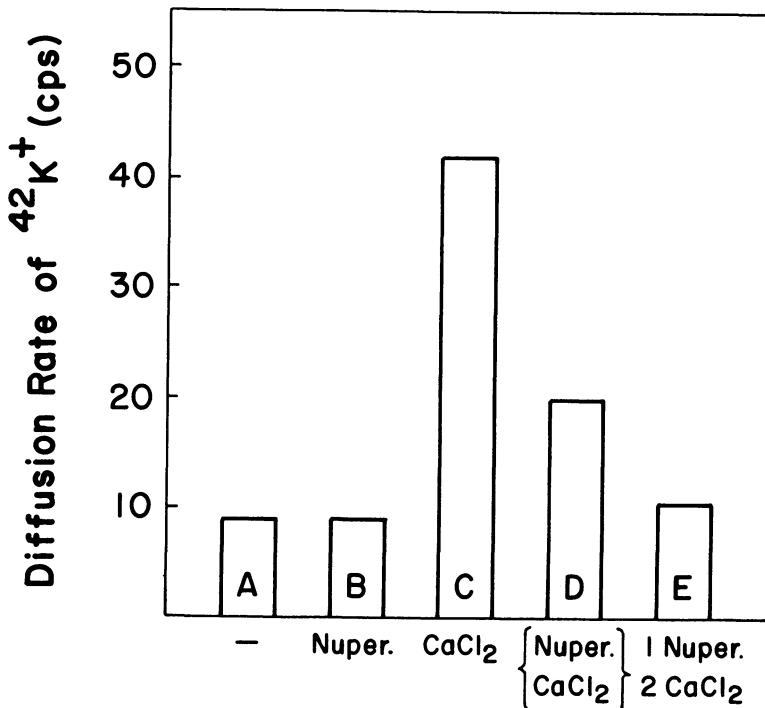


Fig. 5. Effect of $CaCl_2$ on PS vesicles in the presence of Nupercaine. Diffusion rate of ^{42}K from PS vesicles in 0.14 M KCl and 10 mM Tris-Cl at pH 7.4. A: no further additions. B: 0.5 mM Nupercaine added. C: 1.0 mM $CaCl_2$ added. D: Same concentrations of Nupercaine and $CaCl_2$ added simultaneously outside the vesicles. E: Same amounts as above but with Nupercaine added 1 hour before $CaCl_2$.

K^{42} out of vesicles (Fig. 5, C). When nupercaine is added simultaneously with $CaCl_2$, the increase in $^{42}K^+$ diffusion rate is limited (Fig. 5, D). When nupercaine is added first, followed by $CaCl_2$ the effect of Ca^{2+} is completely inhibited (Fig. 5, E). Local anaesthetics have been shown to decrease the negative charge on the surface of phospholipid vesicles (6) producing a small decrease in $^{42}K^+$ diffusion. However the effect shown here probably represents inhibition of Ca^{2+} binding, with subsequent failure of Ca^{2+} to produce permeability changes. Inhibition of Ca^{2+} binding to phospholipids has been shown earlier in two-phase systems (8) and monolayers (42). The results presented here, represent further evidence implicating changes in permeability properties as a result of Ca^{2+} - local anaesthetic antagonism. This subject is now being actively pursued in this laboratory.

Theoretical Consideration of Asymmetrical Membranes:

To understand the instability of the asymmetric membranes mentioned, we have considered the following membrane model. The membrane is composed of a monomolecular layer, each molecule of which, is a long chain with an equal length and has a dissociable polar head group at both ends of the molecule. The molecules lie with their molecular axes normal to the plane of the membrane such as in a unimolecular crystal, while the head groups coordinate in two outer surfaces facing the aqueous phases. The head group is able to chelate with a metal ion according to both the concentration of metal ions and the degree of dissociation of the polar group. It is assumed that if a polar head group chelates with a metal ion, the polar group loses its net charge, or the polar group does not receive any electrostatic interaction from the other charged polar groups.

Let us denote the position of the head groups on the surface of the membrane as "sites". We may denote the number of total sites on one surface of the membrane by N . When N_1 sites out of N are chelated with metal ions, the number of the sites which are not occupied by the metal ions is

$$N - N_1 = N_2 \quad (1)$$

We may define the average probability with which a polar group is chelated with the metal ion as follows:

$$X = \frac{N_1}{N} \quad (2)$$

From Eqs. (1) and (2), we have

$$\left. \begin{aligned} N_1 &= NX \\ N_2 &= N(1-X) \end{aligned} \right\} \quad (3)$$

As extreme cases, if all sites are chelated with the metal ions, $X = 1$, and if all sites are not chelated, $X = 0$.

Let us suppose in the following case: On one surface of the membrane, each site is chelated with a metal ion with a probability X_o . In other words, the number of chelated sites is NX_o and the number of unchelated sites is $N(1-X_o)$ on the surface, and on the other surface of the membrane, there is no chelated site; $X = 0$. Then, total energy for this system is given by

$$F(X_o) = F^{\text{bulk}} + F^{\text{surface}}(X_o) \quad (4)$$

where F^{bulk} is the free energy of the inside phase of the membrane, F^{surface} is the free energy of both surfaces of the membranes which interact with water phase. F^{surface} may be expressed by

$$F^{\text{surface}}(X_o) = [E(X_o)^{\text{sites}} - (ST)^{\text{sites}} + F_o^{\text{surface}}] \quad (5)$$

where E^{sites} is the electrostatic interaction energy due to the dissociated polar groups; $(ST)^{\text{sites}}$ is the entropy due to the mixing of the sites; and F^{surface} is the free energy of the surface excluding the contribution from the polar groups. If we assume that F^{surface} does not change whether or not the polar groups chelate with the metal ions, F^{surface} varies only with the variation of the probability X_o . In the above case, let us suppose that NX_o molecules out of NX_o chelated molecules on one side of the membrane turn over to the other side of the membrane, or NX_o sites out of NX_o on one side exchange with NX unchelated sites on the other side. Then the probability of unchelation for a site on the one side of the membrane will be $(1-X_o+X)$ and the probability of unchelation of a site on the other side of the membrane will be $1-X$. The energy of electrostatic interaction due to charged polar groups is

$$E^{\text{sites}}(X_o) = E_1^{\text{sites}}(X_o) + E_2^{\text{sites}}(X_o) \quad (6)$$

where E_1 and E_2 are the energies of electrostatic interaction at side 1 and the other side 2, due to all polar groups on the surface of side 1 and side 2 of the membrane. E_1 and E_2 may be expressed by

$$E_1 = \frac{1}{2} N e q \psi_1 (1-X) \quad (7)$$

$$E_2 = \frac{1}{2} N e q \psi_2 (1-X_o + X)$$

where ψ_1 and ψ_2 are the electrostatic potentials at a site on side 1 with surface charge density σ and on side 2 with surface charge density σ' , respectively. ψ_1 and ψ_2 are given as follows (24)

$$\psi_1 = \frac{4\pi}{\epsilon_0 \kappa} \frac{\sigma + \sigma' + \sigma' \frac{\epsilon_0 \kappa h}{\epsilon_1}}{2 + \frac{\epsilon_0 \kappa h}{\epsilon_1}} \quad (8)$$

$$\psi_2 = \frac{4\pi}{\epsilon_0 \kappa} \frac{\sigma + \sigma' + \sigma \frac{\epsilon_0 \kappa h}{\epsilon_1}}{2 + \frac{\epsilon_0 \kappa h}{\epsilon_1}}$$

where ϵ_0 and ϵ_1 are the dielectric constants of aqueous and lipid phases, respectively, and σ is the average charge density due to dissociated polar groups. If the area per molecule is A and the net charge per molecule is eq , we have

$$\sigma = \frac{eq}{A} (1-X) \quad (9)$$

$$\sigma = \frac{eq'}{A} (1-X_o + X) \quad (10)$$

Then, the total energy due to the electrostatic interaction of the polar groups is

$$\begin{aligned} E(X_o) &= E_1(X_o) + E_2(X_o) \\ &= \frac{2\pi e^2 q^2}{\epsilon_0 \kappa A} \frac{1}{2 + \frac{\epsilon_0 \kappa h}{\epsilon_1}} \left\{ (1-X_o + X)^2 + (1-X)(1-X_o + X) \right. \\ &\quad \left. + \frac{\epsilon_0 \kappa h}{\epsilon_1} (1-X_o + X)^2 + (1-X)^2 + (1-X)(1-X_o + X) \right. \\ &\quad \left. + \frac{\epsilon_0 \kappa h}{\epsilon_1} (1-X)^2 \right\} \end{aligned} \quad (II1)$$

The partition function of the total system is

$$\begin{aligned}
 Z &= e^{-F/kT} = e^{\frac{ST}{kT}} \frac{\text{sites}}{e^{-E/kT}} \frac{\text{sites}}{e^{-F_o/kT}} \frac{\text{surface}}{e^{-\frac{F^{\text{bulk}}}{kT}}} \\
 &= N_{\text{NX}_o}^{C_{\text{NX}}} \frac{N_{\text{NX}}^{C_{\text{NX}}}}{e^{-\frac{E}{kT}}} \frac{N_{\text{surface}}^{C_{\text{surface}}}}{e^{-\frac{F_o}{kT}}} \frac{N_{\text{bulk}}^{C_{\text{bulk}}}}{e^{-\frac{F^{\text{bulk}}}{kT}}} \\
 &= N_{\text{NX}_o}^{C_{\text{NX}}} \frac{N_{\text{NX}}^{C_{\text{NX}}}}{e^{-\frac{E}{kT}}} e^{-\frac{F_o}{kT}}
 \end{aligned} \tag{12}$$

where $N_{\text{NX}_o}^{C_{\text{NX}}} N_{\text{NX}}^{C_{\text{NX}}}$ is the number of various distributions of the sites, and $F^o = F^{\text{bulk}} + F^{\text{surface}}$.

The free energy of the membrane is

$$F = -kT \log Z = E^{\text{site}}(X_o) - kT \log \left\{ N_{\text{NX}_o}^{C_{\text{NX}}} N_{\text{NX}}^{C_{\text{NX}}} \right\} + F_o \tag{13}$$

Using the approximation $N! \approx N \log N$ for $N!$, we have

$$F = E^{\text{site}}(X_o) = kT N \left[\log \frac{1}{1-X_o} - X_o \log \frac{X_o-X}{1-X_o} - X \log \frac{X}{X_o-X} \right] + F_o \tag{14}$$

Since we assume that F_o is not affected with the change of polar groups, in order to express the free energy change of the membrane it is sufficient to know the relative free energy ($\frac{F^{\text{rel}}}{N} \equiv \frac{F-F_o}{N}$) per molecule due to the change of the polar groups.

The relative specific free energy is defined as follows:

$$\frac{F-F_o}{N} \approx F^{\text{rel}} = \epsilon(X_o) - kT \log \frac{1}{1-X_o} - X_o \log \frac{X_o-X}{1-X_o} - X \log \frac{X}{X_o-X} \tag{15}$$

where $\epsilon(X_o) = \frac{E(X_o)^{\text{sites}}}{N}$

For given X_o , the stationary state of the system can be determined by

$$\frac{\partial F^{\text{rel}}}{\partial X} = 0 \tag{16}$$

With the value X_1 which satisfies Eq. (16), the relative free energy per molecule will be a minimum. We call this state $F(X_1)$ a

stable state of the membrane. The difference ΔF between the specific free energies at $X = 0$ and $X = X_1^o$, is expressed in terms of X_0^o and q with Eqs. (11), (15) and (16).

$$\Delta F^{rel} = F^{rel}(X_0^o) - F^{rel}(X_1^o) \quad (17)$$

The numerical values of F with respect to the probability of initial chelation X of a site and the degree of dissociation q of the polar groups can be calculated. For the case of $X_0^o = 1$, the numerical value of ΔF is shown with various values of q , in Fig. 6.

According to Salem (37, 38), the London van der Waals dispersion energy per molecule in lipid monolayer films is given by

$$W_{dis} = \frac{n}{2} \frac{A}{4\ell^2 D^4} \rho \left(3 \tan^{-1} \rho + \frac{\rho}{1+\rho^2} \right), \quad \rho = L/D \quad (18)$$

where A is the coefficient of the dispersion interaction between two basic molecular units (CH_2 hydrocarbon units), n is the number of the nearest neighbor hydrocarbon chains, ℓ is the length of a CH_2 unit, D is the mutual distance of two hydrocarbon chains, L is the length of a hydrocarbon chain and N_c is the number of hydrocarbon molecules.

Since the phospholipid is composed of two aliphatic hydrocarbon chains, if we use 60 \AA^2 for the area per lipid molecule, the mutual distance of two nearest hydrocarbon chains D is estimated to be 5.48 \AA for a square lattice packing. If we apply the formula of Eq. (18) to the bilayer membrane with the following numerical values:

$$A: 1340 \text{ \AA}^6 \text{ Kcal/mole for } CH_2-CH_2 \text{ (Ref. 38)}$$

$$\ell: 1.26 \text{ \AA}$$

$$N_c: 18$$

$$D: 5.48 \text{ \AA} \text{ for a square lattice}$$

Thus, the cohesive energy of a hydrocarbon chain in the lipid molecular layer due to the dispersion forces of neighboring hydrocarbon chains is

$$W_{dis} = 4.04 \times 10^{-13} \text{ ergs.}$$

In the square lattice molecular arrangement, if energy is added in amounts greater than W_{dis}^2 (which corresponds to the energy to break two nearest neighboring chains) to a lipid molecule, the membrane can break. That is, if ΔF is greater than $W_{dis}^2/2$, the membrane may break. As shown in Fig. 6, for a given concentration of chelation there is a critical degree of dissociation q_c of

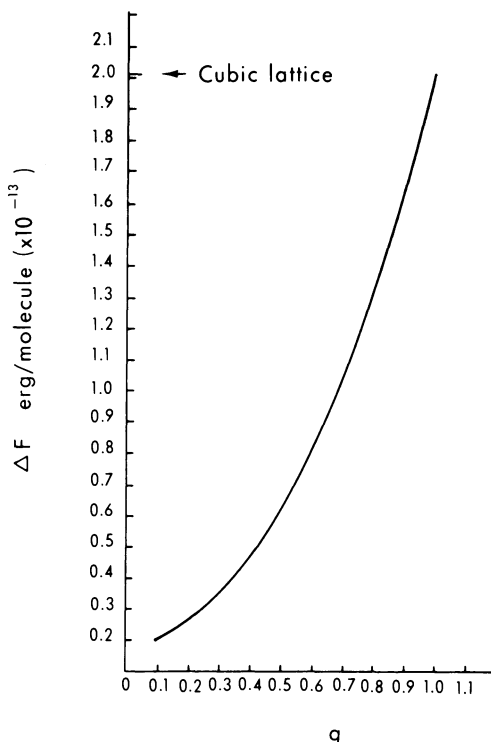


Fig. 6. Relative free energy per lipid molecule with respect to the net charge per molecule. An arrow mark shows the energy necessary to break the membrane with a square lattice packing.

the polar groups which is enough to break the membrane.

$$q_c = 0.95 , \quad X_o = 1 \quad (19)$$

It is appreciated that the analysis given here is oversimplified and contains a number of assumptions (such as the nonspherical character of CH_2 groups, orientation effect, and the neglect of microscopic dielectric constant) which will be valid only in extreme cases. However, the treatment is qualitatively adequate to indicate the significance of the instability of the asymmetrical membrane. The instability of the asymmetrical membrane with divalent metals (e.g. Ca^{++}) may be greatly related to the excitation phenomena of biological membranes, as elaborated in the following section.

Another factor which could also be involved in producing instability is entropy changes following the chelation of Ca^{2+} with polar groups of PS. The calculation similar to the one mentioned above, taking into account the fixing of PS "sites" by chelation indicates the enhancement of the instability of the asymmetric

membrane. The detail analysis is in progress.

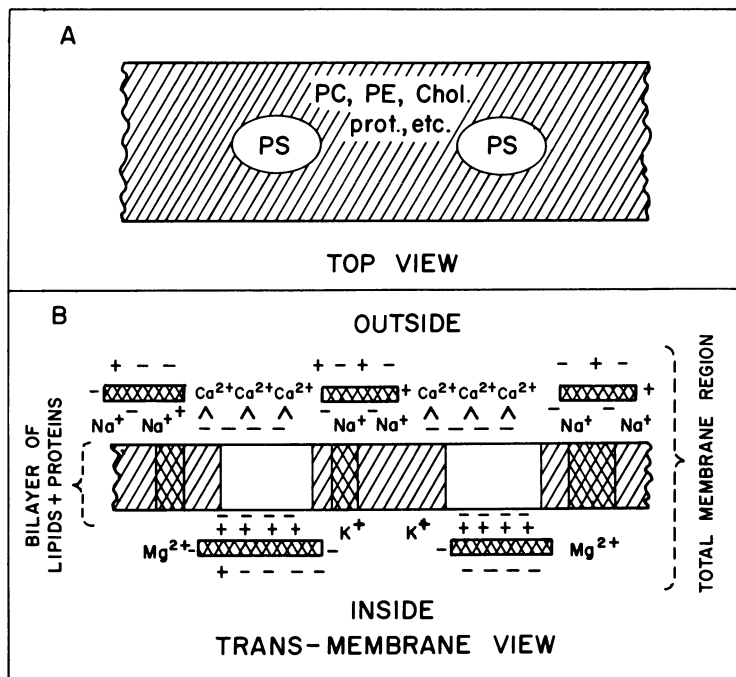
Analogies to Biological Membranes:

The importance of bivalent metals on the structure and function of biological membranes is well recognized. For example, it has been shown that Ca^{2+} has a pronounced effect on the permeability of red cells (14a), epithelial cell junctions (18) and squid axon (9) as well as of many other membranes. In addition, Ca^{2+} is a participant in mitochondrial function (16), cell-contact phenomena and cell deformability (52), and activation of prothrombin by thrombo-plastin(29). All these reactions involve membranous structures containing both phospholipids and proteins. The observations presented here concerning the effect of Ca^{2+} on the permeability of PS membranes seem highly relevant to the effect of Ca^{2+} on whole biological membranes.

Several investigators have considered the possibility of phospholipids being implicated in nerve excitation process. Goldman (10) has speculated on the re-orientation of the dipoles of the phospholipid head-groups as a mechanism accounting for the nerve axon properties. Tobias (48) has proposed a theory of excitation involving Ca^{2+} binding on PS and its replacement by K^+ during action potential. This later postulation was based mainly on the observation that Ca^{2+} increased the electrical resistance of PS-impregnated millipore filter membranes (50). However Tobias' theory did not involve any re-orientation of the whole phospholipid molecules or the effect of asymmetry. Tasaki and Singer (44) have formulated a "macromolecular" theory of the mechanism of action potential involving the binding of divalent metals on membrane negative sites. The actual molecular site for these events was not discussed by these authors, but in view of the observations described in this paper, the PS- Ca^{2+} complex appears as a reasonable possibility. Recent evidence on birefringence charges of whole nerve membranes (7) and spectroscopic changes of dye molecules incorporated into the membrane (43) during electrical stimulation suggest the occurrence of molecular re-orientation within the axon membrane during excitation. Cohen, Keynes and Hille (7) have speculated that the observed changes in light scattering and birefringence might reflect conformational changes of the protein molecules. However changes in birefringence can also be accounted for by a re-orientation of phospholipid molecules (inversion) as a response to the instability created by asymmetric distribution of fixed negative charges or Ca^{2+} (31).

Based on the observed instability of asymmetric PS membranes and various other experimental evidence from other laboratories, we propose the following mechanism for nerve excitation: Let us

suppose that the plasma membrane of a nerve is "variegated" in composition. The neutral phospholipids and proteins constitute the majority of the membrane, interdispersed with small areas (patches) rich in PS or other acidic phospholipids with a high binding constant for Ca^{2+} (Fig. 7A). At the resting state, the membrane areas ("sites") containing high proportions of PS are "balanced" by binding to Ca^{2+} on the outside surface of the membranes and to the positively charged groups of a protein on the inside of the membrane (Figure 7B). Removal of the stabilizing factor (protein) from the inside surface by electrical impulse, produces an asymmetry (31) characterized by instability. As a result of the difference in surface energy between the two planes of the membrane, PS molecules or clusters of molecules "invert" in order to equilibrate the difference in surface energy. During this reorientation, the membrane undergoes profound changes in conductivity and quickly reverts back



■■■ Lipids PC, PE, Chol □ PS XXXX proteins

Fig. 7. Diagrammatic representation of a nerve axon membrane. A: Top view showing areas rich in PS surrounded by areas composed of the rest of (neutral) phospholipids, cholesterol and proteins. B: Trans membrane view showing phospholipids present in a central area of bimolecular thickness with proteins present both in the bilayer region and at the water interface. Calcium ions are shown bound to the PS areas.

to a stable state. During the "inversion", Ca^{2+} is transported into the interior, along with Na^+ , and K^+ is transported out. Ca^{2+} diffuses into the cytoplasm and the internal PS molecules bind again to the basic groups of the "stabilizing" protein. During the Ca^{2+} induced high permeability stage, Na^+ influx would increase first, predominantly due to the potential difference across the membrane, followed by K^+ efflux due to diffusion. This may correspond to the early Na^+ and late K^+ conductance postulated by Hodgkin and Huxley (14). The areas of the membrane composed of the neutral phospholipids and proteins with low binding for Ca^{2+} would not be affected under these conditions.

There is experimental evidence to support the suggestion that a protein involved in the mechanism of the action potential is situated "inside" and not "outside" the axon membrane (49, 35, 45). Tasaki and Singer have calculated the extra ionic flux accompanying the electrical excitation of squid axon as 3.6×10^{-8} moles, $\text{cm}^{-2} \cdot \text{sec}^{-1}$ (44). A very relevant question would be whether the amount of PS present in the nerve axon membrane is enough to transport the calculated number of ions. From various data presented by Ansel and Hawthorn (3) and also more recently by Sheltawy and Dawson (41) it appears that non-myelinated axons have a relatively high percentage of cephalin, of which approximately 40% is PS. Based on total dry weight, a value of 5% can be calculated for the PS content of non-myelinated nerve. Assuming a value of 55 \AA^2 area per molecule of PS (26) it can be calculated that a bilayer membrane consisting 100% of PS would contain 550×10^{-8} moles $\cdot \text{cm}^2$. Taking into account the value of 5% PS content within the axon membrane, the amount of PS molecules present within a cm^2 would be 22×10^{-8} moles $\cdot \text{cm}^2$, more than enough to accommodate the observed ionic flux. This calculation assumes an equal distribution of all the membrane components w/w within the membrane surface, which is probably not the case. It is difficult to state with any certainty the magnitude of the error involved in this assumption because of lack of direct evidence on the fine structure of biological membranes. However it would probably be within the order of magnitude. In any case, if one assumes a modified Danielli-Davson structure with protein both in the region of the bilayer, and also at the water interface, the percentage (per unit area) of each liquid component within the bilayer would be higher than the percentage based on total dry weight.

The membrane model presented in figure 7 should be considered only as a very schematic representation of some of the membrane features that seemed relevant for the discussion. It illustrates proteins as present both in the bilayer region and also adsorbed at the water interface.

Acknowledgement:

This work was supported partly by grants from the U. S. National Institute of Neurological Diseases and Stroke, Grant No. 1 R01 NB08739-01 (S. O.); and from the American Heart Association, Grant No. A.H.A. 68698 (D. P.).

References:

1. Abramson, M. B., Katzman, R., and Gregor, H. P., *J. Biol. Chem.*, 239, 70 (1964).
2. Abramson, M. B., Katzman, R., Gregor, H. P. and Curci, R., *Biochemistry*, 5, 2207 (1966).
3. Ansell, G. B. and Hawthorne, J. N., *Phospholipids*, Elsevier Publ. Co., Amsterdam, N. Y., 1964.
4. Bangham, A. D. in "Progress in Biophysics and Molecular Biology" (edit. by J. A. V. Butler and D. Noble), Pergamon Press, Oxford, 1968, p. 29.
5. Bangham, A. D. and Papahadjopoulos, D., *Biochim. Biophys. Acta*, 126, 181 (1966).
6. Bangham, A. D., Standish, M. M., and Miller, N., *Nature*, 208, 1295 (1965).
7. Cohen, L. B., Keynes, R. D. and Hille, B., *Nature*, 218, 438, (1968).
8. Feinstein, M. B., *J. Gen. Physiol.*, 48, 357 (1964).
9. Frankenhaeuser, B. and Hodgkin, A. L., *J. Physiol.*, London, 137, 218 (1957).
10. Goldman, D. E., *Biophys. J.*, 4, 167 (1964).
11. Hauser, H., and Dawson, R. M. C., *European J. Biochem.*, 1, 61 (1967).
12. Hauser, H. and Dawson, R. M. C., *Biochem. J.*, 109, 909 (1968).
13. Hendrickson, H. S., and Fullington, J. G., *Biochem.* 4, 1599(1965).
14. Hodgkin, A.L. and Huxley, A.F., *J. Physiol.*, 117, 500 (1952).
- 14a Hoffman, J. F., *Circulation*, 26, 1201 (1962).
15. Kimizuka, H., Nakahara, T., Vejo, H., and Yamauchi, A., *Biochim. Biophys. Acta*, 137, 549 (1967).
16. Lehninger, A. L., *Ann. N. Y. Acad. Sci.*, 137, 700 (1966).
17. Lesslauer, Richter, J., Lauger, P., *Nature*, 213, 1224 (1967).
18. Loewenstein, W. R., *J. Colloid Sci.*, 25, 34 (1967).
19. Mueller, P. and Rudin, D. O., *Nature*, 217, 713 (1968).
20. Mueller, P. and Rudin, O. D., *J. Theoret. Biology*, 18, 222 (1968).
21. Ohki, S., *J. Coll. Interf. Sci.*, 30, 413 (1969).
22. Ohki, S., *Biophysical J.*, 9, 1195 (1969).
23. Ohki, in F. M. Snell, et al. Eds., "Physical Principles of Biological Membranes", Gordon and Breach, Science Publ. Inc., in press.
24. Ohki, S. and Aono, O., *J. Coll. Interf. Sci.*, in press.
25. Ohki, S. and Goldup, A., *Nature*, 217, 458 (1968).

26. Papahadjopoulos, D., *Biochim. Biophys. Acta*, 163, 240 (1968).
27. Papahadjopoulos, D., *in preparation*.
28. Papahadjopoulos, D. and Bangham, A. D., *Biochim. Biophys. Acta*, 126, 185 (1966).
29. Papahadjopoulos, D., and Hanahan, D. J., *Biochim. Biophys. Acta*, 90, 436 (1964).
30. Papahadjopoulos, D. and Miller, N., *Biochim. Biophys. Acta*, 135, 624 (1967).
31. Papahadjopoulos, D. and Ohki, S., *Science*, 164, 1075 (1969).
32. Papahadjopoulos, D. and Ohki, S., *J. Amer. Oil Chem. Soc.*, *in press* (*Symposium on Model Membranes*, San Francisco, April 1969).
33. Papahadjopoulos, D. and Ohki, S., *Symposium on "Ordered Fluids and Liquid Crystals"*, *Advances in Chemistry*, Number 43, American Chemical Society, *in press*.
34. Papahadjopoulos, D., Watkins, J. C., *Biochim. Biophys. Acta*, 135, 639 (1967).
35. Rojas, E. and Luxoro, M., *Nature*, 199, 78 (1963).
36. Rojas, E. and Tobias, J. M., *Biochim. Biophys. Acta*, 94, 394 (1965).
37. Salem, L., *Molec. Phys.*, 3, 441 (1960).
38. Salem, L., *J. Chem. Phys.*, 37, 2100 (1962).
39. Rothfield, L. and Finkelstein, A., *Annual Reviews of Biochem.* p. 463 (1968).
40. Shah, D. O. and Schulman, J. H., *J. Lipid Res.*, 8, 227 (1967).
41. Sheltawy, A. and Dawson, R. M. C., *Biochem. J.*, 100, 12 (1966).
42. Skou, J. C., *Acta Pharmacol. Toxicol.*, 10, 325 (1954).
43. Tasaki, I., Carnay, L., Sandlin, R. and Watanabe, A., *Science*, 163, 683 (1969).
44. Tasaki, I. and Singer, I., *Ann. N. Y. Acad. Sci.*, 137, 792 (1966).
45. Tasaki, I., and Takameaka, T., *Proc. Nat. Acad. Sc.*, 52, 804 (1964).
46. Tasaki, I., Watanabe, A. and Lerman, L., *Amer. J. Physiol.*, 213, 1465 (1967).
47. Tien, H. Ti, and Diana, A., *Chem. Phys. Lipids*, 2, 55 (1968).
48. Tobias, J. M., *Nature*, 203, 13 (1964).
49. Tobias, J. M., *J. Gen. Physiol.*, 43, Suppl. 57 (1960).
50. Tobias, J. M., Agin, D. P. and Pawlowski, R., *J. Gen. Physiol.*, 45, 989 (1962).
51. Van Deemen, L. L. M., *in "Progress in the Chemistry of Fats and Other Lipids"*, Vol. 8, part 1, Pergamon Press (1965).
52. Weiss, L., *J. Cell. Biol.*, 35, 347 (1967).

DISSOCIATION OF FUNCTIONAL MARKERS
IN BACTERIAL MEMBRANES

Martin S. Nachbar and Milton R. J. Salton

Department of Medicine and Department of Microbiology
New York University School of Medicine, New York

INTRODUCTION

While much is known of the gross structural, chemical and biochemical properties of biological membranes, (1-4) little is yet known of their existing structure - function relationships, (5) intermolecular architecture, (6) inherent informational content or possible dynamic changes occurring in response to extra - and intracellular stimuli. There exists no universally accepted model of membrane architecture and, indeed, several patterns may exist, not only in different membranes, but in portions of the same membrane.

The elucidation of these problems would seem to require the combined knowledge of gross changes in membrane architecture as determined by alterations of (1) protein and lipid conformations and interactions as described from IR, NMR, CD and ORD spectroscopy and (2) the study of the properties of and the interrelationships between the individual building blocks.

The membrane system we have chosen to discuss is that of the microorganism Micrococcus lysodeikticus (ML) (Fig. 1).

An outer cell wall composed of a peptidoglycan, an outer plasma membrane and an inner mesosomal membrane structure (comprised predominantly of lipid and protein) and the cell sap are evident. In common with other bacteria, ML lacks the

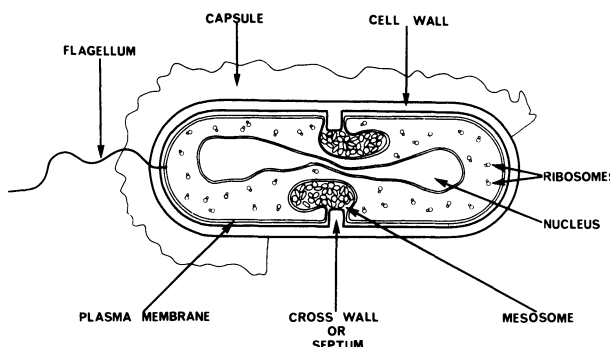


Fig. 1 A diagrammatic representation of the anatomy of a gram-positive bacterium indicating surface appendages, surface layers and internal structures. The discontinuity of the capsule indicates that not all species possess this surface component (Ref. 16).

intracellular membranous organelles i. e. - mitochondria, golgi apparatus, endoplasmic reticulum, nuclear membrane, etc. which are found in higher biological forms.

The membrane systems of ML appear relatively simple but they must be so organized as to be able to perform various complex functions such as ionic and organic transport or translocation, electron transport and oxidative phosphorylation, wall and membrane synthesis, nuclear anchoring and separation during cell division. The challenge is to know which components of the membrane perform these specific functions and whether these components are scattered randomly over the membrane or whether a more highly organized and probably more efficient distribution of activities is to be found.

The membrane systems of this organism are easily obtained. The outer wall can be removed by digestion with the enzyme lysozyme and the membranes obtained by differential centrifugation. As shown by Salton (5) successive washing of the particulate or membranous fraction by 0.1M Tris buffer pH 7.5 results in progressively less release of protein into the supernatant washes. A minimum seems to be reached after about 3-4 washes. This suggests that any components released after this

stage are probably located in the membrane.

Examination of washed, sonicated membranes reacted against protoplasmic antisera in double diffusion tests shows a progressive reduction of reactive material with successive washes. Little or no reactivity with cytoplasmic antisera after the 3rd wash is demonstrated.

These results would tend to militate against much entrapment of cytoplasmic material in membrane bound vesicles. However, upon sonication of the membrane after 5 washes and a subsequent high speed centrifugation, the supernatant revealed the presence of an enzyme thought to be cytoplasmic (TPN specific Isocitric Dehydrogenase). Without sonication, this enzyme could not be found in the supernatant fraction after the third wash. (9) (Fig. 2). Therefore some cytoplasmic trapping within membrane bound vesicles cannot be ruled out.

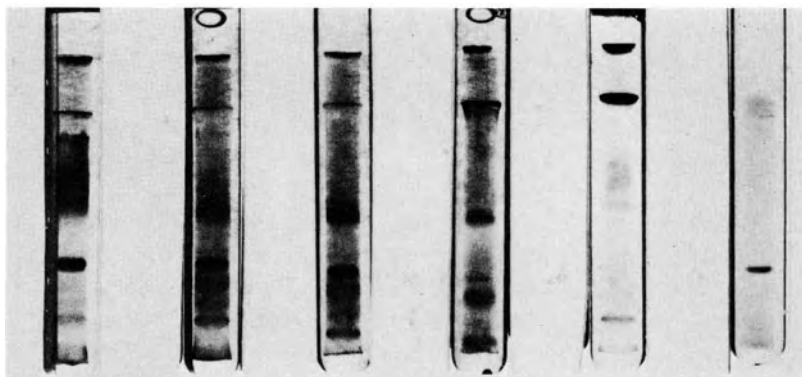


Fig. 2 Disc electrophoresis of washes and supernatant fraction of sonicated membrane stained for various enzyme activities (8). From left to right gels represent washes 1-5, 0.03M Tris pH 7.5, gel on far right is supernatant fraction of sonicated membrane after 5 washes, stained only for TPN-specific Isocitric Dehydrogenase (9). Comparable zone of staining is seen in washes 1-3, faintly in wash 4 and not in wash 5. Standard 7% separating gel run at pH 9.5, stacking gel pH 8.9 (17, 18).

The gross chemical composition of the membrane (Table 1) reveals a preponderance of protein with a protein/lipid ratio of about 2:1, very little carbohydrate and a small but constant amount of RNA.

TABLE 1

CHEMICAL COMPOSITION OF Micrococcus lysodeikticus MEMBRANES

	<u>PROTEIN</u> LOWRY	<u>LIPID</u>	<u>CARBOHYDRATE</u> ANTHRONE	<u>RNA</u> ORCINOL
% (by weight)	49	64.5	23.8	4.2

What are the functional markers that characterize this membrane fraction? We will define a marker as any component (i. e. protein, lipid, lipoprotein, glycoprotein, polysaccharide, etc.) which is found in significant amounts in the membrane fraction after washing and which can be recognized by its enzymatic, antigenic, chemical or physio-chemical properties. Phospholipids, carotenoids and menaquinones have been shown to reside exclusively in the membrane (10) fraction after separation from cytoplasm.

Individual proteins may not behave in this all or none manner. As can be seen in Fig. 3, the distribution of enzyme activities between membrane and cytoplasm varies over a wide range from those exclusively found in the cytoplasm such as DPN-TPNH transhydrogenase to those found entirely in the membrane fraction such as phosphatidic acid-cytidyl transferase (Nachbar - unpublished). A large bipartite region can also be seen. Most of those enzymes associated predominantly with the cytoplasm can be released by repeated washing, i. e. in 0.03-0.1M Tris buffer pH 7.5, and these have arbitrarily and perhaps wrongly excluded from consideration as "true" membrane markers. It should be realized that these proteins may be associated with the membrane by weak ionic or hydrophobic bonds which are disrupted by even the mildest of procedures.

As can be seen the "true" markers (i. e. those firmly attached to the membranes) belong to the electron transport and

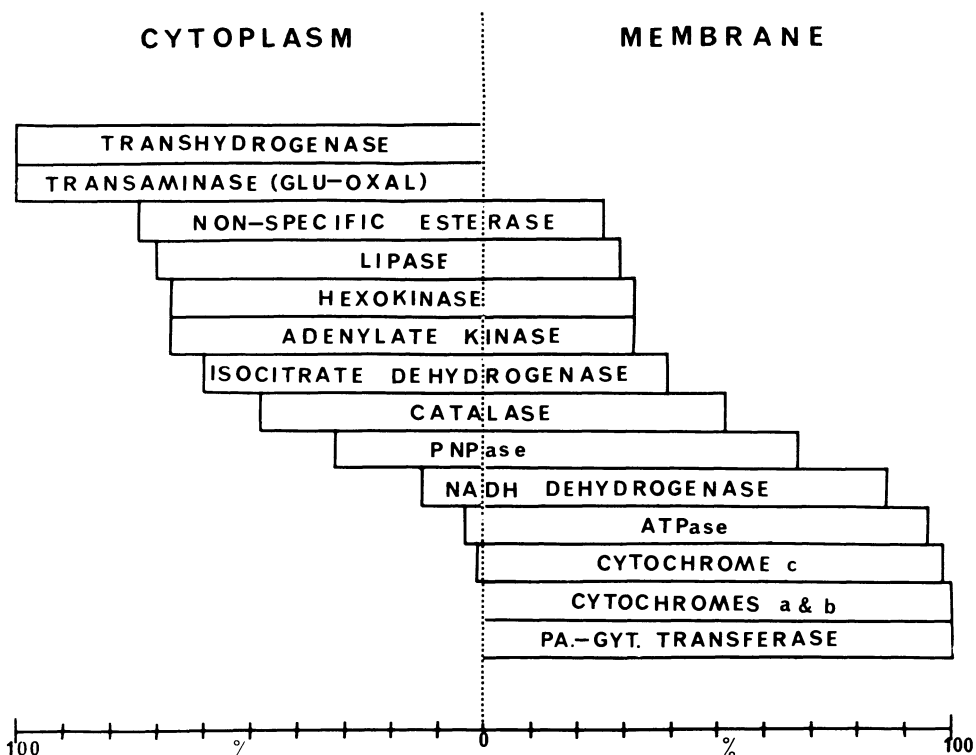


Fig. 3 Histogram of distributions of enzymes between cytoplasm and membrane after separation of cytoplasm and membrane fractions by 30' centrifugation at 0°C at 30,000 xg (Nachbar - unpublished).

oxidative phosphorylation chains, a finding almost universal for all biological membranes, and to enzymes concerned with phospholipid synthesis as recently found by Dr. August De Siervo (unpublished) in our laboratory. Two other systems suspected of being present but not yet identified are the cell wall synthesizing enzymes and components necessary for specialized transport.

The problem which now arises is that of the dissociation of individual components of the membrane while retaining some recognizable characteristics. Table 2 demonstrates the various methods we have thus far employed, the bonds believed to be involved and enzymes partially purified by these techniques. They differ in degree of severity but with each, certain markers

TABLE 2
METHODS OF MEMBRANE DISSOCIATION AND COMPONENTS ISOLATED

<u>PROCEDURE</u>	<u>BOND</u>	<u>MAIN COMPONENTS RELEASED AND ISOLATED</u>
1. Low Ionic Strength Environment	Weak Hydrophobic Bonds Ionic Bonds Via Cations	ATPase
2. Chelation	Ionic Bonds	NADH Dehydrogenase, Cardiolipin, ? Glycolipid
3. Detergents	Hydrophobic Bonds	Cytochromes, Succinic Dehydrogenase
4. Organic Solvents	Hydrophobic Bonds	ATPase, Cytochromes
5. Mechanical Disruption	Weak intermolecular Bonds Hydrogen Bonds	ATPase, Cytochromes

can easily be recognized.

What follows is a more detailed description of the procedures employed and results obtained.

1) Low Ionic Strength Environment

Dr. Emilio Munoz, while working in our laboratory demonstrated that a Ca^{++} -dependent ATPase could be released from ML membranes by lowering the ionic strength of the wash solution. Membranes were washed four times in 0.03M Tris buffer pH 7.5 and then with 0.003M Tris pH 7.5. The results may be seen in Fig. 4.

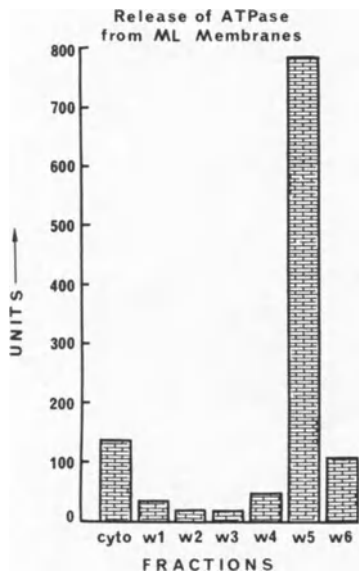


Fig. 4 Histogram showing release of ATPase from ML membranes.
 cyto=cytoplasm, w1-w4=0.03M Tris pH 7.5 washes, w5=first 0.003M Tris wash, w6=second 0.003M Tris wash. Assayed according to Munoz (11).

This treatment results in a marked release of the enzyme as measured by total activity and, in addition, the specific activity of the 5th and 6th washes are 4 to 5 times that of any preceding wash. The specificity of the procedure and identification of the enzymes are demonstrated in Fig. 5. The complexity of the regular washes can be seen and the selectivity of the low ionic strength or "shock" wash can be appreciated. Enzymatic staining of the gel shows the major component of the "shock" wash to have the ATPase activity. Dr. Munoz has further purified this enzyme. The details are beyond the scope of this paper.

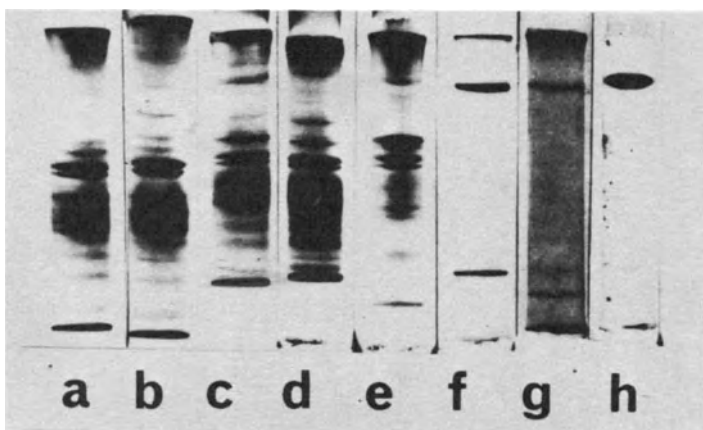


Fig. 5 Disc electrophoresis showing aniline black staining of proteins in a) cytoplasm; (b-g) six consecutive washes of the membranes, and enzymatic staining for ATPase (h). Method of Weinbaum and Markman (19).

The morphology of the membranes before and after treatment by low ionic strength buffer demonstrates some interesting changes. Fig. 6a shows the particle studded membrane prior to low ionic strength treatment. Fig. 6b demonstrates the apparent disappearance of the particles after treatment. The electron micrograph of purified ATPase (Fig. 6c) demonstrates a particulate structure similar to those seen in previous slides. The calculated size of the smaller membrane particles and of purified ATPase are about 100 angstroms. We believe that the two are the same.

In summary, ATPase dissociation from membrane is dependent upon prior removal of poorly defined materials (cation, protein, lipids) with subsequent release upon exposure to a low ionic strength environment. Hydrophobic and/or ionic linkages seem to be the most important bonds in this enzyme's association with the membrane.

2) Cation Depletion by Chelating Agents (EDTA)

Selective release of NADH dehydrogenase activity (Nachbar - unpublished) may be achieved in the following manner. After three to four washes with 0.03M Tris pH 7.5, the membranes are washed again in same buffer but this time made

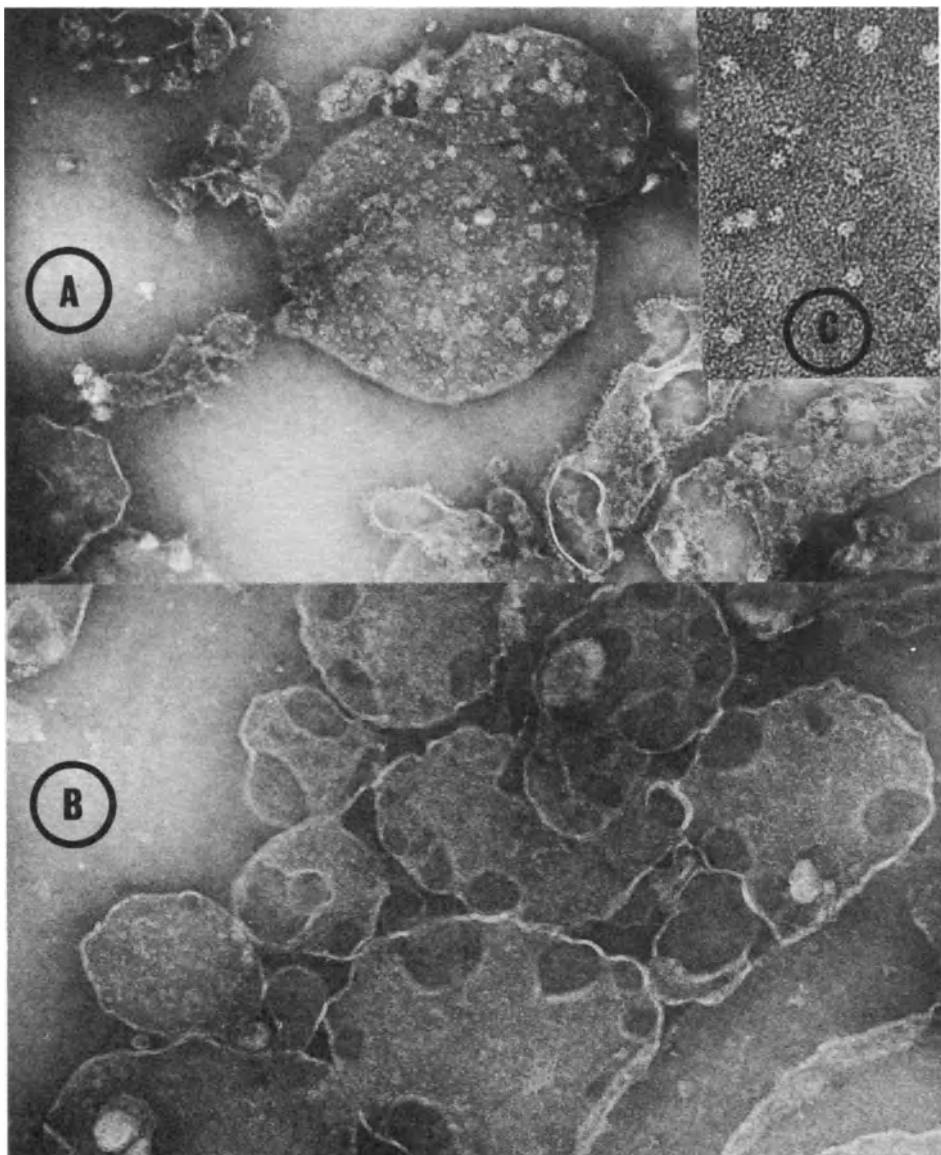


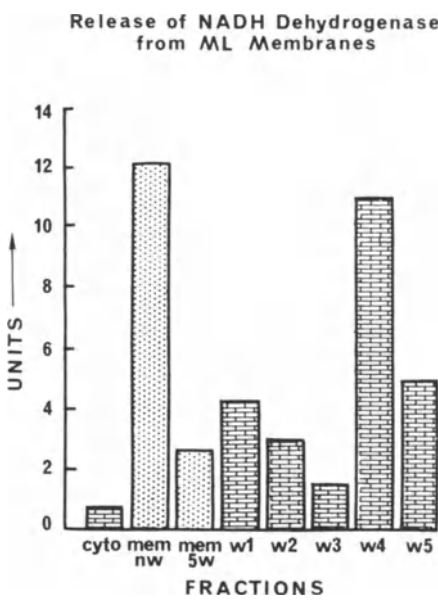
Fig. 6a-c Negatively stained membrane fragments and ATPase preparations. (a) membrane fragments prior to "shock wash" showing associated particles $\times 95,000$, (b) membrane fragments after shock wash showing loss of particles $\times 95,000$, (c) active ATPase preparation after purification, (Ref. 12) showing spherical particles of approximately 100 \AA diameter $\times 260,000$.

0.005M with respect to EDTA. NADH dehydrogenase activity is assayed using 2,6-Dichlorophenolindophenol as the electron acceptor. The units are arbitrary and an O. D. change of 0.1 in 30 seconds at room temperature using a Bausch and Lomb Spectrometer at 600 nm is defined as 1 unit of activity. As can be seen in Fig. 7, treatment with EDTA results in a dramatic release of the activity. Less than 15% of the original activity remains in the membrane. In addition to the large amount of activity released, the specific activity of the EDTA wash is 3 to 4 times that of the original membrane and the preceding washes.

Fig. 7 Histogram showing release of NADH dehydrogenase from ML membranes.

cyto=cytoplasm; mem nw=membranes before washing; mem 5w=membranes after 5 washes, w1-w3=consecutive washes with 0.03M Tris pH 7.5; w4=0.03M Tris pH 7.5 and 0.005M EDTA wash; w5=0.003M Tris pH 7.5 wash.

Assay modified from Saurge (13). Assay mixture contain 6.0 μ moles NADH, 100 μ moles sodium phosphate buffer pH 7.5, 0.1 μ moles 2,6-Dichlorophenolindophenol in a final volume of 2.95 ml assay at room temperature read at 600 nm. Zero time reading after addition of indicator. The sample is then added (0.05 ml) with rapid mixing and the mixture read at 30 seconds. A change of 0.1 O. D. units in 30 seconds is equal to 1 unit of activity. The best range is a decrease of between 0.1 and 0.5 O. D. units. Corrections made for control (no enzyme).



Morphological studies demonstrate the vesicular nature of the "soluble" EDTA wash (Fig. 8).

In a sucrose density gradient of 15-30% run at 25,000 rpm for 24 hrs. at 4°C in a Spinco SW 27 head, particles of activity of 11-12s, 21-22s and a pellet were observed.

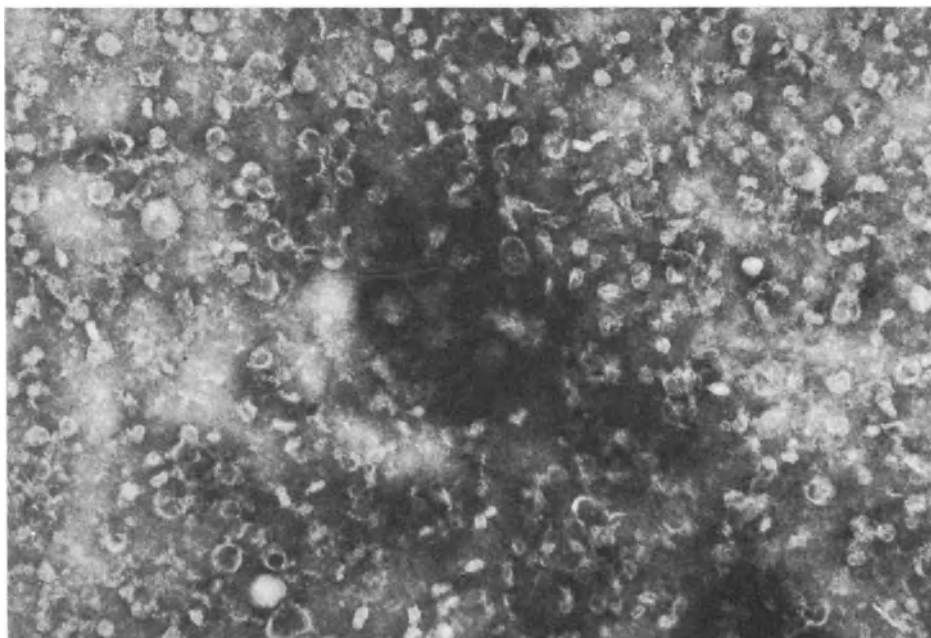


Fig. 8 Negatively stained EDTA wash showing vesicular nature of the wash with smallest vesicles of the order of 300 Å in diameter. ($\times 100,000$). Note the relative uniformity of preparation.

Enzymatic staining of the EDTA wash for NADH dehydrogenase in a 7% polyacrylamide gel after electrophoresis (17, 18) using Triphenyltetrazolium as the indicator, demonstrates 2-3 bands of activity, two in the middle of the gel and one faster moving band. We are not yet sure this represents a group of enzymes or one enzyme in several polymeric forms. (Fig. 9)

An unexpected finding was the apparent selective release of lipid components by EDTA. The protein-lipid ratio of the membrane is of the order of 2:1. The EDTA wash showed a much higher value for the lipid and in addition, selective release of one phospholipid, cardiolipin. (Table 3)

We are tentatively interpreting these results to mean that there may be very specific binding affinities between the various phospholipids and certain membrane proteins, which are highly dependent upon the presence of divalent cations.

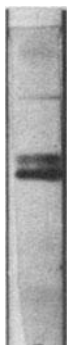


Fig. 9 Disc gel electrophoresis of EDTA wash stained for NADH dehydrogenase activity. Assay mixture contains 6.0 μ moles NADH, 3.0 μ moles triphenyltetrazolium chloride, 100 μ moles 0.03M Tris pH 7.5, 100 μ moles cobalt chloride in a final volume of 3.4 ml. The mixture was allowed to stand 10-30 minutes at 37°C. Note three bands of activity. Positive results appear as red bands.

The selectivity of EDTA can be explained in one of three ways: (1) specific lipids and NADH dehydrogenase exist at different sites on the membrane but are each dependent upon divalent cations for association to the membrane (2) lipids and proteins are located in the same region of the membrane but are not intimately associated and EDTA releases the entire lipid-protein "patch" (3) lipid and protein are intimately associated in a large lipoprotein complex which attaches to the membrane via divalent cations. Combinations of these may also exist. In any event, the findings indicate a heterogeneous makeup of the membrane both for protein and lipid and are perhaps evidence against a simple repeating unit structure for the membrane organization.

TABLE 3

LIPID AND LIPID-PROTEIN RELATIONSHIPS

OF THE MEMBRANE AND EDTA WASHES

<u>PREPARATION</u>	<u>LIPID/ PROTEIN RATIO</u>	<u>CARDIOLIPIN/ PHOSPHATIDYL GLYCEROL</u>
Membrane	0.5	2.2
EDTA Wash	1.3	8.9

3) Detergents

Early work by Salton (8) demonstrated the isolation of cytochromes b, c, a by a combination of ionic and/or non-ionic detergents and salt fractionation. However, this method, while it achieved the separation of the cytochromes from most of the lipids and approximately 2/3 of the proteins left the residue without any obvious structural organization; more recent work with membranes washed with 1% deoxycholate achieved a more remarkable result.



Fig. 10 Electron micrographs of M. lysodeikticus membrane fractions negatively stained with 2% ammonium molybdate A, control membrane after 6 washes with 0.05M Tris B, DOC-insoluble residues after 6 successive washes with 1% DOC in 0.05M Tris.
A and B x 86,000.

The membranes are washed until the supernatant is devoid of yellow color (most of the phospholipids and carotenoids having been removed). These residues contain 10-15% of the initial membrane protein and 3-5% of the original lipid. The absorption spectra of these sheets show that characteristic of the cytochromes. In addition, succinic dehydrogenase activity is found to reside in this residue. The DOC-soluble phase spectra shows little cytochrome absorption but strong carotenoid absorption. Both NADH dehydrogenase activity and ATPase activity are recovered in the soluble phase and not in the residue.

The DOC-treated lipid depleted membranous sheets can be studied (Salton - unpublished) further for their response to other dissociating agents. A neutral detergent Triton-X-100 and 8M urea are not very effective in solubilizing this material. Complete solubilization is achieved with SDS at concentrations of 0.1-0.5%, with Nonidet P-40, 1% with 1% Triton-X-100 solutions containing 0.04M AlCl₃ and with 10.0M acetic acid. The protein concentration for all experiments is 5 mg/ml. Dialysis to remove dissociating reagents usually results in rapid reaggregation into amorphous sheets but membranous sheets are generated in the SDS dissociated fractions dialysed against 0.05M Tris pH 7.5 containing Mg⁺⁺. Precise conditions for optimal reaggregation into membranous sheets requires further study.

Release of cytochrome c from the other cytochromes of this system can be achieved by dissociating this fraction with 0.5% SDS followed by (NH₄)₂SO₄ precipitation (20%). Cytochrome c is released in a soluble form, the a and b cytochrome fraction being precipitated. The major constituents of the fraction seem therefore to be held together by very strong hydrophobic interactions between proteins and to a lesser extent by electrostatic or ionic bonds.

It is possible that with this technique we have skinned the membrane almost down to the bone. The residue may represent its skeleton upon which the other lipids and proteins are deposited.

4) Solvents

A variety of organic solvents have been employed in attempts to solubilize protein components. Of these n-butanol (8) and 3-Pentanol (Nachbar-unpublished) have been the most useful. Extraction of sonicated membranes in a water phase by a saturating solution of n-butanol at 0°C results in removal of (a) almost all of the lipid in a random fashion - greater than 95% (b) solubilization of many enzyme proteins in an active form e.g. ATPase and the recovery of the cytochromes at the interface. However, NADH dehydrogenase activity is almost completely destroyed.

3-Pentanol extraction preserves 30-40% of the NADH dehydrogenase activity while removing > 90% of the lipids. After three extractions, no further lipid can be removed. This solvent appears to selectively remove lipids from the membrane. Analysis

of the remaining phospholipids in the soluble phase by the techniques of P^{32} labelling, methanol-chloroform extraction of lipids (20) followed by silica gel paper chromatography using system 2 of Wurthier (21) and isotope counting demonstrated a marked relative enrichment in this fraction of cardiolipin.

SUMMARY AND CONCLUSION

In summary, we have attempted to dissect the membrane of one organism Micrococcus lysodeikticus into its functional components, using first very mild procedures and progressing to more drastic measures. We have succeeded in partially purifying a few enzymatic markers. We also believe we have demonstrated a great range of strength of binding affinities of lipids to lipids, lipids to proteins, and proteins to proteins. Our data suggest but do not yet prove that there are specific differences between lipids in their participation in various lipo-protein complexes and/or that there may exist a mosaic of lipid or lipoprotein aggregates in different regions of the membranes. Evidence points to a regional distribution of specific proteins, as might be expected for reasons of functional efficiency and not a randomly associated collection of protein molecules bound together by haphazard associations.

We would hasten to point out that our findings may well be peculiar to this organism and generalizations to other membrane systems should be appropriately tempered.

Acknowledgements:

This work was supported in part by a National Science Foundation Grant (GB 7250) and by the P. H. S. General Research Support Grant (FR 05399).

Senior author's (M. S. N.) work done while Public Health Service Training Fellow, P. H. S. Grant GM00466.

We wish to thank Mr. William Winkler, Mrs. Marion T. Schor, Mrs. Marjorie Schmitt and Mr. Charles Harman for their technical assistance and Dr. John H. Freer for the electron micrographs used in this study.

References

1. Korn, E. D. , Fed. Proc., 28, 6, 1969.
2. Korn, E. D. , Ann. Rev. of Biochem. , 38, 263, 1969.
3. Chapman, D. and contribution by D. F. H. Wallach, in Recent Physical Studies of Phospholipids and Natural Membranes in Biological Membranes: Physical Fact and Function, D. Chapman, Ed. , p. 125, Academic Press, New York, 1968.
4. Salton, M. R. J. , in Protides of the Biological Fluids, 15, 279, 1967.
5. Racker, E. and A. Bruni, in Membrane Models and the Formation of Biological Membranes, L. Bolis and B. A. Pethica, Eds.,p. 138, North-Holland Publ. Co. , Amsterdam, 1968.
6. Engelman, D. M. , in Membrane Models and the Formation of Biological Membranes, L. Bolis and B. A. Pethica, Eds. p. 203, North-Holland Publ. Co. , Amsterdam, 1968.
7. Rothfield, L. M. , Weiser M. and A. Endo, J. Gen. Physiol. , 54, 27s, 1969.
8. Salton, M. R. J. , Trans, N. Y. Acad. Sci. , 29, 764, 1967.
9. Bancroft, J. , An Introduction to Histochemical Technique, p. 224, Appleton-Century-Crofts, New York, 1967.
10. Salton, M. R. J. , in Microbial Protoplasts and L-Forms, L. B. Guze, Ed.,p. 144, Williams and Wilkins Co. , Baltimore, 1968.
11. Munoz, E. , Nachbar, M. S. , Schor, M. T. and Salton, M. R. J. , Biochem. Biophys. Res. Commun. , 32, 539, 1968.
12. Munoz, E. , Salton, M. R. J. , Ng, M. H. , Schor, M. T. , European J. Biochem. , 7, 490, 1969.
13. Saurge, N. , Biochem. J. , 67, 146, 1957.
14. Salton, M. R. J. , Freer, J. H. , Ellar, D. J. , Biochem. Biophys. Res. Commun. , 33, 909, 1968.
15. Nachbar, M. S. - in preparation.
16. Salton, M. R. J. , in The Future of the Brain Sciences, S. Bogoch, Ed. , p. 1, Plenum Press, New York, 1969.
17. Ornstein, L. , Ann. N. Y. Acad. Sci. , 121, 321, 1964.
18. Davis, B. J. , Ann. N. Y. Acad. Sci. , 121, 404, 1964.
19. Weinbaum, G. and Markman, R. , Biochim. Biophys. Acta, 124, 207, 1966
20. Bligh, E. G. and Dyer, W. J. , Canad. J. Biochem. 37, 911, 1959.
21. Wuthier, R. E. , J. Lipid Research, 7, 544, 1966.

RNA IN THE CELL PERIPHERY

E. Mayhew and L. Weiss

Department of Experimental Pathology

Roswell Park Memorial Institute, Buffalo, New York

All mammalian cells so far studied carry a net negative surface charge, at neutral pH, as measured by cell electrophoresis. However the nature of the fixed ionogenic groups responsible for the electrokinetic behavior of cells has not as yet been fully elucidated.

This paper is divided into three sections; (1) a presentation of evidence that ionogenic groups specifically susceptible to ribonuclease are present at the periphery of some cell types; (2) a discussion of the dynamic state of the cellular electrokinetic surface, and (3) speculation on the possible importance of this dynamism on cellular properties.

(1) Ribonuclease-susceptible anionic groups

Evidence that there are ionogenic groups within the cell periphery susceptible to ribonuclease comes mainly from measurements of cell electrophoretic mobility.

The original observation (Weiss and Mayhew, 1966) was made that ribonuclease reduced the electrophoretic mobility of two types of cultured human cells. The results showed that this reduction was independent of, and additive to, the known effects of neuraminidase on these cells (Table 1). This was taken as evidence that ribonuclease interacted with sites separate from those acted upon by neuraminidase. Analysis of cell supernatants showed that ribonuclease does not release any neuraminic acids from cells.

On the one hand, loss of cell surface net negativity could result from fission of phosphodiester bonds, indicating the

Table 1

Electrophoretic Mobility of RPMI No. 41 cells
after treatment with HBSS,
Ribonuclease and/or Neuraminidase

1st treatment	2nd treatment	Electrophoretic* mobility	%Decrease in mobility
HBSS	---	-1.09 ± .021	---
HBSS	HBSS	-1.11 ± .022	---
Neuraminidase		-0.65 ± .023	40.4
Neuraminidase	Neuraminidase	-0.63 ± .022	43.2
Ribonuclease	---	-0.78 ± .021	28.4
Ribonuclease	Ribonuclease	-0.77 ± .019	30.6
Ribonuclease	Neuraminidase	-0.43 ± .020	61.3
Neuraminidase	Ribonuclease	-0.45 ± .017	59.5

* $\mu\text{.sec}^{-1} \cdot \text{v}^{-1}\text{cm.}$ ± standard error of mean.

Table 2
Effect of Ribonuclease on Electrophoretic mobility of Cells

Cells	Electro-phoretic mobility	% Change in mobility	p value ³	RNA at cell Periphery ⁴	1. $\mu \text{ sec}^{-1}$. volts $^{-1}$. cm. at 25° pH 7.2-7.4 in PBS or HBSS.
Chicken Erythrocytes	-0.83	-3 to +3	p>0.5	-	2. The extreme ranges of change after ribonuclease treatment in different experiments are shown.
Mouse Erythrocytes	-1.19	-3 to +3	p>0.5	-	
Human Erythrocytes	-1.09	-3 to +3	p>0.5	-	
Human Peripheral Blood Lymphocytes	-0.87	-10 to -15	p<0.01	+	3. Probability value at mean variation in mobility.
Polymorphs	-0.80	-6 to -10	C.C2>p>0.01	?	
Monocytes	-0.57	-3 to -10	0.1>p>0.05	?	
Platelets	5 -0.96	-3 to +3	p>0.5	-	
Acute Lymphocytic Leuk. ⁵	-1.42 ⁶	-8 to +5	p>0.1	?	
Chronic Lymphocytic "S"	-1.18 ⁶	+2 to +10	p>0.5	-	
Human Cultured RPMI No. 41	-1.10	-10 to -35	p<0.01	+	4. - no Peripheral RNase-susceptible sites detectable.
Burkitts Lymphoma	-1.00 ⁶	-3 to +3	p>0.2	-	
Normal Lymphoid	-1.25 ⁶	-11 to -20	p<0.01	+	
Mouse Peritoneal exudate ⁵	-0.77	-5 to -10	0.1>p>0.05	-	? RNase susceptible sites possibly present.
Thymocytes	-0.89	-6 to -10	C.02>p>0.01	?	
Liver	-0.84	-3 to -15	0.02>p>0.01	?	
Lymph node	-1.10	-3 to +3	p<0.1	-	
Mouse Tumour Ehrlich ascites S37	-1.06 -1.00	-10 to -30 -10 to -25	p<0.01 p<0.01	+	+ RNase susceptible sites present under optimal conditions.
Cultured Mouse Ehrlich Ascites 1210	-0.95 -0.83 -0.98	-10 to -25 -6 to +9 +3 to -15	p<0.01 p<0.01 .C5>p>0.02	+	5. Nucleated cells.
929 Fibroblasts				?	6. Measured at 37°.

Table 3

Effect of Ribonuclease A and T₁ on electrophoretic mobility of Ehrlich ascites tumour cells

	Electrophoretic Mobility $\mu\text{sec}^{-1} \cdot \text{v}^{-1} \text{cm.}$	%Decrease in mobility
Control	-1.10 \pm .014 (374)*	---
Ribonuclease A	-0.87 \pm .021 (185)	19.8
Ribonuclease T ₁	-0.96 \pm 0.22 (245)	13.0

*mean \pm standard error (number of determinations)

Table 4

Effects of active and inactive ribonuclease on the electrophoretic mobility of Ehrlich ascites cells¹

Final Concentration Enzyme mg/ml	Electrophoretic Mobility ²	
	Ribonuclease A	Inactivated Ribonuclease A
0	1.11 \pm .026	1.11 \pm .026
10 ⁻³	0.96 \pm .021	1.05 \pm .024
10 ⁻²	0.89 \pm .023	1.08 \pm .030
10 ⁻¹	0.88 \pm .020	1.10 \pm .027

1. cells treated 30 mins at 37°

2. $\mu\text{sec}^{-1} \cdot \text{v}^{-1} \text{cm.}$

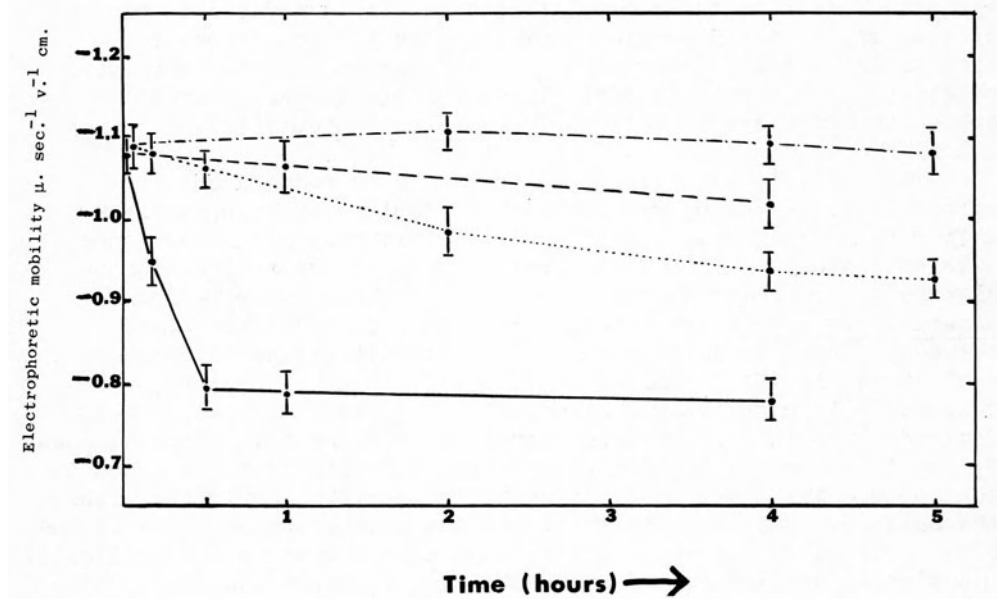


Figure 1. Electrophoretic mobility of Ehrlich ascites cells treated with ribonuclease at 10° or 37° , and measured at those temperatures.

— — — 37° Control, — — 37° ribonuclease-treated
- - - - - 10° Control, 10° ribonuclease-treated

presence of RNA in the cell periphery. On the other hand, as ribonuclease is positively charged at neutral pH, at which most electrophoretic measurements are made, non-specific binding of this enzyme to the cell surface could also reduce net surface negativity.

Several pieces of evidence suggest that non-specific adsorption of ribonuclease is not the cause of the changes in electrophoretic mobility. Table 2 shows the effect of ribonuclease on the electrophoretic mobility of some cell types. Although all these cells carry net negative surface charge, only about a third of the various types have their mobilities appreciably reduced by ribonuclease; and of the RNase-susceptible cells the reductions range from amounts barely detectable by cell electrophoresis (approximately 5%), to more than 30%. These results suggest that any adsorption of RNase to cell surfaces is not nonspecific.

The mobility of Ehrlich ascites cells is reduced both by ribonuclease T₁ and by ribonuclease A (Table 3). (Ribonuclease A from bovine pancreas specifically cleaves phosphodiester bonds between 3' and 5' positions of ribose groups in pyrimidine ribonucleosides (Brown and Todd, 1955) whereas ribonuclease T₁ from Aspergillus oryzae specifically cleaves phosphodiester bonds between 3' guanylic acid groups and 5' hydroxyl groups of adjacent nucleotides in RNA (Egami et al, 1964).) As at neutral pH, ribonuclease T₁ is negatively charged, it is therefore unlikely that the reduction in cell surface charge produced by both ribonucleases T₁ and A can be due to adsorption. The more likely explanation is that both enzymes act by cleaving their specific substrates within the cell periphery. Comparative studies have also been made of the effects of ribonuclease A, and ribonuclease A which was specifically inactivated by Barnard and Stein's method (Barnard and Stein, 1959) (Table 4). The inactivated enzyme differs from native RNase in that histidine residue 119 is carboxymethylated and inactivation produces only minor conformational changes visible by small angle X-ray diffraction at 3 Å resolution (Karthä, personal comm.) and very minor changes in net charge (Crestfield et al, 1963). The inactivated enzyme produced no significant change in cell electrophoretic mobilities. Again these collected data are against the proposition that adsorption of RNase causes the loss of net cell surface negativity. The possible slight effect at high concentrations was probably due to slight residual traces of active ribonuclease in the inactivated enzyme preparation.

In another series of experiments, the effects of temperature of incubation were observed. The mobilities of cells were determined at different times after treatment with ribonuclease at 10° or 37°C (Figure 1). Whereas the mobility of cells treated at 37° decreased rapidly with maximum reduction occurring after about 20 minutes incubation, the mobility of cells treated at 10° decreased

at only approximately 1/5th of this rate. From consideration of Gibbs' adsorption equation it is expected that adsorption at 37° would occur slightly less rapidly than at 10°. As the rate of reaction of ribonuclease against isolated RNA is approximately 8 times faster at 37° than at 10°, the rate of decrease of electrophoretic mobility at the two temperatures is thus more consistent with an enzyme reaction than with adsorption.

More phosphates and nucleotides are liberated from cells treated with ribonuclease than from cells treated with inactive ribonuclease or no enzyme at all (Weiss, Mayhew, 1966). Ribonuclease may well penetrate into cells, act on intracellular substrate and release enzymatic products, as well as acting at the cell periphery. Another possibility is that activity of ribonuclease at the cell periphery causes permeability changes, resulting in leakage of various materials. Thus, analyses of liberated enzymatic degradation products do not necessarily give information on cell surface chemistry.

RNA which leaks from cells could adsorb to their surfaces, and experiments have been made to determine whether the surface RNA is in fact a leakage product. Cells were washed 20 times before treatment with enzyme and their mobilities measured (Table 5). Ribonuclease treatment resulted in a marked reduction in mobility both after 1 or 20 washings. However the control mobilities also decreased slightly from 1 wash to 20 washes, suggesting that some of the ribonuclease-susceptible material can be removed by washing, but most cannot. In another series of experiments, a cell suspension was ultrasonically homogenized and then mixed with either controls, or cells previously treated with ribonuclease. The mobilities were again measured (Table 6), and no changes in mobility were observed. These experiments indicated that cellular debris, containing nucleic acids, does not affect cellular electrophoretic mobility. In cultures where a high percentage of dead cells was present, the amount of detectable peripheral RNA is usually lower than in "healthy" cultures. If adsorbed leaking RNA was the source of cell surface RNA, a higher amount of peripheral RNA would have been expected in "unhealthy" cultures. Other possible sources of peripheral RNA are mycoplasmal or viral contaminants. However, RNase susceptible Ehrlich ascites cells have been shown to be free of mycoplasma (Weiss and Mayhew, 1969) and cell surface viruses (Horoszewicz, personal communications).

The total experimental evidence strongly suggests that in some cell types there are sites in the cell periphery specifically susceptible to ribonuclease, which in view of the specificity of the enzyme, may be taken to indicate the presence of RNA in this region.

Table 5

The Electrophoretic mobility of Ehrlich ascites cells washed different number of times before treatment with ribonuclease

Number of washes before treatment	Electrophoretic mobility*	
	Controls	Treated with Ribonuclease A
1	1.12 \pm .030	0.83 \pm .021
5	1.05 \pm .031	0.85 \pm .022
10	0.98 \pm .027	0.81 \pm .024
15	1.01 \pm .028	0.80 \pm .021
20	0.96 \pm .027	0.78 \pm .021

* $\mu \text{ sec}^{-1} \text{v}^{-1} \text{cm.}$

Table 6

The Effect of Ehrlich ascites cell homogenates on the Electrophoretic Mobility of HBSS and Ribonuclease treated Ehrlich Ascites cells

1st treatment	Electrophoretic mobility	2nd treatment	Electrophoretic mobility
HBSS	-1.06	Medium only 30 min.	-1.08
HBSS	-1.06	Cell homogenates 30 min.	-1.10
Ribonuclease	-0.82	Medium only 30 min.	-0.88
Ribonuclease	-0.82	Cell homogenates 30 min.	-0.89

* $\mu \text{ sec}^{-1} \text{v}^{-1} \text{cm.}$

Following ribonuclease treatment, the loss of anionic groups from the cell periphery can come about in two main ways (Fig. 2). Some ionized phosphates of RNA could be in the cellular electrokinetic surface, and be lost into the environment on enzyme treatment. Cellular RNA is usually bound to proteins, mucopolysaccharides and other materials and a second possibility therefore, is that the RNase susceptible anionic groups at the cellular electrokinetic surface are not part of the actual RNA molecule.

(2) The dynamic state of the cellular electrokinetic surface

(a) Changes with growth rate. The electrophoretic mobilities of untreated cells or cells treated with neuraminidase and ribonuclease were measured in cultures where the growth rate was varied.

Figure 3 shows that when the growth rate of cultures was slowed by not adding fresh medium, the mean electrophoretic mobility of the control cells decreased; their mobility returned to normal one day after adding fresh medium. The mean mobilities of neuraminidase treated cells ran approximately parallel to the controls, and corresponded to a reduction in net negativity of 20-25% throughout the experiment. Fig. 4 shows the effects of ribonuclease. Although there was initial drop of about 25%, after five days without replenishing the medium, ribonuclease did not appreciably decrease the mobility of cells at all. However, within one day of adding fresh medium, decreases in mobility following RNase-treatment were observed. These results indicate that the density of ribonuclease-susceptible ionized groups at the cell surface can be modified by changes in cultural conditions related to changes in growth-rate. In other experiments, the growth-rate was varied by culturing cells in media containing different amounts of calf serum. It can be seen (Table 7), that in the presence of the highest concentration of calf serum, where multiplication was most rapid, RNase-susceptibility was the greatest, and vice versa. In contrast to the variable effects of RNase on cell electrophoretic mobility, neuraminidase-susceptibility did not vary significantly as a function of growth rate.

An attempt was made to follow effects of growth rate changes *in vivo* (Mayhew, 1968), by determining the mobilities of Ehrlich ascites cells at different times after inoculation into mice. The mobilities of cells rose rapidly in the first day after inoculation, and then declined slowly (Table 8). The percentage reduction in the neuraminidase-treated cells remained constant, irrespective of age of tumors. However, after ribonuclease treatment the mobilities fell to a constant value, indicating that the density of ribonuclease-susceptible ionogenic groups at the surfaces of these cells changed with time. The most ribonuclease-susceptible sites were found in the younger tumours, where growth rate is highest. Thus, these results, although not as clear-cut as in the in vitro studies,

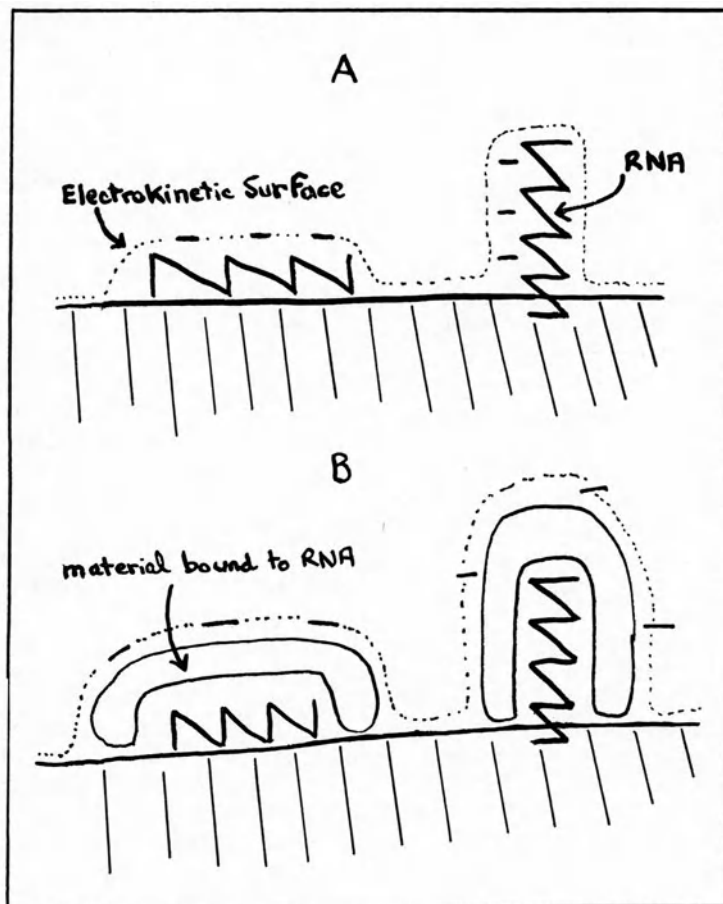


Figure 2. RNA in cell periphery: possible localization. A) Ionogenic groups of RNA are in electrokinetic surface. B) Ionogenic groups of unknown material bound to RNA are in electrokinetic surface.

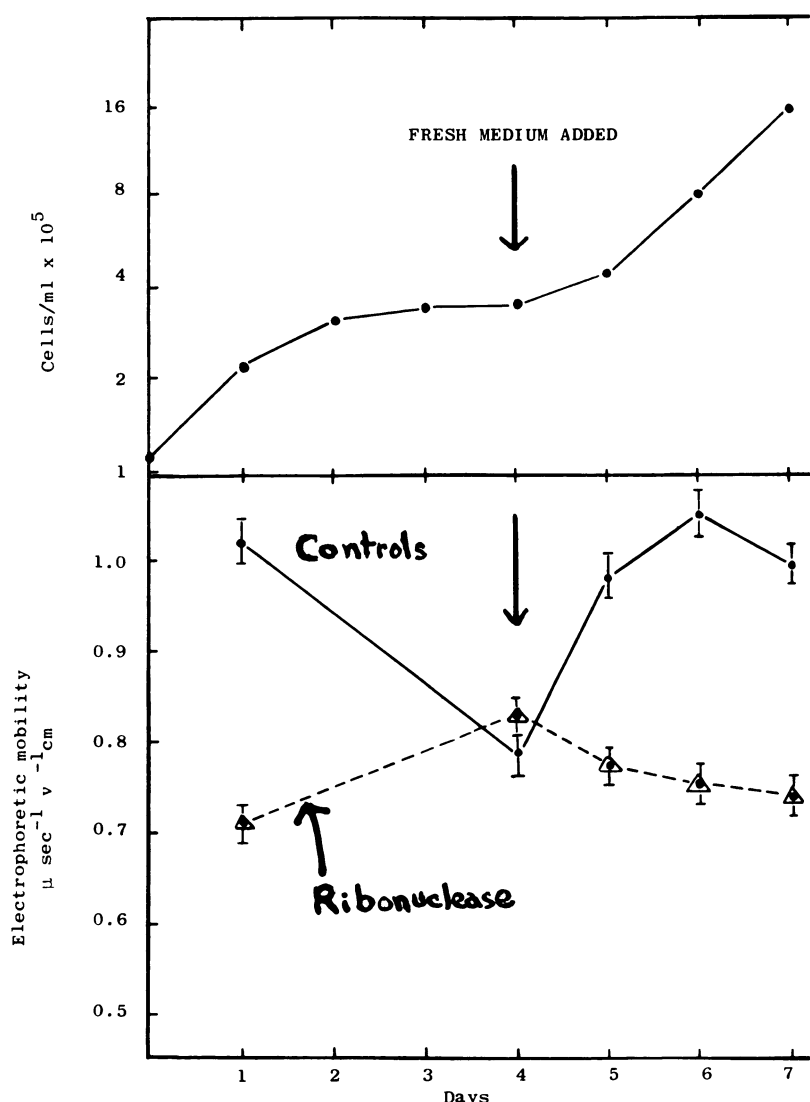


Figure 3. The effect of growth rate changes on electrophoretic mobility of RPMI No. 41 cells.
 — Controls, Δ---Δ ribonuclease-treated,
 ⋄----○ neuraminidase-treated.
 Top graph shows the growth of cells. Cells were not fed from day 0 to day 3 but were refed on day 4.

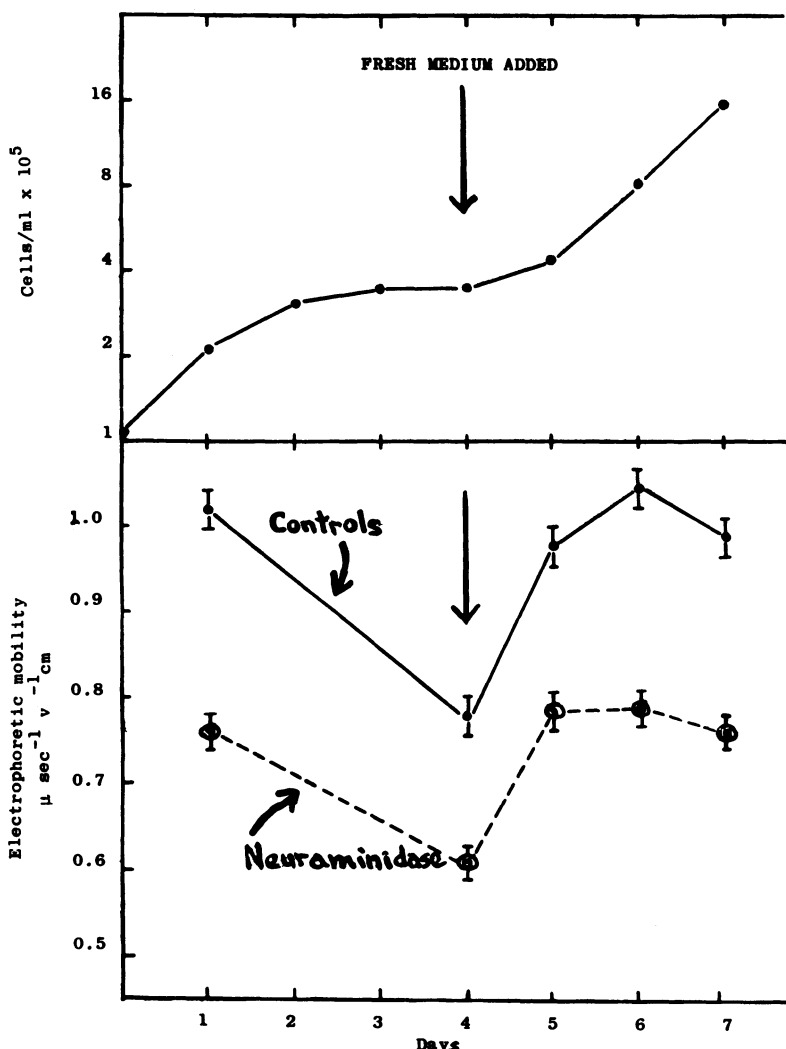


Figure 4. The effect of growth rate changes on electrophoretic mobility of RPMI No. 41 cells.

— Controls, Δ --- Δ ribonuclease-treated,
 \circ --- \circ neuraminidase-treated.

Top graph shows growth of cells. Cells were not fed from day 0 to day 3 but were refed on day 4.

Table 7

Electrophoretic Mobility of RPMI No. 41 cells grown in different calf serum concentrations, with or without treatment with Ribonuclease and/or Neuraminidase

	Calf Serum	0.5% Calf Serum	
	5% Calf Serum	%Reduction	%Reduction
HBSS	1.04	--	0.91
Neuraminidase	0.79	24	0.70
Ribonuclease	0.79	24	0.79
Neuraminidase/Ribonuclease	0.53	48	0.64
Mean Doubling Time	25 Hrs.		51 Hrs.

* $\mu \text{ sec}^{-1} \text{v}^{-1} \text{cm.}$

Table 8

Effect of neuraminidase and ribonuclease on electrophoretic mobility of Ehrlich ascites cells grown in mice

Days after tumour inoculation	Controls	Electrophoretic Mobility*	
		Neuraminidase treatment	Ribonuclease treatment
0	1.02 \pm .030	0.66 \pm .020	0.64 \pm .018
1	1.23 \pm .034	0.76 \pm .019	0.63 \pm .017
2	1.21 \pm .033	0.84 \pm .024	0.59 \pm .019
3	1.18 \pm .025	0.85 \pm .022	0.66 \pm .020
4	1.12 \pm .024	0.75 \pm .017	0.64 \pm .019
5	1.10 \pm .032	0.76 \pm .019	0.67 \pm .019
7	1.00 \pm .026	0.65 \pm .020	0.65 \pm .022
11	0.96 \pm .024	0.66 \pm .021	0.67 \pm .017
14	0.84 \pm .023	0.62 \pm .020	0.66 \pm .019
16	0.78 \pm .026	0.56 \pm .019	0.59 \pm .017

* $\mu \text{ sec}^{-1} \text{v}^{-1} \text{cm.}$

support the concept that growth-rate is directly related to the density of ribonuclease-susceptible groups in Ehrlich ascites cells.

This linkage of electrophoretic mobility to cellular metabolic processes is a subtle one, as short-term experiments lasting approximately 30 minutes, have failed to reveal changes in mobility associated with severe depression of cellular oxygen-consumption, anaerobic glycolysis or uncoupling of oxidative phosphorylation (Weiss and Ratcliffe, 1968).

(b) Changes with cellular life cycle. Cells at specified stages of the cell-life cycle may be obtained in parasychronous cultures and it has been shown that changes occur in the mobility of cells during their mitotic cycle (Mayhew, 1966).

Fig. 5 shows an experiment where synchronized growth was induced in a cultured human cells by double thymidine treatment (Peterson and Anderson, 1964). The top graph shows the growth of the cells after release from the second thymidine block. No cell division occurred for about 7 hours, then wave of division lasting to 10-11 hours took place. No cells were detected in mitosis for about 6 hours, a wave of mitosis then occurred, which reached a peak about 8 hours after release, and then declined. The electrophoretic mobilities of these cells, with or without treatment with ribonuclease and/or neuraminidase, are shown in the bottom graph. The mobilities of the control cells reached a peak at 8 hours and declined afterwards. After neuraminidase-treatment the mobilities fell to a constant level irrespective of time, whereas after ribonuclease treatment there was a slight maximum at 8 hours. These results indicate that the increases in mobility during the mitotic cycles were due mainly to an increased surface density of sialic acid moieties; if there was a variation in the surface density of ribonuclease-susceptible sites it was not detectable in these experiments.

(3) Functional aspects of RNA at the cell periphery

The experimental data show that in the cells examined by us, the density of ribonuclease-susceptible anionic groups at their electrokinetic surfaces varies with growth-rate. The question arises of the functional significance of both the peripheral RNA, and of changes in its surface density.

In addition to the processes discussed earlier, it should also be remembered that changes in the physicochemical nature of the cell periphery can be brought about by enzymes released from cells. Examples have been given of non-lethal autolytic changes produced by released lysosomal enzymes (Weiss, 1967), and among these enzymes in RNase. Thus, any of the multitude of factors causing lysosomal activation, can possibly affect the status of the RNA in

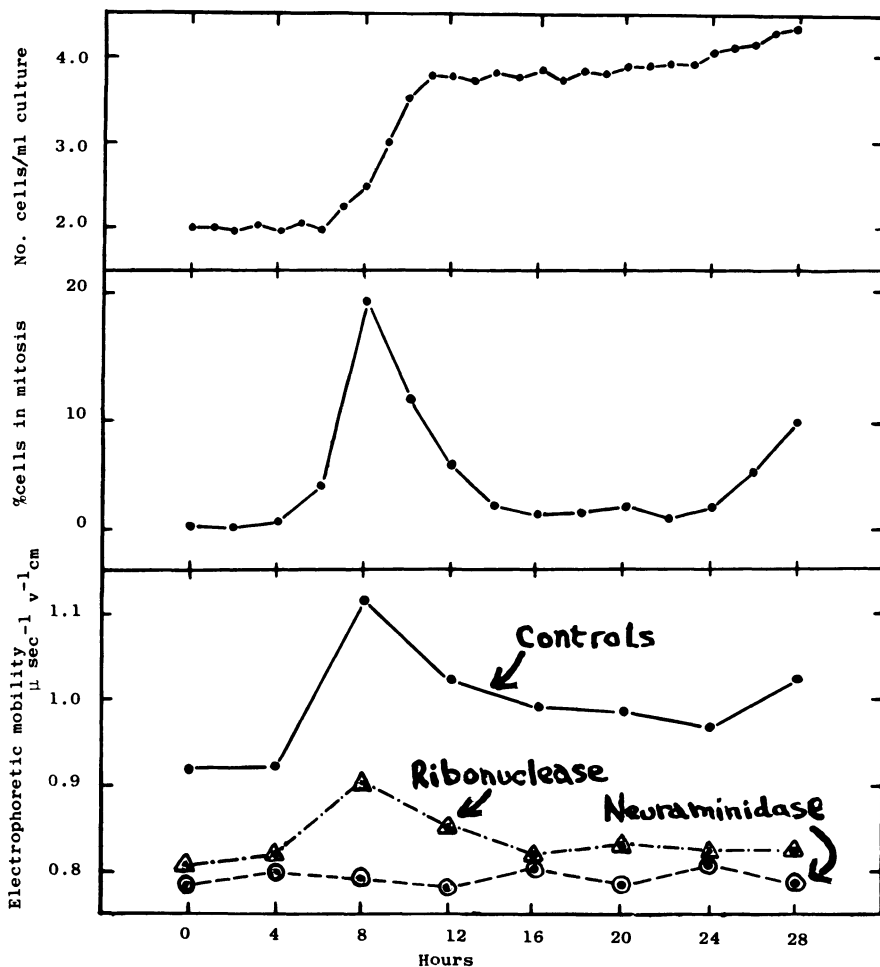


Figure 5. Electrophoretic mobility of RPMI No. 41 cells in parasychronous growth, with or without treatment with ribonuclease or neuraminidase.

the peripheral region of cells.

Previous work has shown that the rigidity of the peripheries of some cells was dependent on sialic acid, possibly due to mutual electrostatic repulsion between its ionized carboxyl groups (Weiss, 1965). When macrophages were treated with neuraminidase, the reduction in net surface negativity and increased deformability were associated with enhancement of phagocytic activity (Weiss, Mayhew, and Ulrich, 1966). However, ribonuclease produces no change in the deformability of a number of cells (Weiss, 1968) and in addition RNase-susceptible groups have not been detected at the macrophage surface (Table 2).

It has often been suggested that ion-binding to carriers is a necessary preliminary step to transmembrane ion movements (Rosenberg and Wilbrandt, 1957). However, studies on Ehrlich ascites tumour cells, have not revealed an effect of ribonuclease-treatment of either net flux of Na^+ or K^+ , or on unidirectional K^+ fluxes (Weiss and Levinson, 1969).

The ionized moieties in the cell periphery may well influence drug adsorption. The charged groups themselves may be the actual receptor or part of the receptor complex; they may orient the drug to invoke drug/receptor specificity as in hapten/antibody interactions; they may affect drug/receptor interactions by altering the conformation of the cell surface and finally, the ionogenic groups may offer steric hindrance to drugs which can react with underlying receptors. Preliminary, unpublished work, suggests that RNase-treatment changes the susceptibility of Ehrlich ascites cells to antitumour drugs.

The observation that whereas normal, human circulating lymphocytes have their electrophoretic mobilities significantly reduced by RNase, whereas circulating lymphoid cells from patients with acute or chronic lymphocytic leukaemia do not, raises the question of whether this difference is capable of diagnostic or chemotherapeutic exploitation (Weiss & Sinks, 1969).

Bennett et al (1969) have studied RNA in the peripheries of rapidly proliferating mouse lymphoid cells, by transplanting lymphopoietic cells into irradiated recipients. Whereas normal lymph-node cells had no detectable peripheral RNA, allogeneic and syngeneic (transplanted) lymphnode cells did, on the evidence that following RNase-treatment, their mean electrophoretic mobilities were reduced by 14.2 and 10.3%, respectively. These observations may be possibly related to those of Mowbray and his colleagues (1969) that pancreatic RNase has immunosuppressive activity, and may be capable of exploitation in transplantation.

The nature of the RNA in the peripheries of some cells is

not known. Speculations have been made on the possible implications if it has genetic informational content (Weiss, 1967), and how this informational material can be transferred from the periphery of one cell to another, where it can be endocytosed and "used".

Contact between the charged surfaces of cells has been treated extensively in terms of lyophobic colloid theory (Curtis 1967, Weiss, 1967). The work presented here suggests that in any consideration of electrostatic interactions between two opposing cell surfaces, the metabolic state of the cells must be considered. If cell contact interactions are in fact dependent on peripheral RNA, then these interactions must also be related to other aspects of cellular activity at that time.

Acknowledgement This work was supported in part by American Cancer Society Grant P403B.

Literature Cited

Barnard E.A. and W.D. Stein, 1959, The histidine residue in the active centre of ribonuclease 1. A specific reaction with bromoacetic acid, *J. Mol. Biol.* 1, 339-349.

Bennett M., Mayhew E., and L. Weiss 1969, RNA in the periphery of rapidly proliferating mouse lymphoid cells *J. Cell. Physiol.* (in press).

Brown D.M. and A. R. Todd, 1955, Evidence on the nature of the chemical bonds in nucleic acids. In "Nucleic Acids" Vol. 1, p.409-446 Eds. E. Chargaff and J. N. Davidson, Academic Press, New York.

Curtis A.S.G., 1967, *The Cell Surface, Its Molecular Role in Morphogenesis*, Logos, Academic Press, London.

Crestfield, A. M., Stein W.D. and S. Moore, 1963, Alkylation and Identification of the Histidine Residues at the active site of ribonuclease *J. Biol. Chem.* 238, 2413-2419.

Egami F., Takahashi K. and T. Uchida, 1964, Ribonuclease in Taka-Diastase; properties, chemical nature and applications. *Prog. in Nucleic acid Res. and Mol. Biol.* Vol. 3, Academic Press, New York.

E. Mayhew 1966, Cellular Electrophoretic mobility and the mitotic cycle *J. Gen. Physiol.*, 49, 717-725.

E. Mayhew, 1967, Effect of ribonuclease and neuraminidase on the electrophoretic mobility of tissue culture cells in parasychronous growth. *J. Cell. Physiol.*, 69 305-310.

E. Mayhew, 1968, Electrophoretic mobility of Ehrlich ascites carcinoma cells grown in vitro or in vivo Cancer Res. 28, 159-1595.

Mowbray J.F., Boylston A. W., Milton J. D. and M. Weksler M. 1969, Studies on the mode of action of immunosuppressive ribonuclease Antibiotica et Chemotherapia, 15, 384-392.

Petersen D. F. and E. C. Anderson, 1964, Quantity Production of synchronized mammalian cells in suspension culture, Nature, 203, 642-643.

Rosenberg T., and W. Wilbrant, 1957, Uphill transport induced by counterflow J. Gen. Physiol., 41, 289-296.

Weiss L. and C. Levinson, 1969, Cell Electrophoretic Mobility and Cationic Flux, J. Cell. Physiol., 73, 31-36.

Weiss L. and E. Mayhew, 1966, The presence of ribonucleic acid within the peripheral zones of two types of mammalian cell J. Cell. Physiol. 68, 345.

Weiss L. and Mayhew E. 1969, Ribonuclease-susceptible charged groups at the surface of Ehrlich ascites tumour cells Int. J. Canc. (in press).

Weiss L., and Ratcliff T. 1968, Effect of Chemotheapeutic and other agents on cellular electrophoretic mobility. J. Nat. Cancer Inst. 41, 957-966.

IMMUNOLOGICAL REACTIONS CARRIED OUT AT A LIQUID-SOLID INTERFACE
WITH THE HELP OF A WEAK ELECTRIC CURRENT

Alexandre Rothen and Christian Mathot

Rockefeller University

New York, New York

We showed more than twenty years ago that monolayers of proteins spread on the water surface of a Langmuir trough and transferred to metalized glass slides were capable of adsorbing specifically corresponding antibodies (1,2). These layers were completely surface denatured, about 8 Å thick per monolayer and in spite of their loss of secondary and tertiary structures they had kept their immunological properties to interact specifically with antisera. The test consisted in smearing on a metalized glass slide coated with the transferred protein layers a drop of dilute antiserum. After 10' or so, the slide was washed and dried and the thickness of the layer adsorbed from the antiserum was measured optically with an ellipsometer, an apparatus developed in our laboratory, permitting the determination of a thickness within a fraction of one Angstrom (3,4). The thickness adsorbed was about 60 Å as compared to approximately 10 Å when the serum was a normal or a heterologous one. Spread films of serum bovine albumin exhibited a unique property not shared by any other protein films investigated, namely the thickness of the layer adsorbed from a homologous antiserum was proportional to the number of monolayers of albumin transferred to the slide. The adsorbed antibody layer was roughly 80 Å thick per double layer of albumin and 240 Å could easily be adsorbed on four underlying double layers of albumin. Protein molecules could also be adsorbed directly on a slide from a dilute solution. In this case the protein molecules were not surface denatured and a layer of antibodies as thick as 80 Å could be specifically immobilized on the subjacent adsorbed layer of antigen. The antigenic layers could also be made of substances other than proteins. Similar experiments carried out with polysaccharides from Types I, III and VIII pneumococcus gave analogous results. In this case the thickness of the adsorbed

layer of antibodies was very large (up to 600 Å) whereas the underlying layer of polysaccharide was only 4 to 5 Å thick (2).

Such results showed that a method for quantitative determinations of immunological reactions might be developed based on the measurements of the thickness of specifically adsorbed layers of antibodies. Theoretically at least, the concentrations of either antigens or antibodies could be determined. In actual practice the method proved to have serious limitations because the antigen solutions had to be relatively pure and concentrated and the antisera could not be greatly diluted. However, when an electric current with the proper polarity was applied during the antigen and antibody adsorption periods, the slide upon which the deposition took place being one of the electrodes, clear cut differentiation between specific and non-specific adsorption could be obtained with very crude antigenic preparations or with highly diluted antisera. These facts were the basis for a new technique to detect immunological reactions which we called "The Immunoelectroadsorption Method". It was successfully applied to the detection of eight arthropod-borne viruses. The antigen solutions were crude extracts of infected new-born mouse brain. In one case immunological reactions could still be detected with an antiserum diluted 1 to 10^5 (5). This method was also used to follow the formation of antibodies in mice against Friend's virus. It was possible to detect the appearance of antibodies already two days after infection (6) and to investigate the influence of the strain of mice on antibodies formation (7). Using pure substances as antigens, we were able to determine the smallest concentration of antigen still detectable with a good rabbit antiserum. For instance the smallest detectable concentration of bovine serum albumin dissolved in water was 10^{-8} g/ml (8). It was important to know the influence of foreign material, protein or otherwise, present in the solutions of antigen on the sensitivity of the method. This information was especially needed if the method was to have wide applications when only very impure antigen preparations were available. The smallest measurable concentration of bovine albumin was $\approx 10^{-7}$ g/ml, when the albumin was dissolved in a 2% guinea pig serum solution named "carrier". In this case the ratio by weight of foreign protein to bovine albumin was roughly 10.000. It is remarkable that the specific adsorption of antibodies was so little influenced by the presence of an overwhelming number of foreign protein molecules present in the solution of the antigen used for the first adsorption.

The determination of circulating human and bovine growth hormones in the physiological range was successfully achieved with the immunoelectroadsorption method (9). The limit of sensitivity was 2×10^{-10} g. of growth hormone per ml of the carrier solution. For an assay of growth hormone the serum to be tested was diluted with a carrier until the thickness adsorbed subsequently from a rabbit immune serum was the same as that observed when the slide was

treated for the first adsorption with the carrier only. The concentration of growth hormone in two sera, one from an acromegalic and the other from a hypopituitary subject were found to be 12×10^{-9} g/ml and 0.8×10^{-9} g/ml respectively.

EXPERIMENTAL

The immunolectroadsorption method was applied to the problem of the interaction between the polysaccharides mainly from type III and VIII pneumococci and their corresponding rabbit antisera. The results obtained are presented in this communication.

Chromium plated slides were used throughout and the intensity of the current was always kept at $300\mu A$. See references (5) and (8) for technical details. The polysaccharides were dissolved either in pure water or in a carrier consisting of a 2% guinea pig serum solution in order to test the influence of foreign material. The results obtained with solutions of polysaccharide from type III pneumococcus in a 2% guinea pig serum have been summarized in Table I. The antiserum solution was a rabbit serum diluted 1 to 10 in veronal buffer.

The tests were conducted as follows: small test tubes were filled with 0.5 ml of the antigen solutions. The chromium plated slides connected to either the negative or positive pole of a D.C. source giving a constant current were inserted into the tubes along with a platinum wire 0.07 cm in diameter connected to the other pole of the D.C. source. After 1' the slides were washed, dried and the thickness adsorbed measured. The slides were then always connected to the positive pole and immersed in 0.5 ml of the immune serum for 1'. After washing and drying, the increase in thickness adsorbed was measured. The figures in column 3 of fig. I are the thicknesses adsorbed from the antiserum in A units. After each test carried out with a sample of the antigen solution, a control test was conducted in a similar way using the same slide but with no polysaccharide in the 0.5 ml of the carrier. Tests and their corresponding controls have been bracketed in column 3. The thickness adsorbed from the antiserum in the control experiment was smaller than that observed when some polysaccharide was present in the carrier solution. The difference in the thickness adsorbed in the test and the corresponding control was a measure of the specific adsorption due to the polysaccharide (see column 4). It was important to use the same slide for both test and control, since the optical thickness adsorbed from an immune serum varied from slide to slide. It is apparent from the table that when the slides were positively charged during the deposition of the polysaccharide, no specific adsorption of antibodies could be observed for concentrations smaller than 10^{-4} g/ml of polysaccharide. However when the slides were negatively charged specific adsorption of antibodies

could still be observed when the titer of the polysaccharide solution was as small as $\times 10^{-7}$ g/ml. At first sight, it would thus appear that the polysaccharide was positively charged. However, when the polysaccharide was dissolved in pure water no specific adsorption of antibodies could be observed if the slide had been negatively charged for the adsorption of the polysaccharide at very low concentrations (10^{-8} g/ml). In contrast, if the slide had been positively charged a specific adsorption could still be observed with aqueous solutions of polysaccharide as dilute as 10^{-13} g/ml. These results showed that the polysaccharide was negatively charged. Therefore, we are inclined to believe that when the slides were negatively charged in the presence of a carrier the adsorption of the protein of the carrier was so reduced as to permit the detection of an immunological reaction at greater dilutions of the antigen solutions.

Table I

Sign of charge on slide for antigen deposition	Concentration of polysaccharide in carrier solu- tion	Thickness adsorbed from antisera in Å	Specific thickness of adsorbed anti- bodies in Å
+	2.1×10^{-4}	166	55
+	0	111	
+	2×10^{-5}	103	0
+	0	105	
-	2×10^{-5}	164	41
-	0	123	
-	1×10^{-5}	140	24
-	0	116	
-	1×10^{-6}	126	10
-	0	116	
-	1×10^{-7}	132	12
-	0	120	

Specific adsorption of antibodies as a function of concentration and polarity of the slide for the first electrodeposition.

When working with extremely dilute solutions of polysaccharide

the nature of the metalized surface played a very important role. This had also been previously observed in the system growth hormone antigrowth hormone rabbit serum. Certain batches of slides metalized apparently under the same conditions did not permit to observe an immunological reaction at the greatest dilutions. However, an adequate surface could be obtained if a metalized slide yielding no results was coated with five monolayers of Ba stearate prior to the electroadsoption of the antigen (8). It was important to use the slides within 4-6 hours after the deposition of the stearate layers. No positive results could be obtained with slides coated 20 hr before they were used for an IEA test, that is the thickness observed after the electroadsoption of the immune serum, was the same on the part of the slide coated with antigen and carrier and the part coated with carrier only. However, if the slides were kept in a test tube in a water vapor saturated atmosphere they could be used at least 24 hr after their preparation. Slides freshly coated with five layer of stearate lost immediately their property for identification of immunological reactions if heated at 50° for 5'. The same thing happened if the slides were placed under vacuum for 10 min.

Most interesting results were obtained when we investigated the reactions between the polysaccharide from types III and VIII pneumococci and their respective rabbit antisera. For the experiments summarized in Table II the adsorption of the antigen as well as of the antibodies were carried out without electric current. It is known that a certain amount of cross reaction takes place between these two systems. This is clearly evident from the first row of the Table. The adsorption period of the polysaccharides was 1' and that of the antisera 10' - the antisera were diluted one to ten in veronal buffer pH 7.5.

The figures in columns 2,3,5 and 6 of the table are the thickness in A units adsorbed from the antisera against polysaccharide III or VIII. It is evident that homologous reactions could still be differentiated from the heterologous in the concentration range of 10^{-6} g/ml of the polysaccharide. It is known that a certain amount of cross reaction takes place between these two systems. This is clearly evident from the first row of the table which shows that when the polysaccharide solutions were concentrated (10^{-3} g/ml) very thick layers could be adsorbed from the immune sera. These thicknesses would vary within large limits depending on whether the slide had been dried or not after the adsorption of the antigen. Layers nearly twice as thick were adsorbed if the slides were kept wet after the adsorption of the polysaccharide until they were immersed into the immune serum solutions. This observation, which has great significance for the mechanism of the adsorption will be more fully discussed in a forthcoming paper.

Table II

Antiserum against polysaccharide from Type III pneumococcus			Antiserum against polysaccharide from Type VIII pneumococcus		
conc. g/ml	poly III Å	poly VIII Å	conc. g/ml	poly III Å	poly VIII Å
3×10^{-3}	278	180	3×10^{-3}	89	158
4×10^{-6}	55	43	2×10^{-4}	35	92
4×10^{-7}	30	27	4×10^{-6}	35	-
4×10^{-8}	-	23	8×10^{-7}	24	36
			1.6×10^{-10}	-	23

Specific adsorption of antibodies as a function of concentration of polysaccharides solutions without the use of an electric current. The figures under the headings poly III and poly VIII which refer to the type of polysaccharide used as antigen, are the thicknesses in Å adsorbed from antisera against either type III or VIII pneumococcus.

Table III

Rabbit antiserum against pneumococcus III			Rabbit antiserum against pneumococcus VIII		
conc. g/ml	poly III Å	poly VIII Å	conc. g/ml	poly III Å	poly VIII Å
3×10^{-12}	80	50	3×10^{-10}	98	122
3×10^{-13}	74	55	3×10^{-11}	94	115
3×10^{-13}	78	50	3×10^{-13}	108	120
3×10^{-14}	60	56	6×10^{-16}	77	86
0	60		6×10^{-18}	75	77

Specific adsorption of antibodies with the use of a current as a function of the concentration of the polysaccharides solutions. The figures under the headings poly III and poly VIII which refer to the type of polysaccharide used in the first electroadSORption, are the thicknesses in Å adsorbed from antisera against Type III or VIII pneumococcus.

The data of Table III show that when a current was used for the deposition of the antigen and antibodies an immunological

reaction was still detectable with concentrations in antigen as small as 3×10^{-13} g/ml, seven orders of magnitude smaller than the limit attained without current. The slides were positively charged for both adsorption periods which lasted 1'.

Dilutions of the antiserum. All experiments reported so far were performed with slides sparsely coated with antigen and treated with relatively concentrated antiserum solutions (1 to 10 dilution). We investigated the effect of the dilution of the antiserum on the immunological reaction carried out on slides fully coated with antigen. The antigen solution contained 10^{-3} g/ml of polysaccharide, and no current was used for the adsorption period which lasted 1'. The adsorbed layer was roughly 5 Å thick. The antiserum adsorption lasted 2', with the slides positively charged as usual. Specific adsorption of 36 Å, 17 Å and 10 Å were recorded on slides treated with rabbit antiserum (against the polysaccharide from type III pneumococcus) diluted 1/4000, 1/40,000 and 1/400,000 respectively. Such specific adsorption could not be obtained without current.

DISCUSSION

It is most remarkable that such minute quantities of polysaccharide could be detected by this method. When the concentration of the polysaccharide solution used for the adsorption was 10^{-12} g/ml, the average thickness attained was at most 5×10^{-5} Å which would be the thickness if all the polysaccharide molecules present in 0.5 ml had been adsorbed. On such a sparsely coated slide, 20 to 30 Å of antibodies could be specifically immobilized. What is then the mechanism which permits to have a ratio by weight of antibodies to antigen of roughly 10^6 ? Whatever the mechanism, the conclusion seems inescapable that a very great number of antibody molecules must be specifically immobilized by a single molecule of antigen. One could assume that the combination antigen antibody adsorbed on the surface could act as a nucleus around which a large number of antibody molecules could congregate especially so under the influence of the electric current. A definite arrangement of the chromium atoms of the metalized surface seems important. As mentioned above it was only with certain types of metalized slides that an IEA test could be successfully conducted. Preliminary electron diffraction patterns obtained with the metalized surfaces have indicated that the crystals size of the chromium surface might play a key role in these interactions.

Finally it should not be forgotten that in the case of the polysaccharide, even without current, a very thick layer of antibodies close to 600 Å could be adsorbed in a few hours on a densely packed layer of polysaccharide 5 Å thick anchored to layers of octadecylamine (2). No such thick layer would be formed

if the polysaccharide was not present. It is therefore not too surprising if with the help of a weak electric current one can detect the presence of polysaccharides in concentrations as small as 10^{-13} g/ml.

These findings seem important from the physical as well as the biological points of view. The forces involved in the building up of thick specifically adsorbed layers are not clearly understood.

From the biological aspect, the immunological reactions taking place at a solid-liquid interface might be much more subtle than it would appear from the present theories based mostly on experiments carried out in the liquid phase. Reactions at interfaces are of prime importance in biology.

REFERENCES

1. Rothen, A., and Landsteiner, K. J., *Exp. Med.*, 76, 437, 1962.
2. Rothen, A., *J. Biol. Chem.*, 168, 75, 1947.
3. Rothen, A., *Rev. Sci. Instr.*, 28, 283, 1957
Rothen, A., in *Physical Techniques in Biological Research*, D.H. Moore, Ed., Vol. IIA Academic Press, 1968.
4. Rothen, A., *Bio-Med. Engineering*, 2, 177, 1967.
5. Mathot, C., Rothen, A., and Casals, J., *Nature*, 202, 1181 1964.
6. Mathot, C., Rothen, A., and Scher, S., *Nature*, 207, 1263, 1965.
7. Mathot, C., Rothen, A., and Scher, S., *Experientia*, 22, 833 1966.
8. Rothen, A., and Mathot, C., *Immunochemistry*, 6, 241, 1969.
9. Rothen, A., Mathot, C., and Thiele, E., *Experientia*, 25, 420, 1969.

ELECTROPHORESIS AND ADSORPTION STUDIES OF PROTEINS AND THEIR
DERIVATIVES ON COLLOIDS AND CELLS

D. J. Wilkins¹ and P. A. Myers
With the technical assistance of C. A. Warren

New England Institute for Medical Research
Ridgefield, Connecticut 06877

INTRODUCTION

The work to be described concerns the adsorption of some proteins and their derivatives at the solid/water interface. This study is derived from previous work on the modification of model particles by adsorption in an attempt to investigate the problem of what constitutes "foreignness" as far as the body is concerned. Specifically, a cell system in mammals, the reticulo-endothelial system identifies foreign particles from native ones and removes them by phagocytosis. The mechanism of this process is but poorly understood and previous work has been directed toward the initial step of recognition. This was studied using a model colloidal system of polystyrene latex (PSL) with its surface properties modified by adsorption of various macromolecules (1). It was found that such surface modification influenced the organ distribution of injected particles.

¹ Present address: Battelle Institute
7 Route de Drize
1227 Carouge/Geneva
Switzerland

The changes in surface properties were monitored by micro-electrophoresis and during work on the change of electrophoretic mobility of the PSL as a function of added macromolecule adsorption behavior was found which strongly indicated orientation of the adsorbing species. This communication describes some of this work in detail in an attempt to understand the interaction of the adsorbing molecules with the substrate. In view of the invariable presence of protein at the cell surface, indeed it is required by the Danielli bilipid layer theory (2), it is felt that such a study may be of interest. Further it is known that many enzymes function at intracellular interfaces and the fact that they lose their activity, both quantitative and qualitative, upon cell destruction inclines one to inquire if this is not perhaps because the orientation or conformation of the enzyme molecule is not unfavorably altered.

METHODS AND MATERIALS

Microelectrophoresis was carried out in an apparatus similar to that described by Bangham *et al* (3). This consists of a cylindrical cell with platinized platinum electrodes suspended in a water bath at $25 \pm 0.1^\circ$. Particles in the stationary layer were observed via a microscope linked to a closed circuit television system. All measurements represent the mean of at least ten particles timed in both directions and are expressed in terms of mobility in microns/sec/v/cm rather than converting to ζ -potentials. Unless otherwise mentioned all measurements were made in 0.145 M NaCl, otherwise referred to as saline. Measurements of mobility as a function of pH were made as follows: 25.0 mg. of protein or derivative was dissolved in 4.0 ml. of NaCl solution. To this stirred solution was added 1.0 ml. of 2% w/v PSL and stirring continued at room temperature for at least one hour. At that time 0.2 ml. samples were removed and added to 20.0 ml. of saline with pH adjusted with either 0.145 M HCl or NaOH. The pH of the suspension was then measured and the electrophoretic mobility determined. As was pointed out by Abramson (4), and as will become clear later, it is very important to carry out determinations by coating at a high concentration and then diluting for observation.

The procedure for adding various concentrations of protein or derivatives to various colloidal particles was as follows: One ml. of a suspension of particles at a suitable concentration for electrophoretic mobility determination was added to a series of beakers containing the adsorbate in a suitable concentration range. The total volume in each beaker was 20.0 ml. and the final salt concentration 0.145 M NaCl. After adsorption at 30 minutes the pH and then the electrophoretic mobility was determined. Except at

high concentrations the pH was constant over a large range of concentrations with most of the materials used. If necessary (v. infra) the pH was adjusted with either 0.145 M NaCl or 0.145 M HCl. The following colloidal particles were used as adsorbent in the protein adsorption studies.

1. Polystyrene latex (PSL), diameter 1.099 microns, kindly supplied by Dr. John W. Vanderhoff, Dow Chemical Co., Midland, Michigan. This material was extensively washed with distilled water by Millipore filtration.

2. Methylated polystyrene latex (MPSL) is the above material methylated as follows: One g. of PSL was filtered, washed with methanol, and resuspended in 100 ml. methanol and 0.85 ml. concentrated HCl and after stirring overnight the material was filtered and washed five times with 200 ml. of water and suspended in 50.0 ml. of water.

3. Powdered silica is an ultrapure sample kindly provided by Dr. Vandegrift of Corning Glass, Corning, New York. The material was suspended in distilled water and centrifuged. The very fine particles were removed leaving a sample of average size 1.0 μ diameter (estimated).

4. Sheep red blood cells (SRBC) were fixed with acetaldehyde as described by Heard and Seaman (5). It has been shown (5) that such cells behave electrophoretically like fresh cells and are useful since no complications can arise from hemoglobin released from lysed cells under extreme environmental conditions.

5. Mineral Oil (Drakeol 6-VR) kindly supplied by Pennsylvania Refining Company, Butler, Pennsylvania, was emulsified by adding 0.5 ml. to 50.0 ml. of water and sonifying for 30 secs at position 6 using a Branson Sonifier.

Most of the proteins and their derivatives were prepared by similar means and hence it is not necessary to describe all the preparations in detail. The gelatin used was acid extracted porcine material (kindly supplied by Ucопco Division, Wilson and Co., Chicago, Illinois). Bovine plasma albumin (BPA) powder, was fraction V material obtained from Armour Pharmaceutical Co., Chicago, Illinois. Polylysyl gelatin (PLG) was prepared as follows: ϵ -N-trifluoro acetyl-L-lysine was prepared (6) and converted to its carboxy amino anhydride by bubbling phosgene through a solution in ethyl acetate (7). After recrystallization from ethyl acetate the anhydride in dioxane solution was reacted with an aqueous

buffered solution of gelatin (8). The protective trifluoro acetyl groups were removed using aqueous piperidine and the final material dialyzed exhaustively against distilled water, millipore filtered (0.45 μ diam.) and lyophilized. Poly-L-ornithyl gelatin (POG) and poly-L-lysyl bovine plasma albumin (PLBPA) were prepared in a similar manner. Polylysine (PL) was prepared from the ϵ -N-trifluoro acetyl- α -N-carboxyl-L-lysine anhydride by polymerizing with triethylamine (9). The material was then processed as for PLG (v. supra). Methylated bovine plasma albumin (Me BPA) was obtained by esterifying using methanol and HCl (10).

The adsorption isotherm of PLG on PSL was determined using I^{131} -labelled PLG (11). A PSL suspension containing 5.5 mg. of PSL was added to a series of cellulose nitrate (0.5 x 2.5 inches) centrifuge tubes containing PLG solutions in a suitable range of concentrations. The total volume in each tube was 5.0 ml. and the final salt concentration 0.0145 M NaCl. After equilibration for 30 minutes at 37° the tubes were centrifuged at 35,000 x g for 15 minutes and washed several times with 0.0145 M NaCl solution until the PSL pellet showed no further change in counts. Micro-electrophoresis was also carried out on suspensions of the washed PSL in 0.0145 M NaCl.

For injection into rats I^{125} -labelled PSL (1) was suspended in a range of concentrations of PLG in 0.145 M NaCl. This material was filtered by membrane filtration (Millipore Corporation, Bedford, Mass.) to remove excess PLG and resuspended in 0.145 M NaCl with gentle sonification. Injections were carried out in Nembutal-anesthetized rats and distributions and rate of clearance from the blood determined as previously described (1). The results were expressed as the percentage of the injected dose accumulated in the spleen after 15 minutes.

RESULTS

Determinations were made of the electrophoretic mobility in saline of all of the particles used in these studies, as a function of pH. The results are shown in figure 1 and illustrate the different surface nature of the materials used.

The value for the mobility of acetaldehyde treated SRBC's (-1.40 at pH 7.5) is very similar to that found by Seaman *et al* (5). Although there is a certain amount of controversy concerning the ionogenic groups, at the surface of PSL (12,13) the fact that the mobility is so markedly reduced by esterification strongly suggests the presence of carboxyl groups.

The electrophoretic mobilities of all proteins and derivatives used after adsorption on PSL are shown in figures 2 and 3 as a function of pH.

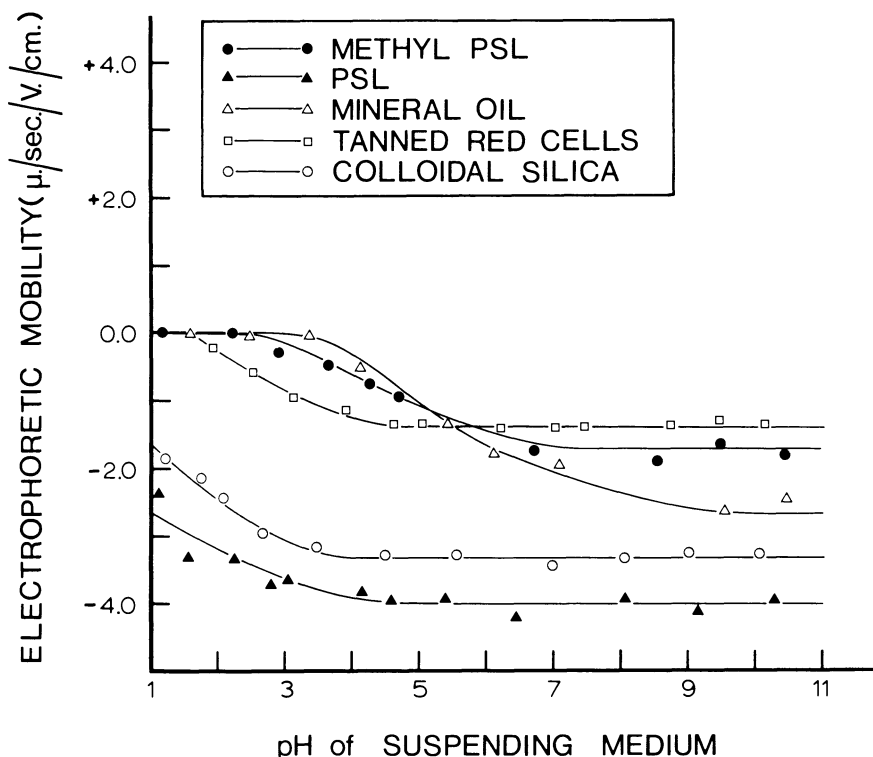


Fig. 1. Electrophoretic mobility of the particles used as a function of the pH of the suspending medium (0.145 M NaCl).

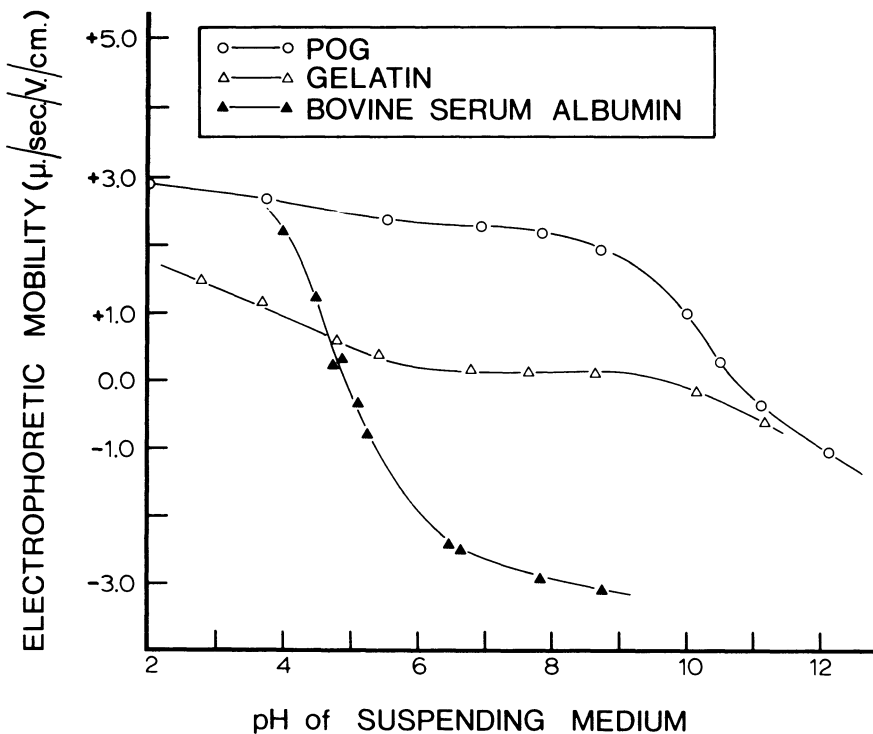


Fig. 2. Electrophoretic mobility of some proteins and derivatives adsorbed on PSL as a function of the pH of the suspending medium (0.0145 M NaCl).

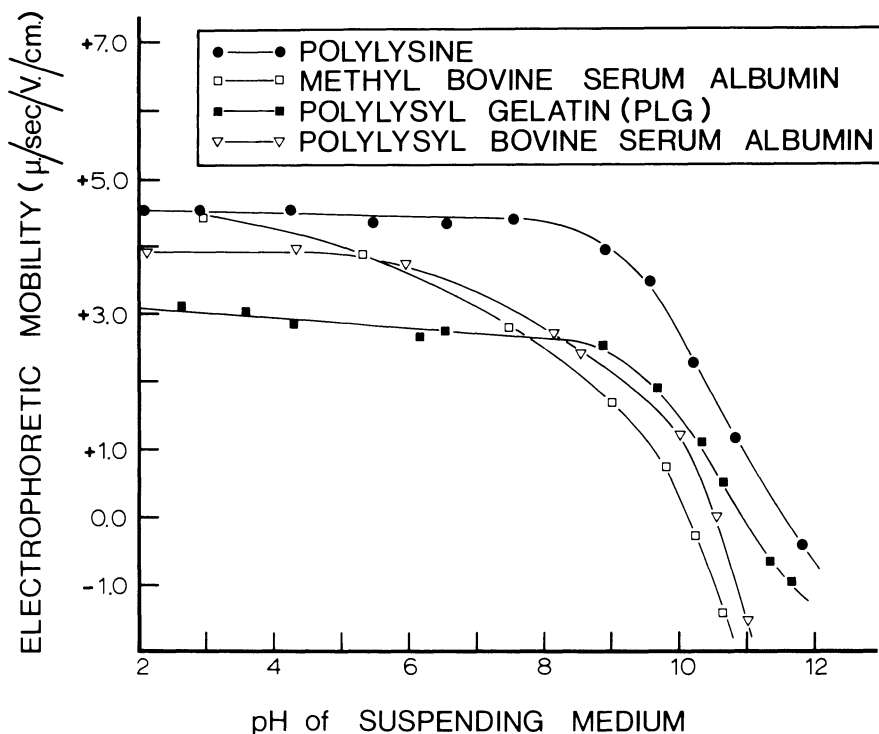


Fig. 3. Electrophoretic mobility of some proteins and derivatives adsorbed on PSL as a function of the pH of the suspending medium (0.0145 M NaCl).

It can be seen that the particular type of gelatin used is near isoelectric over the pH range 6-10, a rather unusual behavior for a protein. Addition of either lysine or ornithine to gelatin can be seen to increase the positive mobility and the isoelectric point. The pH-mobility curve for adsorbed BPA is very similar in shape and isoelectric point to values obtained using the soluble material and a moving boundary method (4). Addition of lysine or indeed esterification with methanol again increase the positive mobility and isoelectric point. Polylysine due to the absence of any acidic groups has the highest positive mobility and isoelectric point.

Figure 4 shows a comparison of the adsorption isotherm of PLG on PSL together with the electrophoretic mobility of the samples.

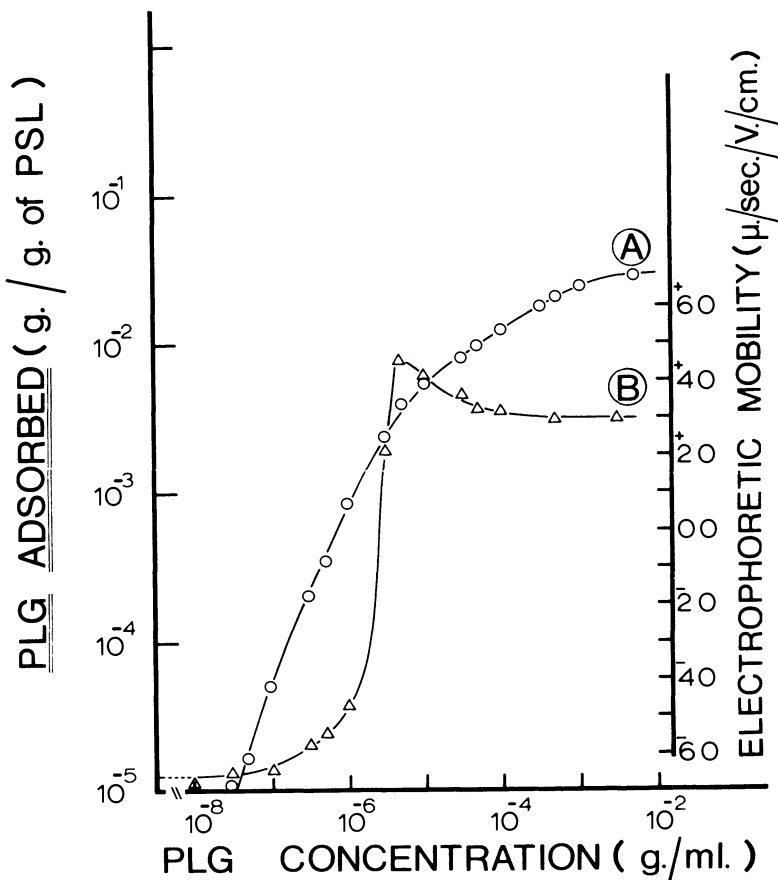


Fig. 4. Adsorption and electrophoresis of PLG on PSL as a function of PLG concentration; curve A- amount of PLG bound by PSL after centrifuging and exhaustive washing; Curve B- electrophoretic mobility of the washed PSL/PLG from A. Both adsorption and electrophoresis in 0.0145 M NaCl.

It will be noted that the electrophoretic uptake (curve B) shows a distinct maximum positive mobility and then decreases to a constant value. It is this maximum in the mobility which is of interest, since it presumably reflects a particular orientation of the PLG molecules upon adsorption. In order to see whether the effect was only obtained by adsorbing PLG on PSL adsorption and electrophoresis was also carried out on the particles examined in figure 1. The results are shown in figures 5 and 6, and it is immediately obvious

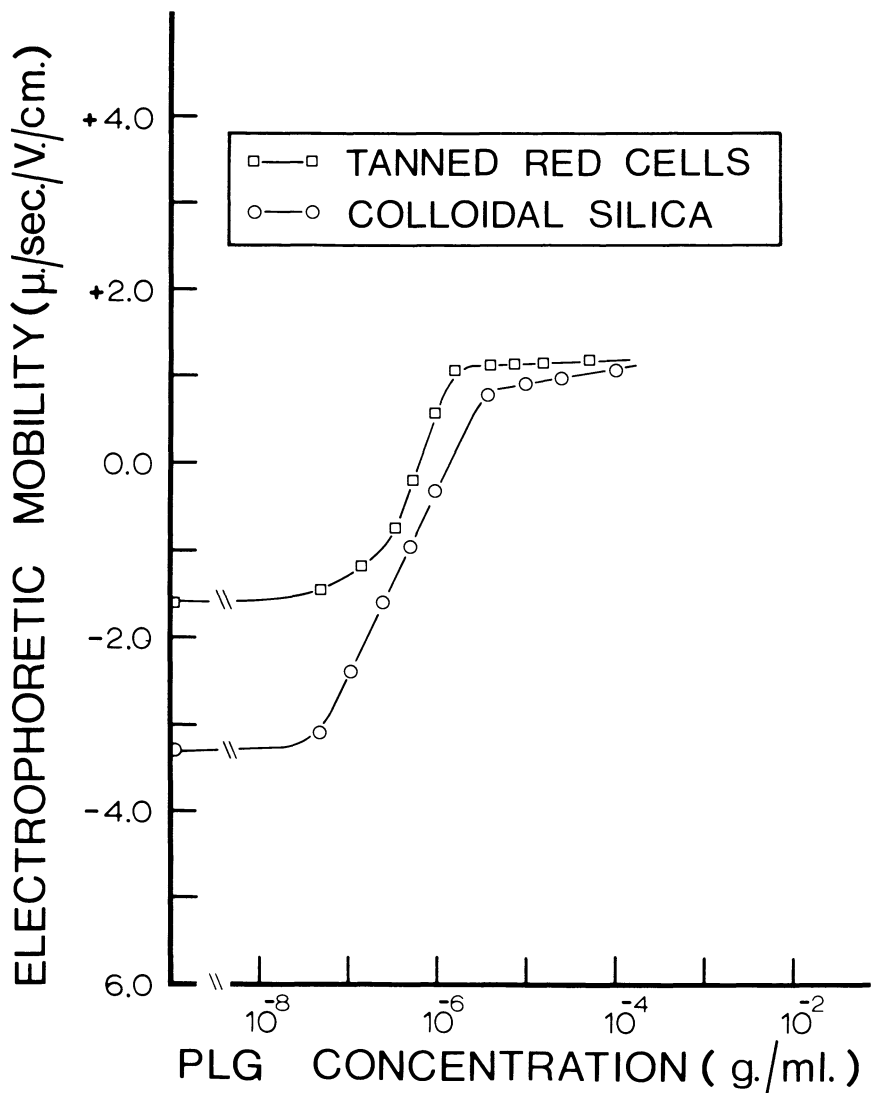


Fig. 5. Electrophoretic mobility of various particles as a function of PLG concentration in the suspension (0.145 M NaCl).

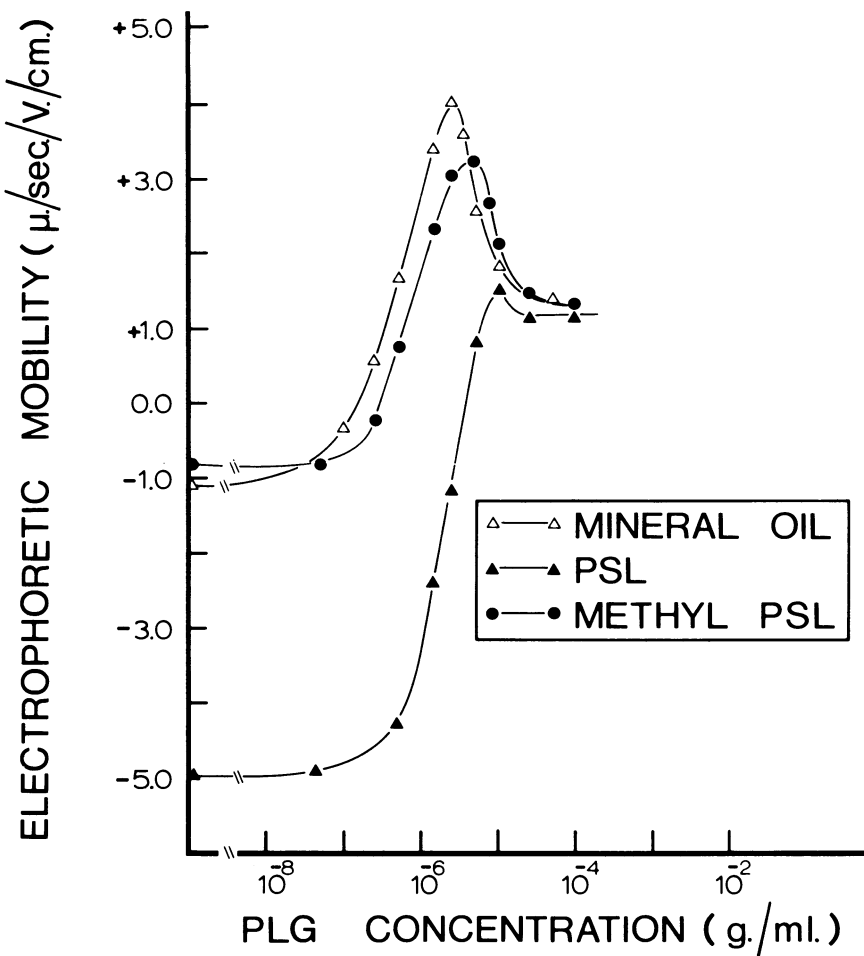


Fig. 6. Electrophoretic mobility of various particles as a function of PLG concentration in the suspension (0.145 M NaCl).

that a maximum in mobility is not obtained on all substrates. The electrophoretic adsorption behavior on different particles of the proteins and derivatives (the pH-mobility characteristics of which are shown in figures 2 and 3) was also examined and the results are shown in figures 7 and 8.

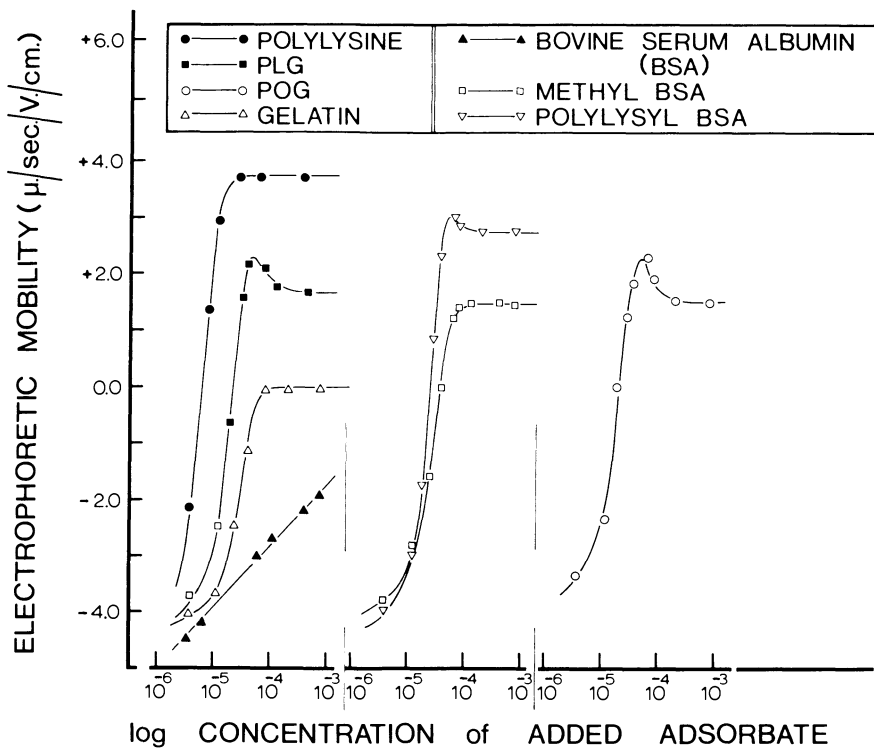


Fig. 7. Electrophoretic mobility of various proteins and their derivatives adsorbed on PSL as a function of the concentration of the adsorbate (0.145 M NaCl).

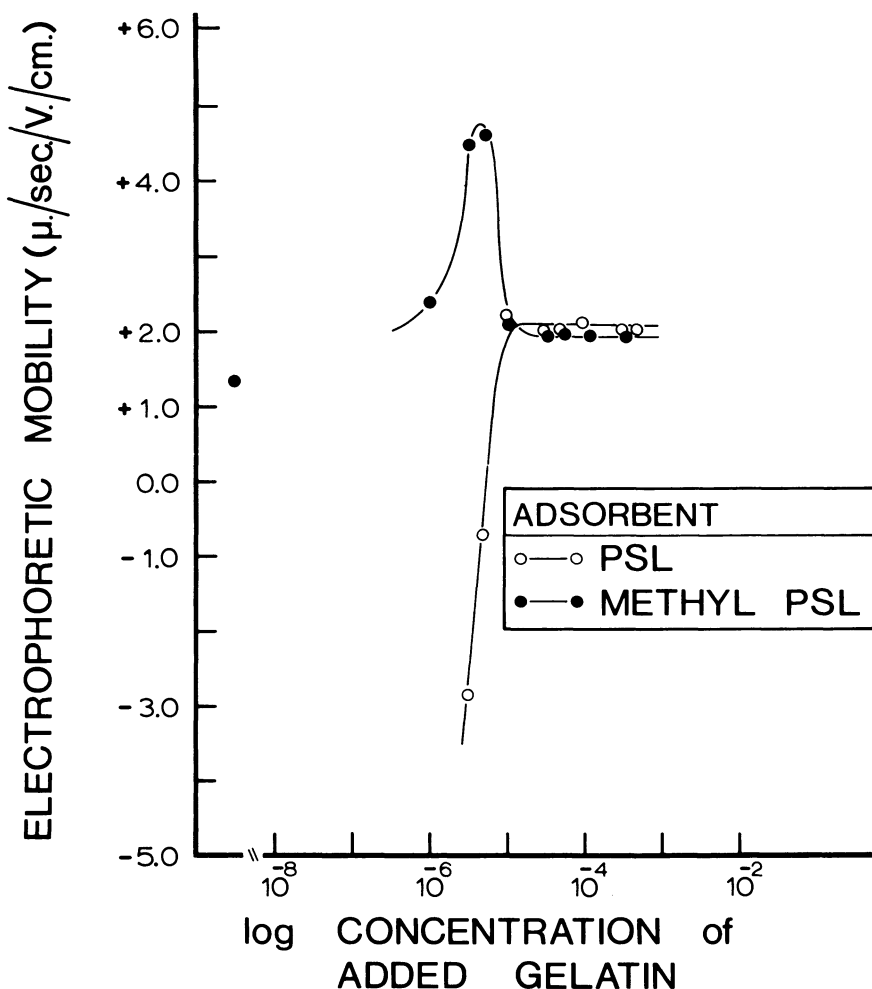


Fig. 8. Electrophoretic mobility of PSL and Methyl PSL as a function of gelatin concentration at pH 2 (0.145 M NaCl adjusted with 0.145 M HCl).

These results demonstrate that the anomalous high positive mobility found with PLG is not limited to lysyl derivatives of proteins or amino acid derivatives of gelatin. In fact with a protein like gelatin under conditions of low pH the effect is seen on MePSL. Gelatin was chosen for this experiment since it is obviously not denatured at pH 2. Figure 9 shows the results of a typical intra-venous clearance experiment, in which the percentage of the injected

dose accumulated in the spleen 15 minutes after injection is plotted as a function of the coating concentration of PLG. It will be observed that the biological behavior is in fact reflected in the electrophoretic characteristics of the particle.

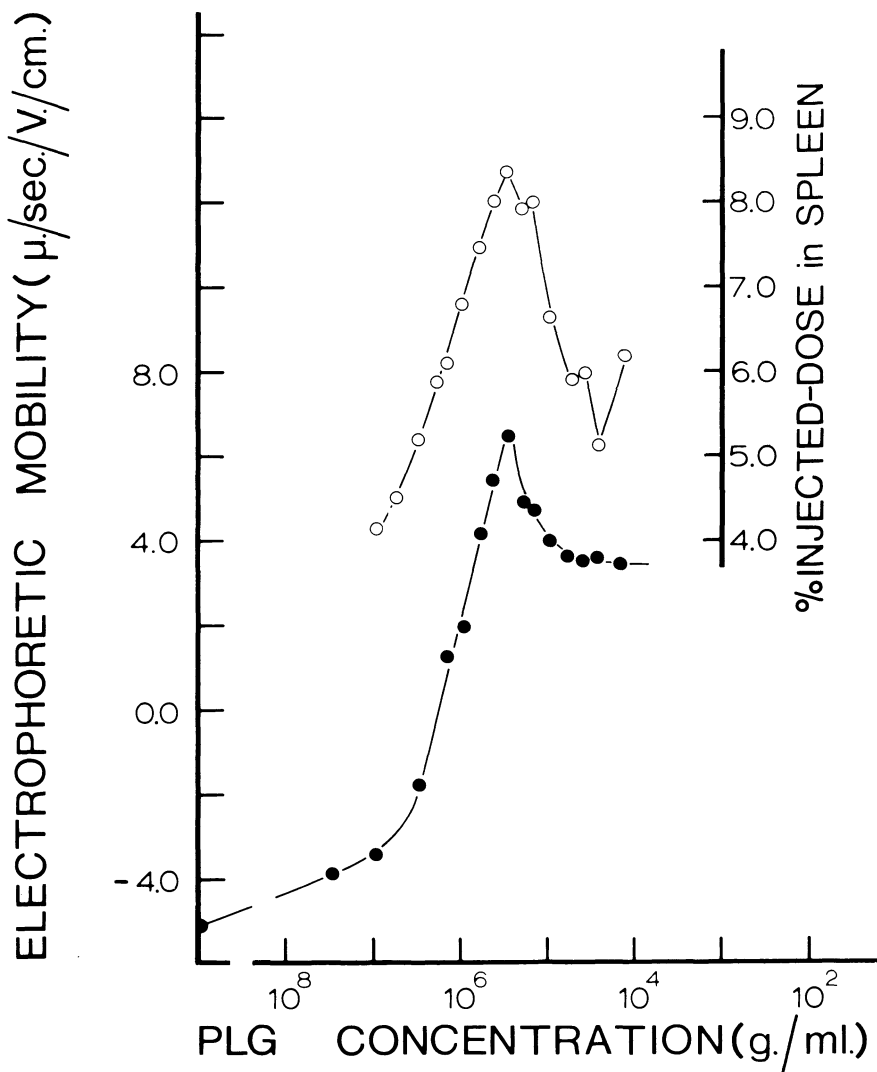


Fig. 9. Electrophoretic mobility and amount of PSL taken up by the spleen fifteen minutes after injection as a function of PLG concentration: -o- mobility of PSL/PLG particles; -o- uptake by the spleen of PSL/PLG particles. Injected dose, 0.73 mg. PSL/100 g. rat (0.145 M NaCl).

DISCUSSION

It is hoped that this presentation has demonstrated the usefulness, and some of the drawbacks, to the technique of microelectrophoresis for protein studies. As with most surface chemistry of this sort the actual interpretation of what is happening at the molecular level is not easy. Furthermore as has been noted in the past (20) and recently by Mathot and Rothen (14) there is not an extensive literature upon which to draw in the area of the adsorption of proteins onto solids. Loeb (15) and Abramson (4) demonstrated just how useful microelectrophoresis of adsorbed proteins could be and how well the results compared to those obtained by other means. Since then the importance of consideration of electrophoretic surface change has been shown to be of great usefulness in a variety of biological problems. Bangham (16,17) has demonstrated the importance of surface charge in blood clotting and in certain enzyme reactions and Bedford has demonstrated correlations of the maturation of sperm with their surface charge (18) while the work of Seaman (5), Weiss (19) and others has added greatly to our knowledge of the nature of cell surfaces, both normal and neoplastic. Hopefully some of the material presented here will clarify some of the ideas on the electrophoresis of adsorbed protein and point to some of the precautions necessary for correct interpretation of data. It is immediately obvious that the surface nature of the colloid particle can affect the electrophoretic results and that the concentration of added protein or polymer is very important. It was pointed out by Abramson (4) that it is preferable to coat at a high concentration to achieve adequate coverage and then dilute to a suitable concentration for observation. It is now obvious that this is also necessary to avoid the possibility that the protein covered surface will show an abnormal high mobility since it can be observed (e.g., fig. 6) that at high enough concentrations the mobilities all reach a similar value. However, at high enough concentrations the choice of particle is unimportant since any interaction is damped out. Of course at high protein concentrations consideration has to be given to possible changes in viscosity and pH which would lead to mobility changes. Another useful feature of the method is its ability to detect changes in protein chemistry or particle surface chemistry. Thus for example the effects of methylation of PSL were demonstrated by figure 1 and of adding lysine to gelatin by figures 2 and 3.

The high positive mobility of basic protein derivatives on PSL, for example, at certain concentrations is interpreted as a configurational change due to interaction with the substrate surface. If the interaction were purely electrostatic then since all the surfaces studied are electrophoretically negative one

would expect basic groups from the protein to be as close as possible to negative sites on the surface leaving a preponderance of negative groups in the plane of shear and hence no excessive positive mobility. Since this is in fact the opposite of what occurs, the proposal is made that anionic groups of the proteins adsorb preferentially to the largely hydrophobic PSL surface exposing an excess of basic groups in the plane of shear and a consequent elevated positive mobility. This hypothesis is supported by several facts: (i) anions due to their lower hydration adhere more readily on hydrophobic surfaces (20), (this is also demonstrated by the fact that mineral oil becomes negative at higher pH); (ii) increasing the hydrophobic nature of the PSL surface increases the positive mobility, and using a completely hydrophobic surface such as mineral oil emulsion shows an even higher positive mobility; (iii) polylysine which has no anionic groups does not show an increased positive mobility; (iv) hydrophilic surfaces such as silica or red cells do not show the effect. From figure 4 it can be seen that at the point of highest positive mobility, the coverage is approximately 1.0 mg. PLG/m^2 of PSL, very similar to the coverage determined by several workers (21) for a protein "monolayer" at the air/water interface. As further PLG is added the mobility decreases again, presumably due to the multi-layer formed "damping" out the effect of the substrate surface. A similar effect was noted by Matijevic and Ottewill (22) who showed a periodic change in electrophoretic mobility of silver halide sols as a function of added cationic detergent. This was ascribed to successive layers of detergent having opposite orientations on a charge basis which was damped out at higher concentrations. It is interesting to note that PLG does not show a Langmuir isotherm on PSL but forms a multilayer, presumably because the PLG-PLG interaction is stronger or more slowly reversible than the PLG-H₂O interaction. It has been noted that although proteins usually show a Langmuir adsorption isotherm, at least on inorganic substrates (23) theoretically at least, they should not, since the adsorption is for all practical purposes irreversible. One final effect of the increased positive mobility should be noted. The elevated positive mobility shown in figure 4 is of a material which after adsorption was filtered, washed and resuspended while those shown, for example, in figure 6 are particles suspended in the adsorbate solution. This suggests that the presumed conformational change is very rigid, and able to withstand fairly harsh physical treatment.

In view of the importance of interfaces in biology, both intracellular and extracellular, it is interesting to speculate on the biological significance of such orientations. It has been shown previously that the distribution of an intravenously administered colloid is influenced by the surface character of the

injected colloid. Electrophoretically positive colloids showed an increase in splenic accumulation over negative colloids (24). Thus the fact that the spleen can recognize far more subtle differences in surface characteristics (see fig. 9) as shown by how precisely the spleen uptake mirrors the anomalous adsorption behavior takes on an added interest. Of course, "recognition" of self from non-self almost certainly is more complex than differentiating between positive and negative surfaces and only when more is understood about the complex interactions between surfaces and blood elements is the problem likely to be completely resolved (25).

It is interesting to speculate on a few further possible implications of oriented proteins on hydrophobic surfaces. It is well known that Danielli's (2) model for the cell membrane depends upon the presence of an exterior coating of globular protein. Yet it has recently been pointed out by Weiss (26) that electrophoretically it is impossible to detect -NH_2 groups at the cell surface. It is tempting to think of some lipid-protein interaction similar to that described above possibly accounting for this anomaly, although preliminary experiments are not very encouraging. Certainly, as Wallach *et al.* (27) have pointed out, the interaction at the cell surface between proteins and lipids is almost entirely hydrophobic. Although doubts have been raised about the validity of the bilipid layer (28) model it certainly accounts for some of the properties of cell membranes. What is rather surprising is that so little attention has been paid to the presence (or absence) of protein exterior to the lipid layers.

Finally, when cells are destroyed the activity of their enzyme systems diminishes, both quantitatively and qualitatively (29). It has been suggested, from this and other arguments, that many intracellular enzyme reactions take place at interfaces. Certainly with phospholipases the surface charge is very important in the enzyme substrate interaction and hence in the rate of hydrolysis (17). It is possible that enzymes at interfaces are adsorbed and interact with the adsorbent layer in a manner sufficiently similar to that discussed above that this might be a worthwhile field of study.

ACKNOWLEDGMENTS

The work was supported in part by grants from The John A. Hartford Foundation, Inc., the National Institutes of Health (Grant Number AL 07161-02), and the Office of Naval Research (Grant Number Nonr-4170 (00, NR 301-740)).

BIBLIOGRAPHY

1. Wilkins, D. J. and Myers, P. A., Brit. J. Exp. Pathol., 47, 568 (1966).
2. Danielli, J. F. and Harvey, E. H., J. Franklin Inst., 214, 1 (1932).
3. Bangham, A. D., Flemens, R., Heard, D. H. and Seaman, G.V.F., Nature, 182, 642 (1958).
4. Abramson, H. A., Moyer, L. S. and Gorin, M. H., "The Electrophoresis of Proteins", Reinhold, N. Y. (1942).
5. Heard, D. H. and Seaman, G.V.F., Biochim. Biophys. Acta, 53, 336 (1961).
6. Sela, M., Arnon, R. and Jacobson, I., Biopolymers, 1, 517 (1963).
7. Fasman, G. D., Idelson, M., and Blout, D. R., J. Amer. Chem. Soc., 83, 709 (1961).
8. Sela, M. and Arnon, R., Biochem. J., 75, 91 (1960).
9. Daniel, E. and Katchalsky, E., in "Polyamino Acids, Poly-peptides and Proteins", Ed. M. A. Stahman, Univ. of Wisconsin Press (1962).
10. Fraenkel-Conrat, H. and Olcott, H. S., J. Biol. Chem., 161, 259 (1945).
11. Bocci, V., Intern. J. Appl. Radiation Isotopes, 15, 449 (1964).
12. Ottewill, R. H. and Shaw, J. N., Kolloid-Z.U.Z. Polymere, 218, 34 (1967).
13. Van den Hul, H. J. and Vanderhoff, J. W., J. Coll. Interfac. Sci., 28, 336 (1968).
14. Mathot, C. and Rothen, R., 43rd National Colloid Symposium (Preprints), p. 105, Case Western Reserve University, Cleveland, Ohio, June 1969.
15. Loeb, J., J. Gen. Physiol., 6, 116 (1923).
16. Bangham, A. D., Nature, 192, 1197 (1961).
17. Bangham, A. D. and Dawson, R. M. C., Biochim. Biophys. Acta, 59, 103 (1962).

18. Bedford, J. M., *Nature*, 200, 1178 (1963).
19. Weiss, L. and Ratcliffe, T. M., *J. Nat. Cancer Inst.* 41, 957 (1968).
20. Bull, H. B., "Physical Biochemistry", John Wiley, N. Y. (1943).
21. Cheesman, D. F. and Davies, J. T., *Advan. Protein Chem.*, 9, 439 (1954).
22. Matijevic, E. and Ottewill, R. H., *J. Colloid Sci.*, 13, 242 (1958).
23. Neurath, H. and Bull, H. B., *Chem. Revs.* 23, 391 (1938).
24. Wilkins, D. J., *J. Colloid Interfac. Sci.*, 25, 84 (1967).
25. Wilkins, D. J., "The Reticuloendothelial System and Atherosclerosis", p. 25, Plenum Press, N. Y. (1967).
26. Weiss, L., Bello, J. and Cudney, T. L., *Int. J. Cancer*, 795 (1968).
27. Wallach, F. H. and Gordon, A., *Federation Proc.*, 27, 1263 (1968).
28. Korn, E. D., *Science*, 153, 1491 (1966).
29. Hundler, R. W., "Protein Biosynthesis and Membrane Biochemistry", John Wiley & Sons, Inc. (1968).

SURFACE CHEMICAL FEATURES OF BLOOD VESSEL WALLS AND OF SYNTHETIC MATERIALS EXHIBITING THROMBORESISTANCE

R. E. Baier

Applied Physics Department, Cornell Aeronautical
Laboratory of Cornell University, Buffalo, NY 14221

R. C. Dutton

Laboratory of Technical Development, National Heart
Institute, Bethesda, Maryland 20014

V. L. Gott, Department of Surgery, Johns Hopkins
Hospital, Baltimore, Maryland 21205

INTRODUCTION

Our problem can be stated simply: What surface properties are required for candidate biomedical materials to be as non-thrombogenic as possible? This symposium paper relates recent progress along three converging paths we have taken while attempting to solve this problem. First, we report qualitative results from in vitro and in situ surface chemical measurements on blood vessels which were carried out by Dutton and Baier at the National Heart Institute. A more quantitative treatment of these data will be published separately. Second, we report at some length the results of Gott, Dutton and Baier -- obtained during two years of collaborative effort -- which suggest an explanation for the excellent thromboresistance observed with prosthetic implants of the metallic alloy Stellite. Third, we briefly review the surface chemical investigation of candidate biomaterials now being prosecuted by Gott and Baier with the support of the Artificial Heart Program of the National Institutes of Health.

These studies rely heavily on contact angle measurements and the critical surface tension concept identified with Zisman's laboratory (1), which has recently been extended to bioadhesional problems (2, 3), and are supported by the surface-specific spectroscopy allowed by new internal reflection techniques (4).

BACKGROUND ON THE APPLICABILITY OF SURFACE CHEMICAL CONCEPTS TO BIOMEDICAL PROBLEMS

The maintenance of favorable blood flow depends upon the lack of adhesion between circulating blood elements and vessel walls (or synthetic materials) with which they make intimate contact. Careful examination of the formation, structure and properties of biological interfaces is required to understand these phenomena, eventually. The more urgent task is to discover which known mechanisms assist or impede biological adhesion, since lack of this information is a limiting factor in producing biocompatible prosthetic implants and nonthrombogenic extracorporeal circuits. Current efforts attempt to extend technical data on adhesive behavior to bioadhesional problems by presenting some basic relations between the surface properties of materials and adhesion, and outlining the useful comparative concept of "critical surface tension" (2, 3). There is little doubt of the importance of these relations when considering some initial interactions at biologically interesting surfaces. Many illustrations can be drawn from the large relevant literature on the role surface phenomena play in determining adhesion in biomedical environments.

The extreme localization of surface forces has been emphasized (5, 6, 7). Examples are plentiful that these physical forces alone, without the need for chemical bonding, are sufficient as a basis for good adhesion (8, 9). Wetting and spreading considerations have been reviewed (5, 11), and the point made that careful attention to the relations between contacting phases is required (2, 3). A parameter called "critical surface tension (γ_c)", derived from contact angle data, allows the empirical ranking of the relative surface energies of organic materials (12). "Critical surface tension" is a unique characteristic of the solid surface, and is readily correlated with the actual outermost chemical constitution of most substances. For example, fluorocarbon surfaces are of intrinsically low surface energy, have low γ_c values, and show poor adhesive qualities; surfaces largely composed of oxygen and nitrogen atoms are of relatively high energy, have higher critical surface tensions, and form good adhesive bonds. Organic surfaces are thus conveniently grouped into high-energy and low-energy categories, and the wetting, spreading, and adhesive behavior on each may be differentiated. The major influence of water on biological adhesion has been suggested to be a reflection of its conversion of intrinsically high energy surfaces into

considerably lower energy surfaces (13, 14, 15). As an illustration of the important role which proteins must play at biological interfaces, the wetting properties of some simpler polyamides have been given (16, 17, 18). Wetting studies on the nylons, for instance, using carefully purified diagnostic liquids showed that hydrogen-bonding across the solid-liquid interface is manifested at polyamide surfaces (16, 17). Polyacrylamide, a model polymer with great affinity for water, shows slightly altered wetting properties, reflecting the presence of adsorbed moisture (18, 19); but this water does not mask the potential H-bonding contribution of the amide groups to adhesion. The wetting properties of a model polypeptide, polymethylglutamate, having various chain conformations show that the H-bonding functionality can be completely masked when certain polymer configurations and side chain arrangements occur, however (18). These concepts are applicable to complex protein molecules as demonstrated in recent surface chemical investigations of collagen and its denatured product, gelatin (16, 20).

Recognition of the role of surface forces in biological adhesion is exemplified in studies of cell-to-cell adhesion (21, 22), and cell-to-foreign surface adhesion (23, 24). Potential correlations of biological interactions with critical surface tension (γ_c) are found in results from tissue culture observations (25), blood contact studies (26, 27), and cell filtration through prepared bead columns (23). The major influence of adsorbed films has been indicated (3, 28). There is growing evidence for "conditioning" films of adsorbed protein as a prerequisite for cell adhesion to foreign surfaces (29, 30, 31, 32). The often overlooked role of adventitious surface-active adhesion modifiers has been brought out (3, 19), and attention directed to the potential utility of deliberately applied surface-active species as coupling agents for biological joints (13, 33). One class of such agents might be used to displace or react with the water already present at biological surfaces (33). Despite the apparently direct carry-over of current knowledge of adhesion to biomedical problems, a number of complications still exist. Among these are disputed theoretical objections, which suggest stable adhesion even in the absence of intimate molecular contact (34), and consideration of the auxiliary role of metabolic processes (35).

Even in the presence of such difficulties, contact angle studies provide a useful body of required data on the wettability and reactivity of materials of biological interest. The critical surface tension concept, as used here, has been amply validated during two decades of its application to well-defined organic polymers. Major influences of surface chemical constitution and of the presence of adsorbed species are admirably reflected in the γ_c parameter. For example, the results reported here indicate that fully hydrated vessel interfaces have general surface characteristics of poor wettability by most organic substances but easy penetrability

Figure 1

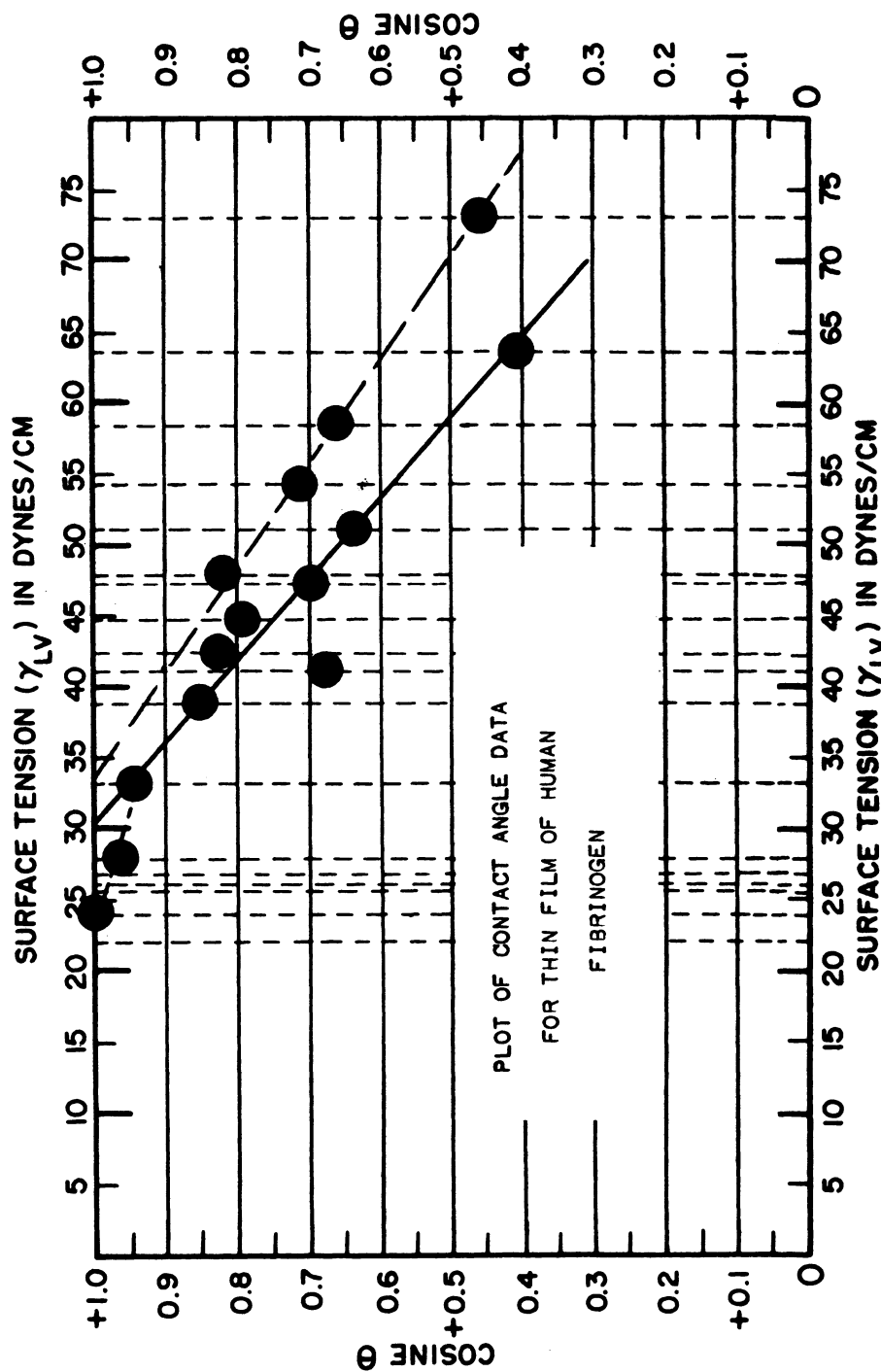
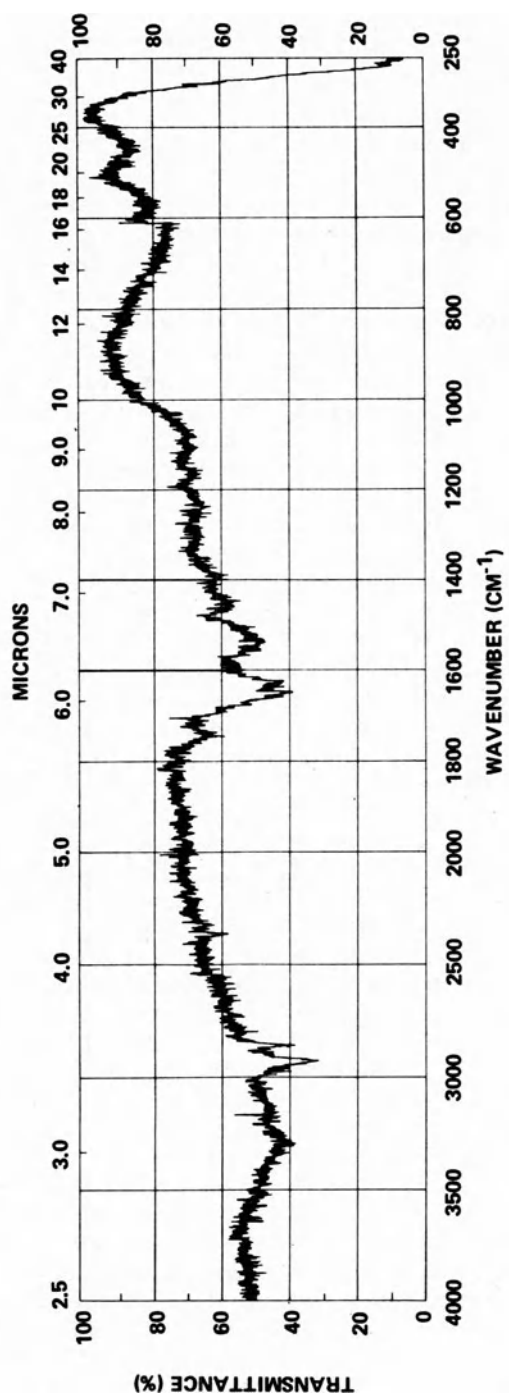


Figure 2



BLOOD VESSEL INTIMA - MAIR

by H-bonding substances. Our results also indicate the importance of adsorbed protein films and of low-energy surfaces in determining thromboresistance.

"WETTABILITY" OF BLOOD VESSEL WALLS

There have been clear disagreements among both Western (36, 37, 38) and Russian publications (39, 40) about the "wettability" of vessel endothelium and its influence on the state of fluidity of blood. There is general agreement, however, that knowledge of the actual surface properties of the inner walls of natural blood conduits would prove valuable in our attempts to mimic nature by providing synthetic nonthrombogenic flow channels. We used contact angle measurements and MAIR (multiple attenuated internal reflection) infrared spectroscopy of excised veins as initial methods to partially reveal their surface chemical makeup.

The type of data produced by these techniques may be judged from Figures 1 and 2. Figure 1 is a plot of contact angle data obtained with a film of human fibrinogen (Fisher Scientific, Purified Fraction F1, Human Fibrinogen Powder), and represents as complex a situation as commonly encountered with biological surfaces. The solid line through the data points (plotted as cosine of the average contact angle Θ versus surface tension of the liquid used γ_{LV}) represents a reasonable trend for the liquids which show stable equilibrium advancing contact angles on the protein surface. These liquids are primarily halogenated organics. The upper dashed line suggests a separate trend for polar, penetrable hydrogen-bonding liquids such as water and glycols. Failure of the H-bonding liquids to cluster more closely about the line drawn through the nonpenetrable, organic liquid data generally indicates the availability of some H-bonding sites in the surface under study (16, 17, 18, 41). The lower dashed line at the upper left of Figure 1 shows the anomalous incomplete spreading for low surface tension hydrocarbon liquids associated with the presence of adsorbed water on the surface being studied (13, 14, 15, 16, 19). In any case, the line drawn through the most reliable data points, when plotted in this format, is used to extrapolate to an intercept with the $\cos \Theta = 1$ axis. This intercept is then defined as the approximate critical surface tension (γ_c) for the surface under investigation. This plot for human fibrinogen has been used to illustrate the maximum scatter of data which must be tolerated; it also serves to illustrate that the estimated critical surface tension for purified fibrinogen films is in the range between 30 and 35 dynes/cm. An even higher γ_c value had been found with bovine fibrinogen (29), although the infrared spectra of human fibrinogen films were essentially the same as that published for bovine fibrinogen samples (29). So, in addition to serving an illustrative role, Figure 1 (together with the previous published data (29)) shows that

critical surface tensions reported below for the vessel intima -- which are substantially lower -- are not artifactually influenced by adsorbed fibrinogen layers masking the actual intimal surfaces.

Figure 2 is the MAIR infrared spectrum typical of the inside surfaces of excised, thoroughly rinsed (in physiologic saline), and dried jugular veins. This spectrum is excellent in quality, and shows that the vessel intimal surface, selectively analyzed to only a micron or so in depth, is definitely proteinaceous in composition. Spectral evidence for mucopolysaccharides in this outermost layer is scant. The strong absorption bands at about 2900 cm^{-1} and 1750 cm^{-1} in Figure 2 are associated with hydrocarbon content and ester components, respectively. These bands show unambiguously that the vessel intima is abundantly supplied with lipids, probably admixed and associated with the protein components. Long chain fatty acids, for instance, are molecules which show specifically similar infrared spectra.

Knowing that fatty acids and other lipids are surface-active compounds, and preferentially orient at interfaces to mask higher-energy protein sites while exposing their own low-energy CH_3 and CH_2 groups, this spectrum prompts the suggestion that the inside walls of blood veins are dominated by outermost layers of lipid -- most likely tightly bound to protein -- and have an intrinsically low surface energy. The critical surface tension range for variously packed fatty acid films runs from about 22 to 28 dynes/cm.

Figure 3 is a simplified plot of the wetting data obtained for these excised jugular vein segments, as laid open and dried into flat sheets on glass slides. The trend line drawn from data taken at 50% relative humidity is an average through both polar H-bonding and non-H-bonding liquids. The low critical surface tension intercept, between 25 and 30 dynes/cm, is certainly consistent with the postulate that hydrocarbons dominate the surface constitution of the intimal surfaces. In an attempt to approach more realistic conditions, these flattened veins were allowed to swell completely by imbibing distilled water from a pool placed around the periphery of each sample. The line on Figure 3 labeled "water swollen" represents the trend of only the halogenated organic wetting liquids, since the water compatible liquids penetrated the swollen, hydrated surface immediately. The shift of the apparent critical surface tension intercept to a value near 32 dynes/cm is completely compatible with a conversion of this surface to one dominated by an adsorbed water film (13, 14, 15).

As a further approach to a realistic assessment of the "wettability" of blood veins *in situ*, experiments with living animals were undertaken. Anesthetized dogs were subjected to a midline laparotomy, their superior mesenteric veins exposed and cannulated, and long venous branches were completely flushed free of blood

Figure 3

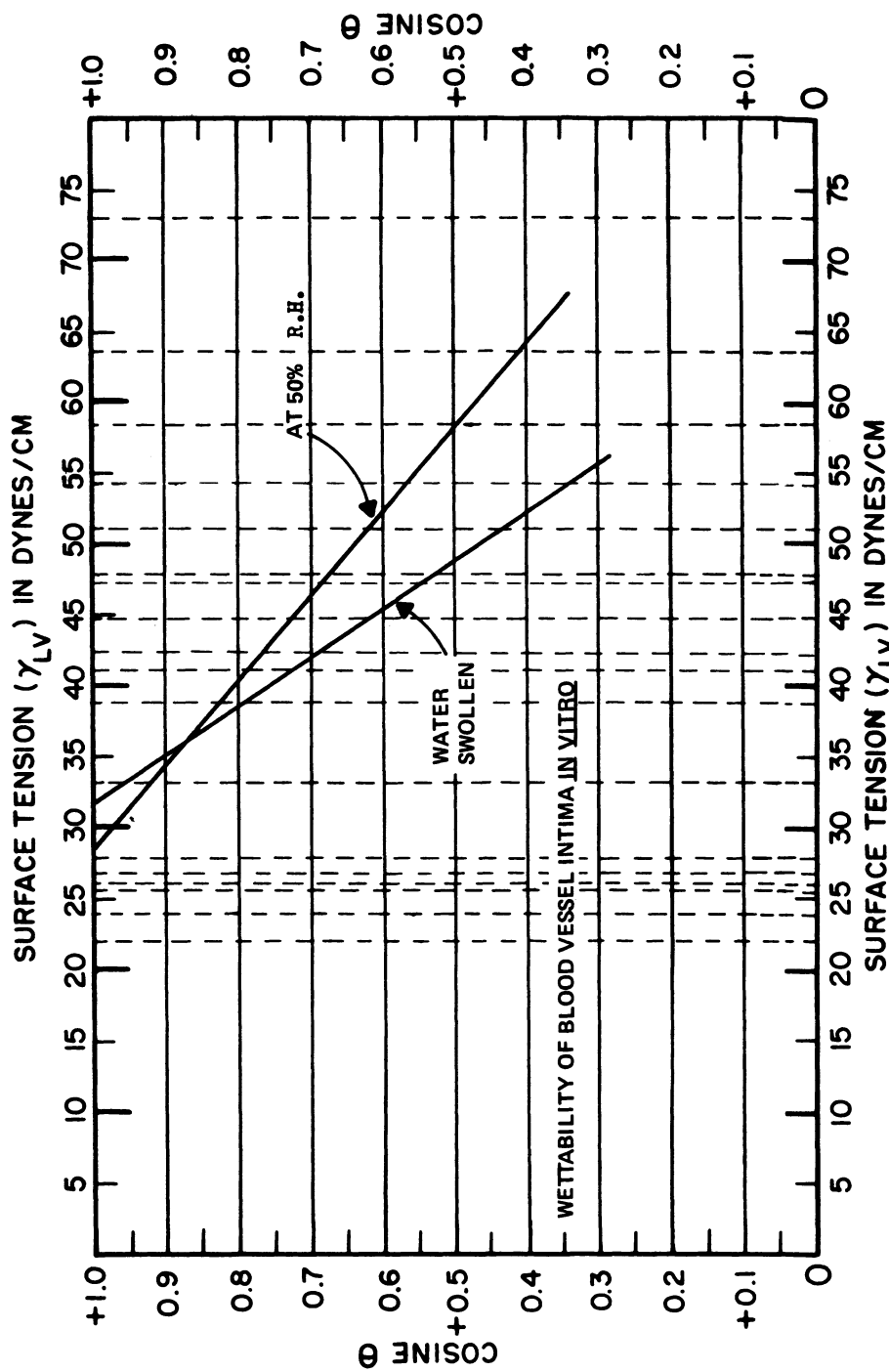
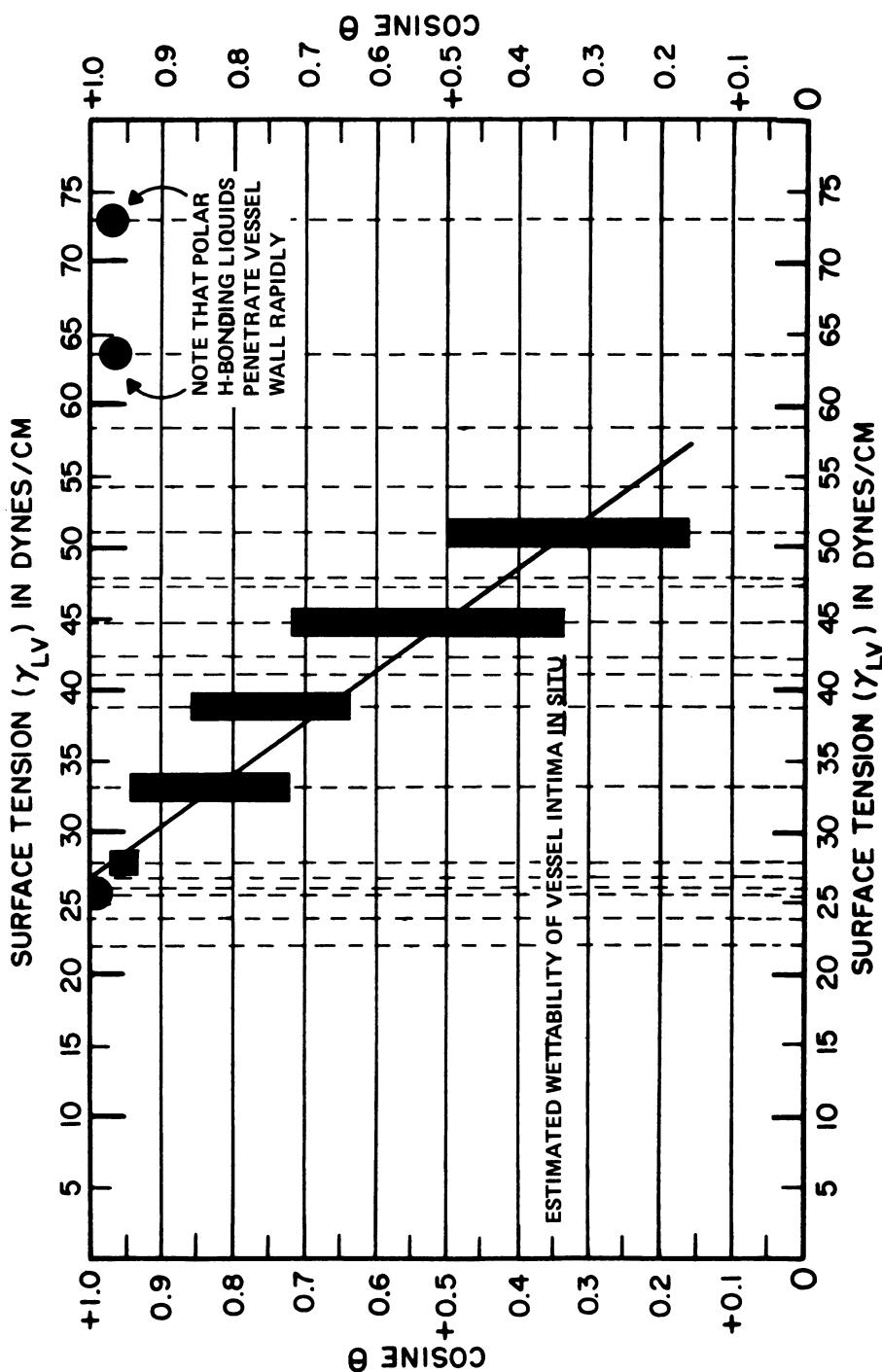


Figure 4



with physiologic saline. Various wetting liquids representing a range of structural types and surface tensions were then injected into the veins. Purposely formed air bubbles in these liquid trains were then microphotographed, and the contact angles at the vein/liquid/air interfaces determined from the photography. Table 1 lists the liquids used, their approximate surface tensions, the estimated contact angles observed, and Figure 4 is a graph of these data. It should be noted that the results are similar to those from veins *in vitro* in the sense that water miscible liquids exhibited very low contact angles -- correlated with their ready penetrability of the hydrated vessel walls -- while non-interacting organics showed a regular progression of decreasing contact angles in accord with their surface tensions. Again, a critical surface tension intercept between 25 and 30 dynes/cm is the best inference from the data and this range correlates well with surface layers dominated by hydrocarbon components.

Our conclusion from these contact angle measurements and from these MAIR infrared analyses is that the blood vessel intima is an intrinsically low-surface-energy lipoprotein lining with an outermost layer of predominantly hydrocarbon composition.

A natural corollary is that damage to this surface layer would expose the higher-energy protein matrix beneath it and result in spontaneous intravascular thrombosis. A further corollary is that adsorption of circulating components to the intima, resulting in increased surface energy, would also carry an increased probability for thrombogenesis.

Table 1
APPROXIMATE CONTACT ANGLES FOR VARIOUS
AIR/LIQUID INTERFACES PRODUCED IN VEINS

LIQUIDS AND THEIR APPROXIMATE SURFACE TENSIONS (IN DYNES/CM)	ESTIMATED CONTACT ANGLE RANGE OBSERVED (IN DEGREES)
NORMAL SALINE	73
GLYCEROL	63
METHYLENE IODIDE	50
1-BROMONAPHTHALENE	44
1-METHYLNAPHTHALENE	38
ISOPROPYLBIPHENYL	33
MINERAL OIL	27
DODECANE	25
	10 - 15
	10 - 15
	60 - 80
	45 - 70
	30 - 50
	20 - 45
	15 - 20
	0 - 10

THE ROLE OF A LOW-SURFACE-ENERGY HYDROCARBON COMPOUND IN DETERMINING THROMBORESISTANCE OF STELLITE 21

There is no obvious reason why Stellite 21 should be intrinsically more thromboresistant than any other metallic alloy, pure metal, or metal oxide. Stellite is simply an alloy of cobalt, chromium, and tungsten -- metals which themselves have shown no thromboresistant character -- which is very hard, brittle, and takes a high polish.

Indeed, metallographically-polished, organic-free Stellite 21 plates and rings show surface properties, as judged from contact angle experiments at high and low relative humidities, identical to those of other high energy materials including many metals and glasses (13, 14, 15). It is no surprise, then, that Stellite prostheses with these surface properties are as adversely thrombogenic as other metallic implants.

Yet, Stellite 21 struts and valve seats used in replacement heart valves admittedly show excellent resistance to thrombus formation, and other metals do not. Our measurements on a Starr-Edwards heart valve, removed after a considerable period of human implantation, were the first to show that the Stellite portions of this prosthetic implant had a remarkably low-energy surface. It was immediately suggested, and later confirmed in discussions with the manufacturer, that this low-surface-energy reflected the attachment to the metal of organic contaminants from a hydrocarbon-based final polishing compound. We have since examined other Stellite surfaces, notably those on the pins and valve seat of the Schimert-Cutter experimental heart valve, and found them to be similarly organic-coated (although not having quite as low critical surface tensions). The common "tallow" additives in commercial polishing agents are simple mixtures of stearic and palmitic acids (long chain fatty compounds).

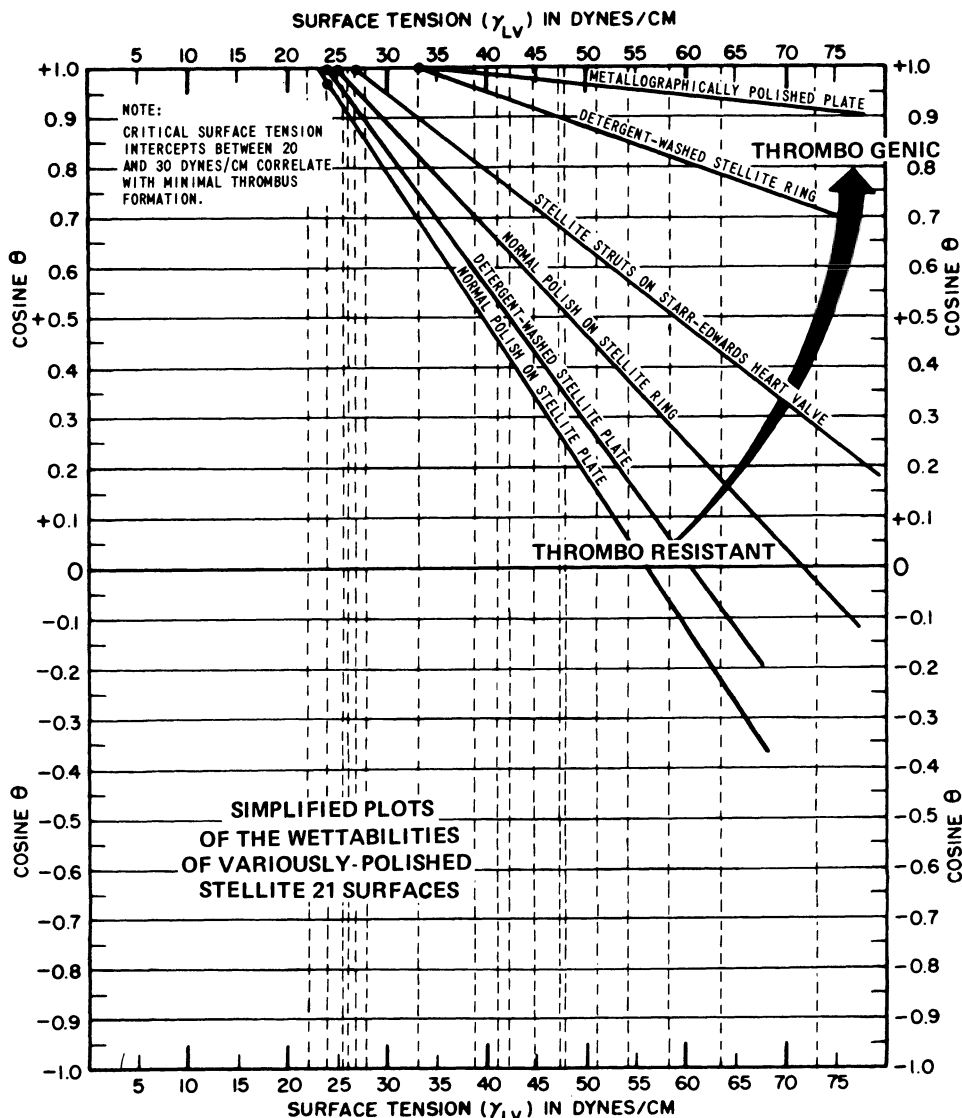
The surface chemistry of such fatty acids is well-known, and the ready arrangement of these molecules into closepacked surface layers during polishing explains the low-energy character of surfaces polished in their presence. Thus, the outermost surface constitution of thromboresistant Stellite 21 is not metallic at all but, rather, consists of closely packed methyl groups of the organic compounds present during the final polishing steps.

We have extensively investigated the surface properties of Stellite plates and rings to better define the role of this adventitious contaminant in determining the blood compatibility of the material as used in prosthetic devices. These are our conclusions:

Table 2
Contact Angles of Various Pure Liquids on Modified Stellite Surfaces

Wetting Liquid and Surface Tension (γ_{LV}) at 20°C, dynes/cm	(a) Stellite Plate Normal Polish Distilled Water	(b) Same After Vigorous Detergent Wash	(c) Same After Vigorous Detergent-Edwards Cage Of Cages	(d) Stellite 21 Ring Normal Polish	(e) Same After Implan-tation And Detergent Wash	(f) Stellite 21 Ring Poorly Organic Coated	(g) Same After Implan-tation And Adsorption Of Protein	(h) Same After Vigorous Detergent-Wash	(i) Stellite 21 Ring Only Partially Organic Coated	(j) Same After Vigorous Detergent And Adsorption Of Protein	(k) Same After Vigorous Detergent Wash
Water	72.8	104	101	73	91	43	93	39	5	68	48
Glycerol	63.4	102	--	--	--	--	--	--	--	--	--
Formamide	58.2	98	--	--	--	--	--	--	--	--	--
Thiodiglycol	54.0	81	80	61	79	37	79	32	5	43	32
Methylene Iodide	50.8	67	63	54	59	32	59	44	34	32	48
Sym-Tetrabromoethane	47.5	66	--	--	--	--	--	--	--	--	--
1-Bromonaphthalene	44.6	62	55	41	54	21	53	35	26	28	37
0-DiBromobenzene	42.0	57	--	--	--	--	--	--	--	--	--
1-Methylnaphthalene	38.7	55	48	31	46	8	48	30	18	19	26
Dicyclohexyl	33.0	45	37	15	29	0	35	16	0	0	15
Hexadecane	27.7	36	30	--	18	0	27	8	0	0	12
Tetradecane	26.7	32	27	--	0	--	--	0	0	0	0
Tridecane	25.9	28	24	--	0	--	--	0	0	0	0
Dodecane	25.4	26	23	--	0	--	--	0	0	0	0
Decane	23.9	14	12	6	0	0	0	0	0	0	0

Figure 5



- (1) Thromboresistant Stellite has an organic, low-surface-energy material as its outermost layer, most likely a long-chain fatty acid, as revealed by both contact angle measurements and MAIR infrared surface spectroscopy.
- (2) On thromboresistant Stellite, and not on other metals tested or thrombogenic Stellite, this layer is tenaciously bonded. This has been demonstrated by surface quality checks after a series of increasingly stringent cleaning techniques ranging from distilled water rinsing through detergent scrubbing to mechanical abrasion.
- (3) Implantation experiments have shown that only surfaces having strongly-bonded low-energy layers are significantly thromboresistant. Incompletely coated surfaces, or weakly-bound coatings, are less thromboresistant.
- (4) Experiments with polished and unpolished plastic surfaces have shown that the influence of surface roughness on the above results is relatively minor.

EXPERIMENTAL DATA supporting these conclusions follows.

Table 2 is a compilation of the average contact angles measured for a number of highly purified liquids placed on variously polished and cleaned Stellite parts. Figure 5 illustrates simplified plots of these data in the Zisman format (as cosines of the contact angles versus liquid-vapor surface tensions for the liquids (1)) which allows determination of approximate critical surface tensions for the materials in question.

Column (a) of Table 2 records the wetting data for a plate of Stellite, polished exactly as valve cages and vena cava rings -- which showed excellent thromboresistance -- had been polished routinely. The very high contact angles for all liquids on this surface show unambiguously that an organic coating, most likely exposing closepacked methyl groups, completely masks the metallic surface. Infrared spectra of this surface, obtained by pressing it tightly against an internal reflection element and using MAIR (multiple attenuated internal reflection) accessories (4), confirmed the presence of a hydrocarbon component in the outermost surface layer. Extensive, and prolonged, distilled water rinsing of this surface did not change the contact angles obtained.

Column (b) of the table records the slightly lower contact angle values obtained after a vigorous detergent washing of the plate. The observation that the wetting was not significantly changed illustrates the firmness with which the organic layer was bound. Further scrubbing of the plate with a hard brush and detergent further lowered the contact angles, but only mechanical

erosion (using an organic-free abrasive) or direct flaming of the surface could completely restore the metallic (i. e. high energy) nature of the surface.

Column (c) records the contact angles on the polished Stellite cage of a Starr-Edwards heart valve which had been implanted and then detergent-washed just before the measurements were made. The fact that these contact angles were lower than those on similarly washed, non-implanted Stellite plates suggests that during removal of the adsorbed protein films (formed during implantation) some of the organic coating was also stripped from the surface. The fact that the critical surface tension of these struts was still very low, between 20 and 30 dynes/cm, even after such stripping indicates that the organic layer was strongly-bound and present in considerable quantity.

Columns (d) and (e) confirm these suppositions by comparing the results on a polished Stellite 21 vena cava ring -- which proved to be significantly thromboresistant when implanted -- and that same ring after implantation and after vigorous scrubbing with a strong detergent and hard-bristle test tube brush. The data in column (e), including a water contact angle greater than 40°, clearly indicate the presence of residual organic material. Rings with this little organic coverage did not prove thromboresistant when reimplanted, but were not as thrombogenic as rings made completely organic-free by flaming.

The last two groups of data in Table 2, comprising columns (f), (g) and (h) and columns (i), (j) and (k), illustrate the surface modification of Stellite rings by adsorbed protein films in vivo and the reason for the ineffectiveness of poorly organic-coated Stellite rings for preventing thrombus formation. Comparison of the contact angle values obtained after detergent washing of both sets of rings (see columns (h) and (k)) with values from thromboresistant rings similarly treated (see column (e)) shows clearly that the organic coating on both sets of rings was extremely labile. It did not survive -- certainly not long enough to influence thrombus formation -- the autoclaving, implantation, and cleaning steps. It is appropriate to recall here the 1968 study of Dutton and co-workers, who showed that monolayer organic coatings on glass and silicone substrates -- although sufficient to completely change the initial wetting properties of these surfaces -- were not sufficient in quantity nor strongly enough bound to influence thrombus formation on these substrates (42).

Nonthromboresistant Stellite surfaces also accumulated similar protein films by adsorption (compare columns (g) and (j)), as is evident in the infrared spectra of these protein films, given as Figure 6.

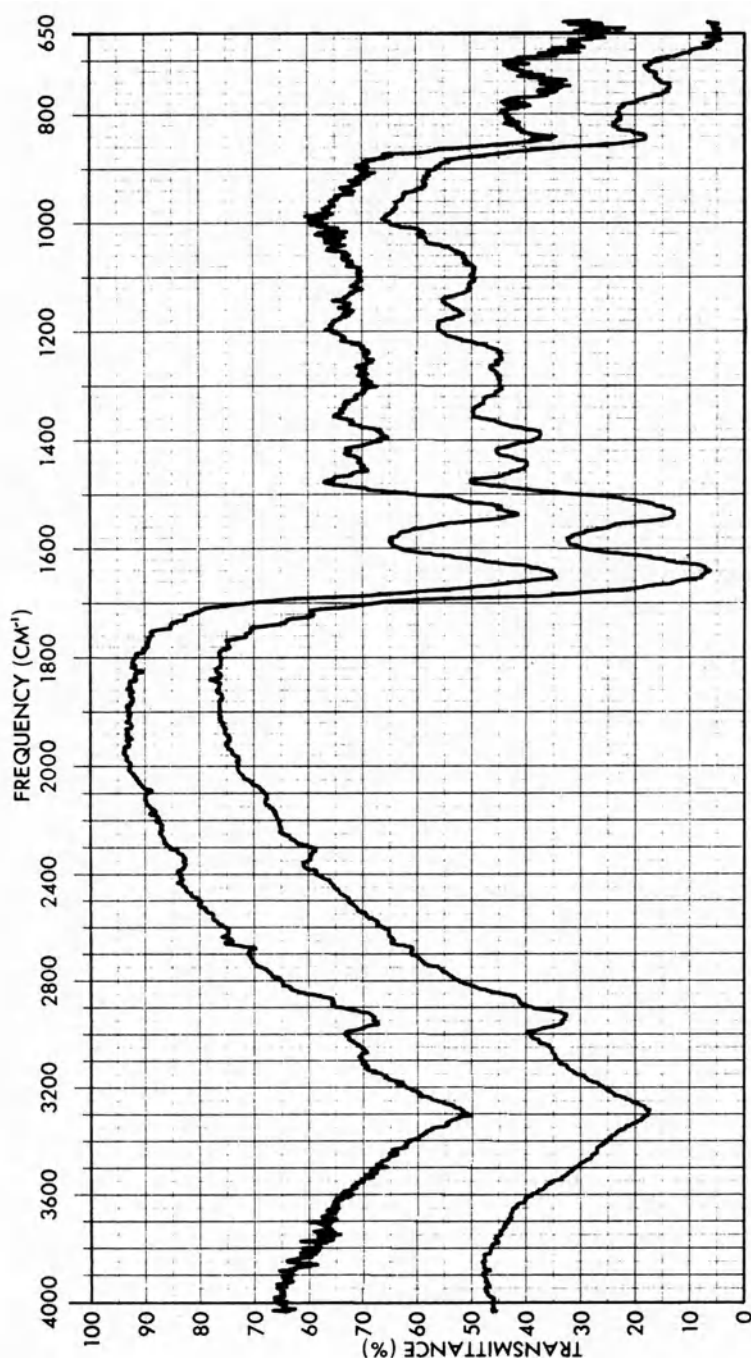


Figure 7

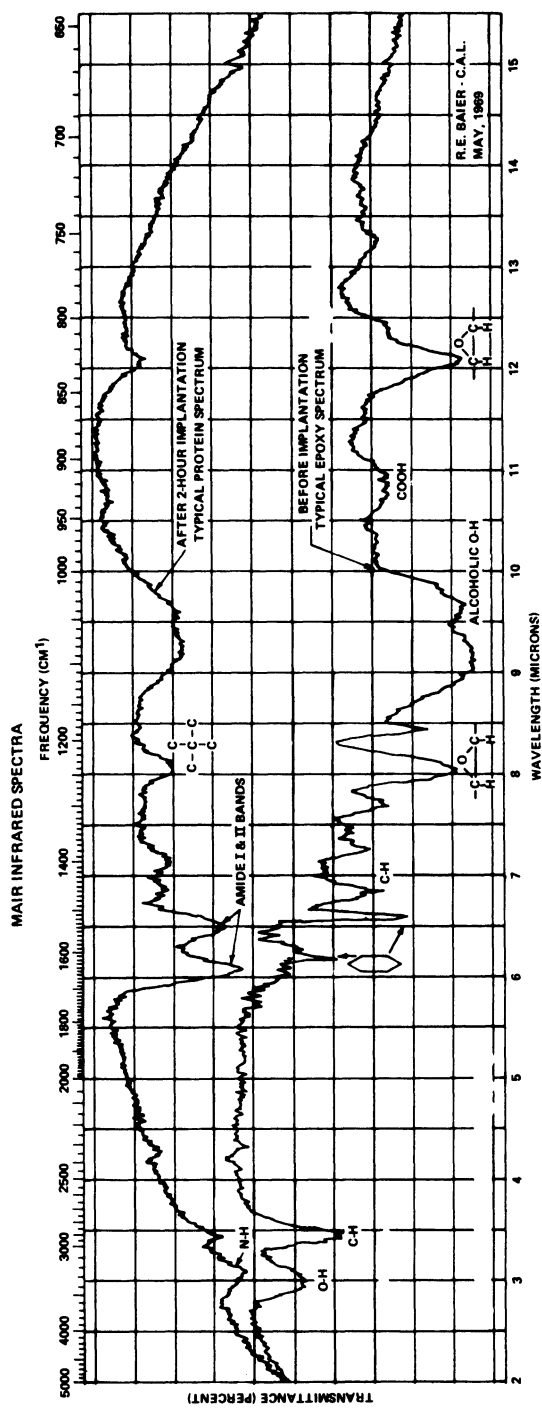
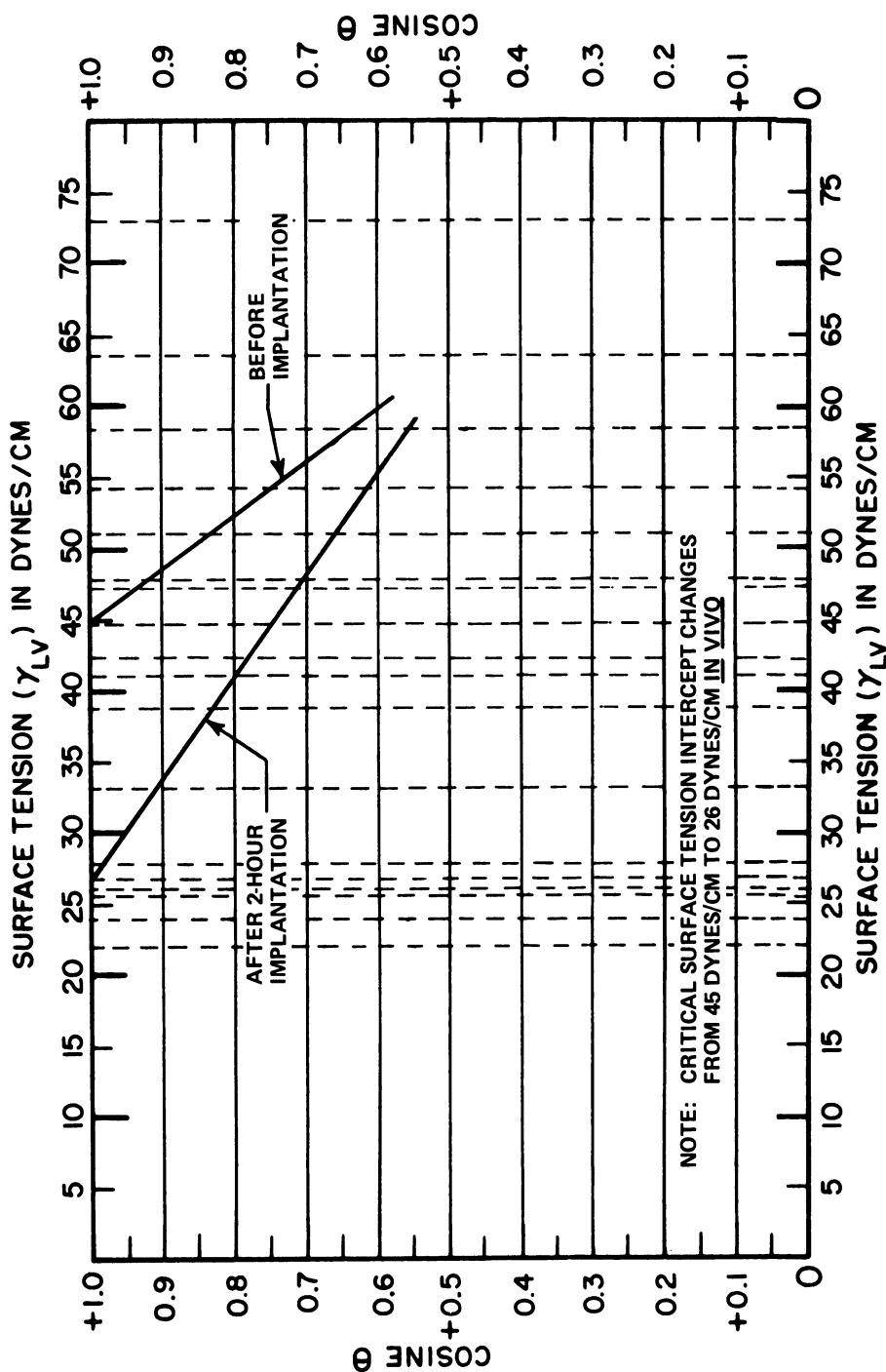


Figure 8



Concurrently with the above-described experiments, investigations of polished and unpolished vena cava rings of Lexan (polycarbonate) were undertaken. These latter studies produced erratic results but, nonetheless, allowed an assessment of the influence of surface roughness on the properties of Stellite specimens. Our most recent experimental series showed that unpolished, visually rougher-surfaced Lexan rings were not detectably more thrombogenic than polished specimens having the same chemical makeup (as shown by both contact angles and infrared spectra). Therefore, it seems safe to conclude that the thromboresistance which has been empirically attributed to polished Stellite is not simply due to the enhanced surface smoothness of the polished specimens.

OTHER CANDIDATE BIOMEDICAL MATERIALS

We are now conducting an investigation of surface properties of new, potentially thromboresistant biomaterials. This study includes in vivo evaluations of implanted rings whose critical surface tensions (γ_c) have previously been determined from the contact angles of specially calibrated liquids on their surfaces. Surface chemical constitution of each material is verified through sensitive surface spectroscopy which utilizes the MAIR (multiple attenuated internal reflection) infrared technique. The materials are re-analyzed after implantation to determine those surface changes, particularly the adsorption of proteinaceous films, which reflect the relative thrombogenecity of the materials in vivo.

Various plastic vena cava rings have been studied. Enough data has been gathered to allow some cautious generalizations to be drawn about the change in the materials' surface properties which occurs during implantation. We hope to correlate the nature of this change with the biocompatibility of the various materials.

Our initial generalizations are these:

- (1) During implantation, all materials rapidly adsorb a tenaciously adherent coating of protein.
- (2) On most materials, this adsorbed protein layer substantially changes the critical surface tension, to higher values for initially low-energy surfaces and to lower values for initially high-energy surfaces.
- (3) Since there are obvious differences in the thrombogenecity of the various materials, and also differences in the wetting data and infrared spectra for the adsorbed films which form on them, the relation connecting the

structure and properties of these absorbed layers with the in vivo test results requires additional investigation.

- (4) Although strongly-bound low-energy surface layers of hydrocarbon composition appear to correlate with the natural thromboresistance of blood vessels and with the observed thromboresistance of commercially polished Stellite, such an initial layer may be neither necessary nor sufficient for imparting thromboresistance to other materials. Relatively high-energy surfaces of some polymers, for example, might be capable of adsorbing components from blood which convert their surfaces to low-energy character and thence become nonthrombogenic.

As an illustration of the type of results being achieved, data for epoxy rings before and after implantation are included as Figures 7 and 8. Figure 7 shows the shift in surface infrared spectrum caused during implantation, and Figure 8 shows the concomitant wettability change accompanying the deposition of the protein film.

Presentation of further results, and specific examples of other new materials, must be postponed until a later time.

DISCUSSION

Our experimental findings are summarized in tabular form as Table 3. We have concluded that the final polish normally given to Stellite, using a polish containing a waxy additive, leaves a hydrocarbon component strongly bound in the outermost metallic layers. This coating imparts a very low wettability to the finished surface. Since Stellite parts polished in the absence of waxy materials, as well as those flamed or lightly abraded after the normal polish, do not resist thrombus formation when in contact with blood, we suggest that the presence of the hydrocarbon materials, when tightly bound or when "lapped" into the surface layers, contributes to the thromboresistance of the normally polished Stellite primarily by providing a semi-permanently decreased critical surface tension. Low critical surface tension is also a feature of naturally thromboresistant blood vessel walls.

The critical surface tension of about 25 dynes/cm for vessel intima and polished Stellite indicates that their surfaces are predominantly composed of methyl groups (43, 44). Critical surface tensions much above 30 dynes/cm, for nonheparinized materials, are not compatible with obtaining significant thromboresistance. Clean metals and metal oxides, including Stellite, generally show very small contact angles, approaching zero in most cases, for the

liquids used here, and these surfaces are known to be thrombogenic. Metals other than Stellite (titanium, for example) do not acquire as strongly-bound organic layers during polishing and do not show significant thromboresistance. On polished titanium, very low contact angles are obtained after detergent-washing, suggesting that the hydrocarbon component is easily removed. During polishing then, the Stellite traps more wax in its surface than other metals do; this hydrocarbon material may be available to replenish the surface from a considerable depth. Alternatively, the mechanism of hydrocarbon fixation may be the formation of a metallic soap between components of the alloy, notably chromium, and fatty acids from the polishing agent. This is an example of how the specific composition and bulk properties of materials can influence their final surface properties. In the case of Stellite, the alloy's extreme hardness dictates a rigorous polishing process, and thus favors strong binding of hydrocarbon.

The Zisman plot (see Figure 5) of data obtained from contact angle measurements on Stellite struts of a Heart Valve cage is most interesting. This valve had actually been implanted, washed clean, handled by many people as a laboratory specimen, and washed with concentrated detergent solution and a soft brush, followed by copious rinsing with distilled water and air-drying, before contact angles were measured. The critical surface tension intercept of about 25 dynes/cm and the generally large contact angles for the liquids used, even after this rather lengthy handling and cleaning, guarantee that the surface of the valve cage as implanted was of very low wettability.

As a demonstration of the longevity of the hydrocarbon embedded in the Stellite surface layers, experiments with Stellite plates are cited in Table 2. The wetting results on a freshly polished plate, rinsed only with distilled water before measurements were made, and of the same plate after a vigorous wash with concentrated detergent and a soft brush are comparable. Gentle hand-stroking of the plates over a Fisher Gamal-B polishing cloth coated with Linde gamma-alumina (0.3 micron), following by copious rinsing with distilled water, did not visually modify the surface finish but did abrade enough material from the plate to make it wettable (i.e. have contact angles of about 5° or less) with most liquids used in this investigation. This indicates that removal of the first few layers of material from the plate surface is sufficient to change that surface from one of low surface energy to one of high surface energy.

When a freshly polished Stellite plate was briefly exposed to a stream of flowing blood followed by copious rinsing first with physiologic saline and then distilled water, it was obvious that a very thin surface film was deposited on the surface, as could be seen by viewing the plate in glancing reflected light. The film was

Table 3

SUMMARY OF FINDINGS

MATERIAL	THROMBORESISTANCE	RELATIVE SURFACE ENERGY	RELATIVE RESISTANCE OF SURFACE LAYER TO EROSION
LEXAN POLYCARBONATE	POOR	HIGH	HIGH
OTHER ORGANIC-FREE METALS	POOR	HIGH	HIGH
ORGANIC-FREE STELLITE	POOR	HIGH	HIGH
"TALLOW-COATED" STELLITE	POOR	LOW	LOW
"TALLOW-POLISHED" STELLITE	GOOD	LOW	HIGH
BLOOD VESSEL INTIMA	GOOD	LOW	HIGH

identified as predominantly proteinaceous in character from infrared spectra obtained using multiple internal reflection techniques. Similarly, protein films were formed spontaneously on the surfaces of implanted Stellite vena cava rings. The initially adsorbed protein films adhered rapidly and tenaciously. After vigorous washing of the filmed surfaces with hot concentrated detergent and a hard brush, all trace of the film was removed, as judged by visual inspection, contact angle measurements, and by infrared spectroscopy.

Since the hydrocarbon component is also eventually removed by washing and slight wear, exposure of the high-energy metal surface gradually occurs. This limitation should also apply to the thromboresistance of the surface.

The most plausible explanation for the favorable biocompatibility of polished Stellite, then, is its low surface energy, as reflected in a low critical surface tension. Although it is known that blood proteins and formed elements (platelets, in the main) do adhere to low energy materials (27, 29, 45), the work of adhesion to distract them is substantially less than that necessary to detach them from higher-energy surfaces (2). Rapid, and turbulent, flow regimes (such as are indeed present with an implanted heart valve) would provide the best conditions for detaching small aggregates from low energy surfaces, and allow them to flow downstream where they could be eliminated by enzymatic and other digestive processes. Thus, it is by no means certain, that synthetic low energy surfaces are intrinsically nonthrombogenic. Rather, they may in fact induce thrombus formation but -- because of the diminished strength of adhesion to low energy surfaces -- allow easier removal of growing thrombic masses before they can impair the action of the prosthetic implant. But the apparently intrinsic low-surface-energy coating of natural blood conduits favors the hypothesis that such surface features are closely correlated with thromboresistance.

Additional study of the mechanism of this action is deserved. Substantive low energy coatings can be provided on other materials which must contact the blood. If such surfaces prove to be as thromboresistant as polished Stellite, other plastic and metal components can be deliberately fabricated to include a surface layer of low critical surface tension, preferably renewable by diffusion from the bulk. Some polymeric materials with diffusible low-energy surfactants have already been created (19).

Table 3 indicates the guidelines for future work. Good thromboresistance correlates best with low-energy surfaces having a high resistance to erosion.

REFERENCES

1. Zisman, W. A. (1964). Advances in Chemistry Series 43, pp 1-51, American Chemical Society, Wash. D. C.
2. Baier, R. E., Shafrin, E. G., and Zisman, W. A. (1968). Science 162:1360.
3. Baier, R. E., "Surface Properties Influencing Biological Adhesion", Chapter 2 in Adhesion in Biological Systems (R. L. Manly, Ed.), Academic Press, in press.
4. Harrick, N. J. (1967). "Internal Reflection Spectroscopy", Interscience Publishers, New York.
5. Zisman, W. A. (1962). In "Symposium on Adhesion and Cohesion", (P. Weiss, Ed.), Elsevier, New York.
6. Langmuir, I. (1916). J. Am. Chem. Soc. 38:2286.
7. Langmuir, I. (1925). In "Third Colloid Symposium Monograph", pp 48-75, New York, Chem. Catalogue Co., Inc
8. Budgett, H. M. (1911). Proc. Roy. Soc. A86:25.
9. Henniker, J. C. (1949). Rev. Mod. Phys. 21:322.
10. Zisman, W. A. (1961). "Constitution Effects on Adhesion and Abhesion", Naval Research Laboratory Report No. 5699.
11. Weiss, L. (1960). Int. Rev. Cytology 9:187.
12. Shafrin, E. G. (1967). In "Polymer Handbook", (J. Brandrup and F. H. Immergut, Eds.) pp 111-113, Interscience, N. Y.
13. Shafrin, E. G., and Zisman, W. A. (1967). Journal of the American Ceramic Society 50:478.
14. Bennett, M. K., and Zisman, W. A. (1968). J. Colloid Interface Sci. 28:243.
15. Bennett, M. K., and Zisman, W. A. (1969). J. Colloid Interface Sci. 29:413.
16. Baier, R. E., and Zisman, W. A. (1967). "Critical Surface Tension of Wetting for Protein Analogues", Presented at American Chemical Society, 153rd National Meeting, Miami Beach.

17. Baier, R. E., and Zisman, W. A. (1968). "Wettability and MAIR Infrared Spectroscopy of Solvent-Cast Thin Films of Polyamides and Polypeptides", Naval Research Laboratory Report No. 6755.
18. Baier, R. E. and Zisman, W. A., "The Influence of Polymer Conformation on the Surface Properties of Polymethylglutamate", Submitted for publication.
19. Jarvis, N. L., Fox, R. B., and Zisman, W. A. (1964). Adv. In Chem. 43:317, American Chem. Soc., Wash., D.C.
20. Baier, R. E. and Zisman, W. A., "Wetting Properties of Collagen and Gelatin", In preparation.
21. Weiss, L. (1967). "The Cell Periphery, Metastasis, and Other Contact Phenomena", Amsterdam:North-Holland Publishing Co.
22. Weiss, L. (1968). Exp. Cell. Res. 51:609.
23. Weiss, L., and Blumenson, L. F. (1967). J. Cell. Physiol. 70:23.
24. Taylor, A. C. (1962). In "Biological Interactions in Normal and Neoplastic Growth", (Ed. by M. J. Brennan and W. L. Simpson), pp 169-182, Little, Brown, and Co., Boston, Mass.
25. Taylor, A. C. (1961). Exp. Cell Res. Suppl. 8:154.
26. Brash, J. L. and Lyman, D. J. (1969). J. Biomedical Materials Res. 3:175.
27. Lyman, D. J., Muir, W. M., and Lee, I. J. (1965). Trans. Amer. Soc. Artif. Int. Organs 11:301.
28. Firich, F. R. (1969). In "Interface Conversion for Polymer Coatings", pp 350-373, (Ed. by P. Weiss and G. D. Cheever), American Elsevier Publishing Company, New York.
29. Baier, R. E., and Dutton, R. C. (1969). J. Biomedical Materials Res. 3:191.
30. Dutton, R. C., Webber, T. J., Johnson, S. A., and Baier, R. E. (1969). J. Biomedical Materials Res. 3:13.
31. Scarborough, D. F., Mason, R. G., Dalldorf, R. G., and Brinkhous, K. M. (1969). Lab. Invest. 20:164.

32. Vroman, L., and Adams, A. L. (1969). J. Biomedical Materials Res. 3:43.
33. Zisman, W. A. (1963). Industrial and Engineering Chemistry 55:19.
34. Curtis, A. S. G. (1962). Biol. Rev. 37:82.
35. Weiss, P. (1958). Int. Rev. Cytology 7:391.
36. Copley, A. L. (1960). In "Flow Properties of Blood and Other Biological Systems", (Ed. by A. L. Copley and G. Stainsby) pp 97-117, Pergamon Press, New York.
37. Moolten, S. F., Vroman, L., Vroman, G. M. S., and Goodman, B. (1949). Arch. Internal Med. 84:667.
38. Ratnoff, O. (1959). In "Connective Tissue, Thrombosis, and Atherosclerosis", (Ed., I. Page), Academic Press, N. Y.
39. Perel'man, I. B. (1965). Colloid J. (USSR) 27:422.
40. Zubairov, D. M., Repeikov, A. V., and Timberlaev, V. N. (1963). Fiziologicheskii Zhurnal SSSR 49:85.
41. Ellison, A. H., and Zisman, W. A. (1954). J. Phys. Chem. 58:503.
42. Dutton, R. C., Baier, R. E., Dedrick, R. L., and Bowman, R. L. (1968). Trans. Amer. Soc. Artif. Int. Organs 14:57.
43. Shafrin, E. G. and Zisman, W. A. (1957). J. Phys. Chem. 61:1046.
44. Shafrin, E. G. and Zisman, W. A. (1960). J. Phys. Chem. 64:519.
45. Lyman, D. J., Brash, J. L., Chaikin, S. W., Klein, K. G., and Carini, M. (1968). Trans. Amer. Soc. Artif. Int. Organs 14:250.

LIPID-PROTEIN ASSOCIATION IN LUNG SURFACTANT^{1,2}

Morton Galdston, M.D.

Associate Professor of Medicine
New York University School of Medicine
and
Dinesh O. Shah, Ph.D.

Surface Chemistry Laboratory, Marine Biology Division
Lamont-Doherty Geological Observatory of Columbia
University, Palisades, New York 10964

ABSTRACT

We investigated the nature of the lipid-protein association and the role of the protein moiety in a highly surface active lipoprotein fraction we isolated from cell-free rabbit lung wash and also compared the surface properties of dipalmitoyl lecithin, generally believed chiefly responsible for the surface properties of lung surfactant, with those of the lipoprotein fraction.

An increase in surface potential of monolayers of the lipoprotein fraction on calcium binding and a decrease in surface potential on enzymatic hydrolysis with phospholipase A suggest the polar groups of phospholipid are free to interact with Ca^{++} and phospholipase A and the lipid-protein association in the lipoprotein fraction is of the van der Waals type. Measurements of relative surface viscosity and of film state indicate the protein moiety presumably increases intermolecular spacing between lipid molecules in the lipoprotein fraction, helping to maintain films in the liquid state under high surface pressure. We observed distinct differences in surface properties of films of dipalmitoyl lecithin and of the lipoprotein fraction.

¹These investigations were supported by U.S.P.H.S. Grant No. HE 05256-10 (CVA) and by the National Science Foundation Grant No. GB-5273 and by the Sea Grants Program Administration Grant GH-16.

²Lamont-Doherty Geological Observatory Contribution No. 1405

INTRODUCTION

The surfactant lining of the alveolar air-liquid interface helps to stabilize the alveolar spaces, to prevent alveolar collapse at low lung volumes and to modulate the retractive force of lung (1). Lung surfactant is thought to consist of an insoluble lipoprotein layer, "lining film", and beneath this an extracellular saline dispersable lipoprotein, the "lining complex" or "alveolar surfactant", which acts as a reserve from which the "lining film" is formed (2). An extracellular layer corresponding to surfactant fixed *in situ* and independent of the external plasma membrane of the alveolar epithelial cells was recently identified by electronmicroscopy (3). Surfactant probably originates in the large alveolar (Type II) cells of the epithelial layer (4).

Though the chemical composition of lung surfactant is unknown the concensus is its high content of disaturated phosphatidyl choline chiefly accounts for its unique surface properties (5). Highly surface active lipoproteins (6, 7, 8), mixtures of phospholipids, neutral lipids and polysaccharides (9); and of lipids, predominantly phospholipids together with cholesterol and triglycerides (10) have been isolated from lung. The lipoprotein we isolated from rabbit lung wash was shown by immunologic techniques to come from lung and not from blood (8).

Our purpose herein is to present the current status of our investigations on the nature of the lipid-protein association and the role of the protein moiety in the lipoprotein fraction we isolated and to compare the surface properties of dipalmitoyl lecithin and of the lipoprotein fraction. The association between lipid and protein appears to be of the van der Waals type; the protein moiety helps maintain films of lung surfactant in the liquid state at high surface pressure; and the surface properties of dipalmitoyl lecithin and the lipoprotein fraction differ in many important respects.

METHODS

A highly surface active lipoprotein fraction, designated fraction B, was isolated from cell-free rabbit lung wash, designated stock 0, as previously described (8). The surface properties of these preparations, of the lipid extract (Folch method, 11) of the lipoprotein fraction and of chromatographically pure L- α -dipalmitoyl lecithin (Dajac Laboratories, Philadelphia, Pa.) were investigated by measurements of surface pressure and surface potential related to M^2/mg of material spread, using intermittent manual film compression.

To learn about the nature of the lipid-protein association in the lipoprotein fraction enzymatic hydrolysis by snake venom Naja naja phospholipase A and calcium binding were investigated. To learn about the role of the protein moiety in the lipoprotein fraction relative surface viscosity and physical state of films were investigated.

Surface pressure, the difference between the surface tension of a clean surface and a film-covered surface, was measured in a lucite trough, 400 cm² surface area, with paraffin-coated glass barriers, by the modified Wilhelmy plate method (12) with a sand-blasted rectangular platinum plate (26 guage and 5 cm perimeter), suspended from a torsion balance (500 mg maximum) mounted on an adjustable elevating stand (Fig. 1). Surface potential, which is related to surface molecular concentration and orientation, was measured with an ionizing (α -radiation air) electrode and a Ag-AgCl electrode connected to an electrometer (13) simultaneously with surface pressure (Fig. 1).

Relative surface viscosity, an index of film fluidity was measured by the canal method (ref. 12, p. 253) with a teflon bar containing a canal (0.1 cm wide, 2 cms. long) with a flood gate attached to its front, placed over the middle of the trough (Fig. 1). A monolayer was spread on the interface between the teflon bar and a paraffin-coated glass barrier used to compress the monolayer. Five minutes were allowed for the monolayer to spread, then it was compressed to arbitrarily selected levels of 8 and 30 dynes/cm.

The flood gate was then opened, allowing the monolayer to pass through the canal with surface pressure held constant by movement of the barrier toward the teflon bar. The time required for 1 cm² of a monolayer to pass through the canal on subsolutions of 0.02 M NaCl or 0.01 M CaCl₂ is designated t_{Na^+} or $t_{Ca^{++}}$, respectively. The average of at least five such measurements was taken at each surface pressure level. The ratio

$$\left(\frac{t_{Ca^{++}} - t_{Na^+}}{t_{Na^+}} \right) \times 100$$

is the percent increase in time due to binding of calcium to monolayers (13) and indicates the increase in relative surface viscosity.

The state of a film was studied by gently blowing air with a bellows on talc previously sprinkled on the film (14). If the talc moves freely the film is in the liquid state, if very little or not at all, in the gel or solid state, respectively.

Films of stock 0, the cell-free preparation of rabbit lung wash, and of its lipoprotein fraction were spread from solutions

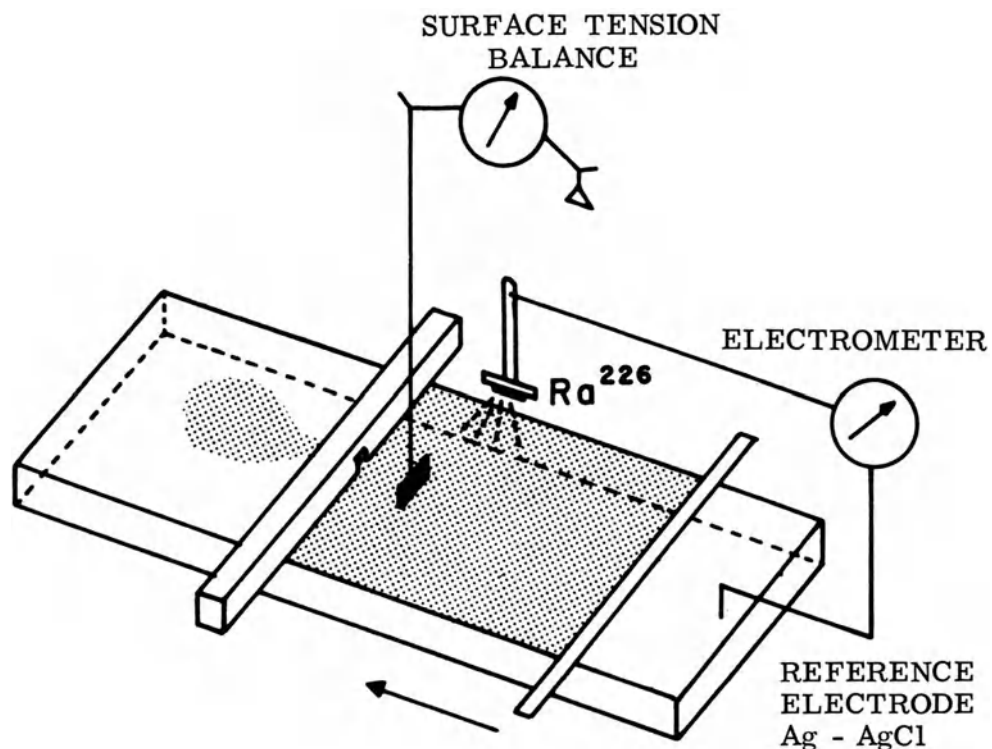


Fig. 1. Schematic presentation of methods used to measure pressure by the modified Wilhelmy plate method, surface potential by radioactive and reference electrodes and surface viscosity by the canal method.

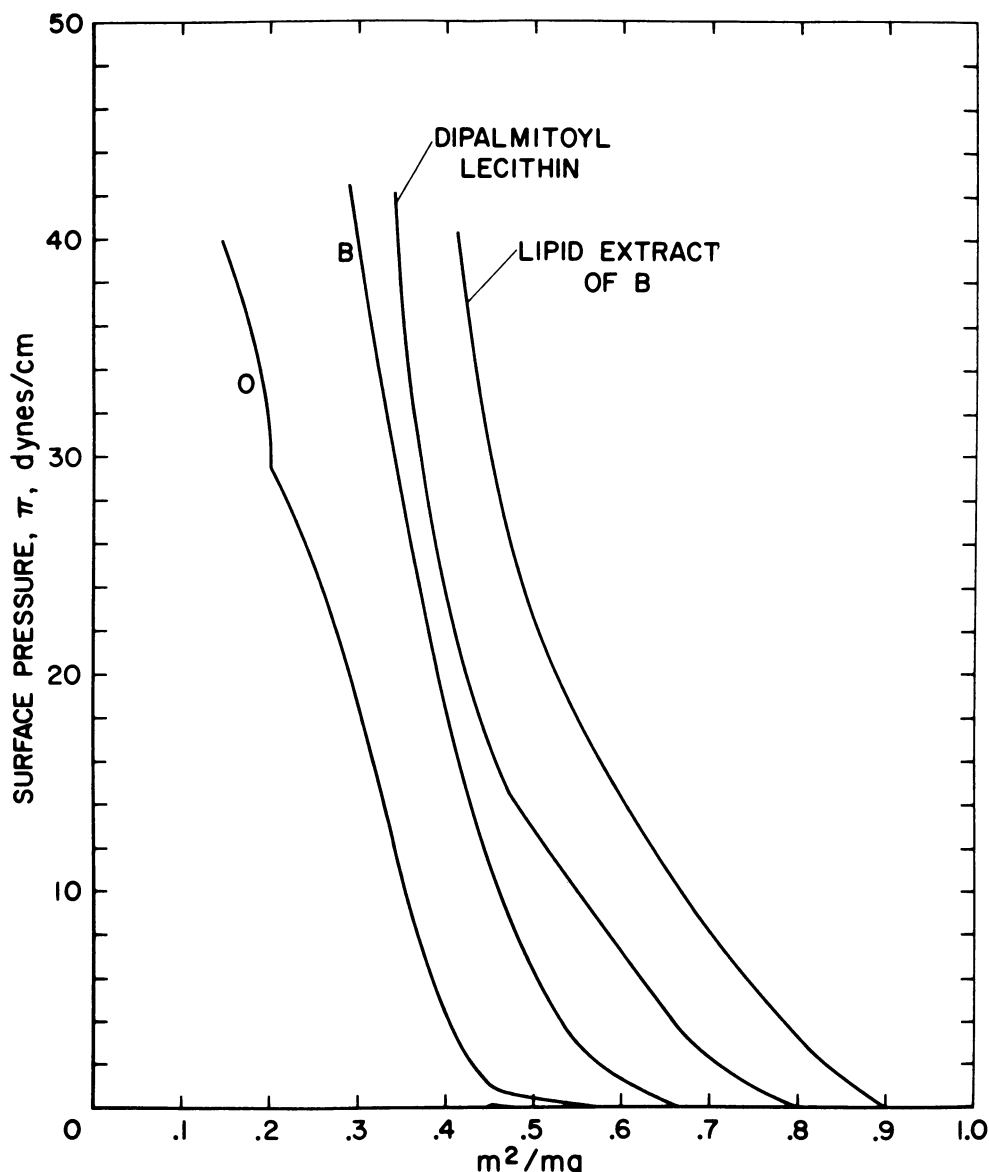


Fig. 2. Surface pressure-area curves of cell-free lung wash, stock O, of its lipoprotein fraction, B, of the lipid extract of the lipoprotein fraction, B, and of dipalmitoyl lecithin on subsolutions of 0.02 M NaCl or 0.01 M CaCl_2 , pH 6.0 and 25 C. The curves were identical on these subsolutions; therefore, only one set is shown. Similar curves were also obtained on 0.155 N NaCl.

TABLE I
SUMMARY OF SURFACE PROPERTIES

Preparation	Film Area	Collapse Pressure	Maximum Surface Potential
	M^2/mg	Dynes/cm	mV
Cell-Free Lung Wash (Stock O)	At onset of surface pressure 0.45	At maximum surface pressure 0.15	Subsolution 0.02 M NaCl 0.01 M CaCl ₂ 400
Lipoprotein Fraction of Lung Wash (Fraction B)	0.66	0.30	Subsolution 0.02 M NaCl 0.01 M CaCl ₂ 43
Lipid Extract of Lipoprotein Fraction	0.90	0.42	Subsolution 0.02 M NaCl 0.01 M CaCl ₂ 41
Dipalmitoyl Lecithin	0.80	0.35	Subsolution 0.02 M NaCl 0.01 M CaCl ₂ 42

TABLE II
 RELATIVE SURFACE VISCOSITY* CHANGES OF DIPALMITOYL LECITHIN AND LIPOPROTEIN FRACTION
 MONOLAYERS IN THE PRESENCE OF Ca^{++} IN SUBSOLUTION, pH 6.0, 25°C.

Difference in surface pressure ($\Delta \pi$) dynes/cm	Substance	t_{Na^+} sec 0.02 M NaCl	$t_{\text{Ca}^{++}}$ sec 0.01 M CaCl_2	$\left(\frac{t_{\text{Ca}^{++}} - t_{\text{Na}^+}}{t_{\text{Na}^+}} \right) \times 100\%$
8	Dipalmitoyl lecithin	1.49	1.49	0
	Lipoprotein fraction	1.50	1.60	
30	Dipalmitoyl lecithin	0.53	0.73	40
	Lipoprotein Fraction	0.50	0.59	

$$*\eta_{\text{monolayer}} = \left(\frac{\Delta \pi w^3}{12 l} \right) t$$

where $\Delta \pi$ = pressure difference across canal

w = width of canal = 0.1 cm

l = length of canal = 2 cm

t = time required for 1 cm^2 of film to flow through canal $\left(\frac{\text{sec}}{\text{cm}^2} \right)$

of known quantities of lyophilized preparations in 0.1% amył alcohol in distilled water (15) by means of an Agla micrometer syringe. Amył alcohol facilitates spreading and increased the reproducibility of the surface pressure-area and surface potential-area curves. Films of lipid extract of the lipoprotein fraction and of dipalmitoyl lecithin were spread from solutions of chloroform-methanol-hexane (1:1:3). Hexane was added to assist spreading of lipid.

Enzymatic hydrolysis of monolayers of the lipoprotein fraction and of dipalmitoyl lecithin by phospholipase A was investigated by injecting 20 µg of boiled snake venom *Naja naja* containing phospholipase A under a monolayer kept at fixed surface pressure levels. The subsolution consisted of 400 ml tris buffer in 0.02 M NaCl and 0.01 M CaCl₂ at pH 7.2. Phospholipase A hydrolyzes lecithin to lysolecithin and free fatty acid, causing a change of surface potential (16). A decrease in surface potential in the first two minutes was assumed to be proportional to the initial rate of hydrolysis.

RESULTS

Consistent force-area curves were obtained with films of all of the preparations studied (Fig. 2). Films of the lipid extract of the lipoprotein fraction are more expanded than films of dipalmitoyl lecithin and these in turn exceed the expansion of films of the lipoprotein fraction and also of stock 0. The steep part of curves of the lipoprotein fraction and of dipalmitoyl lecithin are nearly equally incompressible, somewhat more so than the curve of the lipid extract of the lipoprotein. Though all of the preparations attain about the same maximum surface pressure (40 - 42 dynes/cm) on the NaCl and CaCl₂ subsolutions, surface potential differs: 550 mv for dipalmitoyl lecithin, 410 mv for the lipoprotein fraction and its lipid extract and 400 mv for stock 0, and is consistently about 35 to 70 mv higher with Ca⁺⁺ than with Na⁺ of equal normality in the subsolution (Fig. 3 and Table I).

Films of all of the preparations remain in the liquid state on both subsolutions, except those of dipalmitoyl lecithin. On subsolutions of NaCl dipalmitoyl lecithin films are in the liquid state below a surface pressure of 35 dynes/cm, in the gel state between 35 to 40 dynes/cm and in the solid state above 40 dynes/cm (17). When calcium ions are in the subsolution, lecithin films change to the solid state at a lower surface pressure level (33 to 35 dynes/cm).

The relative surface viscosity of films of dipalmitoyl lecithin and of the lipoprotein fraction is about the same at low surface pressure, 8 dynes/cm, but at high surface pressure,

30 dynes/cm, dipalmitoyl lecithin is about twice as viscous as the lipoprotein fraction in the presence of Ca^{++} (Table II).

Hydrolysis of films of dipalmitoyl lecithin upon injection of phospholipase A into the subsolution occurs until a film surface pressure of 20 dynes/cm, is attained, but with the lipoprotein fraction hydrolysis continues to a film surface pressure of 30 dynes/cm (Fig. 4).

DISCUSSION

We studied rabbit lung washings freed of cells and cellular debris to minimize the likelihood of contamination with blood and tissue elements and separated into fractions having distinct chemical composition (8). One of these fractions consistently gives two bands on disc gel electrophoresis, one staining for lipid and the other for protein, suggesting the lipid and protein are associated. The distribution of these bands is distinctly different from those present in rabbit serum.

The lipid-protein association does not occur during centrifugation nor during lyophilization, since there is similar band mobility in the starting material, cell-free stock 0, and in lyophilized and also in non-lyophilized preparations of the lipoprotein fraction (8).

Immunologic studies indicate the lipoprotein fraction we isolated is indigenous to lung and is not a blood contaminant (8).

Lipid comprises about 63% of the lipoprotein fraction (57% phospholipid and 6% non-phospholipid); the remainder is protein. Of the total lipid, about 90% is phospholipid and 10% non-phospholipid. Lecithin is the predominant phospholipid on thin layer chromatography, having a fatty acid composition similar to egg lecithin, but without polyunsaturated fatty acids normally present. There are also trace amounts of lysolecithin and of phosphatidic acid (8).

The cell-free lung wash, stock 0, and its lipoprotein fraction are normally surface active according to criteria employed by respiratory physiologists, attaining in initially highly compressed films a minimum surface tension of zero or nearly zero dynes/cm upon compression (5 cm/min) from 100% to 20% of the trough area and exhibiting hysteresis on re-expansion to 100% of the trough area (18). For these studies a specially designed trough with a submerged compression bar, avoiding spillage of material over the rim of the trough when compression is continued beyond film collapse area, was used.

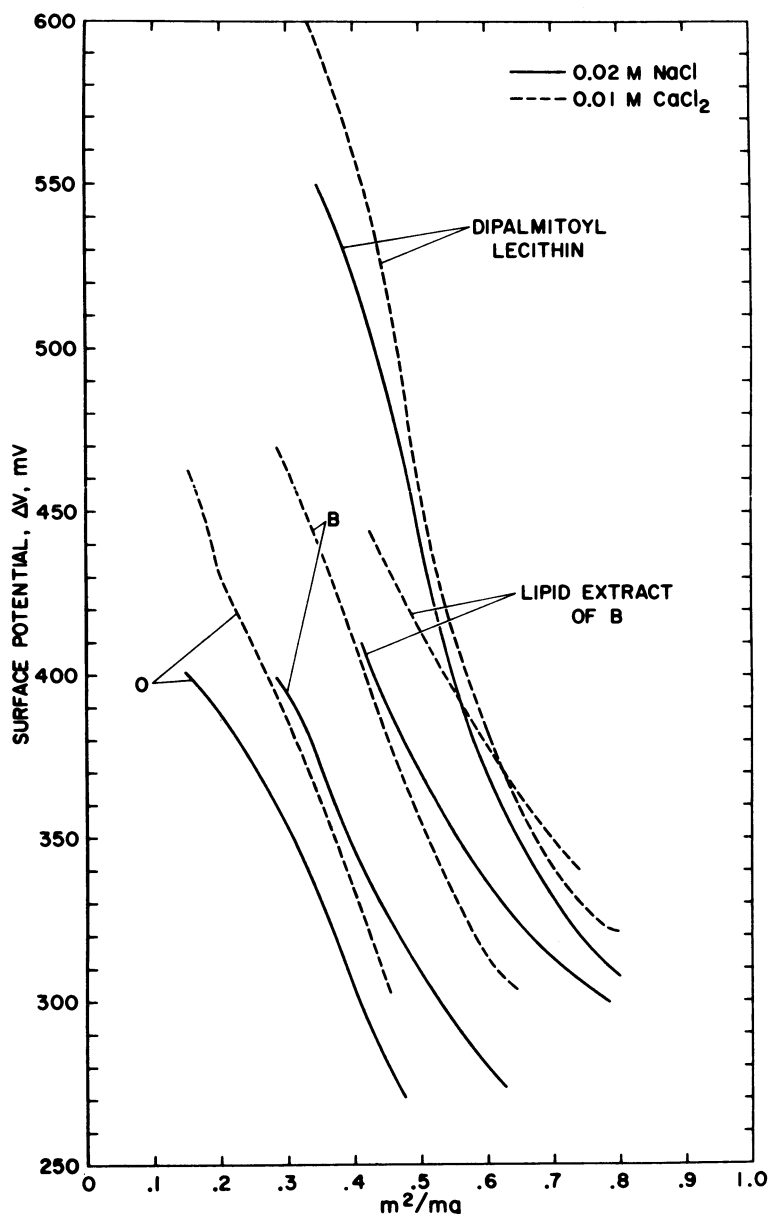


Fig. 3. Surface potential-area curves of cell-free lung wash, stock 0, of its lipoprotein fraction, B, of the lipid extract of the lipoprotein fraction, B, and of dipalmitoyl lecithin on subsolutions of 0.02 M NaCl and 0.01 M CaCl_2 , pH 6.0 and 25 C.

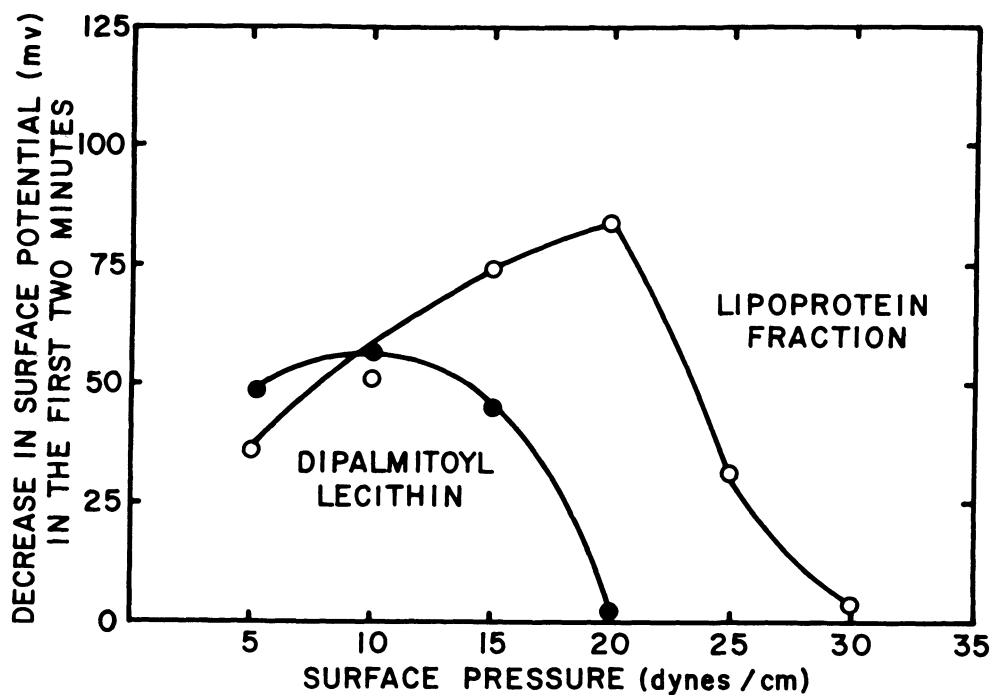


Fig. 4. Comparison of the rate of enzymatic hydrolysis of monolayers of the lipoprotein fraction, B, and of dipalmitoyl lecithin at different surface pressure levels by snake venom *Naja Naja* phospholipase A, based on decrease in surface potential two minutes after addition of the enzyme to the substrate, tris buffer, pH 7.2, 0.05 M and 0.01 M CaCl_2 . Each point represents a newly spread monolayer.

To investigate the surface properties of the several preparations, we applied parameters employed by surface chemists to investigate protein monolayers, i.e., surface pressure and surface potential related to M^2/mg of material spread and physical state of film.

Though films of stock 0, of its lipoprotein fraction and of the lipid extract of the lipoprotein fraction occupy different areas, they all attain about the same collapse pressure (Fig. 2). They also have about the same maximum surface potential on a subsolution of 0.02 M NaCl, (Fig. 3 and Table 1) suggesting at high surface pressure they contain the same chemical species. The kink in the force-area curve of stock 0 (Fig. 2) suggests the less surface-active material present in the original material is squeezed out of the monolayer at high surface pressure.

To learn about the nature of the lipid-protein association in the lipoprotein fraction, we investigated the interaction of calcium ions with monolayers of this fraction and with its lipid extract, and also enzymatic hydrolysis of the lipoprotein fraction by phospholipase A.

Though the presence of Ca^{++} does not affect the collapse pressures of these monolayers (Fig. 2), surface potential is consistently higher in the presence of Ca^{++} as compared with Na^+ (Fig. 3 and Table I). The increase in surface potential is a measure of the magnitude of the interaction. The lipoprotein fraction interacts somewhat more strongly with Ca^{++} than the starting material, stock 0, and the lipid extract of the lipoprotein fraction least of all.

The direction of change in level of surface potential with calcium binding indicates the probable site of interaction and probably orientation of the polar groups of lipid in films of the lipoprotein fraction. Calcium ions could interact with phosphate groups of lipid or carboxyl groups of protein in the lipoprotein. Surface potential decreases with binding of Ca^{++} to carboxyl groups (19) and increases with binding to phosphate groups (13). Since the surface potential of the lipoprotein monolayers increases in the presence of Ca^{++} (Fig. 3 and Table I), calcium binding most likely occurs with phosphate groups in the lipid component of the lipoprotein. This suggests the polar groups of the lipoprotein fraction are exposed to the aqueous phase and are thus available to interact with calcium in the subsolution.

The results of the studies of hydrolysis of monolayers of the lipoprotein fraction by phospholipase A (Fig. 4) tend to support this conclusion. If protein were bound to lipid in this fraction by polar groups or by ionic interaction, the rate of

hydrolysis would have been impeded (20). This did not occur, suggesting the polar groups of phospholipid in the lipoprotein are exposed to the water phase. It, therefore, appears that the interaction between protein in the phospholipid in the lipoprotein fraction is likely of the van der Waals type. Additional indirect evidence comes from the occurrence of about the same maximum surface potential in films of the lipoprotein fraction and in those of the lipid extract of the lipoprotein on a subsolution of Na^{++} (Fig. 3 and Table I). This suggests the lipid-protein association in the lipoprotein does not influence the dipole moment of lipid molecules and is not the result of ionic interaction but probably of the van der Waals type.

Since dipalmitoyl lecithin is commonly believed responsible for the surface properties of lung surfactant we compared the surface properties of the lipoprotein fraction and of dipalmitoyl lecithin. Both attain the same collapse pressure, but films of the lipoprotein fraction are much more condensed (Fig. 2). In the presence of Ca^{++} the surface potential of the lipoprotein fraction increases somewhat more, 70 as compared with 50 mv for dipalmitoyl lecithin (Fig. 3 and Table I).

At low surface pressure (8 dynes/cm) films of dipalmitoyl lecithin and of the lipoprotein fraction have the same relative surface viscosity in the presence of Ca^{++} as compared with Na^+ but at a high surface pressure (30 dynes/cm) dipalmitoyl lecithin is about twice as viscous as the lipoprotein fraction due to interaction with Ca^{++} ions (Table II). This is an important difference between the behavior of films of dipalmitoyl lecithin and the lipoprotein fraction.

The properties of films of dipalmitoyl lecithin differ from those of the lipoprotein fraction in other respects, attaining the gel state on a substrate of NaCl at a surface pressure of 35 to 40 dynes/cm, and the solid state above 40 dynes/cm. With Ca^{++} in the subsolution, lecithin films change to the solid state at a lower surface pressure 33 to 35 dynes/cm. Films of the lipoprotein fraction remain in the liquid state at all levels of surface pressure on the NaCl and CaCl_2 subsolutions used in these investigations.

The studies of the rate of enzymatic hydrolysis of films of the lipoprotein fraction and dipalmitoyl lecithin by phospholipase A (Fig. 4) provide information about the relative intermolecular spacing in these monolayers. Since hydrolysis ceases in films of dipalmitoyl lecithin at a surface pressure of 20 dynes/cm and in films of the lipoprotein fraction at 30 dynes/cm, it appears the intermolecular spacing between lipid molecules is much smaller in dipalmitoyl lecithin than in the lipoprotein fraction. Therefore,

the active site of the enzyme cannot penetrate dipalmitoyl lecithin monolayers above 20 dynes/cm and monolayers of the lipoprotein fraction above 30 dynes/cm.

BIBLIOGRAPHY

1. Radford, E.P., Jr., In "Handbook of Physiology, Vol. 1, p. 447 Amer. Physiol. Soc., Washington, D.C., 1964, Eds. Fenn, W.O. and H. Rahn
2. Pattle, R.E., Advances in Pulmonary Physiology. Ed. C.G. Caro, The Williams and Wilkins Co., Baltimore, 1966.
3. Weibel, E.R. and J. Gil, Resp. Physiol. 4 (1968) 42.
4. Buckingham, S., Heinemann, H.O., S.C. Sommers and W.F. McNary, Amer. J. Pathol., 48 (1966) 1027.
5. Clements, J.A. and D.F. Tierney. 1965. Vol. II, p. 1573 Amer. Physiol. Soc., Washington, D.C., Eds. Fenn, W.O. and H. Rahn.
6. Abrams, M.E., J. Appl. Physiol., 21 (1966) 718.
7. Klein, R.M. and S. Margolis, J. Appl. Physiol., 25 (1968) 654.
8. Galdston, M., D.O. Shah and G.Y. Shinowara, J. Colloid and Interface Sci., 29 (1969) 319.
9. Scarpelli, E.M., B.C. Clutario and F.A. Taylor, J. Appl. Physiol., 23 (1967) 880.
10. Redding, R.A., C.T. Hauck, J.M. Steem and M. Stein, New Engl. J. Med., 280 (1969) 1298.
11. Folch, J., M. Lees and G.H. Sloane Stanley, J. Biol. Chem. 226 (1957) 497.
12. Davies, J.T. and E.K. Rideal, Interfacial Phenomena, Academic Press, 2nd ed., p. 46.
13. Shah, D.O. and J.H. Schulman, J. Lipid Res. 6 (1965) 341.
14. Adam, N.K. 1941, The Physics and Chemistry of Surfaces, Oxford Press, London, 3rd., p. 55.
15. Dervichian, D., Nature, 144 (1939) 629.
16. Shah, D.O. and J.H. Schulman, J. Colloid Interface Sci. 25, (1967) 107.
17. Galdston, M. and D.O. Shah, Biochim. Biophys. Acta, 137 (1967) 255.
18. Tierney, F., Dis. Chest, 47 (1965) 247.
19. Spink, J.A. and J.V. Sanders, Nature, 175 (1955) 644.
20. Hughes, A., Biochem. J., 29 (1935) 437.

ABSENCE OF LIPOPROTEIN IN PULMONARY SURFACTANTS

Emile M. Scarpelli and Giuseppe Colacicco

Department of Pediatrics, Albert Einstein College of
Medicine, New York, N.Y. 10461 and York College,
City University of New York, Flushing, N.Y. 11365

The "alveolar-capillary barrier", which separates the air of the pulmonary alveoli from the blood of the pulmonary capillaries, has been rather well defined by electron microscopy as consisting of the capillary endothelial cell, interstices, alveolar epithelial cell, and acellular lining layer. The latter covers the plasma membrane of the epithelial cell and is the external limiting surface that makes contact with alveolar air (1,2)(Fig. 1). The chemical components of the alveolar lining layer, which have been termed "the surfactant system of the lung" (3), probably include proteins, carbohydrates, phospholipids and other lipids (2,3,4).

The discovery that saline extracts of pulmonary tissue and foam obtained from normal lungs are highly surface-active led to the hypotheses that pulmonary surfactants are essential determinants of alveolar stability (5) and that they modulate alveolar liquid balance to prevent pulmonary edema (6). Indeed, experimental alteration of the surface properties of the lung results in alveolar instability, alveolar collapse, and pulmonary edema (7,8). In addition, several pathological conditions of the lung have been related to disruption of normal surface properties of the alveoli (3).

The pulmonary surfactants reside in the alveolar lining layer and are components of the surfactant system (3). As such they probably form a surface film at the interface between the lining layer and alveolar air, and thus impart to the lung the surface properties that are essential for normal function. The idea that the physiologically important surfactants of the alveolar lining layer are phospholipids was established by Klaus and co-workers (9).

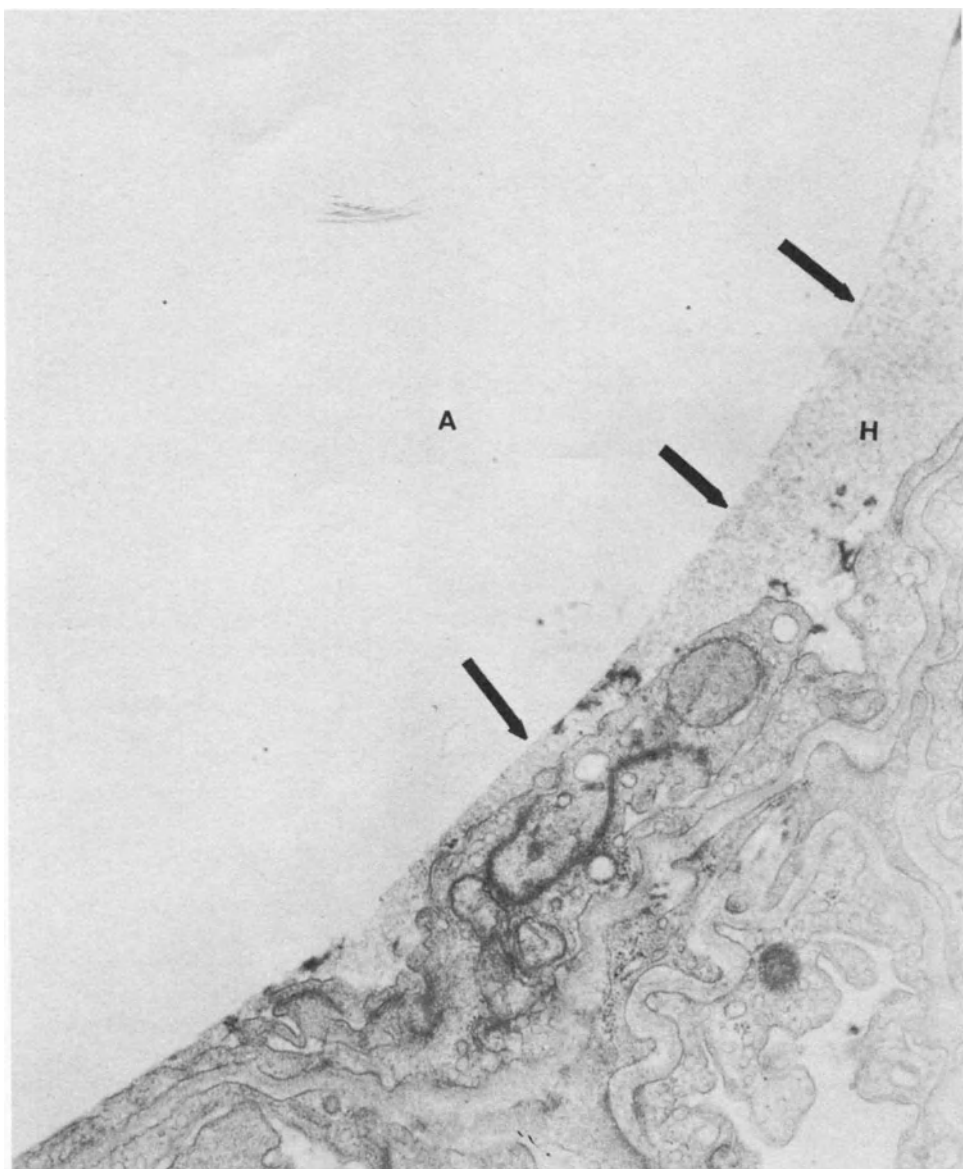


Fig. 1. Electron micrograph of normal rat lung. Magnification 40,000 x. A: alveolus. Arrow: surface film. H: hypophase. (Courtesy of Dr. Yutaka Kikkawa).

This has been confirmed by other investigators (10-13) and it is now apparent that the following phospholipids constitute a "family of pulmonary surfactants": phosphatidyl inositol, lysolecithin, sphingomyelin, phosphatidyl dimethylethanolamine (PDME), and phosphatidyl choline. Since the latter, lecithin, is recovered in highest concentration in pulmonary extracts and the other phospholipids are present in small to trace amounts, it is assumed that lecithin is the essential surfactant.

The natural state of the phospholipid surfactants is not known. It has been generally accepted that they are part of a lipoprotein, notwithstanding the fact that the evidence for this does not exist. Since knowledge of the state of the phospholipids is essential to considerations of the physical and chemical properties of the alveolar lining, we have searched for the lipoprotein in pulmonary extracts. We have found that the phospholipids are not bound to protein, that they cannot be classified as lipoprotein, and that determination of their relationship to other components of the surfactant system, including other lipids, proteins, and carbohydrates, must await further investigation.

PRESUMPTIVE EVIDENCE FOR LIPOPROTEIN SURFACTANTS

Pattle (14,15) and Clements (9,16) and their co-workers were the earliest proponents of the lipoprotein nature of pulmonary surfactants. The evidence upon which the first conclusions were based included the similarity between infrared absorption spectra of pulmonary foam and lecithin-gelatin mixtures (14) and the failure of surface films of total lipid (protein-free) extracts of pulmonary tissue to reduce surface tension below 20 dynes/cm when compressed in a modified Wilhelmy balance (9). Other evidence that was used to support the "lipoprotein theory" included a) the relatively high concentration of nitrogen in films harvested from pulmonary extracts (17), b) the recovery of surface-active precipitates after treatment of pulmonary extracts with trichloroacetic acid (11), and c) the reduced surface-activity of pulmonary foam following incubation with trypsin (14).

More recently three groups of investigators have reported the isolation of a surface-active pulmonary "lipoprotein" (18-20). Abrams (18) working with homogenized and centrifuged pulmonary tissue, isolated a pellicle which floated on NaCl solution of density 1.15 following low speed centrifugation. The pellicle was highly surface-active and contained a protein with the electrophoretic mobility of " α -globulin", in addition to lecithin, phosphatidyl ethanolamine, and other lipids. We repeated these experiments (21) and analyzed the various fractions for protein and lipoprotein content by disc electrophoresis and specific lipid

and protein stains. We have demonstrated that a) the centrifugation method of Abrams neither qualitatively nor quantitatively isolated the phospholipids in the crude extract, b) the pellicle contained up to eight different proteins, c) albumin (whose electrophoretic mobility is near that of α -globulin) was present in highest concentration, and d) there was no lipoprotein as demonstrated by the absence of Sudan Black B staining of the separated proteins. Klein and Margolis (19) obtained a surface-active pellicle of phospholipid and protein after ultracentrifugation of pulmonary extracts in KBr solutions of densities 1.15 and 1.21 at 100,000 g, 0 to 4°C, for up to 18 hours. Although the proteins were not characterized by any qualitative method, it was assumed that a lipoprotein had been isolated. We have demonstrated that Klein and Margolis did not use a sufficiently stringent ultracentrifugation procedure to isolate the surfactants (22,23). The phospholipid surfactants may be purified by 48 hour centrifugation at density 1.080, 115,000 g, 15°C; the purified lipid fraction contains less than 2% protein, which has the electrophoretic mobility of albumin (22,23).

Galdston, Shah and Shinowara (20) reported isolation of pulmonary lipoprotein, which was identified by its reaction with Oil red O stain following disc electrophoresis. We repeated their studies (21,24) and found that a) the Oil red O positive band did not contain phospholipid and was identical with the albumin band from pulmonary extracts, and b) the color reaction of Oil red O was quite different from that obtained with several purified serum lipoproteins. In addition, with the aid of the Sudan Black B prestaining which gave positive reaction with several serum lipoproteins, we demonstrated that none of the protein bands contained lipoprotein.

THE NON-LIPOPROTEIN NATURE OF PULMONARY SURFACTANTS

We have conducted several experiments in search of the pulmonary lipoprotein. These have included standard techniques that are used for the isolation and characterization of serum lipoproteins.

Sephadex G-200 Chromatography

Pulmonary washings were obtained by irrigating excised lungs from dogs with 0.15M NaCl. Samples of the pulmonary washing were applied to Sephadex G-200 columns (4). Five fractions were obtained as indicated by spectrophotometry (280 m μ) of the effluents (Fig. 2). These were monitored for a) lipid phosphorus, b) phospholipid by thin layer chromatography, and c) protein and lipoprotein by disc electrophoresis. These methods have been described elsewhere (4,21,24).

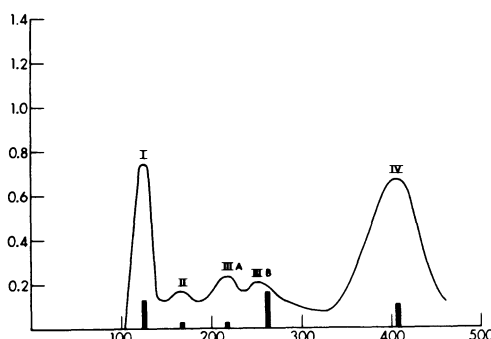


Fig. 2. Absorbance ($280\text{ m}\mu$, vertical axis) of effluent from Sephadex G-200 fractionation of dog pulmonary washing. Horizontal axis = effluent volume. Fraction I was recovered in the "void volume". (See reference 4).

A fact of significance is that phospholipid and protein, which together were supposed to make up the pulmonary "lipoprotein", were recovered in separate fractions: The phospholipids in fraction I and the proteins in the other fractions. Relevant to our discussion is fraction I: it was very turbid and contained all the phospholipids of the original extract, including phosphatidyl ethanolamine, sphingomyelin, lysolecithin (traces), PDME, and lecithin in highest concentration. Its high absorbance was due to the turbidity which was eliminated by the addition of sodium dodecylsulfate. Protein analysis by the quantitative Lowry method, which were performed on concentrated samples of fraction I and on the aqueous layer after extraction of lipid with chloroform:methanol, revealed a weight ratio of protein to phospholipid of less than 1/500. Disc electrophoresis showed no lipoprotein and, in addition, there was no lipoprotein in the other fractions.

When high density lipoprotein from rat serum was applied to the same Sephadex G-200 column, only one fraction was obtained in a sharp peak which was the intact lipoprotein. Thus lipoprotein could not be demonstrated in pulmonary washings by a method that has been used successfully by others (25) and us to isolate and characterize serum lipoproteins.

Preparative Polyacrylamide Electrophoresis

Pulmonary washings of dogs were applied to preparative polyacrylamide gel columns (7.5% gel concentration) and subjected to electrophoresis in the Buchler Instruments "Poly-Prep" apparatus (24).

Up to six peaks were recorded spectrophotometrically ($280 \text{ m}\mu$) in the effluent (Fig. 3). Each fraction was examined for protein by disc electrophoresis and for phospholipid by lipid phosphorus determination and thin layer chromatography. Material was removed from the top of the separation gel after each run and studied in the same way. This included components of pulmonary washings that did not enter the separation gel. Ninety one to 100% of the phospholipids applied were recovered in the top of the gel. Virtually all the proteins were recovered in the various fractions. The phospholipid fraction from the top of the gel, which contained phosphatidyl ethanolamine, PDME, sphingomyelin, lysolecithin, lecithin, and other lipids, contained a trace of protein with the electrophoretic mobility of albumin.

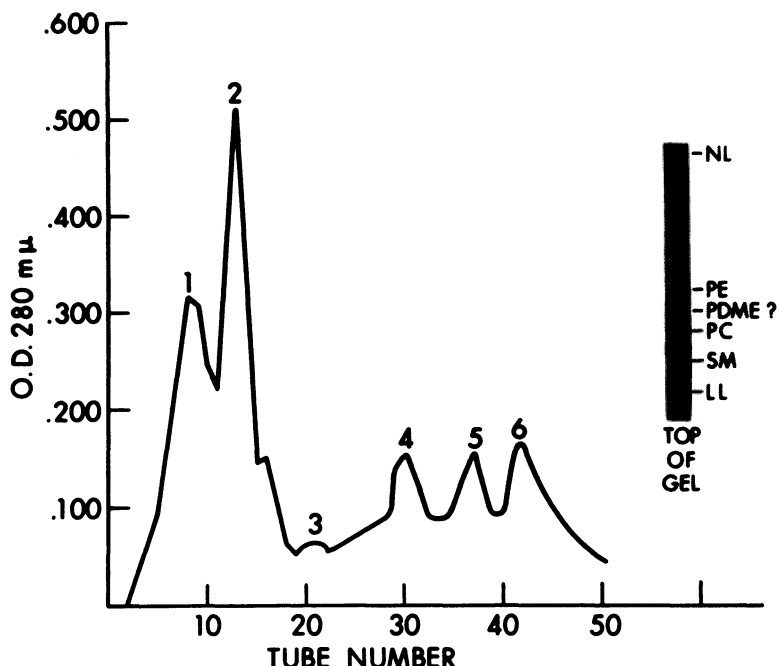


Fig. 3. Preparative electrophoresis of dog pulmonary washings. Vertical axis: Absorbance at $280 \text{ m}\mu$ for protein. Unlike with the lipid Fraction I of Sephadex Column (Fig. 2) the eluates were clear. All the lipids present in the crude pulmonary washings were found on top of gel after electrophoresis: NL, neutral lipids (cholesterol, triglycerides, cholesterol esters, and fatty acids); PE, phosphatidyl ethanolamine; PDME, phosphatidyl dimethyllethanolamine; PC, phosphatidyl choline; SM, sphingomyelin; LL, lysolecithin.

Selective Staining and Disc Electrophoresis

Two extraction methods, viz., pulmonary washing and mincing of pulmonary tissue, were used to obtain samples from several mammalian species including sheep, dog, cat, rabbit, and monkey. Some samples were mixed with Sudan Black B stain for lipoprotein prior to disc electrophoresis; other samples were separated by disc electrophoresis (both 3.75% and 7.5% gels) and the gels were stained with amido black, a non-specific protein stain; a third set of extracts was applied to Sephadex G-200 columns and the effluent fractions were analyzed by the same staining and electro-phoretic methods (24). Serum was analyzed in parallel experiments. None of the proteins in the pulmonary washings reacted with Sudan Black B, whereas three to eight lipoprotein bands were observed in the serum samples. The pulmonary minces of dog, sheep, cat, and rabbit contained no proteins that reacted with Sudan Black B, i.e., no lipoprotein. Similarly, each Sephadex fraction from the separation of dog and sheep extracts contained no Sudan Black B-positive protein. Mince extracts from the lungs of squirrel monkeys, which were heavily contaminated with blood, contained a slow-moving lipoprotein band that was recovered in fraction III of the Sephadex column. This lipoprotein was not associated with the pulmonary phospholipid surfactants since the latter were recovered in fraction I. A similar lipoprotein band was present in monkey serum. The results of these experiments are summarized below.

Table 1. Disc electrophoresis of lung surfactant preparations of normal lung of various species

SUBJECT (NO. OF ANIMALS)	MINCE		WASHING		SEPHADEX FRACTIONS			SERUM*	
	3.75% gel	7.5% gel	3.75% gel	7.5% gel	1	2	3	3.75% gel	7.5% gel
DOG (5)	0	0	0	0	0	0	0	6	6
SHEEP (3)	0	0	0	0	0	0	0	4-6	3
CAT (2)	0	0	0	0	-	-	-	4	3
RABBIT (2)	0	0	0	0	-	-	-	4-6	4
MONKEY (5)	+	+	0	0	0	0	+	7-8	6-7

* = Number of lipoprotein bands observed.

0 = No lipoprotein.

+= Probably serum lipoprotein.

- = Not studied.

Thus surface-active pulmonary washings from several species contained no lipoprotein. Mince extracts contained no lipoprotein except for the samples that were highly contaminated with blood. The lipoprotein found in the latter samples was probably a serum contaminant.

Ultracentrifugation

Pulmonary washings were prepared from the lungs of rabbits with 0.15M NaCl, the density was adjusted to 1.080 with solid KBr, and the samples were centrifuged at 115,000 g, 15°C for 48 hours. All the lipids floated as a single fraction into a pellicle. After dilution and purification by two additional centrifugations, the third pellicle contained less than 2 µg protein for 100 µg phospholipid; on disc electrophoresis the protein was albumin, but there was no lipoprotein (22,23). Each of the three pellicles contained all the lipids and the surface activity of the original pulmonary washing.

Conclusions

The several analytical methods that were used to study pulmonary extracts in our laboratory lend no support to the thesis that pulmonary phospholipid surfactants are part of a lipoprotein. These experiments demonstrate that the physical characteristics of the phospholipids are sufficiently different from those of the proteins to permit the separation of the two on the basis of molecular or aggregate size (Sephadex chromatography), electrophoretic mobility (polyacrylamide gel), and density (ultracentrifugation). It should be noted also that each of these methods has been used successfully by us and others to isolate and identify serum lipoproteins. We have also demonstrated that lipoproteins may find their way into pulmonary extracts when the latter are heavily contaminated with blood, which complicates the interpretation of results.

Corroborative Evidence

Several corroborative reports have appeared since our initial characterization of the phospholipid surfactants as non-lipoprotein (4). According to the electron microscopy studies of Kikkawa (1) (Fig. 1) and Weibel and Gil (2), the alveolar lining layer is composed of two phases: a superficial layer of phospholipids and a base aqueous layer probably containing proteins, lipids and mucopolysaccharides. These layers have been referred to as surface film and hypophase (26,27). In the electron micrographs the surface phospholipids appeared as lamellae, rather than as a monomolecular film, probably because of the tissue fixation method that was used; the

small repeating distances of the lamellae indicated that proteins were excluded (2). Schematic reconstruction of the electron density pattern from the electron microscope permitted an approximation of molecular orientation in the alveolar lining layer; the picture that emerged supports the thesis that phospholipids are not bound to protein. McClenahan and Ohlsen (28) isolated a surface-active fraction from washings of human lung. The proteins were separated and injected into rabbits. The resulting antiserum reacted with human serum albumin only; a water soluble protein other than normal serum albumin was not found in the pulmonary extracts. It should be noted that albumin is the protein present in highest concentration in pulmonary washings, but that other proteins may also be recovered in the washings (4,21,24). Steim and co-workers (29) purified the surface-active phospholipids from an acellular precipitate of pulmonary washings. The precipitate was layered over a linear sucrose gradient and ultracentrifuged for 20 hours at 4°C. A band centering at density 1.035 contained the surface-active phospholipids and less than 3% protein and carbohydrate. This is in agreement with our own ultracentrifugation studies (22, 23). Finally, it is interesting to note that in the disease of humans "alveolar proteinosis", in which there is a large intra-alveolar accumulation of pulmonary phospholipids, the lipids are not bound to protein and are in fact associated with only very small amounts of soluble protein, as determined by electrophoresis of pulmonary washings from patients with the disease (30).

SUMMARY

The evidence that the surface-active pulmonary phospholipids are not part of a lipoprotein is summarized as follows:

Sephadex separation of PL and Proteins	Scarpelli, et al, (4)
Electrophoretic separation of PL and Proteins	Scarpelli, et al, (21)
Absence of specific LP staining reaction	Scarpelli & Taylor, (31)
Purification of surface-active PL by UC	Steim, et al, (29) Colacicco & Scarpelli, (22,23)
Pulmonary ultrastructure compatible with PL but not with LP	Kikkawa, et al, (1) Weibel & Gil, (2)
Absence of antigenic pulmonary LP	McClanahan & Ohlsen, (28)
No recoverable LP in pulmonary washings	Scarpelli, et al, (4,21-24)
Absence of LP in alveolar proteinosis	Ramirez-R. & Harlan, (30)

(PL = phospholipid, LP = lipoprotein, UC = ultracentrifugation)

The most relevant conclusion is that lung surfactants are phospholipids and not lipoprotein. Any specific pulmonary lipoprotein surfactant must be still demonstrated.

REFERENCES

1. Kikkawa, Y., E.K. Motoyama and C.D. Cook. The ultrastructure of the lungs of lambs. Amer. J. Pathol. 47:877-903 (1965).
2. Weibel, E.R. and J. Gil. Electron microscopic demonstration of an extra-cellular duplex lining layer of alveoli. Resp. Physiol. 4:42-57 (1968).
3. Scarpelli, E.M. The Surfactant System of the Lung. Lea and Febiger Publishers, Philadelphia (1968).
4. Scarpelli, E.M., B.C. Clutario and F.A. Taylor. Preliminary identification of the lung surfactant system. J. Appl. Physiol. 23:880-886 (1967).
5. Clements, J.A. Surface phenomena in relation to pulmonary fraction. Physiologist 5:11-28 (1962).
6. Pattle, R.E. Properties, function and origin of the alveolar lining layer. Proc. Roy. Soc. (London) B148:217-240 (1958).
7. Pattle, R.E. and F. Burgess. The lung lining film in some pathological conditions. J. Pathol. Bacteriol. 82:315-331, (1961).
8. Yoshida, S. Effects of surfactants or fat solvent on static pressure-volume hysteresis of excised dog lung. Amer. J. Physiol. 203:725-730 (1962).
9. Klaus, M.H., J.A. Clements and R.J. Havel. Composition of surface-active material isolated from beef lung. Proc. Natl. Acad. Sci. 47:1858-1859 (1961).
10. Fujiwara, T. and F.H. Adams. Isolation and assay of surface-active phospholipid components from lung extracts by thin-layer chromatography. Tohoku J. Exptl. Med. 84:46-54 (1964).
11. Brown, E.S. Isolation and assay of dipalmityl lecithin in lung extracts. Amer. J. Physiol. 207:402-406 (1964).
12. Morgan, T.E., T.N. Finley and H. Fialkow. Comparison of the composition and surface activity of "alveolar" and whole lung lipids in the dog. Biochim. Biophys. Acta 106:403-413 (1965).
13. Gluck, L., E.K. Motoyama, H.L. Smits and M.V. Kulovich. The biochemical development of surface activity in mammalian lung. I. Pediat. Res. 1:237-246 (1967).

14. Pattle, R.E. and L.C. Thomas. Lipoprotein composition of the film lining the lung. *Nature* 189:844 (1961).
15. Pattle, R.E. Surface tension and the lining of the lung alveoli, In *Advances in Respiratory Physiology*, C.G. Caro (Ed.), Williams and Wilkins Publishers, Baltimore (1966), pp. 83-105.
16. Clements, J.A. The alveolar lining layer, In *Development of the Lung*, A.V.S. deReuck and R. Porter (Eds.), Little, Brown and Co., Publishers, Boston (1967), pp. 202-221.
17. Buckingham, S. Studies on the identification of an anti-atelectasis factor in normal sheep lung. *Amer. J. Dis. Child.* 102:521-522 (1961).
18. Abrams, M.E. Isolation and quantitative estimation of pulmonary surface-active lipoprotein. *J. Appl. Physiol.* 21:718-720 (1966).
19. Klein, R.M. and S. Margolis. Purification of pulmonary surfactants by ultracentrifugation. *J. Appl. Physiol.* 25:654-658 (1968).
20. Galdston, M., D.O. Shah and G.Y. Shinowara. Isolation and characterization of a lung lipoprotein surfactant. *J. Colloid Interface Sci.* 29:319-334 (1969).
21. Scarpelli, E.M., S.J. Chang and G. Colacicco. Evaluation of methods for isolation and identification of pulmonary surfactants. (Submitted for publication).
22. Colacicco, G. and E.M. Scarpelli. Purification of pulmonary surfactants by ultracentrifugation. (Manuscript in preparation).
23. Colacicco, G. and E.M. Scarpelli. Physico-chemical properties of lung surfactants, this symposium.
24. Scarpelli, E.M., S.J. Chang and G. Colacicco. A search for the surface-active pulmonary lipoprotein. (Submitted for publication).
25. Fleischer, B. and S. Fleischer. Interaction of the protein moiety of bovine serum α -lipoprotein with phospholipid micelles. II. Isolation and characterization of the complexes. *Biochim. Biophys. Acta* 147:566-576 (1967).

26. Heinenmann, H.O. and A.P. Fishman. Nonrespiratory functions of mammalian lung. *Physiol. Rev.* 49:1-47 (1969).
27. Scarpelli, E.M., K.H. Gabbay and J.A. Kochen. Lung surfactants, counterions and hysteresis. *Science* 148:1607-1609 (1965)
28. McClenahan, J.B. and J.D. Ohlsen. Protein components of human surfactant. *Clin. Res.* 16:134 (1968).
29. Steim, J.M., R.A. Redding, C.T. Hauck and M. Stein. Isolation and characterization of lung surfactant. *Biochem. Biophys. Res. Comm.* 34:434-440 (1969).
30. Ramirez-R, J. and W.R. Harlan, Jr. Pulmonary alveolar proteinosis. *Amer. J. Med.* 45:502-512 (1968).
31. Scarpelli, E.M. and Taylor, F.A. Unpublished observation.

RELATION OF WATER TRANSPORT TO WATER CONTENT IN SWELLING BIOLOGICAL MEMBRANES

Joel L. Bert and Irving Fatt

Department of Mechanical Engineering, University of
California, Berkeley, California 94720

ABSTRACT

In biological and some synthetic polymer materials, which swell on imbibing water (corneal stroma, costal and articular cartilage, skin, cellulose acetate, and polymethyl methacrylate), the phenomenological parameter, k/η , relating rate of water flow to pressure gradient in Darcy's law [$q = -(k/\eta)(dP/dx)$] has been found to be a function of water content. Log k/η appears to be linearly related to log H , where H is grams of water/grams of dry swelling material. A pore model predicts an increase in "pore" radius with increasing hydration. The "pore" radius of the corneal stroma predicted by the model is in agreement with the radius calculated from light scattering and diffusion data.

INTRODUCTION

Most biological materials have a fixed water content in a living system. If these materials are dehydrated by artificial means they will rehydrate to restore the normal water content. Some biological materials have a smaller water content *in situ* than they can hold if simply immersed in water. The corneal stroma is a well-studied example of such a system. An "active" process is supposedly operating in the living system to keep the water content of the corneal stroma to its normal level.¹

Fatt and Goldstick² have shown that the transient water imbibition process in swelling membranes can be described by an equation analogous to the transient diffusion equation. The Fatt

and Goldstick equation is

$$\frac{\partial H}{\partial t} = D(H) \frac{\partial^2 H}{\partial \psi^2} \quad (1)$$

where the terms of this and all subsequent equations are defined in the nomenclature section. Fatt³ has shown that the water transport coefficient $D(H)$, in corneal stroma, is given by

$$D(H) = \frac{k}{\eta} \frac{\epsilon^2}{(\epsilon+H)} \frac{dP}{dH} \quad (2)$$

The flow conductivity term, k/η , in equation (2) is the same term that appears in Darcy's law,

$$q = -\frac{k}{\eta} \frac{dP}{dx} \quad (3)$$

where equation (3) is for steady state flow of a liquid of viscosity η in a one-dimensional system.

Both transient and steady state studies of water flow in swelling materials (Mishima and Hedbys,⁴ Fatt,³ Bert and Fatt⁵) show that k/η is a function of hydration of the material.

If the swelling material is assumed to consist of a matrix of solid material through which the water flows, then a pore model can be hypothesized and tested. In such a model, the pore radius will be a function of hydration.

PORE MODEL

If in an area A_T of a membrane there are n pores, all of radius r and length ℓ , then Poisueille's law gives the flow rate as,

$$Q = n \pi r^4 \Delta P / 8 \eta \ell \quad (4)$$

For the same membrane Darcy's law gives

$$Q = k A_T \Delta P / \eta L \quad (5)$$

Equating (4) and (5) and letting the tortuosity term be τ , where $\tau = \ell/L$, we obtain

$$k A_T = n \pi r^4 / 8 \tau \quad (6)$$

The volume of water in the membrane is

$$V_w = n \pi r^2 l \quad (7)$$

Combining equations (6) and (7) gives

$$k A_T = V_w r^2 / 8 \tau l \quad (8)$$

The volume of dry membrane material is assumed to be generated by moving a slice with area of solid material A_d through a distance L . Then

$$V_d = A_d L \quad (9)$$

Equation (9) assumes that the fractional area of solid material in any plane is equal to the fractional volume of solid in the total membrane volume. In membranes with high solids content this is only a gross approximation, but it is sufficient for our purposes. By the same argument the area of water is given by

$$A_w = V_w / L \quad (10)$$

Combining equations (7), (9), and (10) gives

$$A_T = V_d / L + n \pi r^2 \tau \quad (11)$$

Combining equations (7), (8), and (11) gives

$$k = (V_w r^2) / 8 V_d \tau^2 (1 + V_w / V_d) \quad (12)$$

If γ is the density of water and σ is the density of the dry material, then the definition of H leads to

$$H = \gamma V_w / \sigma V_d \quad (13)$$

If $\gamma/\sigma = \epsilon$ then

$$H = \epsilon V_w / V_d \quad (14)$$

Combining equations (12) and (14) and dividing both sides by η gives

$$\frac{k}{\eta} = H r^2 / 8 \tau^2 \eta (\epsilon + H) \quad (15)$$

Equation (15) shows that if there is a unique relation between k/η and H then r^2/τ^2 must also be unique for that combination of k/η and H .

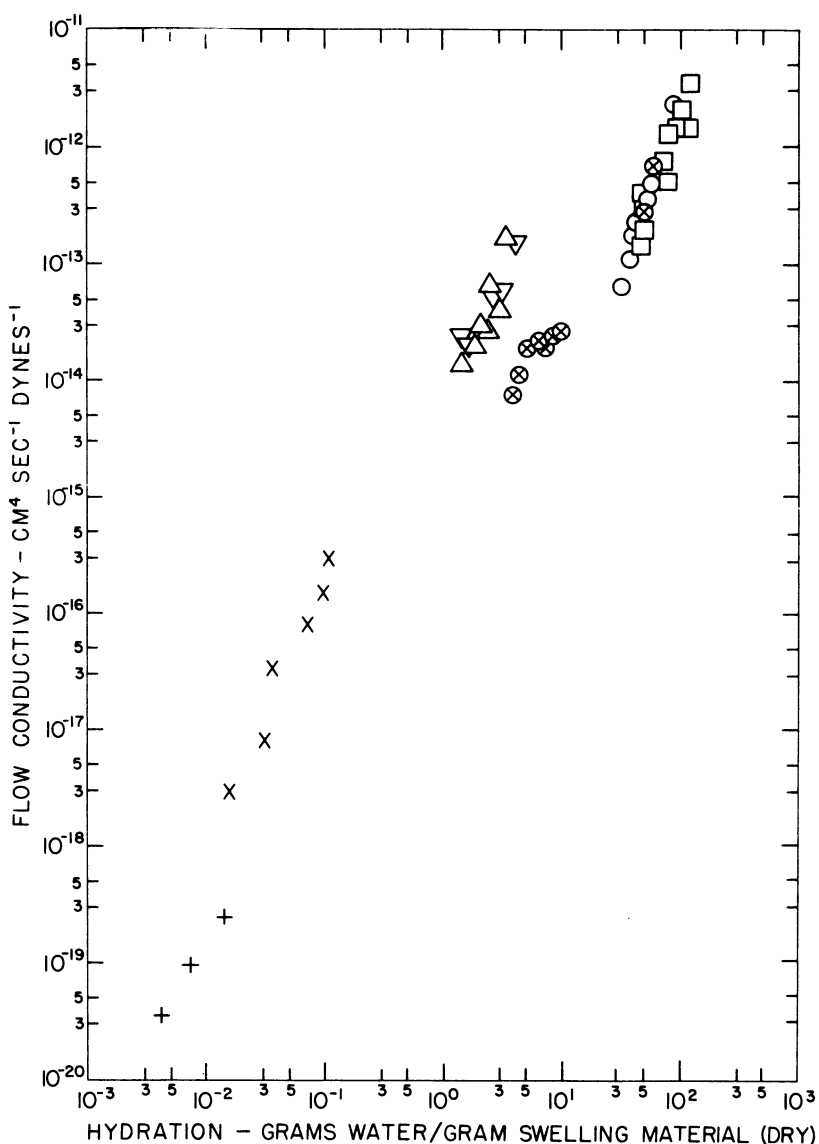


Figure 1. Flow conductivity, k/η , as a function of hydration, H . The materials represented are: Steer corneal stroma (□), rabbit corneal stroma (○), skin (stratum corneum) (⊗), steer costal cartilage (Δ), steer articular cartilage (▽), cellulose acetate (X), and polymethyl methacrylate (+).

TEST OF PORE MODEL

Figure 1 shows experimentally determined values of k/η as a function of H for various biological and synthetic membranes. In this work hydration is considered to be the ratio of water to dry swelling material. This hydration differs from the ratio of water to all dry material for biological tissues, but is the same for homogeneous synthetic polymers shown on the graph. The hydration used here is not the same as the hydration described by previous authors,^{3,5} who considered the ratio to include all dry material. It is assumed in our treatment of water flow in swelling membranes given here, that water flows only in the swelling matrix. The non-swelling material in the corneal stroma, for example, is so widely spaced as to offer no resistance to water flow. Consequently, when dealing with the swelling phenomenon it appears that the non-swelling material is present only for structural reasons and should not, therefore, be included when describing the hydration of the material.

The data of Figure 1 appear to group along a line whose equation is

$$k/\eta = a H^b \quad (16)$$

Combining equations (15) and (16) and solving for r gives

$$r = [8 a H^{b-1} \tau^2 \eta (\varepsilon + H)]^{1/2} \quad (17)$$

Figure 2 shows a plot of equation (17) for r/τ (or $\tau = 1$) and for $\tau = 5$.

Two sets of experimental data are available for testing Figure 2. Maurice¹ measured the "pore" size in corneal stroma by observing the maximum size of a molecule that will diffuse in this tissue. He estimated the pore diameter to be 120 Å. Hart and Farrell;⁶ and Hart, Farrell, and Langham,⁷ using light scattering data, estimated the distance between polymer chains in the ground substance of the stroma, equivalent to the pore diameter of our model, to be 210 Å. Before Figure 2 can be used to estimate an equivalent pore radius, a proper tortuosity must be determined. It is well known that porous materials with large pores have tortuosities approaching unity; and materials with small pores have higher tortuosity factors. In the case of the corneal stroma, a tortuosity approaching unity is an appropriate choice. The hydration of the normal, *in vivo*, corneal stroma is 76. At this hydration then, Figure 2 would estimate a pore radius of approximately 75 Å, or a diameter of 150 Å, for the corneal stroma. This result seems reasonable when compared with the two pore radius estimations that have already been mentioned.

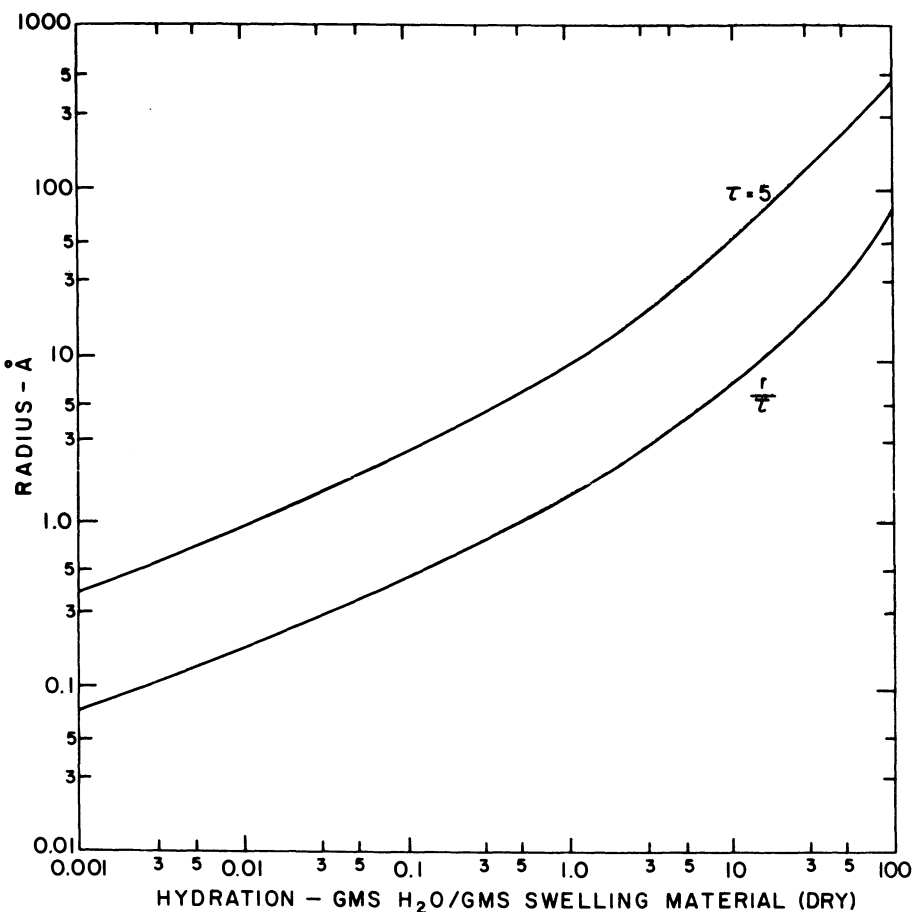


Figure 2. Equivalent pore radius versus hydration for materials of Figure 1, according to Equation (17).

Moreover, Longuet-Higgins and Austin⁸ point out that in membranes with pore diameters greater than 4.5 Å most of the water transport will be by a convective process, whereas in membranes with pore size less than 4.5 Å a diffusive process will predominate. Bert, Fatt, and Saraf⁹ have shown that in cellulose acetate, at hydrations between 0.02 and 0.08, the diffusive and convective fluxes are comparable. Below this range the convective flux falls off rapidly, allowing most of the transport to be by diffusion. For cellulose acetate one would expect the tortuosity to be much greater than one. Carman¹⁰ has suggested that tortuosity is five

for packs of granulated materials. This value is probably applicable for polymeric membranes. For cellulose acetate then, using Figure 2, one would predict that from a diameter of about 3 Å and smaller diffusion is the primary water transport mechanism. On the other hand, for the biological membranes, whose minimum pore diameter from Figure 2 would be about 4 Å, it is known that convection is the significant water transport mechanism. These values of pore diameter seem to agree fairly well with the values theoretically predicted by Longuet-Higgins and Austin.⁸

Finally, although none of the agreement is brilliant, the results of a pore model as given by equation (17) and as shown in Figure 2, do seem reasonable when tested against the results of Maurice;¹ Hart and Farrell;⁶ Hart, Farrell, and Langham;⁷ and Longuet-Higgins and Austin.⁸

This work was supported in part by National Institute of Health grants HE-06796 and GM-1418, and by the Petroleum Research Fund administered by the American Chemical Society.

The authors wish to express their sincere appreciation to Pru Mann and Dr. Helen Fatt, for all they have done for us.

NOMENCLATURE

A_d	= effective surface area of membrane occupied by dry material
A_T	= surface area of membrane
A_w	= effective surface of membrane occupied by water
$D_w(H)$	= water transport coefficient
H	= Hydration, grams of water/grams dry swelling material
k/η	= flow conductivity
ℓ	= length of pore in membrane
L	= thickness of membrane
n	= number of pores per A_T surface area
P	= swelling pressure in equation (2), and total pressure (i.e.--swelling plus hydrostatic, etc.) in other equations
q	= volumetric flow rate across area A_T
Q	= volumetric flow rate
r	= pore radius
t	= time
V_d	= volume of dry membrane material
V_w	= volume of water in membrane
x	= distance variable
γ	= density of water
ϵ	= ratio of densities of water to dry membrane material
η	= viscosity of transported material, water
σ	= density of dry membrane material
τ	= tortuosity, ℓ/L

BIBLIOGRAPHY

1. D. Maurice in *The Eye*, ed. by H. Davson, Vol. 1, 2nd ed., 489-601, Academic Press, New York (1969).
2. I. Fatt and T. K. Goldstick, *J. Colloid Science*, 20, 962-989 (1965)
3. I. Fatt, *Exptl. Eye Research*, 7, 413 (1968).
4. B. O. Hedbys and S. Mishima, *Exptl. Eye Research*, 1, 262-275 (1962).
5. J. L. Bert and I. Fatt, *Life Sciences*, 8, Part 1, 343-346 (1969).
6. R. W. Hart and R. A. Farrell, *J. Optical Soc. of America*, 59 (6), 766-774 (1969).
7. R. W. Hart, R. A. Farrell, and M. E. Langham, *APL Tech. Digest*, Applied Physics Lab., Johns Hopkins Univ., Baltimore, 8 (3), 2-11 (1969).
8. H. C. Longuet-Higgins and G. Austin, *Biophysics J.*, 6 (2), 217-224 (1966).
9. J. L. Bert, I. Fatt, and D. Saraf, *J. Polymer Sci.*, in press.
10. P. C. Carman, *Flow of Gases Through Porous Media*, Academic Press, New York (1956).

KINETIC AND EQUILIBRIUM BEHAVIOR OF SIMPLE SUGARS IN A WATER-BUTANOL-LIPID SYSTEM.

Thomas Jenner Moore, M.D., Ph.D.

St. Luke's Hospital Center, New York, New York

College of Physicians and Surgeons, New York, New York

A word of explanation as to why a pediatrician becomes interested in the plasma membrane seems appropriate. Premature human infants are often found to have plasma glucose levels so low that convulsions would ensue were such levels detected in an older child.⁽¹⁾ Yet clinically these babies generally flourish. To further complicate matters, these prematures compared to older children, when given a glucose load, show a prolongation in the rate of disappearance of glucose from the plasma of their extremities.⁽²⁾

Certain newly born mammals, rats for example, show a difference in toxicity of morphine with age. This difference has been shown to depend on factors that alter drug uptake in the brain.⁽³⁾

These examples suggest that the rate of movement of certain small molecules across plasma membranes differs in the very young when compared to his elder.

In addition, a score of diseases have been described in children where the primary defect is thought to be a disorder in the active or passive movement of small molecules across a cell membrane.⁽⁴⁾

An understanding of any of these related processes is lacking because there exists no satisfactory description of the biophysical and biochemical mechanisms involved in mammalian transport. It is held that a detailed knowledge of simpler forms of biologic transport will provide insights towards solving these clinical problems.

In the nineteenth century, Overton⁽⁵⁾ called attention to the correlation between the rate of penetration of a solute into a cell

and its olive oil-water partition coefficient. This lipoid solubility theory was re-examined quantitatively twenty years ago by Collander and Barlund.⁽⁶⁾ Striking correlations between the rate of penetration of a variety of small hydrophilic molecules into the cell and their oil/water partition were demonstrated. Jacobs and others showed this relationship holds for the human erythrocyte. Many physiologically important solutes, including sugars, were not examined. Collander believed that their distribution coefficient in the lipoid-like organic solvents he employed would be of the magnitude of 1/100,000,⁽⁶⁾ too low for meaningful direct measurements.

If the distribution coefficients of sugars are of this magnitude, penetration into the cell should occur very slowly indeed. Yet many simple sugars rapidly enter the red blood cell. It is believed that a specialized mechanism of penetration resides in the plasma membrane facilitating the diffusion of these solutes into the cell. This mechanism is termed mediated transport.

There exist certain well defined criteria for identifying such a mediated transport system.⁽⁷⁾ It operates exclusively with the existing electrochemical gradient of the permeant and leads to the disappearance of this gradient.

As stated, the rate of penetration exceeds the rate predicted by the lipoid solubility theory.

The rate of penetration is not proportional to concentration but reaches a limiting or saturation value as the concentration is increased.

The entry rates for particular sugars are species-dependent. The conformational properties of the penetrating sugar molecule are thought to be the determinant of this selectivity. As the number of bulky groups in the axial position increases, the rate of penetration decreases. In addition, optical enantiomorphs have been shown to possess different rates of penetration.⁽⁸⁾

A difference in penetration rate exists depending on whether net transfer or unidirectional flux is measured.

Finally the penetration rate can be reduced by the presence of small amounts of inhibitors.

The membrane constituents participating in this process have not been identified with certainty.

Membrane phospholipid might be directly involved in the sugar transport system of the human erythrocyte. Maudsley and Widdas⁽⁹⁾

suspending erythrocytes in an environment of ^{14}C labelled glucose, recovered the label combined to a lipid fraction having the chromatographic properties of triphosphoinositide. Labelling of this fraction could largely be eliminated by pretreating the ghosts with an inhibitor of transport dinitrofluorobenzene.

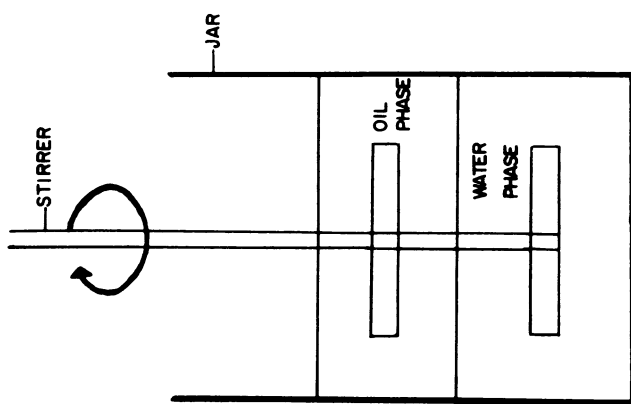
Lefevre(10) has recently demonstrated that erythrocyte membrane phospholipid will markedly accelerate the transport of D-glucose from an aqueous phase through a chloroform phase into a second aqueous phase. The output rate into the second aqueous phase was found to be directly proportional to the input glucose level without limit. In addition, he found that the comparative transfer of glucose, ribose, and inositol in this system did not mimic their penetration rate in the intact erythrocyte.

This laboratory has been attempting to construct qualitative analogies between the penetration of certain sugars into the human erythrocyte and the behaviour of these sugars in a water-butanol and lipid system.

MATERIALS AND METHODS

The principle of the Schulman chamber⁽¹¹⁾, the model membrane used in this laboratory, is that two immiscible liquids, having a stable interface are stirred at the same rate by two blades mounted on a single stirrer shaft. An amphiphilic solute, lipid, introduced into the less polar butanol phase forms a film at the interface. Lipid can also be detected in the bulk aqueous and butanol phases. Radioactive, hydrophilic molecules (sugars in this case) are introduced into the more polar aqueous phase and their rate of appearance in the butanol is measured. Different variables of the system can be changed to measure their influence on the translocation process.

The apparatus consists of battery jars with glass covers and double-bladed stirrers on each stirring shaft. The stirring blades were rotated at a constant speed of 15 rpm. A six unit Phipps & Bird electric stirrer allowed four simultaneous experiments to be conducted. For all experiments 10 ml of 1 M sodium and potassium propionate (included to provide a counter-ion for the interfacial lipid), 200 ml of 1-butanol, and sufficient distilled water to bring the final volume of water--after addition of the sugar solution--to 280 ml, the two layers being mutually saturated, were placed in the jars and allowed to equilibrate. In some experiments, 4 mg of total lipid from erythrocytes was introduced into the butanol in each cell. Then a solution of D-glucose-U- ^{14}C or D-galactose-U- ^{14}C was injected into the aqueous phase, so that the sugar concentration of the aqueous phase at time zero was either



THE SCHULMAN CHAMBER

$$\frac{dn}{dt} = A(K_{WO}C_W - K_{OW}C_O) \quad \dots \dots \dots \quad (1)$$

$$K_{WO} = \frac{P_{OW}}{V_0} \left[\frac{-\ln(1-C_O/C_O^e)}{\left(1 + \frac{V_O}{V_W} P_{OW} \right)} \right] \quad \dots \dots \dots \quad (2)$$

Fig. 1. The Schulman Chamber and the equations describing solute translocation in the system.

0.015 M or 1.3 M. Eight 1.0 ml samples were taken from the butanol phase at 10 min. intervals. After the samples had been collected, the whole system was vigorously stirred to equilibrate the sugar between both phases, and allowed to clear for several hours before samples were drawn from each phase for the determination of the butanol-water distribution coefficient (P_{OW}). Samples were transferred to scintillation vials containing 15 ml of Bray's solution and counted in a Packard model 4000 liquid scintillation spectrometer. Counts per minute were converted to disintegrations per minute by means of an external standard correlation curve. The temperature in the Schulman chamber was maintained at 34°C in a 120 liter circulating water bath.

THEORETICAL CONSIDERATIONS⁽¹²⁾

The kinetic equation for measuring the interfacial transfer coefficient in the Schulman chamber has already been derived. It states that

$$\frac{dn_O}{dt} = A(K_{WO}C_W - K_{OW}C_O) \quad \text{Equation 1}$$

$$K_{WO} = (P_{OW})^{-1} - \left(\frac{C_O}{C_O^e} \right)^{-1} \quad A(t(P_{OW} + 1)/V_O)^{-1} \quad \text{Equation 2}$$

where C_O = concentration of the permeator in the butanol phase at time t ; C_O^e = concentration of the permeator in the alcohol phase at equilibrium, $t = \infty$; C_W = concentration of the permeator in the aqueous phase at time t ; n_O = number of moles of permeator in the butanol phase; P_{OW} = distribution coefficient for the volumes of butanol and water used = C_O^e/C_W^e ; A = area of the interface; K_{WO} = interfacial transfer coefficient from water to butanol ($\text{cm}\cdot\text{hr}^{-1}$); V_O = volume of the alcohol phase; and $a = V_O/(\text{Volume of the aqueous phase.})$

RESULTS

The kinetic and equilibrium experiments were conducted at 34°C in every experiment. Figure 2, a representative experiment, is a plot of K_{WOT} (Calculated from Equation 2) against time in minutes. The slope represents K_{WO} , the interfacial transfer coefficient from water into oil. The figure shows that the K_{WO} for D-galactose is greater when erythrocyte phospholipid is added to the system already containing cholesterol.

Table 1 summarizes the results of numerous experiments where the introduction of the phospholipid species into the chamber was varied. In these experiments d-galactose is the translocating sugar. It is seen that both human erythrocyte phospholipid

A TYPICAL PLOT OF $(P_{ow}) \left[-\ln \left(1 - \frac{C_o}{C_0} \right) \right] / \left(\frac{A}{V_0} \right) (\alpha P_{ow} - 1)$
 VS. t AT 1.3 M SUGAR. THE SLOPE IS K_{wo} , THE INTER-
 FACIAL TRANSFER COEFFICIENT. D-GALACTOSE IS THE
 PERMEATOR.

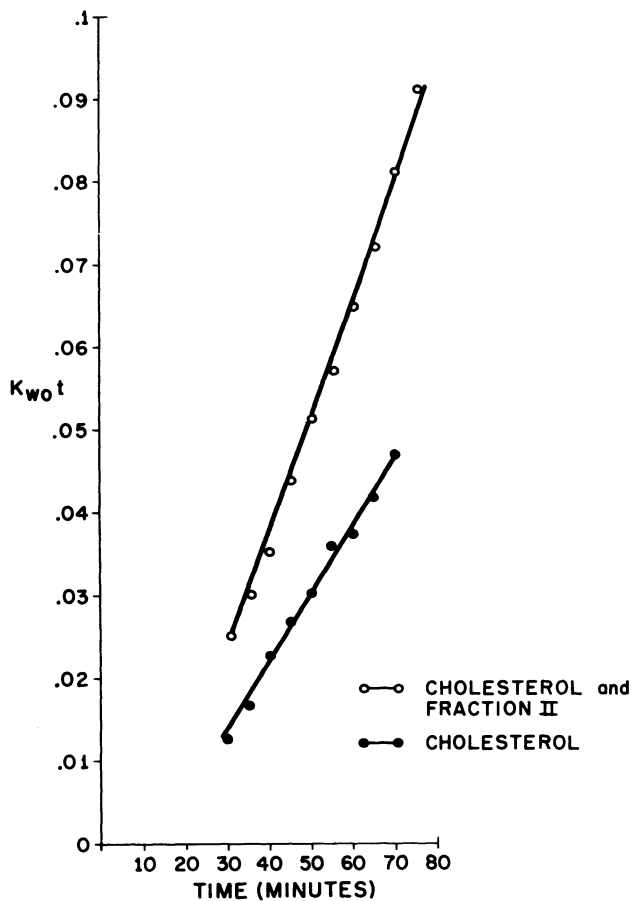


Fig. 2

fractions eluted from the DEAE cellulose column accelerate the translocation process relative to cholesterol alone. Commercially available (Applied Science Laboratories) individual phospholipids known to reside in the human erythrocyte membrane are seen to have a similar effect.

Table 1

INTERFACIAL TRANSFER COEFFICIENT (K_{wo}) WATER INTO OIL
FOR CHOLESTEROL AND PHOSPHOLIPID IN THE CHAMBER

Lipid Species*	n	K_{wo}	D-Galactose	S.D.
Cholesterol 0.5 mgm**	20	0.836	.196	
Fraction II 0.5 mgm***	3	1.570	.089	
Fraction III 0.5 mgm****	6	1.548	.384	
P. Ethanolamine 0.5 mgm**	9	1.071	.106	
Lecithin 0.5 mgm**	6	1.522	.277	
Sphingomyelin 0.5 mgm**	6	1.915	.321	
P. Serine 0.5 mgm**	6	1.568	.560	
P. Inositol 0.5 mgm**	9	1.358	.467	

*3.5 mgm Cholesterol is in every chamber.

**Applied Science Laboratories

***Human erythrocyte Lecithin, Lysolecithin, P. Ethanolamine,
Sphingomyelin

****Human erythrocyte P. Serine, P. Inositol

To determine whether the rate of movement of sugar into the butanol phase reaches a limiting value as the initial concentration of sugar in the aqueous phase is increased, the initial flux of glucose into the oil phase with 4 mgm of human erythrocyte lipid was studied as a function of initial glucose concentration. The flux dn_o/dt was calculated by solving Equation 2 after experimentally determining K_{wo} . Each point represents the mean of three to five experiments. Figure 3 indicates that a limiting value is achieved when the initial aqueous glucose concentration exceeds 0.6 M, the translocation process appears to be saturated.

The previous experiments indicated that the partition coefficient, measured to calculate the interfacial transfer coefficient, varied depending upon the sugar and lipid species in the chamber. Therefore we decided to ask what affect complex lipid, known to reside in the human erythrocyte membrane had on the partition coefficients of a variety of simple sugars. All constituents introduced into the Schulman chamber were reduced in volume by a factor of fourteen and introduced into small vials. The vials were vigorously shaken, equilibrated at 34°C for 24 hours

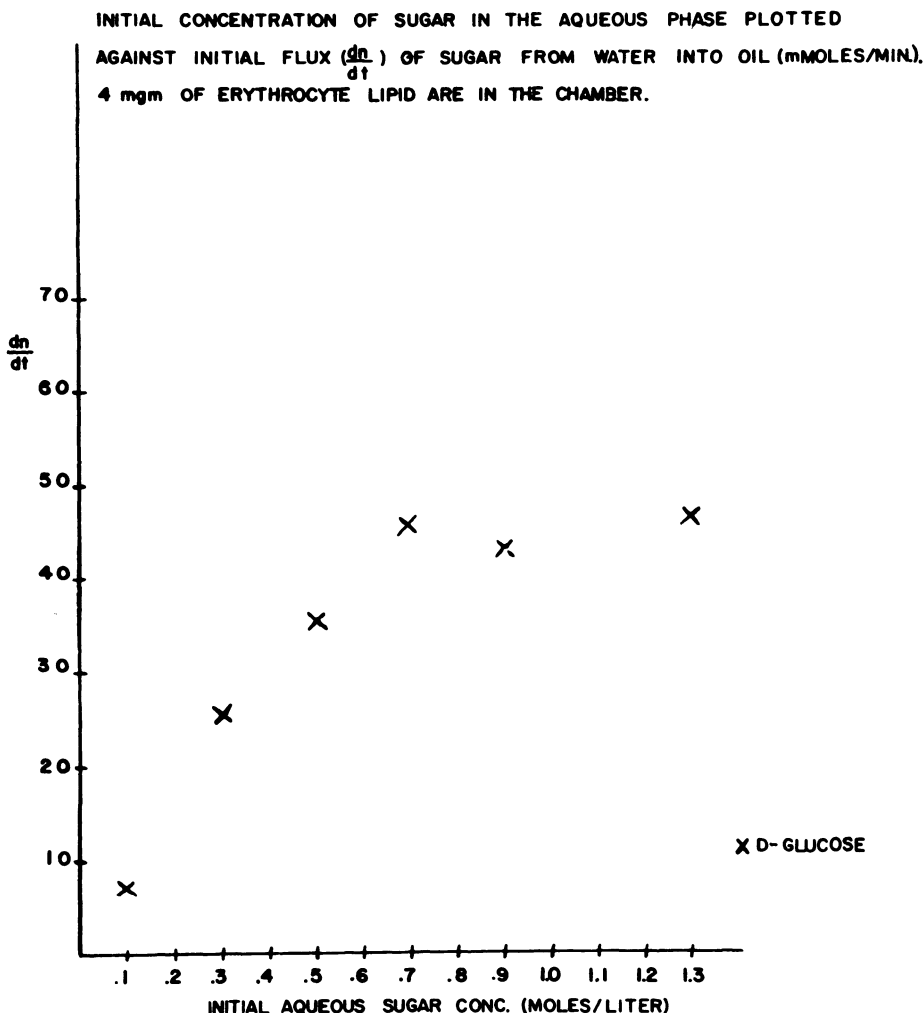


Fig. 3

THE CHANGE IN PARTITION COEFFICIENT IN A WATER-BUTANOL SYSTEM FOLLOWING THE ADDITION OF 0.16 mgm TOTAL HUMAN ERYTHROCYTE LIPID PLOTTED AGAINST LOG K_m (AFFINITY FOR THE ERYTHROCYTE CARRIER APPARATUS). INITIAL AQUEOUS PHASE SUGAR CONCENTRATION IS 0.01 M.

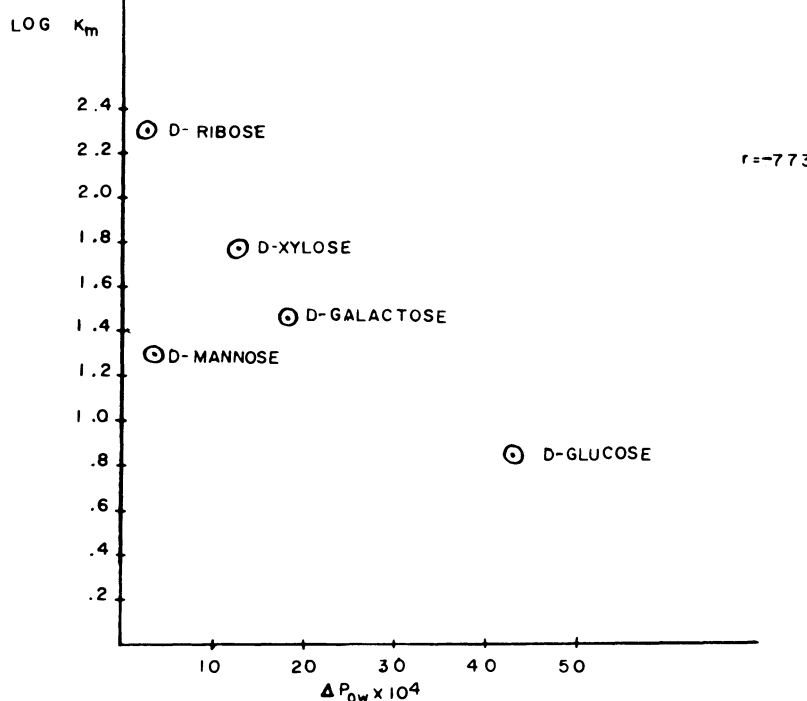


Fig. 4

and sampled. Lipid was then added, the vial re-equilibrated, and sampled. The differences in partition coefficients were then calculated. The results represent the mean of from ten to twenty individual experiments. These differences were then plotted against the log of the affinity for human erythrocyte carrier, measured by Lefevre and Marshall⁽⁸⁾ and correlation coefficients calculated. The next figure illustrates the effect of total erythrocyte lipid on the change in partition coefficient for five sugars at 0.01 M. It is seen that d-glucose is driven into the oil phase, but sugars that penetrate the erythrocyte membrane slowly are not. There is a fairly good correlation between the lipid induced solubilization and the affinity for carrier, and hence the rate of penetration into the red cell.

To determine the effect of individual phospholipids known to reside in the erythrocyte membrane, chromatographically pure phospholipids were tested at the same sugar concentration. Figure 4 illustrates the behaviour of phosphatidyl ethanolamine. Again lipid drives d-glucose into the oil phase and a significant correlation holds. Table 2 summarizes the behaviour of five phospholipids individually examined. It is seen that a significant correlation holds between the penetration rate into the erythrocyte of the five sugars studied and the change in partition coefficient following addition of phosphatidyl ethanolamine. Suggestive but nonsignificant correlations hold for lecithin and phosphatidyl inositol, while there is no correlation for sphingomyelin or phosphatidyl serine. Because the biologic measurements are subject to some uncertainty⁽¹³⁾, correlation coefficients were calculated using penetration rates calculated by a third laboratory.⁽¹⁴⁾ The resulting r values were in fairly good agreement with those presented, phosphatidyl ethanolamine again being the phospholipid with the greatest r value.

D-glucose enters the erythrocyte very much faster than its optical enantiomorph l-glucose. If the correlation holds for optical enantiomorphs, phospholipids added to the system should drive d-glucose into the oil phase and l-glucose out of the oil phase. Table 3 indicates that this did not take place. Each of the five phospholipids introduced drove both d and l glucose into the oil phase. The discriminatory property possessed by certain phospholipids for the d sugars studied does not exist when these optical enantiomorphs are compared, suggesting non-lipid membrane constituents also participate in the selectivity process of the sugar transport apparatus.

SUMMARY

In summary, certain analogies between sugar transport in the human erythrocyte and the translocation of sugars from an aqueous to butanol-lipid phase have been presented. The addition of a

THE CHANGE IN PARTITION COEFFICIENT IN A WATER-BUTANOL SYSTEM FOLLOWING THE ADDITION OF 0.10mgm PHOSPHOTIDYL ETHANOLAMINE PLOTTED AGAINST LOG K_m (AFFINITY FOR THE ERYTHROCYTE CARRIER APPARATUS). INITIAL AQUEOUS PHASE SUGAR CONCENTRATION IS 0.01 M.

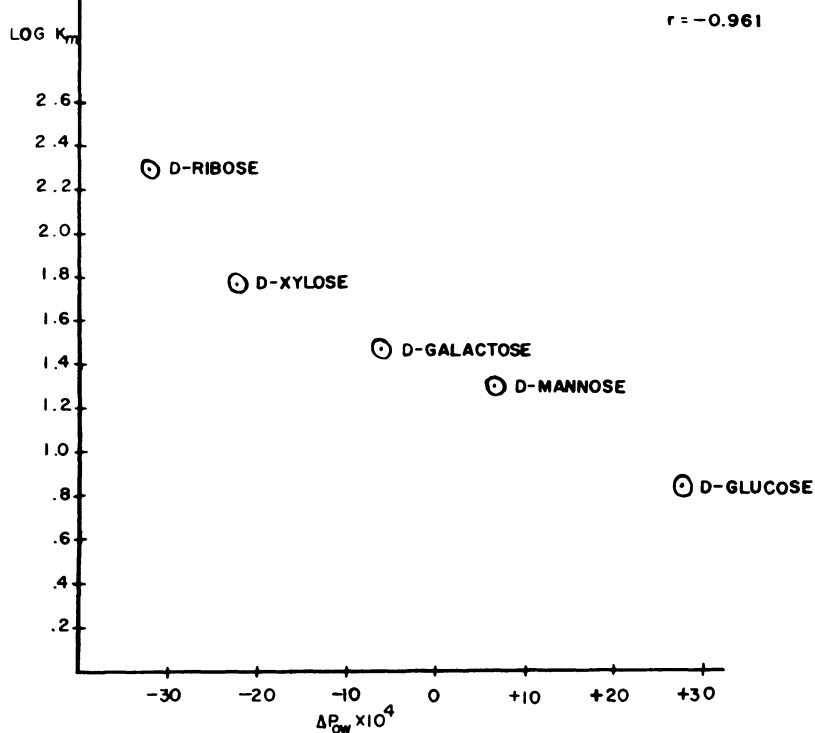


Fig. 5

Table 2

THE EFFECT OF INDIVIDUAL PHOSPHOLIPIDS ON THE
CHANGE IN PARTITION COEFFICIENT OF FIVE SUGARS*
IN A WATER-BUTANOL SYSTEM

Phospholipid	r Value of Log K_m vs ΔP_{ow} for 5 Sugars* at 0.01 M.	P 3 d.f.
P. Ethanolamine	-0.961	0.01
P. Inositol	-0.764	N.S.
Lecithin	-0.653	N.S.
Sphingomyelin	-0.394	N.S.
P. Serine	-0.162	N.S.

*D-Mannose, D-Glucose, D-Galactose, D-Ribose, D-Xylose.

Table 3

THE EFFECT OF INDIVIDUAL PHOSPHOLIPIDS ON THE CHANGE IN
PARTITION COEFFICIENT OF THE OPTICAL ENANTIOMORPHS,
D AND L GLUCOSE, IN A WATER-BUTANOL SYSTEM

Phospholipid	D Glucose	L Glucose
P. Ethanolamine	+	+
P. Inositol	+	+
Lecithin	±	+
Sphingomyelin	+	+
P. Serine	-	+
Predicted from erythrocyte penetration rate.	+	-

+ indicates lipid drives sugar into oil phase

- indicates lipid drives sugar out of oil phase

variety of erythrocyte or commercial phospholipids to the system will accelerate the process when compared to a water-butanol and cholesterol system. As the initial aqueous sugar concentration is increased the initial translocation rate does not increase without limit but achieves a maximum value. Examining the effect of complex lipid on the partition coefficient of sugars illustrates certain properties these lipids possess that parallels to a remarkable degree the hypothetical sugar transport apparatus. They

are capable of moving certain sugars into the oil phase, one phospholipid is capable of distinguishing the five d sugars, but not the l sugar. The d sugars are distinguished in a manner highly reminiscent of the red cell carrier.

In recent years membranes have been considered in terms of their dynamic function and more attention has been focused on the protein components of membranes.⁽¹⁵⁾ The present experiments indicate that understanding the physical interaction between complex membrane lipid and permeating solute is a promising avenue for investigating certain of these dynamic functions.

REFERENCES

1. Cornblath, M. and Schwartz, R., 1966, Disorders of Carbohydrate Metabolism in Infancy, W. B. Saunders Co., Phila.
2. Tiernan, R., 1967, Personal Communication.
3. Kupferberg, H. J., and Way, E. L., 1963, J. Pharm. Exp. Therapy, 141:105.
4. Rosenberg, L. E., 1969, in Biological Membranes, Dowben, ed. Chap. 8, Little, Brown & Co., Inc., Boston.
5. Overton, E., quoted in Davson, H., 1964, A Textbook of General Physiology, 3rd ed., p 282, Little, Brown & Co., Inc., Boston.
6. Collander, R., 1947, Acta Physiol. Scand. 13:363.
7. Stein, W. D., 1967, The Movement of Molecules Across Cell Membranes, Academic Press, Inc., New York, Chap. 4.
8. LeFevre, P. G. and Marshall, J. K., 1958, Am. J. Physiol., 194:333.
9. Maudsley, D. A. and Widdas, W. F., 1967, J. Physiol., London, 189:75.
10. LeFevre, P. G., Jung, C. Y., and Chaney, J. E., 1968, Arch. Biochem. and Biophys., 126:677.
11. Schulman, J. H., 1966, Ann. N. Y. Acad. Sci., 137:860.
12. Ting, H. P., Bertrand, G. L., and Sears, D. F., 1966, Biophys. J., 6:813
13. LeFevre, P. G., 1969, Personal Communication.

14. Stein, W. D., 1967, *The Movement of Molecules Across Cell Membranes*, Academic Press, Inc., New York, p 164. (Widdas' results at 37°C were used for comparison.)
15. Korn, E. D., 1969, *Annual Review of Biochemistry*, Annual Reviews, Inc., p 263.

USE OF SYNTHETIC MEMBRANE MODELS IN THE STUDY OF GASTRIC SECRETORY PROCESSES

Jesse M. Berkowitz and Melvin Praissman

Division of Gastroenterology, Department of Medicine,
Meadowbrook Hospital, East Meadow, N.Y. and The Department
of Physiology, Mount Sinai School of Medicine, New
York, N.Y.

Synthetic membrane models have been used in the study of gastric secretory problems for over thirty years. These techniques were employed to elucidate the mechanisms by which ions were secreted in gastric juice. Modern studies of gastric secretory processes began in the 1930's with the studies of the ionic composition of gastric juice by the late Franklin Hollander (1), a physical-organic chemist turned physiologist, and the membrane model experiments of Torsten Teorell, a physical chemist interested in physiologic problems.

Hollander (1,2) was primarily concerned with the origin of the inorganic constituents of gastric juice and he systematically studied its composition as a function of the volume rate of secretion. These studies were performed in dogs and after an extensive series of experiments, Hollander concluded that the primary secretory product of the gastric glands was a slightly hypertonic (with respect to the interstitial fluid) solution of HCl. The original studies were carried out at a time when flame photometry techniques for Na and K assay were not available. We now know that the primary inorganic secretory product of the gastric glands is a solution of HCl and KCl (the ratio of H to K is approximately 15:1). At low rates of secretion Hollander found that the "basic" chloride, which is now known to be primarily sodium, appeared in the gastric juice at a concentration higher than hydrogen. The sodium-rich solution found at low rates of secretion was hypotonic. By a regression analysis, Hollander concluded that the sodium and the hypotonicity could be accounted for by the leakage of sodium-rich interstitial fluid into the gastric lumen. The combination of the bicarbonate from the alkaline interstitial fluid and the

secreted hydrogen ions would result in the evolution of CO₂ producing a decline in solute concentration. The hypothetical entry of the alkaline interstitial fluid was utilized to account for the decreased hydrogen ion concentration, the sodium content and the hypotonicity of basal gastric juice.

STUDIES ON ION AND WATER FLOW ACROSS THE RESTING GASTRIC MUCOSA

Hollander's treatment of the problem was based on a mathematical analysis. In contrast, Teorell approached the problem experimentally: he placed 5 ml. of a slightly hypertonic solution of pure HCl into the resting stomach of anesthetized cat and followed the changes in its ionic composition with time (3). The volume of the instilled fluid remained constant, the hydrogen concentration fell and the "basic" fraction of the chloride concentration increased. Concomitantly, there was a fall in total chloride concentration. As chloride accounted for almost the total concentration of anions, a decline in its concentration reflected a decline in tonicity. Teorell extended these studies with a synthetic membrane system (4). Isosmotic HCl was placed on one side of an uncharged cellophane membrane and isosmotic NaCl on the other side. As the exchange progressed the hydrogen concentration declined, the sodium concentration rose and the volume remained constant on the acid side of the system. Simultaneously, the chloride concentration declined reflecting a fall in solute concentration. There was no Donnan effect because the membrane was uncharged; Teorell reasoned therefore, that HCl, as an ion pair, left the acid side of the system faster than NaCl entered as an ion pair. In both the synthetic membrane studies and the cat stomach, the unequal exchange rates of the ion pairs with no change in volume was assumed to indicate a net loss of solute from the acid solution. However, changes in the volume of the instilled fluid may not have been detected because of the small volumes used (5.0 ml). If there had been a change in the volume of the instilled acid solutions in Teorell's cat experiments, then the model he proposed would be invalid.

To minimize the problems of Teorell's experiments, we instilled large volumes of isosmotic HCl solutions containing a non-absorbable dilution indicator into unstimulated canine gastric pouches (5). The non-absorbable indicator (phenol red) enabled us to assess two things: (1) Whether the instilled material was quantitatively recovered and (2) Any changes in the volume of the fluid placed in the pouch. The change in fluid volume was determined by measuring the indicator concentration. In Table I is a typical instillation experiment, one of twelve. With time, the hydrogen ion concentration declined, the sodium ion concentration increased, and the measures of solute concentration, chloride and osmolality fell. The decline in phenol red concentration (Table I) reflecting an

entry of fluid was confirmed by the recovery of 96.3 per cent (S.E. \pm 0.6) of the indicator in twelve experiments (5). In other words, the high recovery of phenol red demonstrated that the change in indicator concentration was not the result of diffusion of the compound across the gastric mucosa but the consequence of fluid entry. The results seem paradoxical because the fluid continued to enter the pouch from the mucosa even though the pouch solute concentration was less than that of the interstitial fluid.

TABLE I
CHANGES IN IONIC CONCENTRATIONS
Typical Canine Instillation Experiment

TIME hours	Na mEq./L.	H mEq./L.	Cl* mEq./L.	OSMOLALITY mOsm./Kg. \cdot H ₂ O	PHENOL RED mg./L.
0	0	155	155	295	40.0
1	2	146	151	290	35.4
2	12	125	144	267	32.4
3	31	98	135	252	28.9
4	52	69	129	238	26.1
5	68	52	130	237	24.3

*The sum of the cation concentrations, Na and H, is less than the concentration of chloride. This difference is primarily accounted for by K which has not been listed in the table.

We calculated the net changes in solute and fluid in each hourly period for each experiment (5). In Table II are the net ionic and fluid changes from a typical experiment. The net gain in sodium always exceeded the net hydrogen loss and the net gain in chloride correlated almost quantitatively with the differences between the sodium and hydrogen changes indicating a net gain in solute, i.e., there was not a simple 1:1 exchange of sodium for hydrogen. The changes in fluid volume were always positive indicating a gain in solution (Table II). The solute concentration of the solution transported across the gastric mucosa was calculated and is expressed in mEq./L. In the middle three hours there was a net flow of hypotonic solution into the gastric pouch (concentration of 75 mEq./L.). During these periods the greatest observed fall in osmolality occurred (see Table I).

TABLE II

NET IONIC AND VOLUME CHANGES
Typical Canine Instillation Experiment

Hour	ΔNa	mEq.	ΔH	ΔCl	ml. $\Delta \text{H}_2\text{O}$	mEq./L conc. of solute
1	1.40	-0.62	1.04		6.5	160
2	0.57	-0.44	0.44		5.6	75
3	1.25	-0.80	0.50		7.3	68
4	1.54	-1.18	0.56		7.3	76
5	1.51	-0.95	0.78		6.4	122

The observations in the canine pouches contradict Teorell's findings in the cat stomach. Teorell found no change in volume and an unequal exchange of NaCl and HCl ion pairs with a decline in solute concentration, i.e., a net loss of solute and a fall in tonicity. In contrast, we found a sodium-hydrogen exchange accompanied by a net gain in solute and fluid-the concentration of this solution being hypotonic. Dr. Harry Gregor of Columbia University proposed that our observations concerning the flow of hypotonic fluid might be the result of an anomalous osmotic flux of water produced when ions of different ionic size such as sodium and hydrogen exchange across fixed-negative charge surfaces.

In order to relate the anomalous osmotic flux of solvent to ion transport the studies that follow were undertaken initially in Dr. Gregor's laboratory and have been extended in our laboratory in collaboration with Doctors Gregor and Irving Miller of the Polytechnic Institute of Brooklyn. In Figure 1 is a schematic representation of the apparatus used to study sodium-hydrogen exchange across a fixed negative charge membrane. After the sodium solution was passed over the membrane it was not recirculated. In this manner, the sodium concentration on the open side was kept constant and the hydrogen concentration on the sodium side was negligible. This maximized the gradient of both ions across the membrane. In one set of experiments the amount of solvent moved across the membrane was quantitatively determined as a function of time. The closed side of the system was filled to the upper stopcock and side-arm; as fluid entered the closed side as a result of the exchange, the excess volume of solution flowed out of the side-arm. The fluid was collected in tared vessels and the amount of solution transported determined gravimetrically. In a parallel set of experiments the change in the ionic composition of the acid side was

determined as the exchange progressed by removing solution for assay from the stopcock in the main flow line. In Figure 2 is depicted the water flow rate produced by sodium-hydrogen exchange across a polyanionic membrane (polystyrene-sulfonic acid) containing 20 per cent water (transference number 0.95) (6). A net gain in water always occurred on the closed side and this water flow produced a decline in solute concentration which is shown in Figure 3 (6) in terms of the chloride concentration and osmolality. The decline in solute concentration was the direct result of the observed water entry produced during the sodium-hydrogen exchange (see Figure 2) and does not reflect a loss of solute from the acid side of the system.

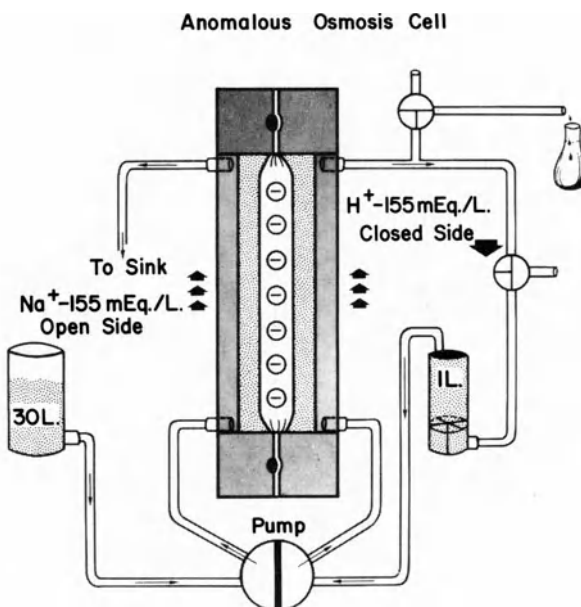


Figure 1. Schematic representation of cell used to study bi-ionic exchanges and secondary anomalous osmosis.

Studies were then undertaken to relate ion size and membrane hydration to the anomalous osmotic fluxes of solvent. In Figure 4 (6) are presented the anomalous osmotic fluxes resulting from the exchange of hydrogen for a series of larger cations in two membranes of different hydration. Water flows were two to three times higher for the 60 per cent hydrated membrane than those found for the 20 per cent hydrated membrane. The effect of ion size is clear: in the exchange of hydrogen for tetramethylammonium

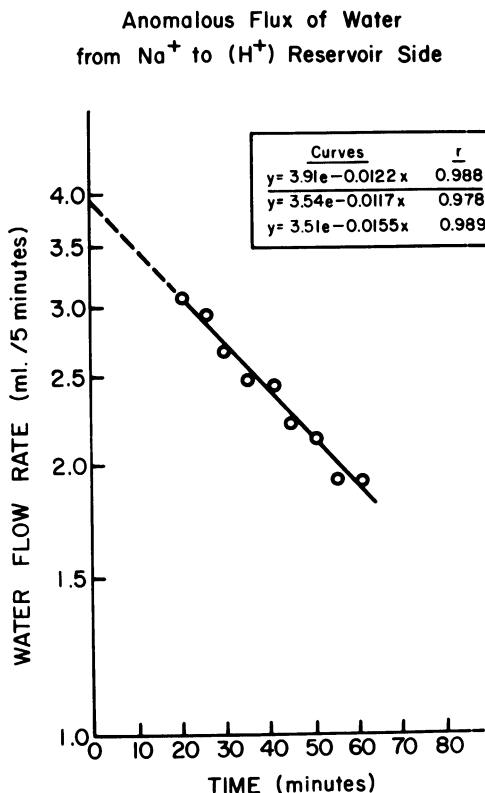


Figure 2. Anomalous osmotic water flow produced by sodium-hydrogen exchange across a sulfonic acid membrane containing 20 per cent water (6).

(crystal size 3.47\AA (7)) and tetraethylammonium (crystal size 4.0\AA) larger anomalous osmotic fluxes are observed than in the hydrogen-sodium (crystal size 0.95\AA) exchange. The differences in water flow become much greater when the results are computed on the basis of a molar rate of ions exchanged. For both membranes the half-time for the exchange of hydrogen for the larger ions, tetramethylammonium and tetraethylammonium, is considerably greater than the half-time for the sodium-hydrogen exchange (see table at top of Figure 4). If each water curve (Figure 4) is integrated from the zero-time to the half-time of the ion flux--relating the water flows to an equal molar exchange of ions--the differences in solvent carried per ion become larger than those seen when the integration is performed as a simple function of time. These studies indicate that an anomalous osmotic flux is dependent on the membrane hydration,

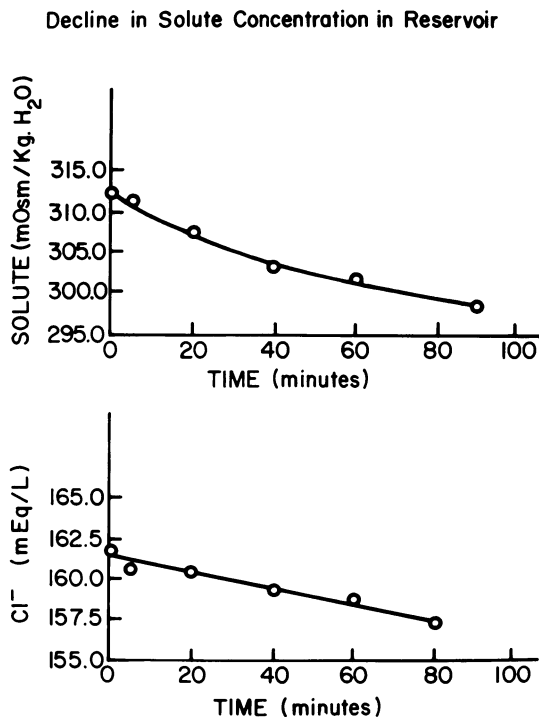


Figure 3. Decline in solute concentration produced by an anomalous flux of water shown in Figure 2. (6)

the number of ions exchanged and their ionic size.

Water flow related to ion movement has also been observed when ions pass through ion-exchange membranes under the influence of an applied electric field. The term electroosmosis (8) has been used to describe the transference of water per mole of ion moved through a highly perm-selective membrane (transference number approaching 1). It has been proposed by Tombalakian, Worsley and Graydon (9), in preliminary experiments, that anomalous osmotic fluxes of water produced by a bi-ionic exchange could be predicted from the electroosmotic fluxes produced by the individual cations. It was shown that the greater the difference in the electroosmotic transport of the ions, the greater the anomalous flux of solvent. Breslau and Miller (10) in a recently advanced mathematical interpretation (of electroosmosis) related the velocity of the solution (in cm/sec) to the electroosmotic coefficient $E_0 d$ (expressed as moles of solution transported per faraday of current). The formulation was in terms of the hydrodynamic drag of a migrating spherical particle in a bounded medium. Based on this interpretation and the work of

Tombalakian, et al.(9) we should be able to predict the anomalous osmotic fluxes for any system of univalent ions by:
 Anomalous Osmosis (moles of solution pumped/mole of ion exchanged)=
 $(E_{O_d})_2 - (E_{O_d})_1$ (moles of solution transported/faraday). (For univalent ions a faraday is equal to an equivalent). We are currently studying the relationship between the electroosmotic fluxes produced by a variety of univalent cations and the anomalous osmotic fluxes produced by bi-ionic exchange of these ions. Hopefully these experiments can be extended to natural polymers.

COMPARISON OF ANOMALOUS OSMOTIC FLUXES ACROSS TWO MEMBRANES

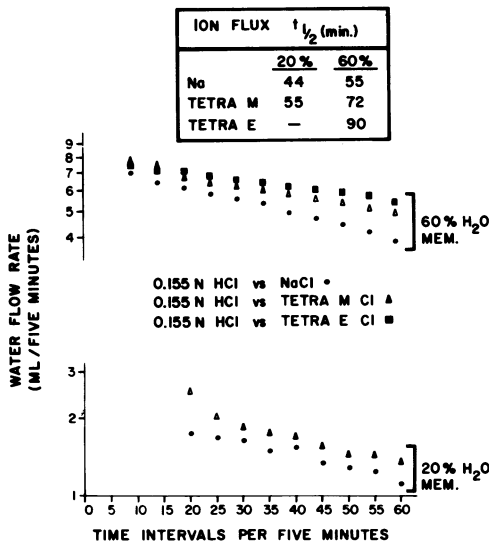


Figure 4. Summary of experimental data relating ion size and membrane hydration to anomalous osmotic fluxes of solvent. (6)

SIGNIFICANCE OF pH AND ANTRAL PERMEABILITY IN GASTRIN RELEASE

Acid glycoproteins are the principle polymeric constituents of the mucus coat on the surface of the stomach. Electron microscopic studies (11) reveal granular packets in the distal portions of the surface epithelial cells and these have been shown by histochemical means to be composed of acid glycoproteins (12). The glycoproteins are periodically released and become part of the mucus coat of the stomach.

The mucus is seen as a viscous coat on the stomach surface in the intact animal. The coat appears in electron micrographs as a fuzz on the apical end of the surface epithelial cells (11). In this symposium Doctor Brandt revealed that the surface of amoebic cells is also covered by an amorphous coat. There is an increasing

amount of evidence that this coat, which has been called by Bennet (13) a glycocalyx, is on the surface of all cells in mammalian systems (14).

In non-secreting stomachs the mucus is a clear gel. Upon acidification of the surface it becomes opaque (15). In unrelated studies, a number of investigators have observed upon acidification of the gastric surface that radio-sodium could no longer pass from the surface fluid into the mucosa (16,17). Changes in the ionization state of the acid glycoproteins may be responsible for the pH-dependent variations observed in the physical state of the mucus and the mucosal permeability to sodium. At pH 7 the carboxyl groups of the acid glycoproteins on the luminal side of the mucus are ionized; at pH 1 these groups are probably protonated and un-ionized leading to a loss of charge at the surface. The loss of surface charge would decrease the osmotic activity of the coat with a loss of water and secondary shrinkage. These pH-dependent physical changes could decrease the ionic permeability and increase the opacity of the mucus.

The release of gastrin, the primary humoral stimulant of gastric acid secretion is regulated by a pH-dependent servo-mechanism (18). An alteration in mucosal permeability, comparable to the pH-dependent change in sodium permeability, may be the molecular basis of this servo-mechanism. Gastrin, a peptide hormone, is produced in the distal part of the stomach known as the antrum. The surface of the gastrin containing cells is exposed to the lumen of the antral glands (19). The proximal part of the stomach known as the fundus, contains the acid and pepsinogen secreting parietal mucosa. Acid and pepsinogen are both released when the parietal mucosa is stimulated by the vagus nerve or by gastrin.

It has been known since the 1920's that when neutral solutions of glycine and other small amino acids which are normally released by peptic digestion are placed in the stomach, they stimulate acid secretion (20). We now know that the amino acids stimulate secretion by causing the release of gastrin from the antrum (21). The hormone is released into the venous blood, goes to the heart and returns to the fundic mucosa via the arterial blood. The fundic mucosa then secretes acid, the contents of the antrum decline to pH 1 and the glycine-stimulated release of gastrin is blocked (22). The mucosa at pH 1 is impermeable to the cation sodium (16,17); it should therefore be impermeable to glycine which is also a cation at this pH. We are proposing that the decline in pH prevents the permeation of the coat by glycine and leads to a diminished rate of gastrin release.

To test whether antral permeation by glycine is altered at pH 1 antral pouches were prepared in dogs by Doctors Gerald Buetow and Robert Cali of the Department of Surgery. 60 mM solutions of glycine-C¹⁴ and ethanolamine-C¹⁴ were instilled into the pouches at pH 7 and 1. The pH 7 and 1 solutions were isosmotic and contained a mixture of NaCl-KCl and HCl-KCl, respectively. At neutral pH after two hours about 15 per cent of each compound passed through the mucosa (Table III). There was a negligible loss of the compounds from the acid solution (Table III) (23).

TABLE III

PERMEATION OF ANTRAL POUCHES
BY GLYCINE AND ETHANOLAMINE

	<u>PER CENT LOSS/2 HOURS</u>	
	Glycine	Ethanolamine
pH 7	16.8 (27)	14.4 (9)
pH 1	2.4 (23)	3.5 (9)

() = number of studies

differences significant to $p < 0.01$ by non-parametric tests

At pH 7, glycine is a zwitterion and ethanolamine is a cation and the mucosa is permeable to both. The cation and zwitterion selectivity may be the result of the carboxyl groups of the glycoproteins being ionized which imparts a negative charge to the surface. At pH 1 glycine and ethanolamine are cations and the mucosa is impermeable to them. This may be the consequence of a reduction in the number of unionized carboxyl groups and the accompanying physical changes---loss of water and membrane shrinkage.

To test this hypothesis, we studied the rate of diffusion of sodium, ethanolamine and glycine across a methacrylic acid membrane at pH 7 and pH 1. At pH 7 the membrane had a water content of 35 per cent and was cation selective. At the lower pH it had a water content of 5 per cent. The membrane was placed in a Lucite cell similar to that in Figure 1. Solutions containing sodium, glycine, and ethanolamine were placed on one side of the cell respectively, and circulated over the membrane. In addition the solutions contained buffer or acid to maintain the pH at 7 or 1. We measured the loss of sodium, ethanolamine and glycine from the closed side of the system. On the open side of the system the solutions were of identical ionic composition to the closed side, but they did

not contain the permeating species.

When the membrane is in its salt form at pH 7, 89 per cent of the sodium, 79 per cent of the ethanolamine and 40 per cent of the glycine pass through the membrane after 75 minutes of exchange (Table IV). At pH 1 when the membrane is in its acid form, only 10 per cent of the sodium, 17 per cent of the ethanolamine, and 15 per cent of the glycine pass through in the same time (Table IV) (24). These experiments indicate that a change in pH alters the cation permeability of surfaces composed of weakly acidic groups.

TABLE IV

PERMEATION OF ACID AND SALT FORMS OF METHACRYLIC
ACID MEMBRANE BY SODIUM, ETHANOLAMINE AND GLYCINE

(PER CENT LOSS)

TIME (min.)	SODIUM		ETHANOLAMINE		GLYCINE	
	ACID	SALT	ACID	SALT	ACID	SALT
15	2.2	32.1	- -	25.1	2.8	5.4
45	5.8	73.2	8.9	60.6	9.7	26.2
75	10.0	89.3	16.9	78.7	15.1	39.7

SUMMARY

The experiments with the canine fundic pouches and the sulfonic acid membranes suggest that the exchange of hydrogen for sodium across the fixed negative charges of the gastric mucus coat yield an anomalous osmotic flow of solvent. Although many of the carboxyl groups at the luminal surface are unionized when the coat is bathed with acid, the pH at the cellular side probably approaches 7 and the carboxyl groups located there are ionized. The bi-ionic exchange across the asymmetrically distributed anionic groups produces a secondary flow of solvent which transforms the primary acid secretory product into a sodium-rich hypotonic fluid.

The experiments with the antral pouches and the methacrylic acid membrane indicate that the natural stimulants of gastrin release, such as glycine, can pass through the ionized, hydrated mucus gel that lies on the surface of the antrum. On permeating the gel, these compounds diffuse into the gland and penetrate the gastrin containing cells. (How they effect gastrin release is not understood at present). The release of gastrin causes the

fundic mucosa to secrete acid which diffuses over the surface of the antrum leading to the protonation of the carboxyl containing groups in the glycoproteins. With the loss of the negative charges, membrane hydration declines and the permeability to cations is altered. These changes are probably the basis of the servo-mechanism by which acid secretion diminishes the release of its primary hormonal stimulant gastrin.

Acknowledgements: This work was supported by the citizens of Nassau County, New York, and by grants from the National Cystic Fibrosis Research Foundation and the National Institutes of Health (grant # AM13674).

BIBLIOGRAPHY

1. James, A.H., THE PHYSIOLOGY OF GASTRIC DIGESTION, ch. 3 (Edward Arnold, Ltd., London, 1957).
2. Hollander, F., Fed. Proc., 11, 706 (1952).
3. Teorell, T., J. Gen. Physiol., 23, 263 (1939).
4. Teorell, T., Gastroenterology, 2, 425 (1947).
5. Berkowitz, J.M., and Janowitz, H.D., Am. J. Physiol., 210, 216 (1966).
6. Praissman, M., Miller, I.F., Gregor, H.P., and Berkowitz, J.M. Unpublished observations.
7. Nightingale, E.R., Jr., J. Phys. Chem., 63, 1381 (1959).
8. Helfferich, F., ION EXCHANGE, 402. (McGraw-Hill Book Company, Inc., New York, 1962).
9. Tombalakian, A.S., Worsley, M., and Graydon, W.F., J. Am. Chem. Soc., 88, 661 (1966).
10. Breslau, B.R., Ph.D. Dissertation, Polytechnic Institute of Brooklyn, Brooklyn, N.Y. (1969).

11. Ito, S., in HANDBOOK OF PHYSIOLOGY, Section 6: Alimentary Canal, II, 705. (Code, C.F., Ed., American Physiological Society, Washington, D.C., 1967).
12. Spicer, S.S., and Sun, D.C., Ann. N.Y. Acad. Sci. 140, 762 (1967).
13. Bennet, H.S., J. Histochem. Cytochem., 11, 14 (1963).
14. Ito, S., Fed. Proc., 28, 12 (1969).
15. Davenport, H.W., PHYSIOLOGY OF THE DIGESTIVE TRACT, 114. (Year Book Medical Publishers, Inc., Chicago, 1966).
16. Cope, O., Cohn, W.E., and Brenzier, A.G., Jr., J. Clin. Invest., 22, 103 (1943).
17. Code, C.F., Higgins, J.A., Moll, J.C., Orvis, A.L. and Scholer, J.F., J. Physiol., London, 166, 110 (1963).
18. Schofield, B., in GASTRIN, 171. (Grossman, M.I., Ed., UCLA Forum in Medical Sciences, University of California Press, Los Angeles, 1966).
19. McGuigan, J.E., Gastroenterology, 55, 315 (1968).
20. Ivy, A.C., and Javois, A.J., Am. J. Physiol., 71, 591 (1925).
21. Elwin, C.-E., and Uvnas, B., in GASTRIN, 69. (Grossman, M.I., Ed., UCLA Forum in Medical Sciences, University of California Press, Los Angeles, 1966).
22. Elwin, C.-E., Acta Physiol. Scand. 175, 36 (1960).
23. Berkowitz, J.M., Praissman, M., Beutow, G., and Cali, R. Unpublished Data.
24. Praissman, M., Miller, I.F., and Berkowitz, J.M. Unpublished Data.

PROPERTIES OF THE PLASMA MEMBRANE OF AMOEBA

Philip W. Brandt¹ and Klaus B. Hendil²

Columbia Univ., 630 W. 168th St., New York 10032 (1)

Carlsberg Laboratory, 10 Gl. Carlsbergvej. Valby, Dk.(2)

Pinocytosis in amoeba was described, and its brief history reviewed at an earlier ACS meeting (4). It was pointed out that pinocytosis is the descriptive term for a behavioral pattern. In amoeba this pattern is initiated by a step increase in the cation concentration at a suitable pH and pCa. This report will consider in detail the initial phase of pinocytosis, the reaction of the amoeba plasma membrane to the cationic stimulus.

The initial signal in pinocytosis is almost certainly the adsorption (2, 19, 20) or exchange of cations at the outer layer of the plasma membrane. Shortly thereafter, or simultaneously in parallel with the surface reaction, the transmembrane conductance (D.C.) increases (3) more than a decade and the impedance decreases (13). This conductance change, like pinocytosis, is dependent in magnitude upon the concentration of the stimulating cation, and upon the background pH and pCa (3). A low pCa tends to block pinocytosis (11, 14) or arrest it if the pCa is lowered after pinocytosis is initiated (3, 4). The conductance increase is time dependent, in parallel with the induction of pinocytosis channel formation (10, 12).

The plasma membranes of amoeba fixed in the high conductance state and studied with the electron microscope are thicker in comparison to control membranes. The increase in thickness, which appears to be mostly a thickening of the electron transparent zone, could be due to an increase in total lipoprotein, or more likely to an imbibition of partially hydrated ions (3, 4). Since the process

of fixation and image interpretation is not known with certainty (15, 21), the thickening may accurately represent the *in vivo* dimensions or be a propensity towards thickening brought out by fixation. Fixation studies, which currently are being designed to explore the area, must necessarily be indirect. However if the thickening were due to an *in vivo* increase in the content of hydrated ions, the partition coefficient of the solution: membrane system should change for nonelectrolytes. Therefore permeability studies on *in vivo* membranes will provide a direct test of the consequences of the membrane changes.

A change in partition coefficient should alter the permeability coefficient (P_n) for a given nonelectrolyte. The flux rates of polar penetrants should increase as the membrane becomes relatively richer in water and that of nonpolar penetrants should decrease. P_n should vary with the quantities of ions in the membrane and with the degree to which each species is hydrated. In turn these ionic quantities will depend on the geometry, concentration, and type of sites available in the membrane. Since changes in the pH and pCa greatly affect the conductance changes and amount of pinocytosis induced by a given cation, it seemed reasonable to systematically study the effect of these variables on P_n .

After P_n was determined for a number of nonelectrolytes under standard conditions, isopropanol was selected for intensive study. P_n for isopropanol is about 4.5×10^{-6} cm/sec with a time constant of about 1200 seconds in our system. Therefore the influx of ^{14}C labeled isopropanol is sufficient in 200 seconds to be readily separated from the background, and even when the P_n is considerably elevated by the experimental treatment the flux rates are easily determined.

MATERIALS AND METHODS

The amoeba Chaos chaos B was grown in mass cultures by methods quite well standardized in the Carlsberg Laboratory, Department of Physiology. Thus large numbers of cells of a uniform state of nutrition were available. In each experiment, several thousand cells were separated according to size by passage through a 2 mm ID polyethylene tube about three meters long wound around a ring stand post 1.25 cm in diameter. The larger cells tended to ride in the center of the flowing saline stream, while the small cells tended to fall into the more slowly flowing saline near the tube wall; therefore, the first cells to arrive at the lower end were the largest. The first 1500 cells to emerge were mixed to randomize their order

then used in the experiments.

Groups of 100 cells in about 50 μl of fluid were placed in each of 12 (approximately 1 ml capacity) pre-weighed polyethylene capsules. The weight increase with loading was taken as the fluid + cell volume. For each experiment, two groups were packed by centrifugation in calibrated capillary tubes and the volume of the cells calculated. This cell volume was confirmed by two alternate methods, an isotope dilution method and an isotope loading method (5).

To determine an experimental point, six capsules containing 100 cells each were shaken for five minutes in a temperature regulated water bath. After this equilibration period, a low (1 $\mu\text{M/L}$) concentration of a ^{14}C labeled non-electrolyte dissolved in the experimental saline was added quantitatively. A measured number of seconds after addition of the isotope, the cells were rapidly washed and collected by a filtration method or a centrifugation method, and the quantity of isotope trapped in the cells was determined. In the filtration method, the cells were transferred with a breaking pipette from the capsule to a one inch Gelman vacuum funnel (#1112) which contained 10 ml of wash fluid. The fluid was drawn down by a slight vacuum to a level about 2 mm from the surface of the filter disk and then a five ml. wash was added. This was repeated once more, then the fluid was completely filtered off.

The filtration procedure caught the cells on the surface of the filter only after the final wash, then the filter disk and cells were quickly removed from the apparatus and dropped into a scintillation vial filled with Bray's scintillation fluid. The scintillation fluid extracted the non-electrolyte from the cells and dissolved the filter disk. The entire wash procedure took about 30 seconds. A similar washout of the same quantity of label, in the absence of cells, provided a background count.

In the centrifuge method, brief centrifugations to pack the cells were alternated with washes until the extracellular ^{14}C label was minimal. It required at least 1.5 minutes but provided a check against cell loss in the filtration method, since the surviving cells were counted in control experiments.

The results reported here were gathered using the filtration method; however, they suggest that amoeba in solutions in which P_n is minimal are relatively stable during filtration while cells in solutions which greatly increase P_n are unstable and tend to leak or rupture during washing by filtration. Thus the curves shown in

figure 1 are probably flatter than they should be. The error is to minimize the effects of high concentrations of cations on the apparent permeability of the cells.

The experiments reported here are influx studies and the following calculations were used:

$$P_n = \ln \frac{C_o}{C_o - C_i} \quad \frac{V}{A t}$$

P = cm sec $^{-1}$ Permeability coefficient

C_o = ^{14}C Concentration outside

C_i = ^{14}C Concentration inside

$\frac{V}{A} = 60 \times 10^{-4}$ cm (9)

t = time

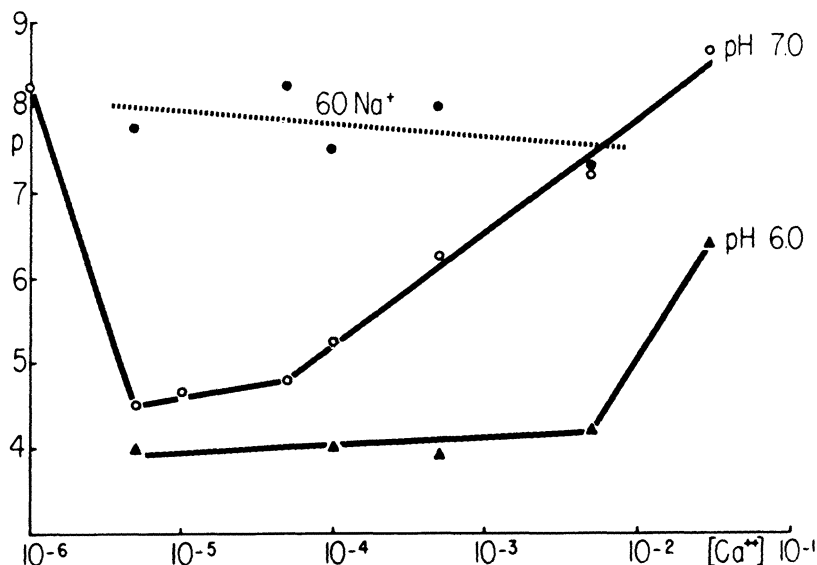
Each point was determined six times; therefore, the calculator was programmed to calculate and accumulate the P_n 's from the raw data and compute the mean and the standard deviation (SD). The coefficient of variation ($\frac{SD}{mean} \times 100$) was 10% to 20% with some higher values in conditions which maximize P_n . Therefore, the exact magnitudes on the curves in figure 1 are not as accurate as the direction of changes in P_n with a given variable. The centrifugation method has an average coefficient of variation less than 10% and this technique is currently being used to repeat and extend the experimental curves.

The solutions all contained approximately 2 mM/L Na^+ but the buffer was varied dependent on the Ca^{++} level. When Ca^{++} was below 1.0 mM/L, a phosphate buffer was used and adjusted so that the total Na^+ remained close to 2 mM/L. The calcium was simply added as a chloride between 100 $\mu\text{M}/\text{L}$ and 30 mM/L. Between 5 $\mu\text{M}/\text{L}$ and 50 $\mu\text{M}/\text{L}$ Ca^{++} , a 1 mM/L citrate buffer for Ca^{++} was employed. The apparent association constant (at the given pH) was calculated from the H^+ and Ca^{++} association constants (5). The Ca^{++} buffer employed at 1 $\mu\text{M}/\text{L}$ Ca^{++} was EGTA and the apparent association constants employed were taken from Portzehl et al.(17), or recalculated from their tables of absolute association constants (5).

RESULTS

The P_n (isopropanol) of the amoeba plasma membrane increases with Ca^{++} concentration and pH at 20C (Figure 1). At pH 7.0 P_n is

Figure 1



The abscissa is the Ca^{++} concentration in M/L while the ordinate is the permeability coefficient in $cm/sec. \times 10^{-6}$. The curves indicated by pH are in a background of 2mM/L Na^+ while the curve identified as 60Na^+ is the P_n of the membrane during the 200-400 second interval after the Na^+ was increased to this level (in mM/L) from the same Ca^{++} concentration point on the pH 7.0 line.

4.5×10^{-6} cm/sec. in a saline containing 5 $\mu\text{M}/\text{L}$ Ca^{++} and increases progressively to 8.5×10^{-6} cm/sec. in 30 mM/L Ca^{++} . At pH 6.0 however, P_n is lower at all Ca^{++} concentrations than at pH 7.0 and only increase when the Ca^{++} exceeds 5 mM/L. Little further decrease in P_n is observed at pH's lower than 6 (table 1). P_n can decrease below that recorded at low pH. When the cells are cooled to 4.5 C, P_n is about 2.3×10^{-6} cm/sec. At very low Ca^{++} concentrations (1 $\mu\text{M}/\text{L}$) the cells are very fragile and tend to be shaken apart during the experiment, especially at pH 6.0 or lower.

At pH 8.0 P_n is higher than it is at any corresponding Ca^{++} level at a lower pH and it increases sharply with rising Ca concentration (Table 1). At 30 mM/L Ca^{++} the cells are too fragile to test, because the stirring necessary to obtain accurate P_n values homogenizes them. Thus the cells are most fragile at two extremes — low pH and low Ca^{++} and at high pH and high Ca^{++} .

Because the conductance changes induced by a step increase in the Na^+ concentration are time dependent, the time course of the change in P_n with a step increase (from 2 to 60 mM/L) in the Na^+ concentration was determined. The influx period was kept at 200 seconds, therefore, this limited the time resolution. It appeared that P_n reached a maximum during 200 to 400 second interval after the Na^+ increase, and fell off towards control values with a time constant of about 10 minutes. This approximates the time course of the conductance changes (3, 4) and the time course of pinocytosis (9).

P_n was determined during the 200 to 400 second interval after a step increase in Na^+ at different Ca^{++} and H^+ concentrations. At pH 7.0 P_n increased to about 8.0×10^{-6} cm/sec. at all concentrations of Ca^{++} tested. As a consequence the high Na^+ P_n line (Figure 1) crosses the low Na^+ P_n line at about 5 mM/L Ca^{++} . We have not yet tested the effect of high Na^+ on P_n when the latter is elevated above 8.0×10^{-6} cm/sec. in high Ca^{++} . We have not systematically examined the effects of varying Na^+ concentration but a few experiments using even higher Na^+ levels (than about 60 mM/L) lead us to believe that the Na^+ effect is saturated by 60 mM/L. Chapman-Andresen (10) reports that the saturation Na^+ concentration for pinocytosis is about 70 mM/L (in a phosphate buffer) which is in reasonable agreement with our data considering the accumulated errors in the two types of studies. The relative effect on P_n of 5 mM/L Ca^{++} , Sr^{++} , Ba^{++} , and Mg^{++} was tested at pH 7.0, and P_n decreased in comparisons between solutions

DATA TABLE 1

Exp.	Date	pH	Ca^{++} mM/L	Na^{+} mM/L	Pn	C.V.
14/11		5.1	0.1	2	3.8	11.4
11/11		5.1	0.5	2	3.6	18.8
29/11		5.0	5.0	2	4.0	18.9
8/11		6.1	0.1	2	4.0	8.5
7/11		6.1	0.5	2	3.9	13.7
15/11		6.1	5.0	2	4.2	12.7
25/11		6.0	30.0	2	6.4	12.7
12/12		6.0	.005	~60	3.9	15.3
6/12		6.0	.01	~60	4.9	34.5
5/12		6.0	0.5	~60	5.8	20.7
9/12		6.0	5.0	~60	4.6	21.5
18/11		7.1	.001	2	8.3	38.7
25/11		7.0	.005	2	4.5	13.6
21/11		7.0	.01	2	4.7	18.2
21/11		7.0	.05	2	4.8	26.2
8/11		7.1	0.1	2	5.2	11.2
7/11		7.1	0.5	2	6.3	23.0
15/11		7.1	5.0	2	7.2	20.2
25/11		7.0	30.0	2	8.6	17.4
13/12		7.0	.005	~60	7.8	19.0
13/12		7.0	.05	~60	8.3	17.5
6/12		7.0	0.1	~60	7.5	26.6
5/12		7.0	0.5	~60	8.0	21.2
9/12		7.0	5.0	~60	7.3	20.5
14/11		8.1	0.1	2	5.5	13.3
11/11		8.0	0.5	2	6.5	16.0
28/11		8.0	5.0	2	9.7	39.0
21.7		8.0	0.1	~60	11.9	7.5

C.V. is the coefficient of variation (see text), Pn is the permeability coefficient of the membrane to isopropanol.

in the above order.

The osmotic pressure of the amoeba cytoplasm corresponds to that of a 107 to 117 milliosmolar solution (Løvtrup and Pigon, Riddick), therefore all of the solutions tested including the culture solution are hypotonic or nearly isotonic. P_n in low Ca^{++} and low or high Na^+ was unaffected by the addition of 120 mM/L sucrose, therefore solvent drag is not a likely factor in our system.

DISCUSSION

There are several reasons to interpret the data in table 1 and figure 1 cautiously. The coefficients of variation are roughly between 10 and 20%. It is our impression that the cells are more fragile at higher P_n 's, therefore the high values are most liable to err on the low side. (Current techniques promise to reduce the coefficients of variation to about 5% and decrease the breakage of cells at high P_n).

Conceivably all our data could be generated if the cells are rapidly changing in surface area or in volume to surface ratio. There are four arguments against this possibility. First the range of P_n 's measured to date are from 2.3×10^{-6} cm/sec (at 4.5°C, 100 $\mu\text{M}/\text{L}$ Ca^{++} , pH 6.75) to 13×10^{-6} cm/sec (at 20°C, 100 $\mu\text{M}/\text{L}$ Ca^{++} , 60 mM/L Cs^+ , pH 8.0). This range would have to represent an overall five fold increase in surface to volume ratio, and a three fold change within 200 seconds. Second, the capsules are rapidly shaken for five minutes before an experiment begins and throughout the experiment. This causes amoeba to round up and restricts the formation of major pseudopods. Third, the high P_n values in high Na^+ are (at pH 7.0, 20°C) associated with a ten to fifty fold increase in conductance (3, 4) over the controls. Thus an area change alone cannot simultaneously explain a two fold increase in P_n and a 50 fold increase in conductance.

Fourth, Wolpert and O'Neill (22) have measured the turnover time of amoeba membrane by tagging it with fluorescent antibody. In control, and in experiments in high Na^+ , no evidence was found for a rapid turnover or formation of new membrane in less than a half time of about five hours. New membrane is thus formed at about .2% per minute. Since our experiments last five minutes, the area change and/or turnover is about 1% and can be neglected. Chapman-Andresen (8) has also argued that during pinocytosis, membranes are decreased, if anything. We conclude, therefore,

our increases in Pn's maybe too small as a consequence of a decrease in surface area during the exposure to high concentrations of cations. However, the volume of the cell may decrease slightly in 60 mM/L Na⁺ although this is nearly isomotic (7). Therefore, we chose to use a constant volume/area ratio throughout all experiments and anticipated that only small errors of variation are introduced into the Pn values by this assumption, although it may contain a constant error.

Thus the Pn's given are all calculated by assuming a volume to surface ratio of 6×10^{-3} cm and may have to be adjusted on this account. It is doubtful if the ratio is larger, but it could be as small as 3×10^{-3} cm (9, 16). The standard errors are large if single points (the mean of six experiments) alone are considered, but the points fall on reasonable curves with little scatter. This improves the reliability of the data in determining the direction in which Pn changes with a given variable.

The data on the permeability of the amoeba to non-electrolytes was collected for two reasons. We believed, on the basis of the earlier morphological and electrophysiological data (3, 4), that the membrane in the high conductance state is very different from the same membrane in the low conductance state. The present data confirm this conclusion. Second, we hoped to establish some link between pinocytosis and the structural and physiological change in the membrane. The present data add little to our understanding of this link. Our current hypothesis of the process of "excitation-pinocytosis-coupling" states that the redistribution of ions or a specific ion in the cytoplasm as a consequence of the permeability change, is the trigger for pinocytosis. Similar models exist for directing amoeboid motion (1). Thus our data support the hypothesis in so far as they demonstrate a permeability change in the presence of pinocytosis activators (5).

In high Ca⁺⁺ (at pH 7.0), Pn is about double that in low Ca⁺⁺ (figure 1). In contrast to the effect on Pn, high Ca⁺⁺ causes the conductance and presumably the Na⁺ and K⁺ permeabilities (Pe) to decrease (3, 4, 6). In low Ca⁺⁺ (5 - 50 μM/L), increasing the concentration of monovalent cations (Na⁺, K⁺, Li⁺, Cs⁺, Rb⁺) is associated with about a doubling of Pn (5) and a 10 to 50 times

increase in conductance (3, 4, 13) and presumably an increase in the permeability of the membrane towards these monovalent cations. The cell is quite impermeable to chloride (6). From these data it is apparent that delta Pn is not necessarily related to delta Pe's. One possible generalization of this data is that Pn increases whenever the instantaneous concentration in the membrane of cations increases. Thus when Ca^{++} is low, a high membrane load of monovalent cations causes an increase in Pn. In high Ca^{++} it can be argued that Ca^{++} bound in the membrane diminishes Pe for Na^+ but increases Pn.

There are several lines of evidence in support of the qualitative model just suggested. Pn varies directly with pH. This suggests that sites in the membrane are not available for association with other cations when they are in the hydrogen form. This is demonstrated by the changes in Pn at pH 6 in comparison to pH 7 at all Ca^{++} and Na^+ levels. Presumably the sites are more hydrated when they are in the non-hydrogen form and it is this factor which most affects Pn.

The total number of groups available to Na^+ is determined by the pH and the Ca^{++} concentration. This is concluded from the horizontal line for high Na^+ in figure 1. The delta Pn is smaller as Ca^{++} is raised until at 5 mM/L Ca^{++} there is no delta Pn. This suggests that either all the available sites are occupied by Ca^{++} , or when Na^+ in the membrane, no net changes in the degree of membrane hydration takes place.

It has often been questioned whether the changes in membrane properties recorded under any experimental condition are due to local changes in a small fraction of the total membrane, or due to a homogeneous membrane change (21). This question resolves formally to asking whether or not the change in property is due to an increase in the diameter of a fixed pore, or due to an increase in the number of transport sites. Whether the sites are confined to a local spot is pertinent only to the second half of the question, since the implication of "new sites" is that they form in an undifferentiated part of the membrane. A few preliminary experiments which probed for an increase in site diameter, as opposed to number, seemed to support the latter. Pn for slower penetrants such as glucose, glycerol or ethylene glycol were not increased to any greater degree by high Na^+ than Pn for isopropanol. A model for the Pn changes based on an increase in pore area, not number, would have to predict a relative increase in the Pn of larger penetrants, especially those limited by pore size.

Although other models and arguments can be adduced from the data (5) the stronger ones have been presented here. We expect to be able to develop a quantitative model of the amoeba. membrane as we increase the size and quality of our data pool. The current model envisages the membrane as a collection of sites which can ionize according to the hydrogen ion concentration, and the ionic strength. The amount of water in the membrane, hence its permeability towards polar non-electrolytes, depends on the quantities of ions in the membrane at any instant. The membrane is plastic and its internal dimensions can change to accomodate different loads of hydrated ions.

SUMMARY

The permeability coefficient (P_n) of the amoeba plasma membrane for polar non-electrolytes has been found to be a function of the concentration of H^+ , monovalent cations, and divalent cations. P_n increases with pH and Ca^{++} concentration. At pH 7.0 a time dependent increase in P_n to a constant value at its maximum accompanies a step increase in the Na^+ concentration at all Ca^{++} concentrations tested. A model is proposed which relates P_n to the degree of membrane hydration. The membrane is hydrated according to its total load of cations and the degree to which these ions are hydrated when bound in the membrane.

ACKNOWLEDGMENTS

Dr. Brandt wishes to acknowledge the warm hospitality of Dr. Heinz Holter, Professor of Physiology, and the other members of this department of the Carlsberg Laboratory during the year he spent in the Laboratory while this study was carried out. Dr. Brandt held a Guggenheim Fellowship over this same period, 1968-9. Supported by NIH Grant 5 RO1 - 05910.

REFERENCES

1. Bingley, M. S., and Thompson, C. M., "Bioelectric Potentials in Relation to Movement in Amoebae", J. Theoret. Biol., 2: 16-32, 1962.
2. Brandt, P. W., "A study of the Mechanism of Pinocytosis", Exp. Cell Res., 15: 300-313, 1958.

3. Brandt, P. W., and Freeman, A. R., "Plasma Membrane: Sub-structural Changes Correlated with Electrical Resistance and Pinocytosis", Science, 155: 582-585, 1967.
4. Brandt, P. W. and Freeman, A. R., "The Role of Surface Chemistry in the Biology of Pinocytosis", J. Colloid and Interface Science, 25: 47-56, 1967.
5. Brandt, P. W., and Hendil, K. B., in preparation for publication in Comp. Rend. Trav. Lab. Carlsberg.
6. Bruce, D. L. and Marshall, J. M. "Some Ionic and Bioelectric Properties of the Amoeba Chaos chaos", J. Gen. Physiol. 49:151-178, 1965.
7. Chapman-Andresen, C., and Dick, D. A. T., "Volume Changes in the Amoeba Chaos Chaos L.", Comp. Rend. Trav. Lab. Carlsberg, 32: 265-289, 1961.
8. Chapman-Andresen, C., "Factors Affecting the Duration of and the Utilization of Membrane During Pinocytosis", in Progress in Protozoology, Proceedings of the First Internat. Conf. Protozoology, Prague, 1961.
9. Chapman-Andresen, C., and Dick, D. A. T., "Sodium and Bromine Fluxes in the Amoeba Chaos Chaos L.", Comp. Rend. Trav. Carlsberg, 32: 445-469, 1962.
10. Chapman-Andresen, C., "Studies on Pinocytosis in Amoebae", Comp. Rend. Trav. Lab. Carlsberg, 33: 73-264, 1962.
11. Cooper, B. A., "Quantitative Studies of Pinocytosis Induced in Amoeba Proteus by Simple Cations". Comp. Rend. Trav. Lab. Carlsberg, 36: 385-403, 1968.
12. Holter, H., "The Induction of Pinocytosis" in Biological Approaches to Cancer Chemotherapy, Academic Press, Inc., 77-88, 1960.
13. Josefsson, J. O., "Some Bioelectrical Properties of Amoeba Proteus' Acta Physiol. Scand.", 66: 395-405, 1966.
14. Josefsson, J. O., "Induction and Inhibition of Pinocytosis in Amoeba Proteus", Acta Physiol. Scand., 73: 481-490, 1968.
15. Korn, E. D., "Structure of Biological Membranes", Science, 153: 1491-1498, 1966.

16. Løvtrup, S., and Pigon, A., "Diffusion and Active Transport of Water in the Amoeba". Comp. Rend. Trav. Lab. Carlsberg, 28: 1-36, 1951.
17. Portzeh, L. H., Caldwell, P. C., and Ruegg, J. C., "The Dependence of Contraction and Relaxation of Muscle Fibers from the Crab Maia Squinado of the Internal Concentration of Free Calcium Ions". Biochimica et Biophysica Acta, 79: 581-591, 1964.
18. Riddick, D. H., "Contractile Vaciole in Amoeba Pelomyна Carolinensis". Am. J. Physiol., 215: 736-740, 1968.
19. Rustad, R. C., "Molecular Orientation at the Surface of Amoeba during Pinocytosis". Nature, 83:1058-1059, 1959
20. Schumaker, V. N., "Uptake of Protein from Solutions by Amoeba Proteus". Exp. Cell Res., 15: 314-331, 1958.
21. Stoeckenius, W., and Engelman, D. M., "Current Models for the Structure of Biological Membranes", J. Cell Biol., 42: 613-646, 1969.
22. Wolpert, L., and O'Neill, C. H., "Dynamics of the Membrane of Amoeba Proteus studied with Labelled Specific Antibody". Nature, 196: 1261-1266, 1962.

INDEX

Adsorption

and electric currents, 209 ff
of ions in amoeba, 323 ff
of protein films at the air-water interface, 1 ff
of proteins on colloids and cells, 217 ff
of proteins on synthetic materials, 235 ff
of lung surfactant, 261 ff, 275 ff

Atheromatous plaques

composition, 55 ff

Bilayer lipid membranes

asymmetric membranes, 155 ff
effects of modifiers, 135 ff
effects of pH and Ca^{2+} , 155 ff

Biological systems

(see also Atheromatous plaques
Gastric secretion
Intravascular prostheses
Lung surfactant
Natural membranes
Thromboresistance)

amoeba, 323 ff
bacterial membranes, 175 ff
blood vessel walls, 235 ff
lining of lung, 261 ff, 275 ff
lining of stomach, 309 ff
various cells including erythrocytes and tumor cells, 191 ff
various systems including corneal stroma, cartilage, 287 ff

Calcium

Ca^{++} dependent ATPase, 181
effect on lecithin monolayers, 268
effect on pinocytosis in amoeba, 323 ff

Calcium (continued)

- interactions with bilayer lipid membranes, 155 ff
- interactions with fatty acids, 23 ff

Differential thermal analysis

- phospholipids in water, 37 ff, 55 ff

Dispersions

- of phospholipids, 37 ff, 85 ff

Electrostatic effects

- and adsorption at solid-liquid interface, 209 ff
- and film pressure, 15
- and ion transport in amoeba, 323 ff
- leading to osmotic flow in stomach, 309 ff
- surface potential, 27

Experimental techniques

- adsorbed monolayers, 4
- bubble stability, 103
- differential thermal analysis, 39, 58
- immunolectroadsorption, 211
- interfacial transport using the Schulman chamber, 297
- microelectrophoresis, 218
- polarized light microscopy, 39
- spread monolayers, 3, 24, 103, 263
- surface potential, 24
- thin-layer chromatography, 88
- titrations of dispersed systems, 87

Gastric secretion

- control mechanism, in vivo, 309 ff

Hexadecyltrimethylammonium bromide

- interaction with bilayer lipid membranes, 141
- interaction with DNA, 119 ff

Interactions

- calcium with fatty acid monolayers, 23 ff
- choline phospholipids with sulfatide, 85 ff
- DNA with positively charged monolayers, 119 ff
- immunological reactions, 209 ff
- lipid-protein association in lung surfactant, 261 ff, 275 ff
- modifiers with bilayer lipid membranes, 135 ff
- phospholipids in water, 37 ff
- poly-L-lysine with stearic acid, 101 ff

Intravascular prostheses

- study of materials, 235 ff

Lipids

as "carriers" in water-butanol system, 295 ff
cholesterol and cholestryl esters, 55 ff, 85 ff, 162, 295 ff
fatty acids, 23 ff, 62 ff
in lung surfactant, 261 ff
oxidized cholesterol, 144
phospholipids, 37 ff, 85 ff, 139, 261 ff, 295 ff
sodium dodecyl sulfate, 93
sulfatides, 85 ff
triglycerides, 55 ff

Lung surfactant

composition and surface properties, 261 ff, 275 ff

Model systems

(see Bilayer lipid membranes
Dispersions
Interactions
Lipids
Monolayers)

Monolayers

acyl derivatives of casein, 1 ff
bovine serum albumin, 1 ff
casein, 1 ff
lung surfactant, 261 ff, 275 ff
lysozyme, 1 ff
fatty acids, 23 ff, 101 ff
oleic acid, 23 ff
phospholipids, 261 ff
polypeptides, 101 ff
proteins, 1 ff
stearic acid, 23 ff, 101 ff

Natural membranes

analogy of bilayer lipid membrane, 135 ff, 155 ff
lipid composition, 55 ff, 76 ff, 175 ff
phospholipid composition, 50 ff, 175 ff
pore model, 288 ff
red blood cells
sheep, 217 ff
human, 295 ff
RNA in cell periphery, 191 ff
surface composition of lung, 261 ff
swelling due to water absorption, 287 ff

Nucleic acids

DNA interaction with monolayers, 119 ff
RNA in the cell periphery, 191 ff

Phospholipids

- as "carriers" in water-butanol system, 295 ff
- in aqueous dispersions, 37 ff, 85 ff
- in monolayers, 261 ff

Pinocytosis

- in amoeba, 323 ff

Polymers

- DNA, 119 ff
- poly-L-lysine, 101 ff
- polylysyl gelatin, 217 ff
- polypeptides (copolymers of L-lysine and L-phenylalanine), 119
- polysaccharides, 209 ff
- polystyrene latex, 217 ff
- polystyrene-sulfonic acid membranes, 309 ff
- protein monolayers, 1 ff, 209 ff, 217 ff
- RNA, 191 ff

Proteins

- enzymes in bacteria, 175 ff
- in lung surfactant, 261 ff, 275 ff
- in monolayers, 1 ff, 209 ff, 217 ff

Sugars

- kinetic and equilibrium behavior in a water-butanol-lipid system, 295 ff

Surface Chemistry

- (see Adsorption
 - Experimental techniques
 - Interactions
 - Model systems
 - Monolayers
 - Wettability

Thromboresistance

- "Stellite 21," 245
- surface chemical features, 235 ff

Transport

- effect of pH and Ca^{++} in amoeba, 323 ff
- of ions and water across gastric mucosa, 310 ff
- of sugars in water-butanol-lipid system, 295 ff
- of water through membranes, 287 ff

Wettability

- of blood vessel walls, 240